The Role of Innate Lymphoid Cells in Intestinal Inflammation

Anna-Lena Schaupp

Magdalen College

University of Oxford

A thesis submitted in fulfilment of the requirements for the degree of Doctor of Philosophy, Trinity Term 2015

The role of innate lymphoid cells in intestinal inflammation

Anna-Lena Schaupp
Magdalen College, University of Oxford

A thesis submitted in fulfilment of the requirements for the degree of Doctor of Philosophy, Trinity Term 2015

Abstract

A breakdown of intestinal homeostasis due to dysregulated immune responses against intestinal bacteria underlies the pathogenesis of inflammatory bowel disease (IBD) in genetically susceptible individuals. Amongst mucosal immune cells, innate lymphoid cells (ILCs) are a heterogeneous group of cells whose functions in pathogenic inflammatory processes in the intestine are beginning to emerge from experimental murine models. However, less is known about the role of ILCs in chronic intestinal inflammation in humans.

In this thesis, human ILCs were examined in the context of IBD and potential mechanisms by which these cells may contribute to IBD pathogenesis were investigated. We identified phenotypically and functionally distinct ILC1, ILC2 and ILC3 populations in the human intestinal lamina propria and peripheral blood and found that ILCs enriched for expression of IL-17A and IFNγ accumulated in the inflamed intestine, potentially through increased *in situ* proliferation and chemokine-mediated recruitment from blood. Based on their *in situ* localization, we investigated potential functional interactions between ILCs and $CD4^+$ T cells and found that a proportion of human ILCs in peripheral blood and the intestinal lamina propria expressed HLA-DR and co-stimulatory molecules. ILCs were capable of taking up and processing protein antigen at levels equivalent to B cells, but in contrast to monocytes, antigen-pulsed ILCs failed to activate antigen-specific memory $CD4^+$ T cells *in vitro*. Reciprocal activation between ILCs and monocytes enhanced the antigen-presenting potential and bactericidal capacity of myeloid cells and induced upregulation of co-stimulatory ligand expression by ILCs. This innate activation loop resulted in an augmentation of $CD4^+$ T cell activation.

These findings extend our knowledge of the complex interactions between human ILCs and other key immune cell populations, and suggest mechanisms by which rare ILCs may contribute to the pathogenesis of IBD by augmenting myeloid cell and $CD4^+$ T cell responses.

Acknowledgements

I would like to thank my supervisors Dr Holm Uhlig and Professor Fiona Powrie for giving me the opportunity to work on this project and for all their advice and discussions along the way. Thank you also to Dr Kevin Maloy and Professor Graham Ogg, who have provided additional feedback and support over the years.

Thank you to all past and present members of the TGU who have helped to shape this project through their comments and criticisms, have always been approachable in times of experimental crisis and have made the TGU a pleasant environment to work in. In particular, I would like to thank Ahmed Hegazy for invaluable advice on all matters T cell-, transcription factor- and flow cytometry-related; Sumit Pandey and Tobias Schwerd for generously sharing their expertise in the handling of bacteria; Helen Ferry for tirelessly performing long ILC sorts, which more often than not involved going beyond her normal working hours (thank you also to Ahmed, Claire and Julie for helping out whenever that wasn't possible!); Claire Pearson and Alessandra Geremia for critical reading of this thesis; and Hannah Chen and Corinne Lochmatter for their friendship and support.

Many thanks to the members of the ORB Biobank for collecting and allocating the intestinal tissue specimens that were used in this study, and, of course, all the patients who kindly agreed to donate their tissues. Thanks also to James Chivenga and Priya Siddhanathi for collecting patient blood from the IBD clinic and to all my colleagues who, repeatedly, fearlessly and incentivised only by the reward of small pieces of chocolate, agreed to donate their blood.

Finally, I would like to express my deepest gratitude to Ben, who recognized a potential in ILC-stroma interactions, and without whom this project would not have been possible; and to my parents, my grandmothers and Dieter, for being unfailingly supportive and believing in me. Auf die Familie!

List of abbreviations

AAHR	Allergic airway hyperresponsiveness
AAM	Alternatively activated macrophage
Ag	Antigen
AHR	Aryl hydrocarbon receptor
AIEC	Adherent-invasive *Escherichia coli*
AMPs	Antimicrobial peptides
APC	Antigen-presenting cell
APRIL	A proliferation-inducing ligand
Areg	Amphiregulin
Arg	Arginine
ATG16L1	Autophagy-related 16-like 1
BAFF	B cell activation factor of the TNF family
Bcl11b	B-cell CLL/lymphoma 11b
BDCA-2	Blood dendritic cell antigen-2
bHLH	Basic helix loop helix
Bif	*Bifidobacterium*
CIITA	Class II transactivator
CCL	C-C chemokine ligand
CCR	C-C chemokine receptor
CD	Crohn's disease
CDH1	Cadherin 1
CFSE	Carboxyfluorescein succinimidyl ester
CFU	Colony-forming units
ChIP	Chromatin immunoprecipitation
ChILP	Common helper ILC progenitor
CILP	Common ILC progenitor
CLP	Common lymphoid progenitor
cNK	Conventional natural killer
CRC	Colorectal cancer
C.rodentium	*Citrobacter rodentium*
CRTH2	Chemoattractant receptor-homologous molecule expressed on T_H2 cells

CUL2	Cullin 2
CXCL	C-X-C chemokine ligand
CXCR	C-X-C chemokine receptor
DC	Dendritic cell
DN	Double-negative
DNA	Deoxyribonucleic acid
dnMAML	Dominant-negative Mastermind-like 1
DR3	Death receptor 3
DSS	Dextran sulfate sodium
DTT	Dithiothreitol
EBF1	Early B cell factor 1
ECM	Extracellular matrix
E. coli	*Escherichia coli*
ED	Embryonic day
EDTA	Ethylenediaminetetraacetic acid
EMA	European Medicines Agency
Eomes	Eomesodermin
ER	Endoplasmic reticulum
ERRFI1	ERB receptor feedback inhibitor 1
FACS	Fluorescence-activated cell sorting
FCGR	Fc gamma receptor
FCS	Foetal calf serum
FITC	Fluorescein isothiocyanide
Flt3	Fms-related tyrosine kinase
Fm	Fatemap
Foxp3	Forkhead box P3
F. prausnitzii	*Faecalibacterium prausnitzii*
FRC	Fibroblastic reticular cell
Fut	Fucosyltransferase
GATA3	GATA-binding protein 3
γ_c	Gamma chain
G-CSF	Granulocyte colony-stimulating factor
GFP	Green fluorescent protein
Gln	Glutamine

GM-CSF	Granulocyte-macrophage colony-stimulating factor
GVHD	Graft-versus-host disease
GWAS	Genome-wide association studies
HBSS	Hank's balanced salt solution
H. hepaticus	*Helicobacter hepaticus*
HLA	Human leukocyte antigen
HNF4A	Hepatocyte nuclear factor 4 alpha
HRP	Horseradish peroxidase
HSC	Haematopoietic stem cell
IBD	Inflammatory bowel disease
ICAM	Intercellular adhesion molecule
ICOS	Inducible T-cell co-stimulator
ICOSLG	ICOS ligand
ID	Inhibitor of DNA binding
IEC	Intestinal epithelial cell
IFN	Interferon
IL	Interleukin
IL2rg	IL-2 receptor gamma chain
ILC	Innate lymphoid cell
ILC2P	ILC2 progenitor
Ig	Immunoglobulin
ILF	Isolated lymphoid follicle
iNK	Immature NK
iNKT	Invariant NKT
IRGM	Immunity-related GTPase family, M
iSC	Intestinal stromal cell
ITLN1	Intelectin 1 (galactofuranose binding)
JAK	Janus kinase
L	Ligand
LB	Luria broth
LCMV	Lymphocytic choreomeningitis virus
Lin	Lineage
LN	Lymph node
LP	Lamina propria

LPMC	Lamina propria mononuclear cell
LPS	Lipopolysaccharide
LRRK2	Leucine-rich repeat kinase 2
LT	Lymphotoxin
LTi	Lymphoid tissue-inducer
MACS	Magnetic-activated cell sorting
MAdCAM	Mucosal addressin cell adhesion molecule
MAIT	Mucosal-associated invariant T
M-CSF	Macrophage colony-stimulating factor
MDM	Monocyte-derived macrophage
MFI	Mean fluorescence intensity
MHC	Major histocompatibility complex
MLN	Mesenteric lymph node
MMPs	Matrix metalloproteinases
MOI	Multiplicity of infection
Mono	Monocyte
MΦ	Macrophage
mRNA	Messenger RNA
MSC	Mesenchymal stromal cell
MUC19	Mucin 19
N. brasiliensis	*Nippostrongylus brasiliensis*
NCR	Natural cytotoxicity receptor
NDM	Nuffield Department of Medicine
NFIL3	Nuclear factor, IL-3 regulated
NFκB	Nuclear factor kappa B
NHS	National Health Service
NICD	Notch intracellular domain
NK	Natural killer
NKR	Natural killer cell receptor
NOD	Nucleotide-binding oligomerization domain-containing protein 1
OD	Optical density
ORB	Oxford Radcliffe Biobank
ORMDL3	Orosomucoid-like 3
OVA	Ovalbumin

PBMC	Peripheral blood mononuclear cell
PBS	Phosphate buffered saline
PD-L1	Programmed death-ligand 1
PGD2	Prostaglandin D2
PHA	Phytohaemagglutinin
PLZF	Promyelocytic leukemia zinc finger
PMA	Phorbol 12-myristate 13-acetate
PP	Peyer's patch
PRR	Pattern recognition receptor
PTGER4	Protaglandin E receptor 4
qRT-PCR	Quantitative real-time polymerase chain reaction
R	Receptor
RA	Retinoic acid
RAG	Recombination activating gene
RANK	Receptor activator of nuclear factor kappa-B
RANKL	RANK ligand
Reg	Regenerating
REL	Reticuloendotheliosis oncogene cellular homolog
RELM	Resistin-like molecule
RNA	Ribonucleic acid
ROR	Retinoic acid receptor-related orphan receptor
RT	Room temperature
Rxrg	Retinoic X receptor gamma
Sca-1	Stem cell antigen-1
SCID	Severe combined immunodeficiency
SEB	Staphylococcal enterotoxin B
SEM	Standard error of mean
SFB	Segmented filamentous bacteria
SI	Small intestine
siRNA	Small interfering RNA
SLC11A1	Solute carrier family 11A1
SLO	Secondary lymphoid organ
SM	*Salmonella*
SMAD	Mothers against decapentaplegic homolog 7

SNP	Single nucleotide polymorphism
STAT	Signal transducer and activator of transcription
S. typhimurium	*Salmonella typhimurium*
T-bet	T-cell-specific T-box transcription factor
TCF1	T cell factor 1
TCR	T cell receptor
TGF-β	Transforming growth factor-β
T. gondii	*Toxoplasma gondii*
TGU	Translational Gastroenterology Unit
T_H	T helper
TL1A	TNF-like ligand 1A
TLO	Tertiary lymphoid organ
TLR	Toll-like receptor
TNFα	Tumour necrosis factor
TNFSF	TNF superfamily
TOX	Thymocyte selection–associated high-mobility group box protein
TRAIL	TNF-related apoptosis-inducing ligand
T_{Reg}	Regulatory T cell
TRUC	$Tbx21^{-/-}Rag^{-/-}$
TSLP	Thymic stromal lymphopoietin
TYK2	Tyrosine kinase 2
UC	Ulcerative colitis
VAT	Visceral adipose tissue
VCAM	Vascular cell adhesion molecule
XBP1	X-box binding protein 1

Contents

Chapter 1: Introduction

With a surface area of approximately 100m^2 the intestinal mucosa represents the largest mucosal interface of mammalian host organisms with the external environment. A single layer of columnar intestinal epithelial cells (IECs) separates the sterile host environment from the luminal contents of the gastrointestinal tract, which include food, invading pathogenic viruses, bacteria, fungi and parasites and a vast community of symbiotic commensal microbes (1). An estimated 10^{14} commensal bacteria, comprising over 30 genera and more than 500 species, are thought to colonize the intestinal mucosa, beginning at birth. In exchange for a nutrient-rich environment, these bacteria aid the host organism in the breakdown of food, supply essential nutrients and vitamins to the host, and provide colonization resistance to invading pathogenic organisms (2). In addition to commensal bacteria, the gut also harbours communities of commensal viruses and fungi (3,4).

The intestinal mucosal immune system faces the challenging task of mounting effective host-protective immune responses to invading pathogens and commensal species that breach the intestinal epithelial barrier, while at the same time maintaining a state of tolerance to innocuous non-self antigens such as dietary antigens and the luminal commensal microbiota (2). A breakdown of intestinal homeostasis in response to food or commensal antigens leads to intestinal inflammation, as exemplified by coeliac disease and inflammatory bowel disease (IBD), respectively. Intestinal homeostasis is achieved through a complex network of innate and adaptive immune cells and their interactions with the intestinal epithelium (see Figure 1.1).

Innate lymphoid cells (ILCs) have emerged as important players in intestinal immune homeostasis. In this general introduction, we will describe what is known about the transcriptional pathways and cytokine requirements that underlie the development of ILCs from common lymphoid progenitors (CLPs) and will discuss the developmental relationships between the different ILC populations identified to date. We will outline the functions of ILCs in intestinal immune homeostasis, including their role in the induction of organised lymphoid tissues during foetal development; their contribution to protective immunity to infections; their role in the maintenance of a tolerogenic host-commensal relationship; their involvement in tissue remodelling and repair processes; and their role in the maintenance of metabolic homeostasis. We will then discuss inflammatory bowel disease (IBD) as a breakdown of immune homeostasis and outline what is known, mostly from mouse models of colitis, about the contribution of ILCs to pathogenic immune responses during chronic intestinal inflammation.

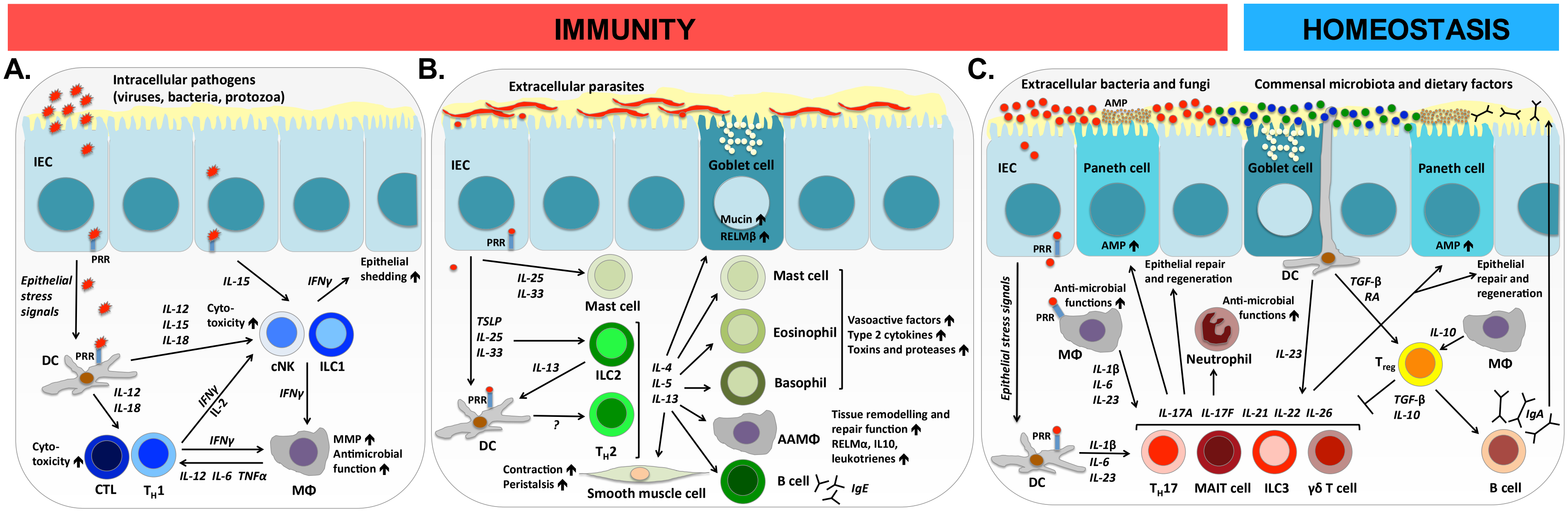

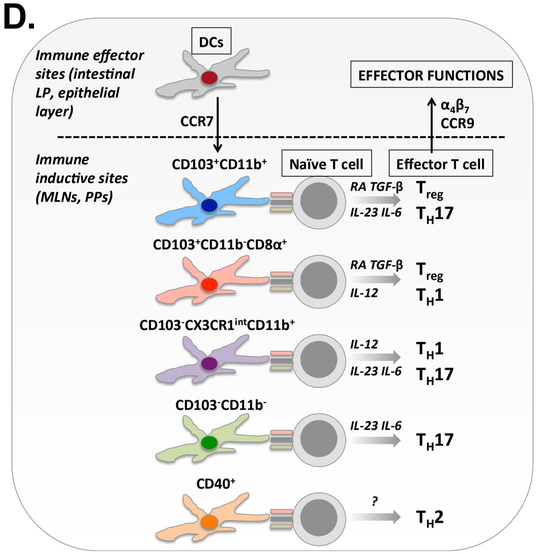

Figure 1.1: Mechanisms of intestinal immunity and homeostasis. A-C. Three major types of cell-mediated immune effector functions contribute to intestinal immunity and homeostasis. Type 1 immune responses characterised by IL-12 and IL-18-driven production of IFNγ and cytotoxicity by adaptive (T_H1, CTL) and innate (cNK, ILC1) immune cells provide host defense to infections with intracellular pathogens (viruses, bacteria, protozoa) (A). Type 2 immune responses characterised by IL-25, IL-33 and TSLP-dependent poduction of IL-4, IL-5 and IL-13 by adaptive (T_H2) and innate (ILC2, mast cells, eosinophils, basophils) immune cells are required for defense against infection with extracellular parasites (B). Type 17 immune responses characterise by IL-1β, IL-6 and IL-23-dependent production of IL-17A, IL-17F, IL-21, IL-22 and IL-26 by adaptive (T_H17), innate (ILC3) and innate-like (MAIT, γδ T) immune cells provide immunity to infection with extracellular bacteria and fungi and play a crucial role in the maintenance of host-commensal homeostasis in the gut (C). **D.** Distinct populations of mucosal DCs can be identified on the basis of expression of cell surface markers CD103, CD11b, CX3CR1 and CD8α. Following antigen uptake, these DC populations migrate to the draining MLN in a CCR7-dependent manner. Here, they present antigen to naïve $CD4^+$ T cells. Priming by distinct DC populations induces distinct T helper subsets, e.g. $CD103^+$ DCs induce T_{Reg} or T_H17 cells, whereas $CX3CR1^{int}$ DCs induce T_H1 or T_H17 cells. Priming by intestinal mucosal DCs also induces gut-homing receptors such as $\alpha_4\beta_7$ or CCR9 on $CD4^+$ T cells, and following their differentiation into effector cells, they migrate to the intestinal lamina propria.

1.1 Innate lymphoid cells

1.1.1 Overview

ILCs are a heterogeneous family of immune cells that share morphological characteristics of lymphoid cells in the absence of somatically rearranged antigen receptors. ILCs have been implicated in a wide range of homeostatic and inflammatory immune processes in both mice and humans (5). ILCs can be grouped on the basis of shared functional and developmental characteristics (Figures 1.2 and 1.3). These different ILC subgroups closely parallel the distinct $CD4^+$ T helper subsets in terms of their cytokine production and transcription factor expression, suggesting that ILCs may be evolutionarily ancient predecessors to adaptive T helper cells (6,7).

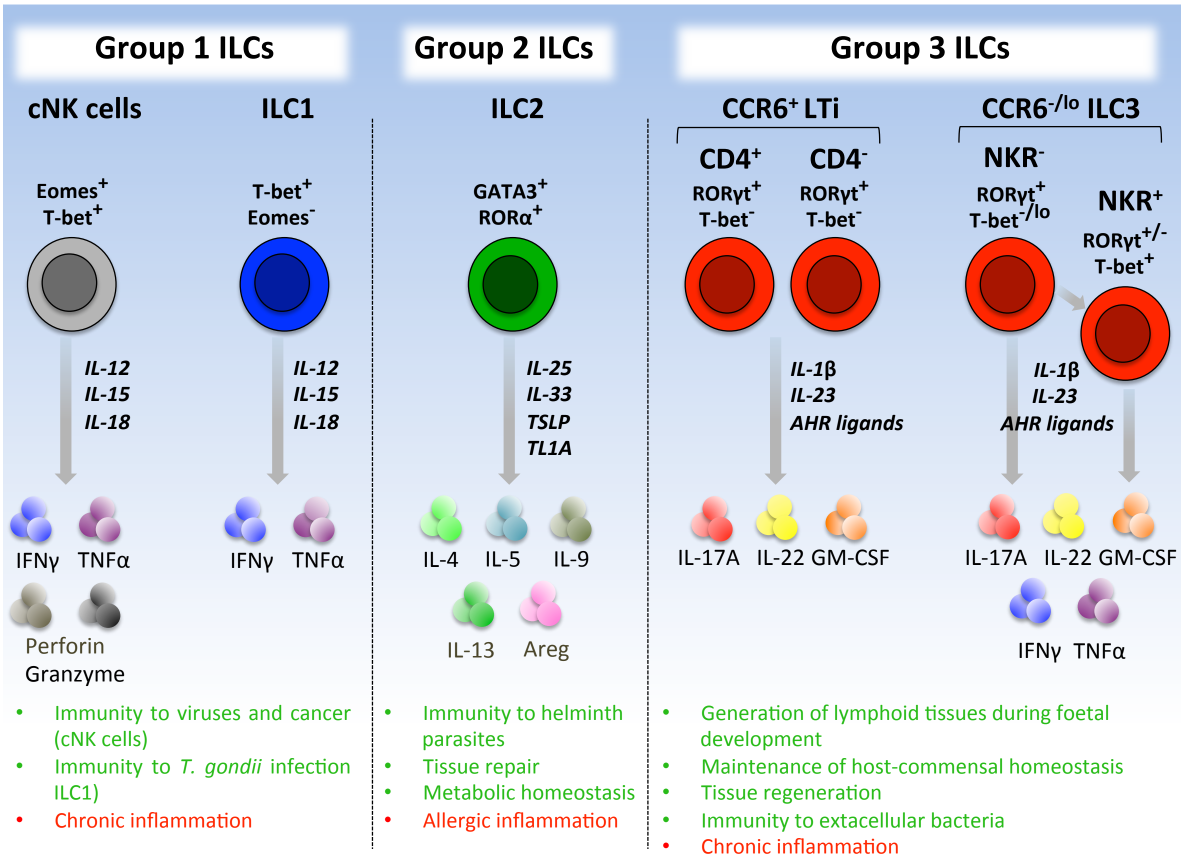

Figure 1.2: Overview of ILC populations and their functions. ILCs are involved in a range of host protective and homeostatic immune functions, but are also implicated in pathogenic inflammatory processes. The distinct ILC populations can be grouped according to shared functions. Group 1 ILCs (cNK cells and ILC1) are characterised by expression of Type 1 cytokines (IFNg) in response to stimulation with IL-12, IL-15 and IL-18. In contrast to cNK cells, ILC1 have not been shown to possess cytotoxic potential. Group 2 ILCs (ILC2) are defined through expression of Type 2 cytokines (IL-4, IL-5, IL-9, IL-13, Areg) in response to stimulation with IL-25, IL-33 and TSLP. Group 3 ILCs comprise a heterogeneous subset of ILCs defined through production of Type 17 cytokines (IL-17A, IL-22, GM-CSF) in response to stimulation with IL-1β and IL-23. CCR6$^+$ LTi cells are crucial for the induction of organised lymphoid tissues during foetal development. In adult organisms, CCR6$^-$ ILC3 can be divided on the basis of NKR expression.

Group 3 ILCs are characterised by a developmental dependence on the transcription factor retinoic acid receptor-related orphan receptor (ROR)γt. The prototypical Group 3 ILCs are foetal lymphoid tissue-inducer cells (LTi cells) which, via interactions with stromal cells, are responsible for the induction of secondary lymphoid tissues during embryonic development. Intestinal Group 3 ILCs also include ILC3 that expand postnatally in response to microbiota-derived signals. Phenotypically, foetal LTi cells and adult ILC3 populations can be distinguished on the basis of C-C chemokine receptor type 6 (CCR6) expression, with LTi cells being of CCR6^{hi} phenotype and adult ILC3 populations of CCR6$^{low/-}$ phenotype (8,9). These CCR6^{-} ILC3 can be further subdivided on the basis of natural killer (NK) cell receptor (NKR), RORγt and T-cell-specific T-box transcription factor (T-bet) expression into NKp46^{-}RORγt^{+}T-bet$^{-/low}$ LTi-like ILC3 and NKp46^{+}RORγt^{+}T-bet^{+} ILC3 enriched for interleukin (IL)-17A and IL-22 expression, and NKp46^{+}RORγt^{-}T-bet^{+} 'ex-ILC3' that have downregulated their expression of RORγt/IL-22 and upregulated their expression of T-bet/Interferon (IFN)γ (6,7). Adult ILC3 populations play important roles in the maintenance of intestinal homeostasis in response to the commensal microbiota, in protective immunity to infections and in tissue repair processes, and can contribute to chronic inflammatory processes through their production of pro-inflammatory cytokines.

Group 2 ILCs (ILC2) are IL-25 and IL-33-responsive ILCs that developmentally depend on the transcription factors RORα and GATA-binding protein 3 (GATA3) and produce the Type 2-cytokines IL-4, IL-5 and IL-13, as well as IL-9 and amphiregulin (Areg) (6,10-17). Under homeostatic conditions, ILC2 can be found widely dispersed in the peripheral tissues of mice, with highest numbers of ILC2 observed in mesenteric lymph nodes (MLNs), spleen, liver and fewer ILC2 observed in lungs and peritoneum (12). ILC2 have been implicated in immunity to helminth parasites, allergic immune responses and metabolic homeostasis.

Group 1 ILCs (conventional natural killer (cNK) cells, ILC1) are defined by expression of the transcription factor T-bet and have been shown to produce IFNγ and tumour necrosis factor (TNF)α in response to stimulation with IL-12, IL-15 or IL-18 (18). ILC1 are involved in protective immunity to protozoan pathogens and can contribute to chronic inflammatory processes in the intestine.

In contrast to cNK cells, Group 3 ILCs, ILC2 and ILC1 lack expression of granzymes and perforin and do not have direct cytotoxic potential. Instead, they are thought to exert their effector functions through the expression of inflammatory cytokines and cell surface molecules. In reference to the classification of T cell subsets, non-cytotoxic ILCs are grouped together as 'helper ILCs', while cNK cells are categorized as 'cytotoxic ILCs'. All helper ILCs are characterised by expression of the IL-7Rα chain (CD127), although not all helper ILCs are developmentally dependent on IL-7 as discussed below. cNK cells do not express CD127 (7).

1.1.2 Early transcriptional control of ILC development

All ILCs develop from CLPs in the foetal liver and adult bone marrow (19-22) (Figure 1.3).

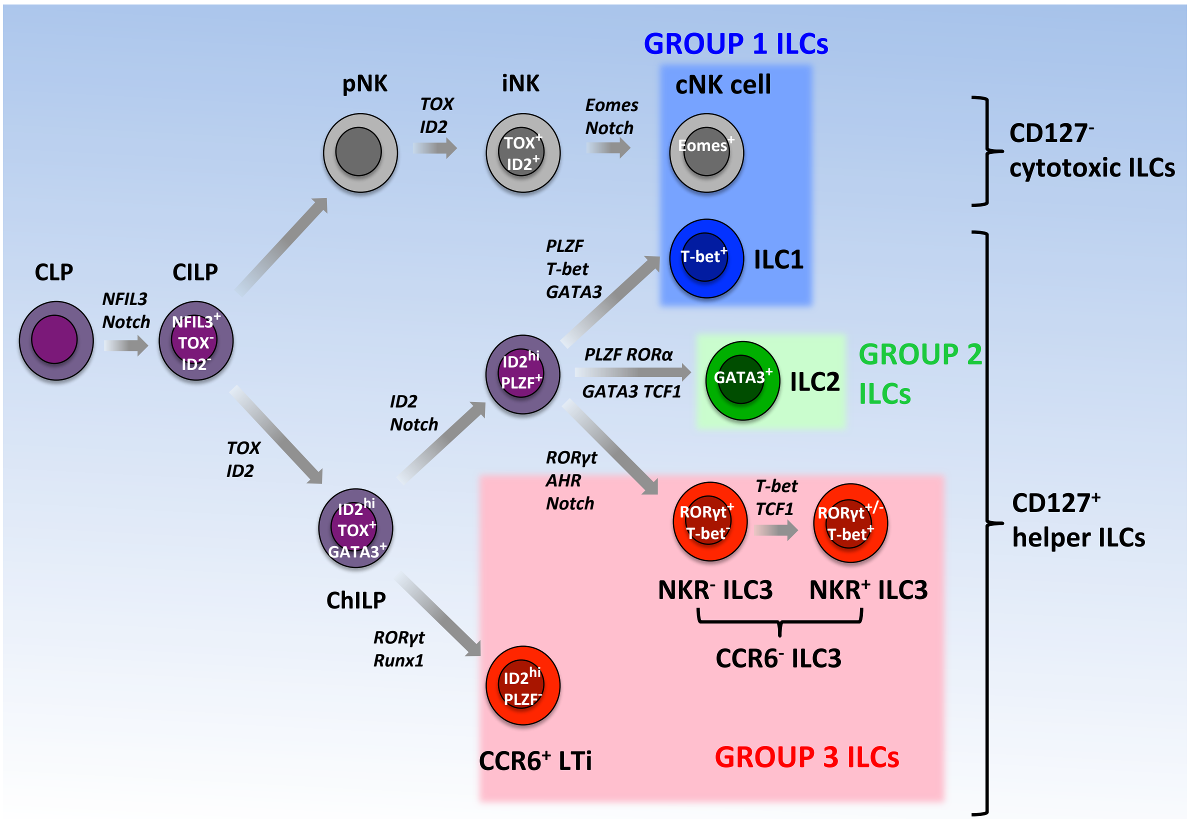

Figure 1.3: Transcriptional regulation of ILC developmental pathways. Like all lymphocytes, ILCs develop from the common lymphoid progenitor (CLP). A common ILC precursor (CILP) shared by cNK and helper ILCs develops from the CLP in an NFIL3 and Notch-dependent manner. cNK and helper ILC lineages diverge at this point, with ID2 and TOX and driving development of a common helper ILC precursor (ChILP) that is shared by ILC1, ILC2, ILC3 and LTi cells. At the ChILP stage, PLZF$^-$ cells differentiate into CCR6$^+$ LTi cells in a manner dependent on RORγt and Runx1, while ID2 and Notch-dependent PLZF$^+$ cells comprise a precursor population from which ILC1, ILC2 and CCR6$^-$ ILC3 are derived. From this precursor, ILC1 differentiation is driven by T-bet, PLZF and GATA3; ILC2 differentiation by GATA3, RORα, TCF1 and PLZF; and ILC3 differentiation by RORγt, AHR, Notch and, in the case of further differentiation into NKR$^+$ ILC3, by T-bet and TCF1.

Specification of ILCs from CLPs

In vivo evidence points to a role for Notch in the specification of α4β7⁺ ILC progenitors downstream of the CLP (23). These progenitors have lost B cell potential, but have retained T cell potential and subsequent downregulation of Notch signalling is thought to be required to prevent their differentiation into T cells and allow commitment to the ILC lineage (23,24). Notch signals have also been shown to be important for differentiation of ILC1, ILC2 and ILC3 subsets *in vitro*. *In vitro* culture of CLPs on OP9-DL1 or OP9-DL4 stromal cells that overexpress Notch ligands DL1 and DL4, respectively, but not on OP9 stromal cells leads to generation of all ILC1, ILC2 and ILC3 subsets (18,20,21,25). However, different requirements for Notch signalling may exist in the development of adult ILC3 and foetal liver LTi cells (20). Adding to the complexity of Notch signalling during ILC development, Notch-dependent signals were also shown to be required at later stages in the differentiation of ILC2 and NKp46⁺ ILC3 subsets (20,26-28).

Nuclear factor, IL-3 regulated (NFIL3) is a transcription factor of the basic leucine zipper family that plays a critical role in the development of the various helper ILC subsets (18,29-32) as well as of cNK cells (32-35). This widespread requirement for NFIL3 in the development of all ILCs suggests that it acts early during ILC development, potentially at the level of a progenitor population shared by all ILC populations. Indeed, *Nfil3*$^{-/-}$ CLPs adoptively transferred into *Rag*$^{-/-}$*Il2rg*$^{-/-}$ alymphoid mice fail to generate ILC1, ILC2, ILC3 and cNK cells in the small intestine and liver. In foetal liver and adult bone marrow, a Fms-related tyrosine kinase (Flt3)⁻ α4β7⁺CXCR6⁺ progenitor population has been identified downstream of the CLP, which, following adoptive transfer into *Rag*$^{-/-}$*Il2rg*$^{-/-}$ mice or *in vitro* culture on OP9-DL4 cells that overexpress the Notch ligand Delta 4, can give rise to all helper ILC subsets and cNK cells but has no B or T cell potential (20,36). This common ILC progenitor (CILP) is lost in *Nfil3*$^{-/-}$ mice, suggesting that NFIL3 acts early during ILC specification and is a critical factor in promoting development of CILPs from CLPs (7,36).

Similarly to NFIL3, the transcription factor thymocyte selection–associated high-mobility group box protein (TOX) is critical for the development of all ILC lineages. *Tox*$^{-/-}$ mice harbour a severe defect in lymphoid organogenesis, resulting from a failure to generate foetal and adult LTi cells and furthermore lack adult ILC3, ILC2 and ILC1 subsets as well as mature cNK cells (37,38).

Inhibitor of DNA binding (ID) proteins are transcriptional regulators that bind to basic helix-loop-helix (bHLH) transcription factors of the E protein family, preventing them from binding to cognate DNA sites and thereby sequestering their transcriptional activity (39). E proteins have important roles in the regulation of T and B cell development and function and overexpression of inhibitory ID2 or ID3 proteins abrogates T and B cell development (5,40). Furthermore, overexpression of the ID2-repressor early B cell factor 1 (EBF1) in pro-B cells leads to alternative differentiation into ILC2 and ILC3 (41). In contrast, mice deficient in ID2 lack mature helper ILC and cNK cells (13,42-44). These findings suggest that ID2 plays a critical role in the development of helper ILC and cNK lineages and may act by inhibiting the commitment of CLPs to T and B cell lineages.

Specification of a progenitor common to all helper ILC populations

However, in contrast to NFIL3, which acts to induce a haematopoietic precursor (the CILP) that is shared by both cNK cells and helper ILCs, TOX and ID2 are required at different time-points in cNK and helper ILC development. While mature cNK cells can no longer be detected in bone marrow, blood or spleen of *Tox*$^{-/-}$ or *Id2*$^{-/-}$ mice, committed cNK progenitors or immature NK cells are present in normal numbers, suggesting that these transcription factors play a role in the later stages of cNK development (37,38,42).

Downstream of the CILP, a lineage (Lin)$^{-}$CD117^{+}IL-7R$\alpha^{+}\alpha 4\beta 7^{+}$Flt3^{-} precursor population capable of differentiating into all helper ILC subsets but not into cNK cells has been identified in murine adult bone marrow and foetal liver (18). This common helper ILC progenitor (ChILP) population highly expresses TOX and is severely reduced in *Tox*$^{-/-}$ mice (37,38). Whole transcriptome analysis of ChILP from *Tox*$^{-/-}$ compared to wild-type mice furthermore revealed that in the absence of TOX there is reduced expression of genes known to be involved in ILC specification, including *Rorc*, *Tbx21*, *Gata3*, *Rora*, *Zbtb16*, *Rxrg*, *Bcl2* as well as Notch target genes such *Tcf7* and *Hes1* (38). Bone marrow-resident ChILP also express high levels of ID2 and give rise to ILC1, ILC2, ILC3 and LTi cells, but not cNK cells, following adoptive transfer into *Rag*$^{-/-}$*Il2rg*$^{-/-}$ alymphoid mice (18,36,37). Both ID2 and TOX expression in ChILPs may be subject to direct regulation by NFIL3 (21,32,36).

cNK cells and helper ILCs constitute developmentally distinct lineages

The developmental relationship between cNK cells and phenotypically related NKR-expressing ILC1 and ILC3 populations has been subject to intense debate. However, the above-described data provide clear evidence that cNK cells and helper ILC populations follow distinct developmental pathways downstream of the shared NFIL3-dependent CILP progenitor stage. ID2$^+$TOX$^+$ ChILP are specified progenitors of helper ILCs but have lost the potential to differentiate into cNK cells (18,36,37). These observations are in agreement with reports that have suggested distinct developmental pathways for cNK cells and phenotypically related ILC1 and ILC3 populations on the basis of differential requirements for the transcription factors T-bet, Eomesodermin (Eomes) and RORγt (18,45-47). Furthermore, GATA3 has been shown to play a critical role in the development of all helper ILCs, whereas cNK cells develop independently of GATA3 (25,48-51). In line with these findings, whole transcriptome analysis of small intestinal and liver ILC1, ILC3 and cNK cells indicates that ILC1 and ILC3 are more closely related to each other than to cNK cells in terms of their gene expression profiles (18).

Heterogeneous expression of PLZF determines the fate of helper ILCs downstream of the ChILP

Fate-mapping studies have revealed transient expression of promyelocytic leukemia zing finger (PLZF) during the development of CCR6$^-$ ILC1, ILC2 and ILC3 populations (52). In contrast, CCR6$^+$ LTi cells do not express PLZF and show no history of PLZF expression. PLZF is a member of the zinc finger protein family of transcription factors that has been shown to control the differentiation invariant NKT (iNKT) cells (53-55). Examination of PLZF expression in precursor populations downstream of the CLP in the foetal liver and adult bone marrow of mice indicates that PLZF expression is upregulated at the ChILP stage, potentially under control of Notch-dependent signals. Approximately 30% of ChILPs express high levels of PLZF (18,52). Following adoptive transfer into *Rag*$^{-/-}$*Il2rg*$^{-/-}$ alymphoid mice, these PLZF^{hi}

ChILPs have the potential to differentiate into ILC1, ILC2 and ILC3 but not into LTi cells (52).

These findings suggest that LTi cells branch off a developmental pathway shared by the other helper ILCs at the stage of the ChILP. PLZF expression at the ChILP stage marks a precursor population with the potential to differentiate into CCR6$^-$ ILC1, ILC2 and ILC3 subsets, but not into CCR6$^+$ LTi cells. In reverse, following *in vitro* culture on OP9 stromal cells or adoptive transfer into irradiated newborn mice, foetal LTi cells cannot differentiate into other Group 3 ILC populations (8).

In a recent report Xu et al. linked NFIL3, ID2 and PLZF in a functional pathway and showed that ID2 overexpression in *Nfil3*$^{-/-}$ CLPs can rescue the inherent defect in ILC development via induction of PLZF expression in ChILPs. This suggests a linear pathway of transcription factor activity in the specification of the helper ILC subsets from CLPs, in which NFIL3 acts to induce ID2 which, perhaps in conjunction with Notch signals, in turn promotes PLZF expression by ChILPs (32). PLZF$^+$ ChILPs then give rise to ILC1, ILC2 and ILC3 populations, while PLZF$^-$ ChILPs differentiate into CCR6$^+$ LTi cells. However, while deficiency in *Zbtb16* (the gene encoding PLZF) results in impaired development of ILC2 and ILC1, ILC3 develop normally in these mice. This suggests that other factors may compensate for loss of PLZF function during ILC3 development (52).

1.1.3 Transcriptional control of helper ILC differentiation

Immature ILC1, ILC2 and ILC3 precursors with highly restricted differentiation potential have been identified in the murine bone marrow. Following *in vitro* culture or adoptive transfer into $Rag^{-/-}Il2rg^{-/-}$ alymphoid hosts, these precursors give rise only to mature ILC1, ILC2 and ILC3 populations, respectively, but not to other ILC subsets (18,20,23,25). ILC subset-specific precursors express particular master transcription factors (T-bet in pre-ILC1, RORα/GATA3 in pre-ILC2 and RORγt in pre-ILC3) that, as outlined below, drive their differentiation into the mature ILC populations and attribute them with the specific functional characteristics associated with each ILC subset.

Group 3 ILCs

Group 3 ILCs, including $CCR6^{+}CD4^{+/-}$ foetal LTi cells and $CCR6^{-}NKp46^{+/-}$ ILC3 populations, are defined by a developmental dependence on the transcription factor RORγt. An essential role for RORγt in the development of foetal LTi cells was first reported by Eberl et al., who showed that RORγt-deficient mice lack LTi cells, resulting in impaired formation of Peyer's patches (PPs) and lymph nodes (LNs) (56). Following upregulation of RORγt expression during development, fully differentiated foetal LTi cells stably maintain expression of this transcription factor (8).

Similarly to foetal LTi cells, adult $CCR6^{low/-}$ ILC3 are critically dependent on $ROR\gamma t^{+}$ for their development (9,57-59). However, graded expression of $ROR\gamma t^{+}$ in conjunction with T-bet expression plays a role in modulating ILC3 phenotype and function (9,47). Amongst $CCR6^{low/-}$ ILC3, a precursor-progeny relationship exists between NKR^{-} and NKR^{+} ILC3. Using RORγt reporter and fate-mapping mice, Vonarbourg et al. reported that adoptively transferred RORγt$^+$NKp46$^-$ ILC3 isolated from the small intestinal lamina propria can give rise to NKp46$^+$ ILC3, although a proportion of transferred cells stably maintained an NKp46$^-$ phenotype. Differentiation of NKp46$^-$ ILC3 into NKp46$^+$ ILC3 is associated with downregulation of RORγt expression and upregulation of T-bet expression (9,47). Thus, while RORγt$^+$NKp46$^-$ ILC3 and foetal LTi cells express little or no T-bet, RORγt$^+$NKp46$^+$ ILC3 highly express T-bet at levels equivalent to cNK cells (9,60,61).

Upregulation of T-bet expression is critically required for the differentiation of NKp46$^+$ ILC3. In *Tbx21*$^{-/-}$ mice NKp46$^+$ ILC3 are severely diminished, while normal numbers of NKp46$^-$ ILC3 and foetal LTi cells are present in the intestinal lamina propria (9,60,61). *In vitro* lentiviral transduction of the Notch intracellular domain (NICD) into *Tbx21*$^{-/-}$ NKp46$^-$ ILC3 can restore their ability to differentiate into NKp46$^+$ ILC3, indicating that Notch acts downstream of T-bet in the NKp46$^+$ ILC3 differentiation pathway (61). Chromatin immunoprecipitation (ChIP) analysis of T helper (T_H)1 cells and cNK cells has revealed T-bet binding sites in the Notch2 promoter and it is conceivable that a similar mechanism underlies T-bet-mediated regulation of Notch activity in NKp46$^+$ ILC3 (61). Downstream of Notch, TCF1 has been implicated in driving differentiation of and IL-22 production by intestinal NKp46$^+$ ILC3 (27,62).

Graded expression of RORγt and T-bet by CCR6$^{low/-}$ ILC3 is associated with functional plasticity. Both RORγt$^+$T-bet$^-$NKp46$^-$ and RORγt$^+$T-bet$^+$NKp46$^+$ ILC3 express IL-23R and respond to stimulation with IL-23 by producing IL-22. In contrast RORγt$^-$T-bet$^+$NKp46$^+$ 'ex-ILC3' downregulate IL-23R and instead upregulate IL-12Rβ2 expression. In response to stimulation with IL-12, these cells mainly produce IFNγ (47).

Environmental factors influence the development and plasticity of CCR6$^{low/-}$ ILC3. CCR6^{high} LTi cells can be found in the intestinal lamina propria from embryonic day (ED)12.5 and are the major intestinal Group 3 ILC population in the developing embryo (7,9,56,63). In contrast, CCR6$^{low/-}$ ILC3 are present only in small numbers during embryonic development, but expand rapidly in the first 4 weeks following birth (7,9). This postnatal expansion appears to be dependent on microbiota-derived signals, since adult CCR6$^{low/-}$ ILC3 populations are diminished in the intestinal lamina propria of germ-free mice (9,47,57,58). Foetal LTi cells develop and function normally in germ-free mice, indicating that they are a developmentally programmed population of cells that operates independently of microbiota-derived signals (8,56,57,64).

The postnatal expansion and maintenance of CCR6$^{low/-}$ ILC3 furthermore requires the transcription factor aryl hydrocarbon receptor (AHR). *Ahr*$^{-/-}$ mice have reduced numbers of CCR6$^{low/-}$ intestinal NKp46^{+} and NKp46^{-} ILC3 populations, indicating that the pool of adult ILC3 is subject to environmental regulation through dietary and/or microbial-derived AHR ligands (9,26,65-67). In contrast, CCR6^{high} LTi cells are present in normal numbers in *Ahr*$^{-/-}$ mice and appear to function normally in the induction of developmentally programmed lymphoid tissues such as PPs and LNs. Interestingly, however, inducible lymphoid tissues such as cryptopatches and small intestinal isolated lymphoid follicles (ILFs) are diminished in *Ahr*$^{-/-}$ mice (9,26,65,66). This suggests that perhaps foetal LTi cells are responsible for lymphoid tissue induction during embryonic development, while CCR6$^{low/-}$ ILC3 populations control formation of inducible lymphoid tissues in adult organisms. Alternatively, AHR may regulate inducer functionality in CCR6^{high} LTi cells during adult but not foetal lymphoid organogenesis (7).

Finally, the differentiation of NKp46$^-$ ILC3 into NKp46$^+$ ILC3 appears to be subject to regulation by environmental factors. The extent of RORγt downregulation during the differentiation of NKp46$^+$ ILC3 appears to be regulated by tissue microenvironmental factors. While the majority of transferred RORγt$^+$ ILC3 that homed to the small intestine continued to express RORγt$^+$, a significant proportion of cells that homed to the colon or spleen downregulated RORγt expression. Only approximately 20% of differentiated NKp46$^+$ ILC3 in the colon and spleen still expressed RORγt. The remaining cells had lost expression of RORγt and become NKp46$^+$RORγt$^-$T-bet$^+$ 'ex-ILC3' (47). Depletion of the commensal microflora by means of antibiotics treatment drastically reduced the proportion of RORγt$^+$NKp46$^+$ ILC3 in the intestinal lamina propria, indicating that microbial signals may play a role in the stabilization of RORγt expression in NKp46$^+$ ILC3, potentially via induction of IL-7 production by intestinal epithelial and stromal cells (47). However, the commensal microbiota has also been suggested to play a role in driving T-bet expression by NKp46$^-$ ILC3 in a Toll-like receptor (TLR)- and IL-23-dependent manner (9).

Taken together these findings show that the development of both CCR6$^+$ foetal LTi cells and CCR6$^{low/-}$ intestinal ILC3 populations is critically dependent on RORγt. The development and function of foetal LTi cells is developmentally programmed and occurs in the absence of microbiota-derived signals. In contrast, the post-natal expansion of CCR6$^{low/-}$ ILC3 is dependent on the intestinal commensal microflora and AHR, indicating a role for environmental regulation. Amongst CCR6$^{low/-}$ ILC3, NKp46$^-$ ILC3 can differentiate into NKp46$^+$ ILC3 under control of microbiota-derived signals. This differentiation is associated with downregulation of RORγt and upregulation of T-bet expression. Graded expression of these transcription factors results in functional plasticity within CCR6$^{low/-}$ ILC3.

ILC2

The transcription factor B-cell CLL/lymphoma 11b (Bcl11b), a member of the zinc finger family with reported roles in T cell specification and maintenance, has been reported to be involved in the specification of a committed ILC2 progenitor (ILC2P) from the ChILP. Approximately 30% of ChILPs in bone marrow were found to express Bcl11b (68). *In vivo* Bcl11b$^+$ ChILPs adoptively transferred into *Rag*$^{-/-}$*Il2rg*$^{-/-}$ alymphoid mice exclusively generated ILC2 while Bcl11b$^-$ ChILPs gave rise to LTi cells and NKp46$^{+/-}$ ILC3 (69). In line with these findings, tamoxifen-induced deletion of Bcl11b expression in *Bcl11b*$^{fl/fl}$*Rosa26*$^{CreERT2/CreERT2}$ transgenic mice led to a reduction in bone marrow-resident ILC2P (69). While Bcl11b is also expressed by mature peripheral ILC2, normal numbers of ILC2 were detected in peripheral tissues 2-3 weeks after tamoxifen administration. Thus, Bcl11b appears to be required for the development of committed ILC2P at the ChILP stage, but not for the maintenance or function of mature tissue-resident ILC2 (68,69).

Ex vivo ILC2 highly express *Rora* transcripts (21,70,71). RORα is a transcription factor of the ROR family and has previously been reported to be involved in the differentiation of T_H17 cells (72). The 'staggerer' mutation is a spontaneous deletion within the *Rora* gene, leading to truncation of the RORα ligand-binding homology domain and loss of transactivation capacity. This functional defect is associated with a ‘staggering’ phenotype in mice, due to impaired development of Purkinje cells and severe cerebellar ataxia (73). Absolute numbers of ILC2 are reduced in the MLN, small and large intestine and lungs of *Rora*$^{sg/sg}$ mice compared to wild-type mice. This defect appears to be specific for ILC2, since normal numbers of CD4^{+} and CD8^{+} T cells, ILC3, NKT cells, cNK cells and B cells are present in spleen and MLN of *Rora*$^{sg/sg}$ mice (21,71). The deficiency in peripheral ILC2 in *Rora*$^{sg/sg}$ mice is likely secondary to loss of committed ILC2P in the bone marrow (25,71). In line with these findings, wild-type but not *Rora*$^{sg/sg}$ bone marrow cells efficiently generate ILC2 in mixed bone marrow chimeras (21,71). Unlike their wild-type counterparts, remnant ILC2 in *Rora*$^{sg/sg}$ mice are functionally deficient and fail to expand and produce Type 2 cytokines in response to intestinal helminth infection, resulting in impaired anti-helminth immunity and increased worm burden at day 6 post-infection (21). Thus, these data suggest that RORα regulates the differentiation of ILC2 from a specified bone marrow progenitor and in addition may play a role in the maintenance and function of mature peripheral ILC2.

In addition to RORα, peripheral ILC2 and bone marrow ILC2P highly express the transcription factor GATA3, a known regulator of T$_{H}$2 differentiation and function (12,13,22,25,74). Tamoxifen-induced deletion of GATA3 in all ID2-expressing cells (i.e. ILCs) in transgenic mice *in vivo*, has been reported to result in selective loss of mature peripheral ILC2 as well as a reduced population of bone marrow-resident ILC2P (25). In turn, adoptively transferred wild-type but not *Gata3*$^{-/-}$ foetal liver-derived haematopoietic stem cells (HSCs) can reconstitute a peripheral ILC2 pool in *Rag*$^{-/-}$*Il2rg*$^{-/-}$ alymphoid recipient mice (74). Thus, GATA3 is a critical regulator of ILC2 differentiation. Furthermore, GATA3 has been shown to functionally regulate ILC2 in a dose-dependent manner. ILC2 from *Gata3*$^{lacZ/+}$ mice with only one functional GATA3 allele produce lower amounts of IL-5 and IL-13 compared to wild-type mice. Conversely, overexpression of GATA3 in *CD2-Gata3tg* mice results in increased Type 2 cytokine production by ILC2 (74). Collectively, these data indicate that GATA3 is required for the differentiation of ILC2P into mature ILC2 and in addition plays a critical role in the maintenance and function of mature peripheral ILC2. ChIP analysis of double-negative (DN) thymocytes has revealed GATA3 binding to the RORα promoter (75). It is therefore conceivable that GATA3 may act upstream of RORα during ILC2 differentiation (74).

Finally, a role for the transcription factor T cell factor 1 (TCF1) (encoded by the *Tcf7* gene) has been identified in the differentiation of ILC2 (27,28). TCF1 is highly expressed by tissue-resident ILC2. *Tcf7*$^{-/-}$ mice have severely reduced numbers of ILC2 in lungs and bone marrow, as well as a near complete loss of ILC2P in the bone marrow. Moreover, the remnant ILC2 found in the lungs of *Tcf7*$^{-/-}$ mice are functionally deficient and produce reduced amounts of IL-5 and IL-13 compared to wild-type cells following intranasal challenge with papain. *Tcf7*$^{-/-}$ ILC2 express lower levels of GATA3, suggesting that TCF1 may be involved in the regulation of GATA3 expression. Indeed, TCF1 overexpression in multipotent Lin^{-}Sca-1^{+}CD117^{+} bone marrow progenitors induces expression of GATA3 as well as additional markers implicated in ILC2 development, including CD127. Furthermore, TCF1 overexpression can rescue ILC2 development in transgenic mice retrovirally transduced with the pan-Notch inhibitor dominant-negative Mastermind-like 1 (dnMAML), indicating that Notch signalling acts upstream of TCF1 in the ILC2 differentiation pathway (28).

ILC1

Murine ILC1 were first identified as an NKp46^{+}NK1.1^{hi} ILC subset in the intestinal lamina propria enriched for expression of T-bet that produces IFNγ and TNFα in response to stimulation with IL-12 (9). Using *Eomes*$^{gfp/+}$ RORγt-fatemap (fm) double-reporter mice, Klose et al. showed that these ILC1 are developmentally distinct from other phenotypically and functionally similar ILC populations (18). In contrast to cNK cells, ILC1 do not express and are developmentally independent of Eomes. Unlike NKp46^{+}RORγt^{-} 'ex-ILC3' that have downregulated RORγt expression, ILC1 show no current or previous expression of RORγt. Fluorescence-activated cell sorting (FACS)- purified Eomes^{-}RORγt^{fm-} ILC1 adoptively transferred into *Rag*$^{-/-}$*Il2rg*$^{-/-}$ alymphoid mice maintain their surface phenotypes and do not upregulate Eomes or RORγt expression, indicating that they indeed represent a stable lineage (18).

Compared to ILC2 and ILC3 populations, much less is known regarding the transcriptional control of ILC1 differentiation. ILC1 appear to be critically dependent on T-bet. *Tbx21*$^{-/-}$ mice are characterised by a loss of intestinal ILC1, amongst other cells. This requirement for T-bet is haematopoietic cell-intrinsic as only *Tbx21*$^{+/+}$ but not *Tbx21*$^{-/-}$ HSCs were shown to regenerate the intestinal ILC1 population in mixed bone marrow chimeras (18).

As mentioned above, early expression of GATA3, potentially at the ChILP stage, is required for the development of all CD127-expressing helper ILC populations (50,51). However, transgenic mice in which GATA3 is inducibly deleted in all *Ncr1*-expressing cells show a selective deficiency in intestinal ILC1, while normal numbers of NKp46^{+} ILC3 and cNK cells are observed. This points to an additional role for GATA3 in the later stages of ILC1 differentiation or maintenance (18).

A TRAIL$^+$NKp46$^+$NK1.1^{hi}T-bet$^+$ population of cells has been identified in the foetal and adult liver of mice that produce IFNγ in response to stimulation with IL-12 (45,48,76,77). In contrast to TRAIL$^-$ cNK cells, these cells lack expression of CD49b and Eomes, but express high levels of CD127. Similar to ILC1 in the intestinal lamina propria, Eomes$^-$NKp46$^+$ liver cells are developmentally dependent on T-bet and GATA3 (48,77). However, unlike intestinal ILC1, Eomes$^-$NKp46$^+$ liver cells have cytotoxic potential and can efficiently lyse Yac-1 cells following overnight stimulation with IL-15 (77). Moreover, contradictory results have been published regarding the capacity of Eomes$^-$NKp46$^+$ liver cells to differentiate into Eomes$^+$NKp46$^+$ cNK cells following adoptive transfer into *Rag*$^{-/-}$*Il2rg*$^{-/-}$ alymphoid mice (45,76,77). Thus, it is currently unclear whether Eomes$^-$NKp46$^+$ liver cells represent a progenitor population that can mature into Eomes$^+$NKp46$^+$ cNK cells or an ILC1 population distinct from cNK cells (7,45,77).

1.1.4 Cytokine requirements in the development of ILCs

The common gamma chain (γ_c) is a cytokine receptor subunit shared by receptors for IL-2, IL-4, IL-7, IL-9, IL-15, and IL-21 (78,79). All ILCs including cNK cells and foetal LTi cells are developmentally dependent on γ_c signalling. Mice deficient in the γ_c lack cNK, ILC1, ILC2 and Group 3 ILC populations, although different ILC populations depend on distinct γ_c cytokines (13,18,57,58,80).

IL-7 plays a critical role in the development and differentiation of ILC2 and Group 3 ILC populations, but not of intestinal ILC1 or cNK cells. ILC2 are critically dependent on IL-7 as evidenced by the absence of ILC2 in *Il7*$^{-/-}$ mice (13,21,81). Similarly, *Il7*$^{-/-}$ or *Il7ra*$^{-/-}$ mice have severely reduced numbers of foetal LTi cells, intestinal NKp46$^{+/-}$

RORγt^{+} ILC3 and NKp46^{+}NK1.1^{hi} RORγt^{-} 'ex-ILC3', while ILC1 and cNK cell develop normally (18,43,47,82,83). Microbiota-induced IL-7 signals have been shown to stabilize RORγt expression in adult ILC3, providing a potential link between microbial colonization of the intestine and post-natal expansion of lamina propria RORγt^{+} ILC3 (47).

Additional cytokines have been shown to influence Group 3 ILC plasticity. IL-23 has been reported to promote maturation of T-bet^{-}RORγt^{+}NKp46^{-} ILC3 into T-bet^{+}RORγt^{+}NKp46^{+} ILC3, while IL-12 is thought to promote destabilization of RORγt expression in peripheral ILC3 (9,47).

Mature ILC2 are highly responsive to the cytokines IL-25 and IL-33 and the receptors for both cytokines, IL-17RB and ST2, are highly expressed by committed ILC2Ps in bone marrow (25,69,84). *In vitro* IL-33, in conjunction with IL-7, has been reported to promote ILC2 development from CLPs (21). However, no *in vivo* requirement for IL-25 or IL-33 for development or maintenance of ILC2 has been demonstrated. While both cytokines are thought to be involved in driving ILC expansion following infection with *N. brasiliensis* or intranasal administration of the protease allergen papain, normal numbers of ILC2 are present in bone marrow and peripheral tissues of *Il17rb*$^{-/-}$ or *St2*$^{-/-}$ mice under steady-state conditions (11,70). This suggests that IL-25 and IL-33 regulate the activation, expansion and effector function of mature ILC2, but do not play a role in their development (11).

IL-15 is required for the development and function of intestinal ILC1 and cNK cells but not for the differentiation of NKp46^{+} ILC3. *Il15*$^{-/-}$ mice have normal numbers of RORγt^{+} ILCs, while much reduced numbers of ILC1 and cNK cells are found in the intestinal lamina propria (18,43,57,58,83,85). However, a role for IL-15 in the maintenance of NKp46^{+}NK1.1^{hi}RORγt^{-} ‘ex-ILC3’ has been suggested, correlating with their downregulation of CD127 and upregulation of CD122 (IL2/IL-15R β-chain) expression compared to NKp46^{+}NK1.1$^{-/low}$RORγt^{+} ILC3 (18).

1.2 Host-protective and homeostatic functions of intestinal ILCs

ILCs are involved in a range of host-protective and homeostatic immune responses in the gut, as summarized in Figure 1.4.

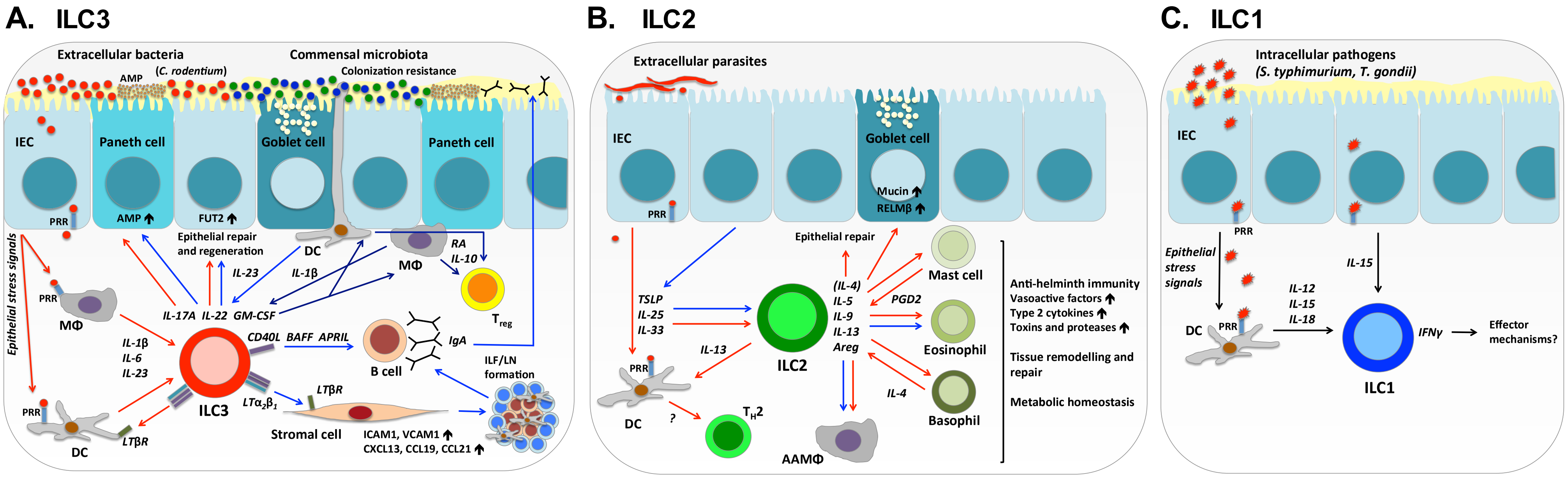

Figure 1.4: Homeostatic and host-protective immune functions of intestinal ILC populations. A. Foetal LTi cells and adult ILC3, via interactions with stromal cells, are responsible for the induction of organised intestinal lymphoid tissues during foetal development (MLNs, PPs) and adult life (ILFs). Intestinal ILC3 are important players in the maintenance of host-commensal homeostasis. ILC3-derived IL-22 and LT have critical functions in the containment of commensal bacteria and potential pathobionts in the gut through induction of anti-microbial responses in IECs and promotion of IEC regeneration and barrier function. ILC3 also promote the generation of low-affinity commensal-specific IgA and IgG antibodies by mucosal B cells, which help to prevent commensal microbial dissemination. ILC3-derived GM-CSF induces tolerogenic DCs and macrophages which promote the generation of T_{Reg}. Through production of pro-inflammatory mediators (IL-17A, IL-22, LT) ILC3 are also involved in host-protective immunity to extracellular bacteria such as *C.rodentium*. **B.** ILC2 play an important role in immunity to intestinal helminth infections through their early secretion of Type 2 cytokines. ILC2-derived IL-9 and potentially Areg also promote epithelial repair and regeneration. Furthermore, ILC2 associated with visceral adipose tissue function in metabolic homeostasis by maintaining eosinophils and AAM. **C.** Only little is known regarding the role of ILC1 in tissue immunity and homeostasis. ILC1 are an important early soure of IFNγ during *T.gondii* infection.

1.2.1 Foetal LTi cells and the generation of organized lymphoid structures

In the gut, RORγt$^+$ LTi cells, in conjunction with stromal cells, are responsible for the induction of secondary lymphoid organs (SLO) such as MLNs and PPs during embryogenesis and contribute to the dynamic modulation of lymphoid tissues during adult life (86,87).

The mechanisms underlying lymphoid organogenesis have been elucidated using knock-out mice characterised by impaired lymphoid organogenesis (87). LTi cells seed developing LN anlagen by ED12.5 and PP anlagen by ED16 (56,64). CXCL13 produced by mesenchymal stromal cells in response to neuronal-derived retinoic acid (RA) signals are thought to regulate the initial recruitment of LTi cells to LN anlagen, where they are retained in a manner dependent on stromal expression of mucosal addressin cell adhesion molecule (MAdCAM)-1 and LTi cell expression of integrin $\alpha_4\beta_1$ (64,87,88). IL-7 secretion by stromal cells promotes LTi survival and function and receptor activator of nuclear factor kappa-B (RANK)-RANK ligand (RANKL) signals promote further LTi clustering. LTβR-dependent activation of stromal organiser cells by lymphotoxin (LT)$\alpha_2\beta_1$-expressing LTi cells then leads to upregulation of chemokines (CXCL13, CCL21, CCL19) and adhesion molecules (intercellular adhesion molecule (ICAM)-1, vascular cell adhesion molecule (VCAM)-1, MAdCAM-1) that attract and retain dendritic cells (DCs), B cells and T cells to the primordial LN (87). Deletion of genes involved in LTi cell development or function (*Id2*, *Tox*, *Rorc*, *Il7*, *Il7r*, *Il2rg*, *Rank*, *Rankl*, *Lta*, *Ltb*, *Cxcl13*, *Cxcr5*, *Ccr6*) or stromal cell function (*Ltbr*) result in impaired LN and/or PP development (5,87).

Interestingly, the size of SLOs in adult mice was found to depend on maternal levels of dietary retinoids during pregnancy. RA signalling controls differentiation of foetal LTi cells upstream of RORγt and availability of RA *in utero* presumably regulates the differentiation and pool size of foetal LTi cells. The implications of this for the effectiveness of immune responses in adult life are currently unclear (89).

In addition to the developmentally programmed induction of MLNs and PPs, intestinal ILFs are organised lymphoid structures that arise after birth in response to colonization of the gut by commensal microbes (90,91). ILFs arise from cryptopatches, small clusters of immune cells composed mainly of RORγt$^+$ ILC3 and DCs, which are distributed throughout the intestinal lamina propria. Like MLNs and PPs, cryptopatches are developmentally programmed structures that arise independently of the microbial flora (92-94). However, post-natal cryptopatch maturation into ILFs is dependent on microbial signals relayed via nucleotide-binding oligomerization domain-containing protein 1 (NOD1) as well as AHR, and is mediated by LT-LTβR interactions between ILCs and stromal cells in a manner reminiscent of foetal lymphoid organogenesis (65,90,91). ILFs have been recognized as primary sites for production of homeostatic immunoglobulin (Ig)A antibodies by B cells, which are important for the anatomical containment of microbial commensals (90,91,93). Thus, the dynamic induction of ILFs in response to microbial signals acts as a feedback mechanism to generate commensal-specific IgA antibodies required for the maintenance of a homeostatic host-commensal relationship. There is a critical requirement for RORγt$^+$ ILC3 in this process. ILFs can form in RORγt-deficient mice that lack ILC3 through B cell-mediated LT signals. However, these ILFs support IgG rather than IgA production by B cells following epithelial damage, resulting in an inability to contain infiltrating commensal bacteria, leading to intestinal inflammation and systemic wasting disease (95).

1.2.2 ILCs and protective immunity to infection

ILC3

Under homeostatic conditions, RORγt^{+} ILC3 populations resident in the intestinal lamina propria are the predominant producers of IL-22 (58,59,96). IL-22 promotes epithelial restitution and regeneration and induces expression of mucins and antimicrobial peptides (AMPs) by IECs, including proteins of the S100 family, β-defensins, regenerating (Reg) proteins, lipocalin-2 and matrix metalloproteinases (MMPs) (97-103). In addition, IL-22 can enhance pro-inflammatory responses via induction of mediators such as IL-6 and TNFα and chemokines (CXCL1, CXCL5, CXCL8, CCL20, CCL2) by IECs that recruit and activate immune effector cells (102,104-109). Together, these processes promote intact intestinal epithelial barrier function required for containment of commensal and pathogenic microbes.

IL-22 production by ILC3 is constitutive and subject to negative and positive regulation by commensal and inflammatory signals, respectively, that are relayed to ILC3 via the epithelium and myeloid cell populations. In response to commensal microbial signals, IECs produce IL-25, which inhibits IL-22 production by ILC3 via inhibitory effects on myeloid cell populations. The inhibitory effect of IL-25 is opposed by IL-23, the expression of which is increased in response to pro-inflammatory signals induced by infection or commensal translocation into the intestinal lamina propria following epithelial damage (59,96,100,110-114).

In mice, protective immunity to the intestinal pathogen *Citrobacter rodentium* (*C. rodentium*) is critically dependent on IL-22 and the downstream induction of AMP secretion by IECs (58,100,115). Following *C. rodentium* infection in *Rag*$^{-/-}$ mice that lack T and B cells, the production of IL-22 by RORγt^{+} ILC3 is critical for prolonged host survival. *Rag*$^{-/-}$ mice deficient in ILCs rapidly succumb to infection (58,115). Importantly, however, ILC3 also contribute to protective immunity to *C. rodentium* in lymphocyte-replete mice that have normal numbers of T and B cells. RORγt^{+} ILC3 are the dominant producers of IL-22 in the intestinal lamina propria during the first six days post-infection, while CD4^{+} T cell-derived IL-22 dominates the later immune response (115). Using a combination of CD90- disparate mice and adoptive transfer, it has been shown that lymphocyte-replete mice specifically depleted of ILCs suffer delayed clearance of *C. rodentium* and increased infection-associated mortality compared to ILC sufficient mice (115). Thus, early ILC3-derived IL-22 plays a non-redundant function in mediating host-protective immunity following *C. rodentium* infection. Induction of IL-22 expression by ILC3 in this setting is dependent on IL-23 and bidirectional interactions between ILC3 and intestinal macrophages/DCs (110-112,115), which will be discussed in Chapter 5.

In addition to their role in protective immunity to *C. rodentium*, ILC3 have been implicated in defence against other bacterial pathogens, including *Streptococcus pneumonia* (116), *Salmonella typhimurium* (9,117), *Mycobacterium tuberculosis* (118) and *Pseudomonas aeruginosa* (119). Furthermore, ILC3 appear to be involved in immune responses against fungal (120) and viral pathogens (121,122) via various mechanisms.

ILC2

ILC2 play an important role in protective immunity against intestinal helminth parasites (11-13). The majority of studies to date have used infection models based on the murine-adapted helminth *Nippostrongylus brasiliensis* (*N. brasiliensis*). However, there is some evidence that ILC2 are important players also during infection with other parasitic organisms, including the helminth *Strongyloides venezuelensis* (123) and the nematode *Trichuris muris* (124). Intestinal ILC2 contribute to anti-helminth immunity through production of Type 2 effector cytokines (IL-4, IL-5, IL-9, IL-13), which help to coordinate effective parasite expulsion through induction of eosinophilia, IgE production, goblet cell hyperplasia, resistin-like molecule β (RELMβ) expression, mucous secretion and smooth muscle contraction (11,125-130). The importance of ILC2 in anti-helminth immune responses is perhaps highlighted by the fact that the intestinal helminth parasite *Heligmosomoides polygyrus* has evolved mechanisms to block activation of ILC2. Secretory products released by the parasite have been found to block release of IL-33 and subsequent activation of ILC2 (131).

Following infection with *N. brasiliensis*, IL-25 and IL-33 produced by IECs, stromal cells, NKT cells and macrophages are thought to be responsible for the recruitment and activation of ILC2 (11,125,128,132-137). ILC2 are directly responsive to IL-25 and IL-33 stimulation and mice deficient in IL-25, IL-33 or the receptors for these cytokines show impaired immunity to *N. brasiliensis* infection (11,128,138). Mast cells and basophils may further contribute to the recruitment and activation of ILC2 following *N. brasiliensis* infection. Activated mast cells produce high levels of prostaglandin D2 (PGD_2), which has been shown to act as a chemoattractant and activator of ILC2 both *in vitro* and during allergic lung inflammation *in vivo*

(139,140). In the lung, mast cell-derived serine proteases have been shown to generate cleaved forms of IL-33 that were extremely potent stimulators of ILC2 *ex vivo*. It is conceivable that similar mechanisms are at play during helminth-induced intestinal inflammation (141). Basophil-derived IL-4 may further add to this innate activatory feedback loop by promoting ILC2 proliferation (142,143).

Several publications have highlighted a role for ILC2 in the induction of effective T_H2 responses via indirect effects on DCs and direct major histocompatibility complex (MHC) class II-mediated antigen presentation to $CD4^+$ T cells (144-146). In the context of *N. brasiliensis* infection, T_H2 responses to *N. brasiliensis* are impaired in mice specifically depleted of ILC2 (146). ILC2-mediated effects on $CD4^+$ T cells will be discussed in detail in Chapter 4.

ILC1

Only little is known to date regarding the role of ILC1 in immunity to infection. There is some indication that T-bet-dependent ILC1 may be involved in control of *Salmonella typhimurium (S. typhimurium)* infection in mice (9). Furthermore, ILC1, but not cNK cells, are the predominant producers of host-protective IFNγ following intestinal infection with the intracellular parasite *Toxoplasma gondii* (*T. gondii*). *Rag2*$^{-/-}$*Il2rg*$^{-/-}$ mice deficient in all ILCs fail to control infection with *T. gondii*, a phenotype which can be rescued following adoptive transfer of ILC1 (18).

1.2.3 ILC3 and the intestinal commensal microbiota

In addition to their functions in promoting host-protective immunity to a variety of pathogens, RORγt$^+$ ILC3 are known to play a role in regulating the tolerogenic relationship between the host immune system and the commensal microbiota which is required for the maintenance of immune homeostasis (147-149).

IL-22 is an important regulator of IEC homeostasis and ILC3 are major producers of IL-22 in the intestinal lamina propria under homeostatic conditions (see Section 2.2.1). Through IL-22-dependent crosstalk with IECs, ILCs promote anatomical containment and prevent systemic dissemination of the intestinal commensal microflora and potential pathobionts. Two independent groups have reported that *in vivo* depletion of ILC3 is associated with decreased levels of intestinal IL-22 and suboptimal expression of antimicrobial factors (Reg3β, Reg3γ, S100 proteins) by IECs, resulting in systemic dissemination of commensal *Alcaligenes* spp. bacteria. Normally, *Alcaligenes* spp. are anatomically contained within gut-associated lymphoid structures such as PP and MLNs. Peripheral *Alcaligenes* spp. dissemination was associated with low-grade systemic inflammation, which could be reversed by treating mice with recombinant IL-22 (96,147,150). ILC3-derived IL-22 has also been shown to protect mice against systemic dissemination of pathobionts following *Clostridium difficile* infection and infection-induced damage to the intestinal epithelium. ILC3-derived IL-22 is required for the induction of complement factor C3 in the liver and intestine, which enhances bacterial phagocytosis and allows effective control of the pathobiont load in peripheral organs (151). Thus, by regulating IEC anti-microbial functions, IL-22 producing ILC3 play an important role in preventing the systemic dissemination of microbial commensals and pathobionts.

Moreover, crosstalk between ILC3 and epithelial cells has been shown to influence the composition of the intestinal microbial flora in mice, resulting in augmented host resistance to colonization with pathogenic organisms such as *C. rodentium* (152,153). Commensal dysbiosis secondary to ILC3 dysfunction can promote systemic inflammatory responses. Outgrowth of commensal segmented filamentous bacteria (SFB), implicated in the development of pro-inflammatory T_H17 cells (154), has been observed in *Ahr*$^{-/-}$ mice that have decreased levels of intestinal ILC3-derived IL-22. Further reduction of ILC3 numbers and IL-22 production in *Ahr*$^{-/-}$ *Rorc(γ)t*$^{GFP/-}$ mice promotes development of spontaneous, T_H17-driven colitis, indicating that ILC3/IL-22-mediated regulation of the commensal flora plays a role in limiting the induction of potentially pathogenic T_H17 responses to commensal antigens (155). Intestinal RORγt$^+$ ILC3 have also been reported to control the composition of the commensal microbiota through regulation of IEC fucosylation. Fucosylated carbohydrates on IECs are thought to be important for the generation of an intestinal niche for commensal microbes (156-158). IEC fucosylation is mediated by the fucosyltransferase enzymes Fut1 and Fut2 (156). Two independent groups have reported that IL-23-dependent IL-22 as well as LT expression by intestinal ILC3 is required for the induction of Fut2 expression in IECs (157,158). Abrogation of IEC fucosylation in *Fut2*$^{-/-}$ mice has been linked to intestinal commensal dysbiosis and leads to increased susceptibility to infection with the pathogens *S. typhimurium* and *C. rodentium* (156-158).

Furthermore, ILC3 can limit commensal dissemination through effects on cells of the adaptive immune system. Through their expression of B cell activating factors such as B cell activation factor of the TNF family (BAFF), a proliferation-inducing ligand (APRIL) and CD40L, as well as through LT-dependent pathways, ILC3 promote the production of T cell-dependent and –independent IgA and IgG antibodies by mucosal and splenic B cell populations (93,159,160). In turn, mucosal IgA and low-affinity systemic IgG antibodies contribute to the maintenance of mucosal homeostasis by regulating the composition, size and anatomical containment of the intestinal commensal microbiota (161-163). ILC3 have also been reported to limit commensal-specific CD4$^+$ T cell responses, through direct inhibitory interactions with CD4$^+$ T cells (164,165) and through induction of tolerogenic RA- and IL-10-secreting intestinal DCs and macrophages (166). These aspects of ILC3 function will be discussed in detail in Chapters 4 and 5.

1.2.4 ILCs in tissue remodelling and repair

ILC3

Through the production of effector cytokines, both ILC3 and ILC2 populations are involved in the remodelling and repair of damaged tissues in response to a variety of insults. Following induction of dextran sulfate sodium (DSS)-mediated epithelial damage, intestinal ILC3-derived IL-22 has been shown to promote epithelial repair and is required for resistance to colitis development (59). Similarly, ILC3-derived IL-22 promotes restoration of intestinal epithelial integrity in a mouse model of graft-versus-host disease (GVHD) via protective effects on intestinal stem cells (63). In the lung, ILC3-derived IL-22 has been reported to limit inflammation and promote epithelial repair processes in a mouse model of allergic airway hyperresponsiveness (AAHR) (167). Moreover, regeneration of thymic epithelial cells following whole-body irradiation of mice was found to be dependent on IL-22 production by radiation-resistant ILC3 (168).

$ROR\gamma t^+$ ILC3 also appear to play a role in the regeneration of damaged lymphoid tissue following infection of mice with lymphocytic choreomeningitis virus (LCMV). LCMV infection leads to a loss of secondary lymphoid organ (SLO) integrity due to $CD8^+$ T cell-mediated destruction of infected stromal fibroblastic reticular cells (FRCs) that provide a structural backbone for SLO architecture. The functional consequence of this is a transient immunodeficiency characterised by failure to induce immune responses to unrelated antigens that rely on intact spatiotemporal interactions between DCs, T helper cells and B cells in SLOs. Restoration of SLO architecture and immune competence is critically dependent on the proliferative accumulation of $LT\alpha_2\beta_1^+ROR\gamma t^+$ ILC3 and their crosstalk with $LT\beta R^+$ FRCs, reminiscent of the stromal-LTi cell interactions responsible for the generation of lymphoid tissues during foetal development (169).

ILC2

Repair functionality of ILC2 has been observed in mouse models of infection-induced tissue damage in the lung. Monticelli et al. reported that intranasal infection of *Rag*$^{-/-}$ mice with influenza virus H1N1 is associated with activation of innate immune responses in the lung and immunopathology characterised by loss of epithelial integrity and reduced lung function (170). Depletion of $CD90^+$ ILCs in this model leads to exacerbation of epithelial necrosis and deterioration of lung function compared to ILC-sufficient animals. In turn, adoptive transfer of ILCs into ILC-depleted *Rag*$^{-/-}$ mice restores epithelial integrity. The group went on to show that the ILC-mediated repair of damaged lung epithelium is dependent on IL-33-induced Areg production by ILC2. Whether ILC2 contribute to epithelial repair in the gut through similar mechanisms is currently unknown.

Furthermore, ILC2-derived IL-9 has been shown to play an important role in the orchestration of innate immune response required to limit immunopathological processes in a mouse model of *N. brasiliensis*-induced lung inflammation (129). In this model, ILC2-derived IL-9 acts in an autocrine amplification loop to boost IL-5 and IL-13 production by IL-9R-expressing ILC2, resulting in the recruitment and activation of eosinophils and alternatively-activated macrophages (AAM) required for the repair of damaged lung tissue.

1.2.5 ILC2 and metabolic homeostasis

Several reports have highlighted a role for ILC2 in the regulation of visceral adipose tissue (VAT), metabolic homeostasis and obesity in mice. ILC2 constitute a substantial proportion of VAT immune cells and are the pre-dominant producers of IL-5 and IL-13 in VAT (13,171,172). IL-5 and IL-13 production by ILC2 in response to IL-25 and IL-33 stimulation was found to be required for the maintenance of VAT-resident eosinophils and AAM (171,172). In response to ILC2-derived IL-5, VAT eosinophils upregulate expression of IL-4, which acts in the induction and function of AAMs (173,174). Interestingly, ILC2/IL-5-mediated eosinophil homeostasis also appears to be regulated by intestinal vasoactive peptide, providing a link between ILC2-dependent metabolic effects, dietary intake and circadian rhythm (175). ILC2-derived IL-13 has also been suggested to directly promote AAM differentiation (171). Through their expression of IL-10, VAT AAM are important players in the prevention of obesity-associated insulin resistance (176-178). Furthermore, AAM-derived catecholamines promote induction of thermogenic beige adipocytes, resulting in increased energy expenditure and improved regulation of adiposity (174,179,180). ILC2-derived IL-13 and encephalin peptides have also been reported to induce beige fat through direct effects on adipocytes and adipocyte precursors (180,181). Confirming the importance of ILC2 in metabolic homeostasis, ILC2-deficient mice show increased susceptibility to high fat diet-induced obesity and insulin resistance as a results of disturbed VAT eosinophil and AAM maintenance (171,172,180).

1.3 Human ILCs

1.3.1 Overview of human ILC subsets

The discovery of foetal LTi cells by Mebius et al. (64) and the characterisation of several ILC subsets that persisted in adult murine tissues prompted investigations into the existence of human ILCs. Human LTi-like cells were identified in 2008 by Cupedo et al. who observed $CD45^{int}Lin^{-}CD127^{+}$ cells in the foetal gut, MLNs and spleen as early as 8-12 weeks of gestation (182). Foetal $CD45^{int}Lin^{-}CD127^{+}$ cells lack expression of lineage markers associated with other leukocyte lineages and show no potential to differentiate into T cells, B cells or DCs following culture on OP9 stromal cells. Furthermore, these cells highly express transcripts for *ID2*, *RORC*, *LTA*, *LTB* and *RANKL* and induce adhesion molecule expression on mesenchymal stromal cells in a co-culture assay, identifying them as the human counterpart of murine LTi cells (182).

LTi-like ILC3 were soon identified in post-natal tissues, including the tonsil, the PPs of the ileum and the appendix. Based on expression of the NK cell markers CD56 or NKp44, these postnatal ILC3 were grouped as NKR^{-} and NKR^{+} ILC3, similar to the grouping of mouse ILC3 into $NKp46^{-}$ and $NKp46^{+}$ cells (182-184). Functionally, human NKR^{+} ILC3 are enriched for production of IL-22 following stimulation with phorbol 12-myristate 13-acetate (PMA)/ionomycin or IL-23, while NKR^{-} ILC3 preferentially secrete IL-17A and IFNγ (183,185-187). In contrast to the heterogeneous expression of CCR6 by mouse Group 3 ILCs, human LTi cells and ILC3 populations all have high expression of CCR6 (16,182,183,188,189).

In addition to NKR$^{-/+}$ ILC3, GATA3-expressing ILC2 have been identified in several human tissues, including foetal gut (16), nasal mucosa (16), skin (190), blood and lung (140). In contrast to RORγt^{+} ILC3, these cells have heterogeneous expression of CD117, lack expression of NKR and can be defined phenotypically by expression of the PGD$_2$ receptor chemoattractant receptor-homologous molecule expressed on Th2 cells (CRTH2) as well as high levels of CD161 and CD25 (16). In response to stimulation with IL-25, IL-33 and thymic stromal lymphopoietin (TSLP), CRTH2^{+} ILCs express high levels of Type 2 cytokines IL-5 and IL-13 (16,17).

Following identification of ILC2, Bernink et al. characterized a population of lamina propria-resident CD127^{+}CD117^{-}CD56^{-}NKp44^{-} ILC1 that are enriched for T-bet expression and respond to stimulation with IL-12 and IL-18 by producing IFNγ. These cells lack expression of RORγt, IL-17A or IL-22 (189). At the same time, another group identified a population of intraepithelial CD103^{+} ILCs enriched for IFNγ expression that phenotypically differed from other known human ILCs due to lack of expression of CD127 (191). Unlike the cells identified by Bernink et al., these cells express the NK markers CD56 and NKp44, but were shown to differ from cNK cells because of a developmental independence from IL-15 signaling. However, in addition to T-bet, intraepithelial CD103^{+} ILC1 express high levels of Eomes and therefore likely constitute an unconventional NK cell subset rather than a helper ILC population.

In reference to a unified ILC nomenclature proposed by a group of researchers in 2013, in humans the distinct helper ILC populations are now classified on the basis of the surface markers CD117, CRTH2 and NKp44. Thus, within the population of total Lin^{-}CD127^{+} ILCs, ILC1 are identified as CRTH2^{-}CD117^{-}NKp44^{-} cells, ILC2 as

CRTH2$^+$CD117$^{+/-}$ cells and ILC3 as CRTH2$^-$CD117$^+$NKp44$^{+/-}$. cNK cells are CD3$^-$CD127$^-$CD94$^+$CD56$^+$ cells (6,16,188,189).

1.3.2 Development of human ILCs

The developmental requirements of and relationships between these different ILC lineages in the human are not as well established as in the murine system. All ILC populations originate from CD34$^+$ HSCs (189,192-194). Recently, a CD34$^+$RORγt$^+$ lineage-specified precursor population that exclusively gives rise to RORγt$^+$ ILC3 has been identified in the human tonsil and intestinal lamina propria (192). Like their murine counterparts, human ILC2 are dependent developmentally and functionally on the transcription factors GATA3 and Notch (17,24). *In vitro,* retrovirus-mediated overexpression of GATA3 in Lin$^-$CD127$^+$CD117$^+$NKp44$^-$CRTH2$^-$ ILCs can drive their differentiation into CRTH2$^+$ ILC2 that produce IL-4, IL-5 and IL-13 following stimulation with TSLP and IL-33 (17).

Furthermore, NKR$^+$ helper ILCs form a developmentally distinct lineage from cNK cells. Unlike mature CD127$^-$CD56$^+$ cNK cells, CD56$^+$ or NKp44$^+$ ILC3 lack expression of the cNK markers CD94, granzyme B and perforin (182-184). However, immature Stage 3 NK (iNK) cells similarly lack expression of CD94 and cytotoxic effector molecules and are enriched for markers such as CCR6, CD161 and CD117 that are also highly expressed by ILC3. This led to the hypothesis that NKR$^+$ ILC3 are a precursor to cNK cells that retain their immature phenotype and associated high AHR and IL-22 expression through IL-1β-dependent signals (184,195). However, a further study revealed that the iNK population is a heterogeneous population comprised of CD117$^+$CD127$^-$CD56$^+$CD94$^-$ cNK precursors and

CD117$^+$CD127$^+$CD56$^+$CD94$^-$ ILC3. CD127$^+$ ILC3 cultured *in vitro* with IL-2, IL-7 or IL-15 do not differentiate into cNK cells, but instead maintained stable expression of CD117, IL-17A and IL-22 in the absence of CD94, granzyme B or perforin upregulation. In contrast, CD117$^+$CD127$^-$ iNK precursors differentiate into IFNγ-producing CD94$^+$ cNK cells that expressed KIRs and showed cytotoxic killing activity (188). Confirming these findings, Ahn et al. reported that CD56$^+$CD117$^+$CD94$^-$ iNK cells derived from CD34$^+$ umbilical cord blood HSCs can be divided into CD11a$^+$ and CD11a$^-$ populations. CD11a$^-$ cells express *RORC* and *IL22* and fail to differentiate into cNK cells, while CD11a$^+$ cells give rise to cNK cells (194). Finally, *in vivo* human evidence for differential developmental requirements for cNK cells and NKR$^+$ ILC3 populations was provided by Vonarbourg et al. who could show that in human severe combined immunodeficiency (SCID) patients with IL-7R deficiency the frequency of CD56$^+$NKp44$^+$ LTi-like cells is severely reduced, while cNK cells is unaffected (47). Thus, convincing *in vitro* evidence shows that human cNK cells and NKR$^+$ ILC3 form developmentally distinct lineages, which is in agreement with data obtained from RORγt fate-mapping mice.

Similar to the mouse, a precursor-progeny relationship exists between adult human NKR$^-$ and NKR$^+$ ILC3. Crellin et al. showed that Lin$^-$CD127$^+$CD56$^-$ ILC3 isolated from the human tonsil can differentiate into Lin$^-$CD127$^+$CD56$^+$ ILC3 following *in vitro* culture with IL-2, IL-7 or IL-15 (188). In mice, a microbiota-induced downregulation of RORγt and concomitant upregulation of T-bet expression in NKR$^-$ ILCs is responsible for differentiation of NKR$^-$ ILCs into NKR$^+$ ILCs (9,47). Whether human NKR$^+$ ILC differentiation is similarly regulated is unknown.

The pathways underlying the development of lamina propria-resident ILC1 are less clear. Similar to murine ILC3, Bernink et al. have described considerable plasticity within human ILC3 populations. *In vitro* culture of tonsillar CD117^{high}NKp44^{+}RORγt^{+} ILC3 with IL-2 plus IL-12 or IL-18 leads to acquisition of an ILC1-like phenotype, including downregulation of CD117, NKp44 and *RORC* expression and acquisition of *TBX21* and *IFNG* expression (189). Thus, it is unclear whether the identified lamina propria-resident ILC1 are *bona fide* ILC1 that, like mouse ILC1 constitute a developmentally independent lineage from other helper ILC subsets, or rather are 'ex-ILC3' that have downregulated expression of CD117, NKp44 and RORγt (189,196).

1.3.3 Functions of human ILCs

In line with mouse findings, adult human ILC populations have been described in a variety of tissues, including the spleen (160), gut (185,189,191,197-199), oral mucosa (16,200-203), skin (190,204-208), lung (140,209-211), uterine mucosa (212,213), brain (214) and synovial tissue (18,215-218).

Like their murine counterparts human ILCs are activated by a range of myeloid-, epithelial- and stromal-derived cytokines, including IL-7, IL-12, IL-15, IL-18, IL-25, IL-33, IL-1β and IL-23. IL-23, IL-1β and IL-6 have been shown to induce proliferation and production of IL-17A, IL-22 and IFNγ in ILC3 populations (183,185,188,195,196,198). IL-12, IL-15 and IL-18 promote IFNγ expression by ILC1 and ILC3 (189,191). IL-25, IL-33 and TSLP act on ILC2 to elicit IL-4, IL-5, IL-13 and Areg expression and promote chemotaxis (16,17,190). Additionally, direct TLR2 stimulation of human ILC3 in conjunction with IL-2 has been reported to induce cell proliferation and expression of IL-22 (219). NKp44$^+$ ILC3 have furthermore been shown to become activated and adopt a pro-inflammatory cytokine profile through direct triggering of NKp44 in conjunction with IL-1β, IL-7 and IL-23, including production of TNFα (187). Cellular ligands for NKp44 are thought to be upregulated on infected or stressed epithelial cells (187,220,221). PGD_2 has been implicated in the regulation of ILC2 function. CRTH2$^+$ ILC2 migrate towards PGD_2 gradients *in vitro* and upregulate Type 2 cytokine production in response to stimulation with PGD_2 (139). Furthermore, E-cadherin and the vitamin A metabolite RA have been shown to negatively regulate human ILC2 function (190,222).

The majority of published data regarding human ILC function is descriptive and inferential. Only few functional experiments involving human ILCs have been performed. With respect to ILC functionality in the gut, co-culture experiments of ILC3 with a colonic epithelial cell line have indicated that ILC3-derived IL-22 can induce STAT3 phosphorylation, proliferation and production of anti-microbial factors and IL-10 in IECs, suggesting that, similar to the mouse, ILC3 may contribute to mucosal homeostasis in the human gut (183).

1.4 IBD

IBD are chronic relapsing-remitting inflammatory disorders of the gastrointestinal tract. Although disease pathogenesis is incompletely understood, evidence from genetic and immunological studies suggests that a breakdown in intestinal homeostasis due to dysregulated immune responses against intestinal bacteria underlies disease development in genetically susceptible individuals (223).

The main forms of IBD are Crohn's disease (CD) and ulcerative colitis (UC), which can be distinguished through a combination of overlapping and distinct histological, endoscopic, radiological and clinical features (224,225). Both CD and UC are highly debilitating relapsing-remitting conditions characterised by recurrent abdominal pain, diarrhoea, intestinal bleeding, fever and malnutrition (226). Extraintestinal disease manifestations can be observed in both CD and UC, and most commonly include ocular (uveitis, episcleritis), musculoskeletal (arthritis) and mucocutaneous (pyoderma gangrenosum, erythema nodosum) complications (227,228). Furthermore, both CD and UC patients are at increased risk for development of colorectal cancers (229). No curative treatments are available for CD or UC and despite the availability of biological and small molecule immunosuppressive agents the rate of surgical intervention remains high. Approximately half of patients require surgery ten years after diagnosis (102,226,230-233).

1.4.1 Epidemiology

In Europe, approximately 1 in 1000 people currently suffer from IBD currently, with a prevalence range at 8-214/100,000 and 21-294/100,000 for CD and UC, respectively (233). The peak of onset for IBD is during early adulthood, ranging from 20-40 years. However, disease onset can occur at any age. In addition, paediatric IBD accounts for 7 -20% of all IBD cases (233,234).

Over the last 50 years, the incidence rates of both CD and UC have been on the rise. While UC incidence appears to have stabilized recently, CD incidence is still increasing (233,235). The highest prevalence of IBD is found in industrialized regions such as Europe and North America. However, epidemiological data indicate that IBD is on the rise also in developing countries and countries that are adopting more Westernized lifestyles (233,235). This suggests that lifestyle and/or environmental factors associated with increased industrialisation may be responsible for the increased rate of IBD in developing countries.

A mild gender bias has been observed in IBD, although this appears to be less pronounced than in other autoimmune diseases. CD occurs slightly more frequently in women, especially among cases diagnosed during adolescence and early adulthood. Furthermore, female CD patients have been reported to experience a more severe disease course compared to male CD patients (236,237). In contrast to CD, UC is more common in men than women (233,238). These findings suggest that hormonal influences may play a role in disease expression (238).

Differences in IBD incidence between ethnic groups have been observed, which are thought to result from both genetic and environmental differences. While the incidence of CD among the Ashkenazi Jews varies depending on where they reside (indicating modulation by environmental influences), it is always higher than in the local non-Jewish population (arguing for genetic predisposition) (233). Similarly, a lower incidence has been reported in Asian and Hispanic populations in North America compared to Caucasian Americans. However, this likely reflects differences in lifestyle, since the rate of IBD among these populations has begun to increase (238,239).

1.4.2 Diagnostic features

CD is characterized by a patchy inflammation that can occur anywhere along the GI tract from the mouth to the anus. Inflamed areas can be interspersed with macroscopically unaffected areas, leading to characteristic ‘skip’ lesions. Inflammatory lesions are most common in the distal ileum, the colon and the perianal region. Inflammation is transmural, i.e. spanning the entirety of the gut wall from the mucosa to the serosa and is characterized by deep ulcerations and formation of non-caseating granulomas (234,239). The deep fissuring ulcers can give rise to fistulae (abnormal connections that form between the gut and surrounding tissues, including the skin, other parts of the intestinal tract, the vagina or blood vessels), strictures (narrowing of the gut lumen) and abscesses, all of which are common complications in CD patients. Based on the disease course, CD can be classified as inflammatory (presence of inflammatory lesions in the gut wall), penetrating (presence of fistulae and abscesses) or stricturing disease. Inflammatory CD is most common in the early years after diagnosis, while the incidence of penetrating and stricturing disease increases with time after diagnosis, indicating that the latter may be a manifestation of disease progression and arise as a consequence of long-term chronic inflammation (234,239).

In contrast to CD, UC is characterized by a diffuse, continuous inflammation that usually commences in the rectum and spreads proximally to the colon. Depending on the extent of inflammation, UC is classified as proctitis (limited to rectum), left-sided (distal to splenic flexure) or pan-colonic (proximal to splenic flexure) (224). The inflammation is more superficial than in CD and restricted to the mucosa and submucosa. Deep ulcerations are uncommon and only found in very severe disease (233). Penetrating disease involving recurrent formation of fistulae is not a feature of UC (233,234). Histological diagnostic features of UC include substantial crypt distortion, cryptitis, mucin depletion and Paneth cell metaplasia (224).

1.4.3 Pathogenesis

The pathogenesis of IBD is incompletely understood but is thought to result from a complex interplay between host genetics, immune responses and environmental factors that are most dominantly represented by the microbial commensal flora (Figure 1.5).

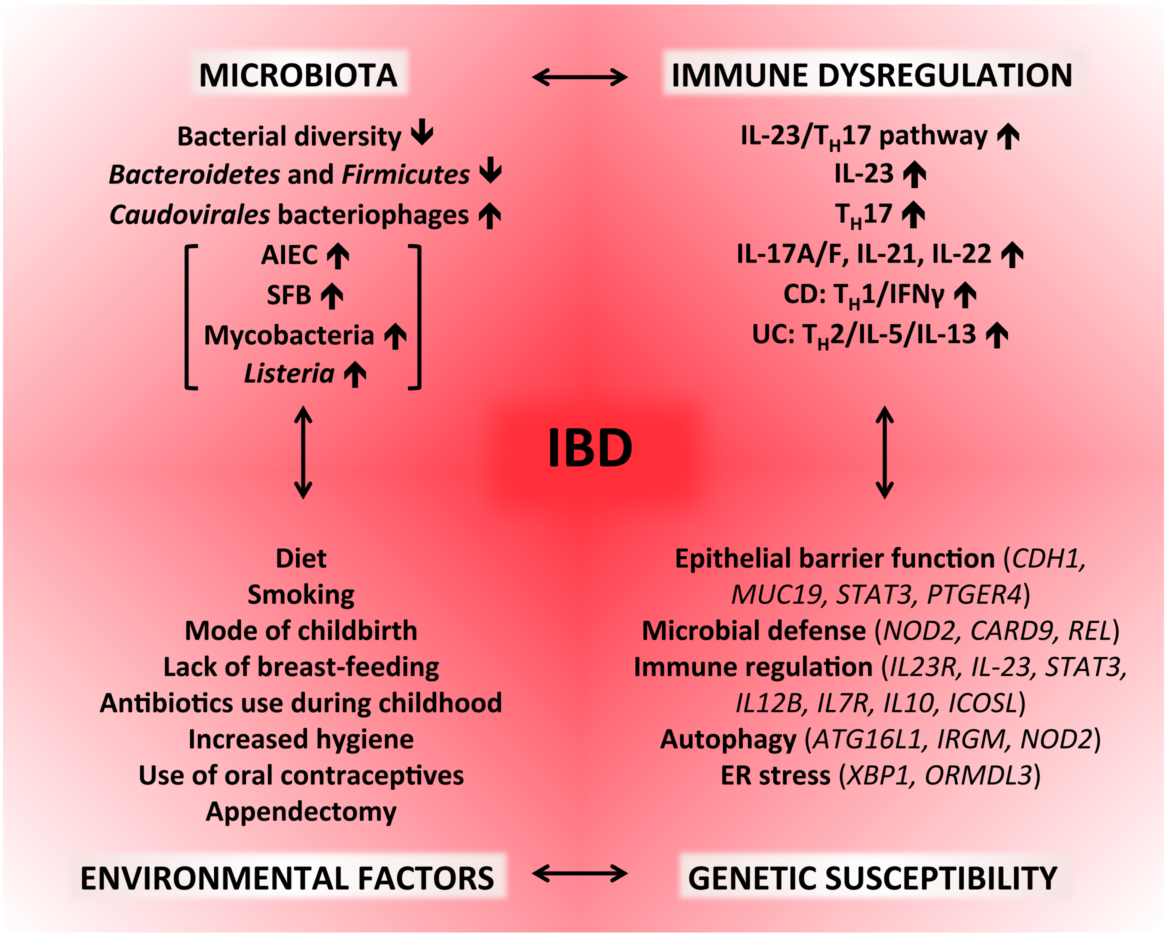

Figure 1.5: IBD pathogenesis. The mechanisms underlying IBD pathogenesis are incompletely understood, but disease is thought to result from a complex interplay of host genetics, immune responses, the microbial commensal flora and environmental factors.

Genetics

In addition to enrichment of IBD within the Jewish population (240), twin and family studies point to a genetic component in the pathogenesis of IBD. Twin studies have indicated concordance rates in monozygotic twins of approximately 30.3% for CD and 15.4% for UC (241). The higher concordance rate in CD suggests a greater genetic component in this disease compared to UC (226).

An 8-10 fold increased risk of IBD has also been reported in first-degree relatives of IBD patients (226,242). In the majority of affected families, all individuals with IBD will suffer from the same disease type. However, approximately 20% of multiply affected families are mixed, with different family members presenting with either CD or UC. These findings point to the existence of genetic risk factors exclusive to either CD or UC, as well as susceptibility loci that are shared by both disease types (226). These observations align with findings from genome-wide association studies (GWAS). To date GWAS have identified single nucleotide polymorphisms (SNPs) associated with 163 genetic loci that confer increased risk of or protection from IBD development. The majority of loci (110 out of 163) are shared by both CD and UC (243). Many of them highlight immune pathways involved in host-commensal homeostasis, such as epithelial barrier function (*HNF4A, CDH1, ERRFI1, MUC19, STAT3, REL, PTGER4*), microbial defence (*NOD2, ITLN1, CARD9, REL, SLC11A1, FCGR2A/B*), innate and adaptive immune regulation (*IL23R, IL23, IL22, JAK2, TYK2, STAT3, ICOSLG, IL21, IL12B, TNFSF15*, *IL5, IL7R, IL2, IL10, IL27, IL1R1/IL1R2)*, as well as cellular processes such as autophagy (*ATG16L1, IRGM, NOD2, LRRK2, CUL2*), and endoplasmic reticulum (ER) stress (*XBP1, ORMDL3*) (234).

IBD is a complex polygenic disorder. With the exception of genetic variants identified in very early-onset IBD patients with monogenic disease (eg. *IL10RA*, *IL10RB*) (244), the majority of individual disease variants identified to date convey only a small risk (<1.5-fold) for disease development (245). The strongest associations relate to *NOD2* polymorphisms in CD (relative risk >20-fold in homozygotes, with 30-50% of European and North American CD patients carrying at least one allele), and a protective Arg381Gln *IL23R* polymorphism in both CD and UC (relative risk reduced approximately 3-fold) (226,240,245-247).

Detailed functional analyses are required to understand precisely how these risk alleles impact the function or expression of their encoded proteins, how such alterations can mechanistically contribute to disease development and ultimately how these changes may be targeted therapeutically. For example, while GWAS clearly indicate that the IL-23/T_H17 pathways plays a prominent role in both CD and UC (risk variants of *IL23R* as well as multiple other genes implicated in this pathway, including *IL-23, JAK2, STAT3, IL17A, IL17F,* and *CCR6*), it is not well understood how these polymorphisms affect protein function or expression (234).

On the other hand, more progress has been made in understanding the effects of *NOD2* risk variants on NOD2 function and how this may contribute to disease development. *NOD2* disease variants have been reported to have a reduced capacity to induce nuclear factor kappa B (NFκB) phosphorylation following *in vitro* stimulation with bacterial peptidoglycans, indicating that these alleles may result in reduced NOD2 function (248). Through inhibitory effects on TLR2, NOD2 has been shown to act as a negative regulator of IL-12-mediated T_H1 activation and it is conceivable that a reduced regulatory capacity of NOD2 may contribute to excessive

T_H1 activation seen in CD (249). CD-associated *NOD2* variants were also reported to inhibit IL-10 production by monocytes (247) and to promote IL-12p40 expression (250), indicating that they may contribute to a loss of immune regulation in disease. Linking NOD2 and autophagy pathways, CD-associated *NOD2* variants have been shown to be defective in the induction of autophagy pathways in DCs following infection with *S. typhimurium* or adherent-invasive *Escherichia coli* (AIEC), resulting in impaired bacterial handling (251). Furthermore, Paneth cells carrying *NOD2* risk variants were reported to produce lower amounts of AMPs compared to cells with non-risk alleles (252). In addition, IBD-associated risk variants in autophagy-related *ATG16L1* and ER stress response-related *XBP1* were found to functionally converge on impaired Paneth cell function and reduced production of AMPs (234).

These findings point to a significant role for innate immunity in IBD pathogenesis and suggest that bacterial sensing and activation of downstream pro-inflammatory/anti-microbial modules may be impaired in patients carrying these risk alleles. In line with the proposed immunodeficiency hypothesis of IBD, this could potentially lead to impaired containment of commensal and pathogenic bacteria, leading to secondary activation of commensal-specific T cells and perpetuation of inflammation (253-255).

Environmental factors

The relatively modest concordance rates for CD and UC in twin studies indicate a prominent role for developmental or environmental factors in IBD pathogenesis (256). Evidence for a role of environmental risk factors also comes from migration studies, which have shown that immigrants moving to areas with higher disease prevalence are more likely to develop disease (257,258).

Smoking is one of the most consistently reported risk factors for IBD (258). Smoking is associated with increased risk for CD development and predictive of an aggressive disease course. In contrast, smoking conveys an inverse risk for UC development. In UC patients, cessation of smoking has been correlated with onset of disease or disease flare-ups. It is unclear why smoking has opposing effects on CD and UC. Moreover, the pathogenic/protective mechanisms behind these effects are not well defined, but appear to be independent of nicotine. Effects of tobacco smoke on epithelial barrier integrity, oxidative stress and the composition of the intestinal microbiota have been proposed (259).

Additional environmental risk factors for IBD development have been suggested, including mode of childbirth, breast-feeding, reduced exposure to intestinal helminths (hygiene hypothesis), antibiotics exposure in childhood, use of oral contraceptives, vaccinations and appendectomy (238,259).

Convincing evidence for the bacterial microbiota as an environmental risk factor comes from colitis studies that report abrogation of disease development in germ-free animals, pointing to a critical role for commensal bacteria in the development of intestinal inflammation (260-263). In humans, faecal stream diversion has been shown to reduce inflammation and to prevent post-operative recurrence in CD patients. In turn, restoration of the faecal stream was associated with development of inflammatory lesions and disease flare-up (264,265). Furthermore, antibiotic treatment can ameliorate inflammation in some IBD patients, particular in those with stricturing disease or perianal fistulae (266).

IBD patients show a disrupted composition of the bacterial intestinal flora compared to control individuals. Both CD and UC are associated with a reduction in bacterial diversity, mainly due to a decrease in symbiotic *Bacteroidetes* and *Firmicutes* phyla (267,268). In contrast, increased numbers of *Proteobacteria* have been reported (268,269). *Bacteroides fragilis* is a prominent symbiotic species that has been shown to protect mice from *Helicobacter hepaticus (H. hepaticus)*–induced colitis and its reduction in IBD patients could facilitate pathogenic colonization of the intestinal mucosa (270). *Faecalibacterium prausnitzii (F. prausnitzii)*, a butyrate-producing Firmicute with confirmed anti-inflammatory properties in mouse colitis models *in vivo*, is reduced in CD and UC patients, which is associated with recurrence of ileal CD following surgical resection (271,272). In mice, SFB have been shown to induce the differentiation of T_H17 cells in the intestinal lamina propria (154,273). Overexpression of Paneth cell α-defensin in transgenic mice has been shown to reduce intestinal SFB (274) and it may be speculated that impaired Paneth cell function in IBD (e.g. as a result of polymorphisms in *NOD2*, *XBP1*, *ATG16L1*) may result in outgrowth of SFB, promoting pro-inflammatory T_H17 responses. However, the role of SFB in IBD is currently unclear.

It is unclear whether the changes in microbial composition observed in IBD play a primary role in disease development or whether they are secondary to inflammation-induced microenvironmental changes. Reduced mucosal colonization with *F. prausnitzii* has been reported in first-degree relatives of UC patients, indicating that host genetics or environmental factors can result in altered microbial composition that may then pre-dispose individuals to IBD development (275). The effects of differences in long-term and short-term diet on changes in the composition of the intestinal microbiota are beginning to be elucidated and are likely to play a significant role in determining a person's risk for IBD development (276,277).

Specific pathogens have also been implicated in the development of IBD and commensal dysbiosis may facilitate colonization of the intestinal mucosa by pathogenic organisms (270). Increased numbers of mucosal AIEC have been reported in CD patients and *E. coli* antigens can be detected in approximately 37-55% of CD patients compared to <5% of healthy controls (278,279). AIEC invade and replicate in macrophages, eliciting production of TNFα in the process, which may contribute to intestinal inflammation (280). It has been suggested that impaired NOD2 signalling in CD patients may promote susceptibility to AIEC infection and contribute to disease development through induction of pro-inflammatory cytokine secretion and granuloma formation (278). However, it is also possible that AIEC accumulation in CD is not a primary inducer of disease but occurs secondary to intestinal inflammation and increased mucosal permeability or commensal dysbiosis. In addition to *E.coli*, mycobacterial species such as *Mycobacterium avium* ssp. *paratuberculosis* have been implicated in IBD development, although this evidence is controversial (281-283). Moreover, *Yersinia* and *Listeria* species have been proposed as potential drivers of IBD, linking their increased prevalence due to refrigeration to the rise of IBD in industrialized countries (284).

More recently, interest has risen in the intestinal virome, the viral equivalent of the commensal bacterial flora, and its modulation of intestinal immune responses and inflammation (3). Both CD and UC are associated with an expansion of enteric *Caudovirales* bacteriophages, although the potential functional implications of this are currently unclear (285).

Immune effector pathways in IBD

As outlined discussed above GWAS data have pointed to a central role of IL-23-dependent pathways in IBD. In line with these findings, multiple mouse models of colitis have highlighted a key role of the IL-23/T_H17 axis in driving intestinal inflammation (286-290). The pro-inflammatory effects exerted by IL-23 in colitis models have been linked to its role in skewing the intestinal immune balance away from forkhead box P3 (Foxp3)$^+$ regulatory T cell (T_{Reg})-driven regulatory responses and towards T_H17-mediated pro-inflammatory responses characterised by elevated expression of cytokines such as IL-17A/F, IL-21, IL-22, IFNγ and TNFα (287,291). In IBD patients, elevated expression levels of IL-23 are observed in the inflamed intestinal mucosa (292-294). Increased IL-23 production by lamina propria-resident myeloid cells that share phenotypic markers of macrophages and DCs, as well as by infiltrating neutrophils have been reported in the inflamed lesions of IBD patients (295-297). This is associated with increased frequencies of circulating and gut-resident T_H17 cells (298) and elevated levels of IL-17A/F, IL-21 and IL-22, effector cytokines downstream of IL-23 (102,231).

In addition to the increased IL-23 driven T_H17-type responses observed in both forms of IBD, CD and UC are associated with distinct, yet complex cytokine profiles. In CD, T_H1-type responses defined by production of IL-12 and IFN-γ are elevated and thought to be driven partly by IL-23 and IL-21, and by IL-12 itself (231,299,300). Conversion of T_H17 cells towards a T_H1-like phenotype, including acquisition of IFN-γ production, seems to correlate with their *in vivo* pathogenicity in mouse models of colitis (107,301,302). In contrast, UC is associated with T_H2-type responses with increased levels of IL-5 and IL-13 in inflamed intestinal lesions (286,289,300,303).

Through the induction of chemoattractant production (CXCL1, CXCL5, CXCL8, CCL2, CCL20) in epithelial, myeloid and stromal cells, IL-17A, IL-17F and IL-21 are involved in the recruitment of neutrophils and inflammatory monocytes to the intestinal mucosa (304,305). IL-17A has also been shown to act on subepithelial myofibroblasts to initiate tissue remodelling processes via induction of MMPs and production of pro-inflammatory cytokines such as IL-6, granulocyte-macrophage colony-stimulating factor (GM-CSF) and granulocyte colony-stimulating factor (G-CSF) (304-309).

The role of IL-22 in intestinal inflammation is controversial. As outlined above, IL-22 plays a key role in the maintenance of intestinal homeostasis. While the majority of mouse colitis models have indicated a protective role of IL-22, a pro-inflammatory contribution of IL-22 in intestinal inflammation has also been reported (311). IL-22 can boost pro-inflammatory responses via induction of IL-6, TNFα, G-CSF and chemoattractant mediators in IECs and subepithelial myofibroblasts (102,104,105,108,109,310).

IFNγ has been shown to induce production of chemokines (CXCL9, CXCL10, CCL2) in IECs that contribute to recruitment of inflammatory monocytes and effector T cells to the intestinal lamina propria (312,313). IFNγ has also been shown to directly reduce intestinal epithelial barrier function by inducing downregulation of tight junction proteins in IECs. This leads to increased epithelial permeability and facilitates translocation of microbes into the intestinal lamina propria (226,230,232,314,315).

TNFα is thought to contribute to colitis through a range of pro-inflammatory effects. TNFα can induce Paneth cell death through necroptosis and can reduce epithelial barrier integrity through induction of myosin light chain kinase activity. Macrophages upregulate production of pro-inflammatory cytokines, including IL-1β, IL-6 and TNFα itself, in response to stimulation with TNFα. Furthermore, TNFα can render effector T cells resistant to apoptosis and can induce expression of MMPs in myofibroblasts (309,316).

IL-13 has been implicated in alteration of epithelial barrier function through modulation of epithelial tight junctions and induction of apoptosis of IECs (309,317). In addition, through effects on macrophages and stromal cells, IL-13 may contribute to intestinal fibrosis (318).

1.4.4 Therapeutic options

Conventional medical management of CD and UC currently includes treatment with anti-inflammatory and immunosuppressive drugs such as 5-aminosalicylic acid compounds, thiopurines (azathioprine, 6-mercaptopurine), corticosteroids, methotrexate and cyclosporine (319). In addition, biologics are emerging as important therapeutic agents for the treatment of IBD patients with severe disease or disease refractory to conventional management. Biologics approved by the European Medicines Agency (EMA) for treatment of IBD patients are listed below in Table 1.1.

Table 1.1: Current list of EMA-approved biologics for treatment of CD or UC (320)

Drug name	*Active ingredient*	*Type*	*Target*	*CD*	*UC*	*EMA approval*
Remicade	Infliximab	Chimeric mAb	TNFα	✓	✓	13/08/1999
Remsima	Infliximab biosimilar	Chimeric mAb	TNFα	✓	✓	10/09/1999
Inflectra	Infliximab biosimilar	Chimeric mAb	TNFα	✓	✓	10/09/2013
Humira	Adalimumab	Human mAb	TNFα	✓	✓	08/09/2003
Simponi	Golimumab	Human mAb	TNFα	×	✓	01/10/2009
Entyvio	Vedolizumab	Humanized mAb	$\alpha_4\beta_7$	✓	✓	22/05/2014

However, with the exception of 5-aminosalicylates and possibly vedolizumab, all above mentioned agents are broadly immunosuppressive and associated with significantly increased risk of infection and other serious side effects (321-327). Furthermore, available treatments do not effectively control disease in a large proportion of patients and approximately 70-80% of CD patients and 30% of UC patients will require surgical intervention during their lifetime. While total colectomy is curative for UC patients, albeit associated with pouchitis development in up to 45% of patients, a high rate of post-operative recurrence exists for CD patients; approximately 15% of CD patients require additional surgery after five years (319,328).

These findings highlight a need for the development of additional, more specific therapies and for improved patient stratification, which will allow more selective targeting of immune pathways active in particular subgroups of CD and UC patients.

Currently, several monoclonal antibodies and small molecule compounds are in development or being tested in clinical trials in IBD patients that aim to inhibit key cytokines involved in disease pathogenesis, including IL-23p19 (BI655066, AMG139), IL-12p40 (ustekinumab, briakinumab), IL-6(R) (tocilizumab, olokizumab, BMS945429, PF04236921, C326), IL-1β (anakinra, rilonacept, canakinumab) and IL-13 (anrukinzumab, tralokinzumab, QAX576). Further drugs are in development aiming to curb leukocyte migration into the gut (etrolizumab, PF-00547659, fingolimod) or to inhibit pro-inflammatory intracellular signalling pathways, including JAK inhibitors (tofacitinib), STAT inhibitors (pimozide), receptor tyrosine kinase inhibitors (masitinib) and a SMAD7 antisense oligonucleotide (Mongersen) (329,330).

1.5 ILCs in intestinal inflammation

While early IBD research was mainly focussed on understanding the contribution of T cells to disease pathogenesis, it soon became apparent that effector cytokines traditionally attributed to CD4$^+$ T cells could also be produced by ILCs. This prompted investigations into the role of ILCs in intestinal inflammation.

The involvement of murine ILC3 and ILC1 in intestinal inflammation has been demonstrated in a variety of colitis models. ILC3 are required for induction of innate bacterial-driven colitis in *Rag*$^{-/-}$ mice following infection with the pathogenic bacterium *H. hepaticus*. Colitis development is dependent on IL-23-induced IL-17A and IFNγ production by ILC3 that accumulate in the gut in response to IL-1β. RORγt$^+$ ILC3 are critical for colitis development, since intestinal inflammation is abrogated in *Rag*$^{-/-}$*Rorc*$^{-/-}$ mice that lack ILC3 (331,332). Pathogenic IL-17A production by intestinal ILC3 has also been shown to underlie the development of spontaneous colitis in *Tbx21*$^{-/-}$*Rag*$^{-/-}$ (TRUC) mice. In this model, ILC3 accumulate in the intestinal lamina propria and are activated in response to TNFα, IL-23 and IL-6 produced by activated DCs (198,333). Moreover, IFNγ- and TNFα-producing NKp46$^+$RORγt$^-$ 'ex-ILC3' and intraepithelial ILC1 are known to mediate intestinal inflammation in mice treated with anti-CD40 antibody (47,191).

It is well documented that murine ILC2 can contribute to allergic inflammation in the lung and skin through their production of the Type 2 effector cytokines IL-4, IL-5, IL-9 and IL-13 in response to IL-25, IL-33, TSLP and TNF-like ligand 1A (TL1A) secreted by activated epithelial, stromal and myeloid cells (10,70,84,133,334-337). However, little is known regarding the potential involvement of ILC2 in intestinal inflammation. One report has described a pathogenic role for IL-13-producing ILC2 in a mouse model of oxazolone-induced colitis (338).

Open questions remain regarding the involvement of human ILCs in intestinal inflammation. At the beginning of this study, data from our lab indicated that IL-23-responsive ILCs enriched for expression of IL-17A and IFNγ accumulated in the inflamed intestinal mucosa of CD patients, suggesting that ILCs may contribute also to human intestinal inflammation (discussed in detail in Chapter 3) (185).

1.6 Aims

Murine studies have highlighted important roles for intestinal ILCs in host-protective and homeostatic immune responses, but also in driving pathogenic intestinal inflammation. However, less is known about the function of human ILC populations. As the majority of murine studies examining ILC function have been performed in *Rag*$^{-/-}$ mice deficient of T and B cells, a crucial open question is how these rare cells impact homeostatic or, in the case of IBD, pathogenic immune responses in the presence of a functional adaptive immune system.

This thesis aims to characterise human ILCs in the context of IBD and to investigate potential mechanisms by which these cells can contribute to intestinal inflammation, focussing on several key areas:

- Characterisation of the frequency, phenotype and activation state of ILCs in peripheral blood and intestinal lamina propria of IBD patients compared to uninflamed controls.
- Examination of the *in situ* localization characteristics of CD3^{-}RORγt^{+} ILCs in the intestinal lamina propria.
- Evaluation of the capacity of human ILCs to act as antigen-presenting cells to CD4^{+} T cells.
- Investigation of functional interactions between ILCs and monocytes and the effects thereof on CD4^{+} T cells.

These experiments aim to provide insight into how ILCs as a rare immune cell population can contribute to pathogenic intestinal immune responses in the context of two key players implicated in IBD pathogenesis, CD4^{+} T cells and monocytes.

Chapter 2: Materials and methods

2.1 Study subjects

IBD and colorectal cancer (CRC) (control) patients were recruited and consented at the John Radcliffe Hospital and Churchill Hospital, Oxford, through the Oxford IBD cohort study and Oxford Radcliffe Biobank (ORB). The diagnosis of CD or UC was made on the basis of established clinical, endoscopic, radiological and histological criteria. In the case of IBD patients, gut specimens were collected from patients undergoing surgical resection for severe or chronically active disease. Intestinal specimens from non-tumour resection margins were collected from CRC patients and used as non-inflammatory controls. For both CRC and IBD patients, ileal, small intestinal, colonic and rectal specimens were collected.

IBD blood samples were collected mainly from patients attending the outpatient clinic, and only in some cases from patients undergoing surgery. Control blood samples were obtained from healthy volunteers or from leukocyte cones obtained from the National Health Services (NHS) Blood & Transplant centre at the John Radcliffe Hospital.

2.2 Ethics

Ethical approval was obtained through the NHS Research Ethics System (Reference numbers: 09/H1204/30 for IBD patients and 11/YH/0020 for controls). Informed written consent was obtained from all study participants.

2.3 Clinical patient data

The tissue specimens received in the Translational Gastroenterology Unit (TGU) were completely anonymised by the ORB prior to hand-over and only identifiable through an assigned IBD or ORB number. Upon request, information regarding diagnosis and in some cases treatment history and would be made available without revealing patient identity.

2.4 Preparation of tissue for histology

2.4.1 Preparation of tissue specimens for frozen sections

Tissues for the generation of frozen sections were cut into small approximately 1 cm^3 pieces, placed in Tissue-Tek® Cryomold® Biopsy containers (Sakura) and immersed in Tissue-Tek® O.C.T. Compound (Sakura). This was followed by rapid freezing on a layer of isopentane (Sigma) pre-cooled on dry ice. Frozen blocks were stored at -80°C.

2.4.2 Cutting of tissue sections

Frozen sections were cut to a thickness of 5μm using microtome and cryostat, respectively. Following adherence to the microscopy slides (Superfrost Plus™, Fisher Scientific), sections were dried at room temperature (RT) for 1h before storage either at RT (FFPE sections) or -20°C (frozen sections).

2.5 Immunofluorescence

Antibodies used for double and triple staining are listed in Table 2.2. Images were acquired on a Zeiss Axioscope. Image analysis was performed using ImageJ (339).

Table 2.1: Primary and secondary antibodies used for immunofluorescence

Specificity	*Clone*	*Species*	*Conjugated*	*Dilution*	*Company*
Primary antibodies					
CD3	SP7	Rabbit	Unconjugated	1:100	Abcam
CD127	eBioRDR5	Mouse	Unconjugated	1:10	EBioscience
RORγ	AFKJS-9	Rat	Unconjugated	1:20	EBioscience
Secondary antibodies					
Anti-rabbit	Polyclonal	Donkey	HRP	1:100	Jackson ImmunoResearch
Anti-mouse	Polyclonal	Donkey	HRP	1:100	Jackson ImmunoResearch
Anti-rat	Polyclonal	Donkey	HRP	1:100	Jackson ImmunoResearch

Frozen tissue sections were obtained from OCT-embedded resection material as described in Sections 2.4 and 2.5. Following defrosting at RT for 5 mins, the sections were fixed in cold acetone for 3 mins at -20°C. In order to preserve better tissue morphology, this was followed by fixation in 2% formalin for 3 mins at RT. Endogenous peroxidase activity and non-specific antibody binding were blocked by incubating the sections in a mixture of 1% (vol/vol) of 0.13% sodium azide + 1 % (vol/vol) of 30% H_2O_2 + 10% donkey serum for 2 x 15 mins at RT. After washing in phosphate buffered saline (PBS) for 3 x 5 mins, primary antibody was added (diluted in PBS + 2% donkey serum). Following incubation for 30 mins at RT, the sections were washed and incubated with horseradish peroxidase (HRP)-conjugated secondary antibody. After additional washing steps in PBS, this was followed by incubation with fluorescent Cy3-tyramide or Cy5-tyramide TSA™ reagents (diluted 1:300 in tyramide amplification buffer) (Perkin Elmer), allowing the visualization of specific signals. If double stainings were performed this was followed by intranuclear staining (see below), whereas for triple stainings, a second round of surface staining was performed after blocking endogenous peroxidase activity as described above.

For intranuclear staining for RORγ, sections were permeabilized by incubating in cold fixation/permiabilization buffer (Foxp3 staining kit, EBioscience) for 5 mins. After blocking endogenous peroxidase activity, the sections were incubated with anti-RORγ antibody for 2h at RT or overnight at 4°C. The sections were then washed in PBS, incubated with anti-rat-HRP antibody (1h, RT) and specific binding visualized using fluorescein isothiocyanide (FITC)-tyramide TSA™ reagent diluted 1:300 in tyramide amplification buffer (Perkin Elmer). Finally, sections were dried at RT and mounted using DAPI-containing Vectashield Mounting Medium for Fluorescence (Vector Laboratories).

2.6 Cell isolation from peripheral blood and tissues

2.6.1 Peripheral blood mononuclear cell (PBMC) isolation

Peripheral blood was diluted in an equal volume of PBS and layered onto 15ml of Lymphoprep™ (Axis-Shield). This was followed by centrifugation at 900 x g at RT for 20 mins. PBMCs were collected from the Lymphoprep™-plasma interface and washed 3x in PBS before further use.

2.6.2 Lamina propria mononuclear cell (LPMC) isolation

LPMCs from surgical resection specimens were isolated following a protocol previously established in the lab. Specimens were washed in Hank's Balanced Salt Solution (HBSS), followed by dissection along the muscularis mucosa to separate the mucosa from the underlying submucosa. To remove the mucous layer, the mucosa was incubated in dithiothreitol (DTT) solution (HBSS supplemented with 1mM DTT (Life Technologies)) on a shaker at RT for 2 x 15 mins. To detach the epithelial layer, the specimen was then cut into small pieces (<25 mm^2) and transferred to a vented Erlenmeyer flask (Corning) for washes in ethylenediaminetetraacetic acid (EDTA) solution (HBSS supplemented with 0.75 mM EDTA) at 37°C for 3 x 30 min. Following this, supernatants were carefully removed and the specimen washed in HBSS in order to remove any remaining EDTA, which is an inhibitor of collagenase activity. The tissue was then immersed in collagenase solution made up of RPMI-1640 supplemented with 10% foetal calf serum (FCS) (Gibco) and 0.1 mg/ml collagenase A solution (Roche Diagnostics), and left to digest overnight (12-18h) at 37°C in a vented Erlenmeyer flask with a magnetic stirrer for additional mechanical disruption. The next day, supernatants were harvested, filtered through 70μm cell strainers (Fisher Scientific) and washed 3x in RPMI-1640 + 10% FCS. Cells were resuspended in a 40% Percoll solution (GE Healthcare) and were then layered onto a 100% / 60% / 40% / 30% Percoll gradient and centrifuged for 30 mins at 600 x g at 4°C. Finally, LPMCs were collected from the 40% / 60% interface and washed in HBSS before further use. All solutions used in the isolation procedure were supplemented with penicillin/streptomycin solution (1% vol/vol) (Life Technologies), gentamicin (40 μg/ml) (Life Technologies), and amphotericin B (0.025 μg/ml) (Lonza).

2.6.3. Fat mononuclear cell isolation

Visceral fat surrounding tissue specimen was separated from the gut tissue, washed in HBSS, cut into small pieces and digested overnight (12-18h) in vented Erlenmeyer flasks (Corning) using collagenase solution (RPMI-1640 + 10% FCS + 0.1 mg/ml collagenase A solution (Roche Diagnostics)). The next day, supernatants were filtered through 70μm cell strainers (Fisher Scientific) and washed 3x in HBSS before FACS staining. All solutions used in the isolation procedure were supplemented with penicillin/streptomycin solution (1% vol/vol) (Life Technologies), gentamicin (40 μg/ml) (Life Technologies), and amphotericin B (0.025 μg/ml) (Lonza).

2.7 Flow cytometry

2.7.1 Antibodies used for flow cytometry analysis

Table 2.2 lists antibodies used for flow cytometry. Stained cells were acquired on a BD Fortessa or LSRII. Analysis was performed using FlowJo software (TreeStar Inc.).

Table 2.2: Antibodies used for flow cytometry

Specificity	***Clone***	***Species***	***Fluorochrome***	***Dilution***	***Company***
Surface					
CD1a	HI149	Mouse	FITC	1:50	Biolegend
CD3	UCHT1	Mouse	FITC	1:100	Biolegend
CD3	OKT3	Mouse	BV510	1:100	Biolegend
CD3	OKT3	Mouse	eFluor 605	1:100	Biolegend
CD3	OKT3	Mouse	BV650	1:100	Biolegend
CD4	OKT4	Mouse	FITC	1:100	Biolegend
CD4	OKT4	Mouse	BV605	1:100	Biolegend
CD8α	HIT8a	Mouse	FITC	1:100	Biolegend
CD8α	RPA-T8	Mouse	PE/TxR	1:100	BD Bioscience
CD11b	ICRF44	Mouse	FITC	1:100	Biolegend
CD11c	3.93	Mouse	FITC	1:100	Biolegend
CD14	61D3	Mouse	FITC	1:50	Biolegend
CD14	M5E2	Mouse	BV605	1:100	Biolegend
CD14	M5E2	Mouse	BV650	1:100	Biolegend
CD16	3G8	Mouse	FITC	1:50	Biolegend
CD19	HIB19	Mouse	FITC	1:50	Biolegend
CD19	HIB19	Mouse	BV605	1:50	Biolegend
CD20	2H7	Mouse	FITC	1:100	Biolegend
CD25	BC96	Mouse	APC	1:50	Biolegend
CD34	4H11	Mouse	FITC	1:50	Biolegend
CD40	5C3	Mouse	APC	1:50	Biolegend
CD45	HI30	Mouse	PE/Cy7	1:100	Biolegend
CD45	RA3-6B2	Mouse	Alexa 700	1:100	Biolegend
CD45RA	HI100	Mouse	PE/Cy7	1:100	Biolegend
CD45RO	BV570	Mouse	UCHL1	1:100	Biolegend
CD56	HCD56	Mouse	PcP/Cy5.5	1:50	Biolegend
CD56	HCD56	Mouse	BV510	1:50	Biolegend
CD70	113-16	Mouse	APC	1:50	Biolegend
CD80	2D10	Mouse	BV650	1:50	Biolegend

CD83	HB15e	Mouse	FITC	1:50	Biolegend
CD86	IT2.2	Mouse	BV605	1:50	Biolegend
CD117	A3C6E2	Mouse	PE/Cy5	1:100	Biolegend
CD117	104D2	Mouse	PE/Cy7	1:100	Biolegend
CD123	6H6	Mouse	FITC	1:20	Biolegend
CD127	A019D5	Mouse	PB	1:50	Biolegend
CD127	A019D5	Mouse	BV421	1:100	Biolegend
CD127	eBioRDR5	Mouse	APC	1:100	EBioscience
CD127	A019D5	Mouse	PE	1:100	Biolegend
CD127	A019D5	Mouse	PE/Cy7	1:100	Biolegend
CD161	HP-3G10	Mouse	APC	1:50	EBioscience
CD161	HP-3G10	Mouse	BV421	1:50	Biolegend
BDCA-2	201A	Mouse	FITC	1:50	Biolegend
CRTH2	BM16	Rat	PE	1:20	Biolegend
CRTH2	BM16	Rat	biotin	1:25	Miltenyi
FcεRI	AER-37	Mouse	FITC	1:50	Biolegend
HLA-DR	L243	Mouse	PcP/Cy5.5	1:50	Biolegend
ICOS	C398.4A	Mouse	PE	1:50	Biolegend
OX40	ACT35	Mouse	PE/Cy7	1:50	Biolegend
OX40L	11C3.1	Mouse	PE	1:25	Biolegend
PD1	EH12.2H7	Mouse	BV711	1:50	Biolegend
PD-L1	29E.2A3	Mouse	BV421	1:50	Biolegend
PD-L2	24F.10C12	Mouse	PE	1:50	Biolegend
TCRαβ	IP26	Mouse	FITC	1:50	Biolegend
TCRαβ	IP26	Mouse	PE	1:100	Biolegend
TCRγδ	B1.1	Mouse	FITC	1:50	Biolegend
TCRγδ	B1.1	Mouse	APC	1:100	Biolegend
CCR6	11A9	Mouse	PE	1:100	Biolegend
CCR6	G034E3	Mouse	BV605	1:100	Biolegend
CCR7	3D12	Mouse	APC	1:50	EBioscience
CCR9	112509	Mouse	Unconjugated	1:50	R&D Systems
Biotinylated Abs for MACS					
CD1a	HI149	Mouse	Biotin	1:500	Biolegend
CD8	HIT8α	Mouse	Biotin	1:500	Biolegend
CD14	HCD14	Mouse	Biotin	1:500	Biolegend
CD16	3G8	Mouse	Biotin	1:500	Biolegend
CD19	HIB19	Mouse	Biotin	1:500	Biolegend
CD25	BC96	Mouse	Biotin	1:500	Biolegend
CD34	581	Mouse	Biotin	1:500	Biolegend
CD45RA	H100	Mouse	Biotin	1:1250	Biolegend
CD56	HCD56	Mouse	Biotin	1:500	Biolegend

NKp44	P44-8	Mouse	Biotin	1:500	Biolegend
CD95	DX2	Mouse	Biotin	1:500	Biolegend
CD123	6H6	Mouse	Biotin	1:500	Biolegend
Secondary antibodies					
SA-PE-CF594	---	---	PE-CF594	1:300	BD Bioscience
SA-PE	---	---	PE	1:100	EBioscience
Intracellular - cytokines					
IL-17A	4S.B3	Mouse	PE	1:10	Biolegend
IL-17A	BL168	Mouse	BV711	1:150	Biolegend
IL-22	2G12A41	Mouse	PE	1:150	Biolegend
IL-22	22URTI	Mouse	PE/Cy7	1:150	EBioscience
GM-CSF	BVD221C11	Mouse	PcP/Cy5.5	1:150	Biolegend
GM-CSF	BVD221C11	Mouse	APC	1:150	Biolegend
IL-4	MP4-25D2	Mouse	PE	1:150	Biolegend
IL-5	TRFK5	Mouse	APC	1:150	Biolegend
IL-13	PVM13-1	Mouse	FITC	1:150	EBioscience
IFNγ	B27	Mouse	A700	1:100	Biolegend
TNFα	MAB11	Mouse	BV605	1:150	Biolegend
IL-2	MQ1-17H12	Mouse	BV650	1:150	Biolegend
IL-10	JES3-9D7	Mouse	BV421	1:150	Biolegend
Intracellular-transcription factors					
Ki67	B56	Mouse	PE	1:50	EBioscience
Ki67	B56	Mouse	FITC	1:50	EBioscience
Foxp3	PCH101	Mouse	PE/Cy7	1:50	EBioscience
RORγt	Q21-559	Rat	PE	1:150	BD Bioscience
Tbet	4B10	Mouse	BV421	1:150	EBioscience
Tbet	4B10	Mouse	BV711	1:150	EBioscience
Eomes	WD1928	Mouse	PcP/Cy5.5	1:150	EBioscience
GATA3	TWAJ	Mouse	APC	1:50	EBioscience
GATA3	TWAJ	Mouse	PE	1:150	EBioscience

2.7.2 Staining for surface antigens

FACS buffer (PBS + 2% BSA + 2mM EDTA) was used to make up antibody dilutions and perform washing and resuspension steps. FACS stainings were performed in V-bottom 96-well plates or 1.5 ml Eppendorf tubes at cell densities of approximately 1-15 x 10^6 cells per well or tube. This was followed by incubation with appropriately diluted antibody mixes supplemented with fixable viability dye eFluor780 (eBioscience) (at a final dilution of 1:1000) for 30 mins on ice. Cells were washed 3x in FACS buffer. For antibody mixes containing biotinylated primary antibodies, this was followed by incubation with streptavidin-labelled secondary antibodies diluted (1:300 in FACS buffer) for 20 mins on ice. After washing 3x in FACS buffer, cells were then fixed at RT in 2% PFA solution (Electron Microscopy Sciences) diluted in PBS for 15 mins or in BD FACS Lysing Solution (BD Biosciences) diluted 1:10 in dH_2O for 8 mins. Finally, cells were resuspended in 200µl of FACS buffer.

2.7.3 Intracellular staining for cytokines

In preparation for intracellular cytokine staining (ICS), cells were stimulated with phorbol 12-myristate 13-acetate (PMA) (100 ng/ml) (Sigma Aldrich) and ionomycin (1 µg/ml) (Sigma Aldrich) at 37°C for 4h in the presence of Golgistop (1:1000) (BD Bioscience) and Golgiplug (1:1000) (BD Bioscience). After washing 3x in FACS buffer, cells were stained for surface markers and fixed as described above. The cells were then washed and resuspended in the anti-cytokine antibody mix diluted in saponin solution (0.1% w/v saponin (Sigma-Aldrich) in PBS) for 1h on ice. Cells were then washed three times before final resuspension in 200µl of FACS buffer.

2.7.4 Intranuclear staining for transcription factors

Unless otherwise indicated, FACS buffer (PBS + 2% BSA + 2mM EDTA) was used to perform washing and final resuspension steps. Following staining for surface markers as described above, cells were fixed in ice-cold fixation/permeabilization buffer (Foxp3 staining kit, EBioscience) for 30 mins on ice. Cells were washed 1x in ice-cold Permeabilization buffer (Foxp3 staining kit, EBioscience). This was followed by re-suspension in antibody mix diluted in Permeabilization buffer and incubation for 30 mins-1h on ice. Immediately before flow cytometry analysis, cells were collected by centrifugation (500 x g, 5 mins at 4°C) and resuspended in 200µl of ice-cold FACS buffer.

2.8 Magnetic-activated cell sorting (MACS)

2.8.1 Monocyte enrichment

Following isolation from human peripheral blood, PBMCs re-suspended in RPMI-1640 + 10% FCS, transferred to petri dishes and incubated at 37°C to allow monocyte adherence to the dish. After 2.5 -3 h of adhesion, non-adherent cells and supernatants were carefully removed from the petri dishes. The adherent cells were collected using vigorous pipetting. Monocytes were then further purified from the adherent fraction by magnetic cell sorting using a MACS® CD14 human microbead kit (Miltenyi Biotec) according to the manufacturer's protocol. Following labelling with beads, cells were sorted using an AutoMACS® separator (Miltenyi Biotec). Monocytes were routinely enriched to purities ≥ 95% as assessed by FACS.

2.8.2 PBMC pre-enrichment for naïve and memory CD4$^+$ T cell

Before FACS sorting naïve and memory CD4$^+$ T cells from human peripheral blood, PBMCs were pre-enriched for these populations via depletion of non-target cell populations. For naïve CD4$^+$CD45RA$^+$ T cell enrichment, PBMCs were labeled using biotin-conjugated anti-CD8, anti-CD19, anti-NKp44, anti-CD14, anti-CD16, anti-CD25, anti-CD45RO, anti-CD34, anti-CD123 and anti-CD1a antibodies. For memory CD4$^+$CD45RO$^+$ T cell enrichment, PBMCs were labeled using biotin-conjugated anti-CD8, anti-CD19, anti-NKp44, anti-CD14, anti-CD16, anti-CD25, anti-CD95, anti-CD45 RA, anti-CD34, anti-CD123, anti-CD1a and anti-CD56 antibodies. The labeled non-target cells were then depleted using MACS® Anti-Biotin MicroBeads (Miltenyi Biotec) according to the manufacturer's protocol on an AutoMACS® separator (Miltenyi Biotec).

2.8.3 PBMC pre-enrichment for ILC sorts

For ILC subset sorts from human peripheral blood, PBMCs were pre-enriched before FACS sorting using a RosetteSep™ human NK cell enrichment kit (StemCell Tehcnologies) according to the manufacturer's protocol.

2.9 Fluorescence-activated cell sorting (FACS)

All sorts were performed in the Nuffield Department of Medicine (NDM) Experimental Medicine flow cytometry facility using a FACSAriaIII cell sorter (BD Biosciences).

2.9.1 Sorting of ILC populations

In a two-step staining approach PBMCs pre-enriched for ILCs (see 2.9.3) were labeled with anti-Lineage (CD1a, CD3, CD4, CD8, TCRαβ, TCRγδ, CD11b, CD11c, CD14, CD16, CD19, CD20, CD34, CD94, CD123, FcεRI, BDCA-2) – FITC; CD45 – AF700; TCRαβ – PE; TCRγδ – APC; CD3 – BV650; CD127 – BV421; CD56 – BV510 or PcP/Cy5.5; CD117 – PE/Cy5 or PE/Cy7; CRTH2 – biotin and SA-PE/TxR antibodies as well as viability dye in eFluor780.

The following four cell populations were then sorted into RPMI-1640 + 50% FCS according to expression of cell surface markers:
ILC3: Live CD45^{+} CD3^{-} TCRαβ^{-} TCRγδ^{-} Lin^{-} CD127^{+} CD56^{-} CD117^{+} CRTH2^{-}
ILC2: Live CD45^{+} CD3^{-} TCRαβ^{-} TCRγδ^{-} Lin^{-} CD127^{+} CD56^{-} CRTH2^{+}
ILC1: Live CD45^{+} CD3^{-} TCRαβ^{-} TCRγδ^{-} Lin^{-} CD127^{+} CD56^{-} CD117^{-} CRTH2^{-}
cNK cells: Live CD45^{+} CD3^{-} TCRαβ^{-} TCRγδ^{-} CD127^{-} CD56^{+}

For ILC sorts from LPMCs, cells were labeled with anti-Lineage (CD1a, CD3, CD4, CD8, T cell receptor (TCR)αβ, TCRγδ, CD11b, CD11c, CD14, CD16, CD19, CD20, CD34, CD94, CD123, FcεRI, BDCA-2) – FITC; CD45 – AF700; TCRαβ – biotin; TCRγδ – biotin; NKp44 – APC; CD3 – BV650; CD127 – BV421; CD56 – BV510 or PcP/Cy5.5; CD117 –

PE/Cy5 or PE/Cy7; CRTH2 – PE and SA-PE/TxR antibodies as well as viability dye in eFluor780.

The following populations were sorted into RPMI-1640 + 50% FCS:

ILC3: Live $CD45^+$ $CD3^-$ $TCR\alpha\beta^-$ $TCR\gamma\delta^-$ Lin^- $CD127^+$ $CD56^-$ $CD117^+$ $NKp44^+$ $CRTH2^-$

ILC2: Live $CD45^+$ $CD3^-$ $TCR\alpha\beta^-$ $TCR\gamma\delta^-$ Lin^- $CD127^+$ $CD56^-$ $NKp44^-$ $CRTH2^+$

ILC1: Live $CD45^+$ $CD3^-$ $TCR\alpha\beta^-$ $TCR\gamma\delta^-$ Lin^- $CD127^+$ $CD56^-$ $CD117^-$ $NKp44^-$ $CRTH2^-$

cNK cells: Live $CD45^+$ $CD3^-$ $TCR\alpha\beta^-$ $TCR\gamma\delta^-$ $CD127^-$ $CD56^+$

2.9.2 Sorting of memory $CD4^+$ T cells

Pre-enriched PBMCs were labeled with anti-CD45 – AF700; anti-CD4 – FTIC; anti-CD8 – PE/TxR; CD45RO – BV570; CD45RA – PE/Cy7 amtibodies as well as viability dye in eFluor780. Memory $CD4^+$ T cells were sorted into RPMI-1640 + 50% FCS as Live $CD45^+$ $CD8^-$ $CD4^+$ $CD45RO^+$ $CD45RA^-$

2.9.3 Sorting of *Salmonella*-specific memory T cells on basis of CFSE dilution

Following expansion of CFSE-labelled $CD4^+$ $CD45RO^+$ memory T cells with irradiated autologous monocytes pulsed with *Salmonella* lysate antigen, *Salmonella*-reactive T cells were sorted on the basis of CFSE dilution and ICOS upregulation. T cells were labeled with anti-ICOS – PE and anti-CD4 – BV605 antibodies as well as viability dye in eFluor780. *Salmonella*-specific T cells were identified as $CD4^+$ $CFSE^{low}$ $ICOS^{high}$ cells and sorted into RPMI-1640 + 50% FCS.

2.10 Absolute cell counts

2.10.1 Full blood counts

Full blood counts from some control and IBD patients were obtained using a haematology analyser (Abx Pentra 60, Horiba Abx Diagnostics).

2.10.2 Absolute cell counts using flow cytometry

Absolute cell counts in *in vitro* experiments were obtained using CountBright™ Absolute Counting beads for flow cytometry (Life Technologies) according to the manufacturer's protocol.

2.11 RNA extraction and cDNA synthesis

Cells were lysed in RLT buffer (Qiagen) supplemented with β-mercaptoethanol and then stored at -80°C. RNA extraction was performed using RNeasy Mini kits (Qiagen) according to the manufacturer's protocol. DNase incubation steps were performed to avoid contamination with genomic DNA. Concentration and quality of RNA were assessed using a NanoDrop (Thermo Scientific). RNA was stored at -80°C. cDNA synthesis was performed using SuperScript® III Reverse Transcriptase (Invitrogen) and Oligo (dT) primers (Invitrogen) according to the manufacturer's protocol. After synthesis, cDNA was diluted in Milli-Q water (Millipore) and stored at -20°C.

2.12 Gene expression analysis

Quantitative real-time polymerase chain reaction (qRT-PCR) was performed using TaqMan® Gene Expression Assays (Life Technologies) according to the manufacturer's protocol. Detection occurred through a CFX384 Touch™ Real-Time PCR Detection System (Bio-Rad). Reactions for all samples were set up in triplicate and β-actin was included as a housekeeping gene. Gene expression levels for each sample were normalized to β-actin and expressed as $2^{-\Delta CT}$ ($\Delta CT = CT_{\text{target gene}} - CT_{\text{ACTB}}$), unless otherwise indicated. The TaqMan® gene expression assays used are listed in Table 2.3.

Table 2.3: TaqMan gene expression assays

Gene	*Entrez Gene ID*	*Transcript*	*Reporter Dye*	*Company*	*Assay ID*
RORC	6097	NM_005060	FAM	Life Technologies	Hs01076122_m1
AHR	196	NM_001621	FAM	Life Technologies	Hs00169233_m1
TBX21	30009	NM_013351	FAM	Life Technologies	Hs00203436_m1
EOMES	8320	NM_005442	FAM	Life Technologies	Hs00172872_m1
GATA3	2625	NM_002051	FAM	Life Technologies	Hs00231122_m1
RORA	6095	NM_002943	FAM	Life Technologies	Hs00536545_m1
ID2	3398	NM_002166	FAM	Life Technologies	Hs04187239_m1
HLADMA	3108	NM_006120	FAM	Life Technologies	Hs00185435_m1
HLADMB	3109	NM_002118	FAM	Life Technologies	Hs00157943_m1
HLADRA	3122	NM_019111	FAM	Life Technologies	Hs00219575_m1
CD74	972	NM_004355	FAM	Life Technologies	Hs00269961_m1
CD80	941	NM_005191	FAM	Life Technologies	Hs00175478_m1
CD83	9308	NM_004233	FAM	Life Technologies	Hs00188486_m1
TNFSF4	7292	NM_003326	FAM	Life Technologies	Hs00182411_m1
TNFSF14	8740	NM_003807	FAM	Life Technologies	Hs00542477_m1
LTA	4049	NM_000595	FAM	Life Technologies	Hs04188773_g1

LTB	4050	NM_002341	FAM	Life Technologies	Hs00242739_m1
IL4	3565	NM_000589	FAM	Life Technologies	Hs00174122_m1
IL13	3596	NM_002188	FAM	Life Technologies	Hs00174379_m1
IL22	50616	NM_020525	FAM	Life Technologies	Hs01574154_m1
IFNG	3458	NM_000619	FAM	Life Technologies	Hs00989291_m1
CSF2	1437	NM_000758	FAM	Life Technologies	Hs00929873_m1
IL1R1	3554	NM_000877	FAM	Life Technologies	Hs00991002_m1
IL2RA	3559	NM_000417	FAM	Life Technologies	Hs00907779_m1
IL6R	3570	NM_000565	FAM	Life Technologies	Hs01075666_m1
IL10RA	3587	NM_001558	FAM	Life Technologies	Hs00155485_m1
IL10RB	3588	NM_000628	FAM	Life Technologies	Hs00175123_m1
IL12RB1	3594	NM_005535	FAM	Life Technologies	Hs00538167_m1
IL23R	149233	NM_144701	FAM	Life Technologies	Hs00332759_m1
IL1RL1	9173	NM_003856	FAM	Life Technologies	Hs00545033_m1
ACTB	60	NM_001101	FAM	Life Technologies	Hs01060665_g1

2.13 Cell culture

2.13.1 Media

Complete growth medium used for ILC and T cell cultures consisted of RPMI-1640 supplemented with with human serum (2% vol/vol) (Sigma-Aldrich), MEM Non-Essential Amino Acids solution (1% vol/vol) (Life Technologies), beta-mercaptoethanol (0.05 mM), sodium pyruvate (1 mM) (Life Technologies), L-glutamine (Life Technologies) and penicillin/streptomycin solution (1% vol/vol) (Life Technologies).

2.13.1 Cytokines used for *in vitro* experiments

Human recombinant cytokines used in the course of this study are listed in Table 2.4.

Table 2.4 Cytokines used for *in vitro* experiments and stimulations

Cytokine	*Concentration used*	*Company*
IL-1β	50 ng/ml	Peprotech
IL-2	100 U/ml or 200 U/ml	Peprotech
IL-2 IS	100 U/ml or 200 U/ml	Miltenyi Biotec
IL-6	20 ng/ml	Peprotech
IL-7	50 ng/ml	Peprotech
IL-7	50 ng/ml	R&D Systems
IL-10	10 ng/ml	Peprotech
IL-12	50 ng/ml	Peprotech
IL-15	10 ng/ml	R&D Systems
IL-17A	20 ng/ml	Peprotech
IL-18	50 ng/ml	Peprotech
IL-23	50 ng/ml	Peprotech
IL-33	50 ng/ml	Peprotech
IFNγ	10 ng/ml	Peprotech
TNFα	10 ng/ml	Peprotech
TGFβ	10 ng/ml	Peprotech
M-CSF	100 ng/ml	Peprotech
LTα	20 ng/ml	Peprotech

2.13.2 ILC expansion

FACS sorted ILC1, ILC2, ILC3 and cNK populations were plated in round-bottom 96-well plates (1 x 10^3 cells/well) on a feeder layer of mixed irradiated PBMCs (45 Gy) from three allogeneic donors (1 x 10^5 cell/well). The culture medium used was complete growth medium supplemented with IL-2 (100 U/ml) and/or IL-7 (50 ng/ml). Phytohaemagglutinin (PHA) (1μg/ml) was added once at the beginning of the cultures. IL-2 and IL-7 were replenished every three days. ILCs were cultured for up to 6 weeks before being used in experimental assays. The culture purity was assessed using flow cytometry before every experiment and if necessary cells were re-sorted.

2.13.3 ILC supernatants

To generate ILC supernatants for use in gentamycin protection assays, ILC2 and ILC3 that had been expanding *in vitro* for approximately 3-4 weeks were washed 3x in PBS in order to remove any remaining PHA. ILCs were resuspended in complete growth medium and re-seeded at a density of 2 x 10^5 cells/well in 96-well round-bottom plates. Supernatants were collected after three days of culture.

2.13.4 Measuring cell proliferation

In vitro proliferation of target cells was measured using CellTrace™ CFSE or Violet reagents (Life Technologies) according to the manufacturer's protocol. Briefly, CellTrace™ reagents were stored at -20°C in the dark. Stock solutions were prepared by resuspension in DMSO at a concentration of 5 mM. Target cells were resuspended in ice-cold PBS + 1% BSA and CellTrace™ CFSE or Violet were added to a final concentration of 5 μM, followed by incubation in the dark for 5 mins at RT. The cells were then washed 3x in ice-cold PBS + 1% BSA.

2.13.5 Expansion of *Salmonella*-specific CD4$^+$ memory T cells

CD4$^+$ CD45RO$^+$ memory T cells were FACS sorted from human peripheral blood as described above and labelled with carboxyfluorescein succinimidyl ester (CFSE). Autologous monocytes were purified using adherence and MACS CD14$^+$ cell enrichment as described above to achieve purities ≥95%. Monocytes were irradiated (45 Gy), resuspended in complete growth medium and seeded onto flat-bottom 96-well plates at densities of 1×10^4 monocytes/well. *S. typhimurium* lysate was added to each well (1:1000) followed by incubation for 6 – 8h at 37°C to allow antigen uptake and processing. Following this, CFSE-labelled T cells were added at a density of 2×10^4 T cells/well and allowed to expand for 10d. Monocyte-T cell co-cultures without addition of bacterial antigens were used as negative controls of T cell proliferation. Addition of staphylococcal enterotoxin B (SEB) (Sigma-Aldrich) was used as a positive control for T cell proliferation. Following expansion for 10d, cells were harvested and stained with anti-CD4, anti-CD8, anti-CD14 and anti-ICOS antibodies as well as viability dye. *Salmonella*-responsive T cells (Live CFSE$^-$ CD8$^-$ CD14$^-$ CD4$^+$ ICOS^{high}) were FACS sorted and seeded in round-bottom 96-well plates at a density of 10^4 cells/well in complete growth medium supplemented with IL-2 (200 U/ml). Dynabead® CD3/CD28 human T activator beads (Life Technologies) were added at a density of 1 bead : 2 T cells, and T cells were allowed to expand for 5 – 7d. Cells were transferred to 48-well plates when the medium turned yellow.

2.13.6 Macrophage differentiation

PBMC were isolated by Ficoll gradient centrifugation. Monocyte-derived macrophages (MDM) were differentiated from the adherent fraction of PBMC over a period of 5 days in RPMI-1640 medium supplemented with 10% FCS and macrophage colony-stimulating factor (M-CSF) (100 ng/ml).

2.13.7 Inducer assay

Depending on the experiment, equal cell numbers of stromal cells (colonic fibroblast cell line CCD18co) and in vitro expanded ILC populations (5×10^3 or 1×10^4, depending on the experiment) were co-cultured in flat-bottom 96-well plates for 3-4d in complete growth medium. Cells were then harvested and stromal cell activation was assessed using FACS. Stroma-ILC co-cultures were compared to stromal cells activated with TNFα (10 ng/ml), LTα (20 ng/ml) and IL-17A (20 ng/ml).

2.13.8 Preparation of bacterial lysates for T cell assays

Bacterial lysates were generated from *Bifidobacterium animalis* subsp. *lactis* Bi-07 (*Bifidobacterium*) and *Salmonella enterica serovar typhimurium* (*S. typhimurium*). Microbes were killed by heating at 65 °C for 1 h according to standard methods, followed by three freeze-thaw cycles.

2.14 Antigen uptake and processing assays

2.14.1 DQ-OVA assay

DQ™ Ovalbumin (Life Technologies) is a self-quenching conjugate of ovalbumin linked to BODIPY® FL dye (Life Technologies). Following uptake and proteolytic degradation through the endocytic pathway, DQ-OVA emits bright green fluorescence that can be detected by flow cytometry. It is therefore a useful tool to assess the capacity of target cells to take up and proteolytically process protein antigen. Lyophilized DQ-OVA was reconstituted in PBS to a stock concentration of 1 mg/ml. Target cells were resuspended in RPMI-1640 + 10% FCS. DQ-OVA was added to a final concentration of 10 µg/ml, followed by 4h of incubation on ice to inhibit antigen uptake (negative control) or at 37°C. The cells were then washed, stained for surface antigens and analysed by flow cytometry.

2.14.2 Phagocytosis assay

A phagocytosis assay kit (Cayman Chemicals) was used according to the manufacturer's protocol. Briefly, MACS purified CD14$^+$ monocytes and *in vitro* expanded ILCs cells were seeded in 24-well plates at a density of 5 x 10^5 cells/well in complete growth medium and incubated for 4h at 37°C with latex beads coated with FITC-labelled rabbit IgG. The cells were harvested, washed, stained with fixable viability dye and analysed by flow cytometry.

2.14.3 Gentamycin protection assay

Salmonella enterica serovar typhimurium (*S. typhimurium*) expressing GFP (NCTC 12023) was used in the gentamicin protection assays. *S. typhimurium* was grown overnight in lysogeny broth (LB) medium and freshly inoculated the next day to achieve an optical density (OD) of 0.5. MDM were seeded in 96-well flat bottom plates at a density of 9 x 10^4 cell/well and rested overnight. Cells were pre-treated with supernatants derived from unstimulated and IL-23-stimulated ILC3 or unstimulated ILC2 cultures overnight. Bacterial infection was performed at multiplicity of infection (MOI) of 10 bacteria per macrophage cell. After 1h cells were washed with PBS and new complete medium supplemented with gentamicin (100 μg/ml) was added for an additional 2h to kill extracellular bacteria. In order to remove all traces of gentamicin, cells were washed with PBS and MDM were lysed in Triton X-100 diluted in deionized water (1% vol/vol). Samples were diluted, and plated by track method onto square LB agar plates to determine the number of colony forming units (CFU) recovered from the lysed macrophages.

2.14.4 Stimulation of antigen-specific CD4$^+$ T cells

Salmonella-specific CD4$^+$ CD45RO$^+$ memory T cells were expanded as described above, harvested and washed 3x in PBS. Cells were then cultured in complete growth medium for 1d in the absence of exogenous IL-2, harvested and labelled with CFSE. Irradiated (45 Gy) autologous monocytes and autologous *in vitro* expanded ILCs were seeded into flat-bottom 96-well plates at densities of 2 x 10^4 cells/well. *Salmonella* lysate was added to each well (1:1000) followed by incubation for 6-8h at 37°C to allow antigen uptake and processing. The unrelated antigen *Bifidobacterium* lysate (1:750) was used as a negative control for T cell stimulation. Addition of SEB was used as a positive control for T cell activation. CFSE-labelled *Salmonella*-specific T cells were then added to each well at a density of 4 x 10^4 cells/well. After co-culture for 5-7d, cells were harvested and T cell proliferation (CFSE dilution), activation (OX40, CD25, ICOS, PD1), cytokine expression (IFNγ, GM-CSF, IL-17A, IL-

22, IL-5, IL-13, IL-10, IL-2, TNFα) and transcription factor expression (T-bet, Eomes, RORγt, GATA3) were assessed by flow cytometry.

2.15 ILC – monocyte co-cultures

MACS purified CD14$^+$ monocytes were labelled with CFSE and plated on flat-bottom 96-well plates at a density of 3 x 10^4 cells/well in complete growth medium. In some cases, monocytes were activated by addition of LPS (1 μg/ml) (Sigma-Aldrich). *In vitro* expanded autologous or allogeneic ILC1, ILC2 and ILC3 were labelled with CellTrace Violet and added to the monocytes at a density of 3 x 10^4 cells/well. All cultures were supplemented with IL-2 (100U/ml) and IL-7 (50ng/ml) to maintain optimal ILC health. The co-cultures were maintained for two days, then cells were harvested, labelled with antibodies and analysed by flow cytometry. Where indicated, blocking antibodies specific for TNFα (Infliximab/Remicade®, MSD), IL-6R (Tocilizumab/Actemra®, Roche), IL-1β (clone H1b-27, Biolegend) and GM-CSF (clone BVD2-23B6, Biolegend) were added at saturating concentrations (10 μg/ml) at the beginning of the co-cultures.

2.16 ILC-monocyte-T cell co-cultures

These experiments were performed using autologous CD4$^+$ memory T cells, CD14$^+$ monocytes and *in vitro* expanded ILC populations. T cell and ILC populations were FACS sorted from peripheral blood, while monocytes were MACS sorted as described above. T cells were labelled with CFSE and ILCs were labelled with CellTrace Violet prior to co-culture in order to assess cell proliferation and allow for careful gating of the individual populations. ILCs and monocytes were seeded in flat-bottom 96-well plates at a density of 2 x 10^4 cells/well, either alone or in combination. This was followed by addition of naïve or memory CD4+ T cells at a density of 4 x 10^4 cells/well. T cell activation was achieved by addition of anti-CD3 antibody (10 μg/ml) (purified NA/LE mouse anti-human CD3, clone HIT3a, BD Pharmingen). After 7d of culture, cells were harvested and analysed by flow cytometry. Cultures were grown in complete growth medium in the absence of exogenous cytokines. In some experiments, CD4+ T cells and monocytes were separated from ILCs using 0.4μm polycarbonate transwell inserts (Corning). In some cultures, inert lymphocyte-sized filler beads (2x10^4/well) (FluoSpheres™ polystyrene microspheres, Life Technologies) were added to the monocyte – T cell co-cultures instead of ILCs.

2.17 Statistics

Statistical analysis was performed using Prism statistics software (GraphPad). The non-parametric Wilcoxon matched-pairs signed rank test was used for analysis of paired samples. For all other analyses, the non-parametric two-tailed Mann-Whitney U test was performed. Mean ± standard error of mean (SEM) was plotted in graphs. Differences between groups were considered to be statistically significant when $p \leq 0.05$.

Chapter 3: *Ex* characterisation of blood and intestinal ILCs in IBD

3.1 Introduction

At the time this study was initiated, human Lin$^-$CD127$^+$ ILCs had been identified in the uninflamed foetal and adult human gut, but little was known about the behaviour of human ILCs during intestinal inflammation. In line with previous reports (102,300,309,340,341), research from our group had shown increased expression at the mRNA level of T$_H$17-associated cytokines *IL17A*, *IL17F*, *IL22* and *IL26* in the inflamed lamina propria of CD and UC patients (185). While no significant differences in the expression of these cytokines among CD3$^+$ cells were detected between uninflamed controls and CD patients, CD3$^-$ cells from CD patients were significantly enriched for *IL17A* and *IL17F* transcripts. Further phenotyping of the CD3$^-$ fraction of lamina propria mononuclear cells (LPMCs) revealed that the producers of T$_H$17-type cytokines corresponded to previously identified ILCs, i.e. they lacked expression of lineage markers (CD14, CD16, CD19) associated with other immune effector populations, but highly expressed CD127. Furthermore, Lin$^-$CD127$^+$ cells expressed *RORC*, *IL23R* and *AHR*, identifying them as LTi-like ILC3 (185).

In agreement with a previous report showing that, similar to murine systems, human ILC3 could be grouped according to their expression of NKRs (NKp44 or CD56) (183), the ILC3 identified in our lab could be subdivided into CD56$^+$ cells enriched for NKp44, *IL22* and *IL26* expression and CD56$^-$ cells enriched for expression of *IL17A and IL17F*. Both CD56$^-$ and CD56$^+$ ILCs isolated from the lamina propria of CD patients expressed *IFNG* (185). Analysis of the frequencies of CD56$^-$ and CD56$^+$ ILCs among Lin$^-$CD45$^+$ LPMCs revealed that CD56$^-$ ILCs were selectively enriched in the lamina propria of CD but not UC patients compared to uninflamed controls, indicating that these cells may accumulate under inflammatory conditions and contribute to intestinal pathology through production of pro-inflammatory cytokines such as IL-17A, IL-17F and IFNγ (185).

Here, we sought to perform a detailed *ex vivo* characterisation of human intestinal CD56$^-$ and CD56$^+$ ILC3 building on the above discussed findings from our lab. We aimed to (i) examine the phenotype and function of these ILC subsets in different inflammation states (control, CD, UC) and tissue sites (colon, ileum, peripheral blood, visceral fat) using flow cytometry; (ii) investigate potential mechanisms of ILC accumulation in the inflamed intestinal lamina propria of IBD patients; (iii) analyse the *in situ* localization characteristics of CD3$^-$RORγ$^+$ ILC3 populations in control and IBD tissues; and (iv) establish a culture system allowing for the stable expansion of human ILC subsets *in vitro*.

3.2 Results

3.2.1 Lin^-CD127^+ ILCs can be detected in the human blood and gut and show enriched frequency in colon compared to blood

Flow cytometric analysis was used to identify Lin^- $CD127^+$ ILCs in peripheral blood and intestinal resection specimens. IBD blood samples were obtained from patients attending the Oxford IBD outpatient clinic and compared to blood from healthy control individuals. Intestinal specimens were derived from IBD patients requiring surgical intervention due to severe, treatment-unresponsive disease. Non-tumour containing resection specimens from colorectal cancer patients were used as uninflamed controls.

As shown in Figure 3.1A, $CD45^+$ cells in human blood and the intestinal lamina propria contain a clear population of $CD127^+$ cells that do not express phenotypic markers associated with other leukocyte lineages (CD1a, CD3, CD4, CD8, TCRαβ, TCRγδ, CD11b, CD11c, CD14, CD16, CD19, CD20, CD34, CD94, CD123, FcεRI and BDCA-2). Under uninflamed conditions, these ILCs were enriched in the intestinal lamina propria compared to peripheral blood, but in both compartments constituted an extremely rare population of immune cells, accounting for approximately 0.35% of total $CD45^+$ leukocytes in the colon and for 0.16% in the blood (Figure 3.1A).

3.2.2 Lin^-CD127^+ ILCs accumulate in the inflamed intestinal lamina propria of IBD patients and produce pro-inflammatory cytokines

Compared to uninflamed controls, we observed a significant increase in the frequency of ILCs in the intestinal lamina propria of IBD patients (Figure 3.1B). Following *in vitro* activation with PMA/ionomycin, ILCs were capable of expressing a range of effector cytokines and in IBD blood showed increased production of pro-inflammatory and fibrosis-promoting cytokines such as IFNγ, GM-CSF, IL-17A, IL-4, IL-13, IL-2 and TNFα (Figure 3.1C). These cytokines have been implicated in the pathogenesis of experimental and human IBD and it is therefore conceivable that cytokine production by human ILCs can contribute to inflammatory processes in the intestine (342).

3.2.3 CD56$^-$ ILCs but not CD56$^+$ ILCs accumulate in the intestinal lamina propria in IBD

Within the Lin$^-$CD127$^+$ ILC population, two distinct ILC subsets have been reported that can be distinguished based on differential expression of the NK marker CD56. Using this strategy, we compared ILC expression of CD56 in colon and blood. In the uninflamed colon, the Lin$^-$CD127$^+$ ILC population contained a similar proportion of CD56$^+$ and CD56$^-$ ILCs, whereas in the blood CD56$^-$ ILCs clearly pre-dominated (Figure 3.1D). Confirming earlier findings from our lab (185), the frequency of CD56$^-$ ILCs specifically increased in the inflamed CD colon compared to control colon, but were in addition found to accumulate in UC colon (Figure 3.1E). Similarly, an increase in CD56$^-$ ILCs was observed in the inflamed CD ileum compared to uninflamed ileum (Figure 3.1F). Thus, CD56$^-$ ILCs appear to accumulate selectively in the inflamed intestinal lamina propria of CD and UC patients.

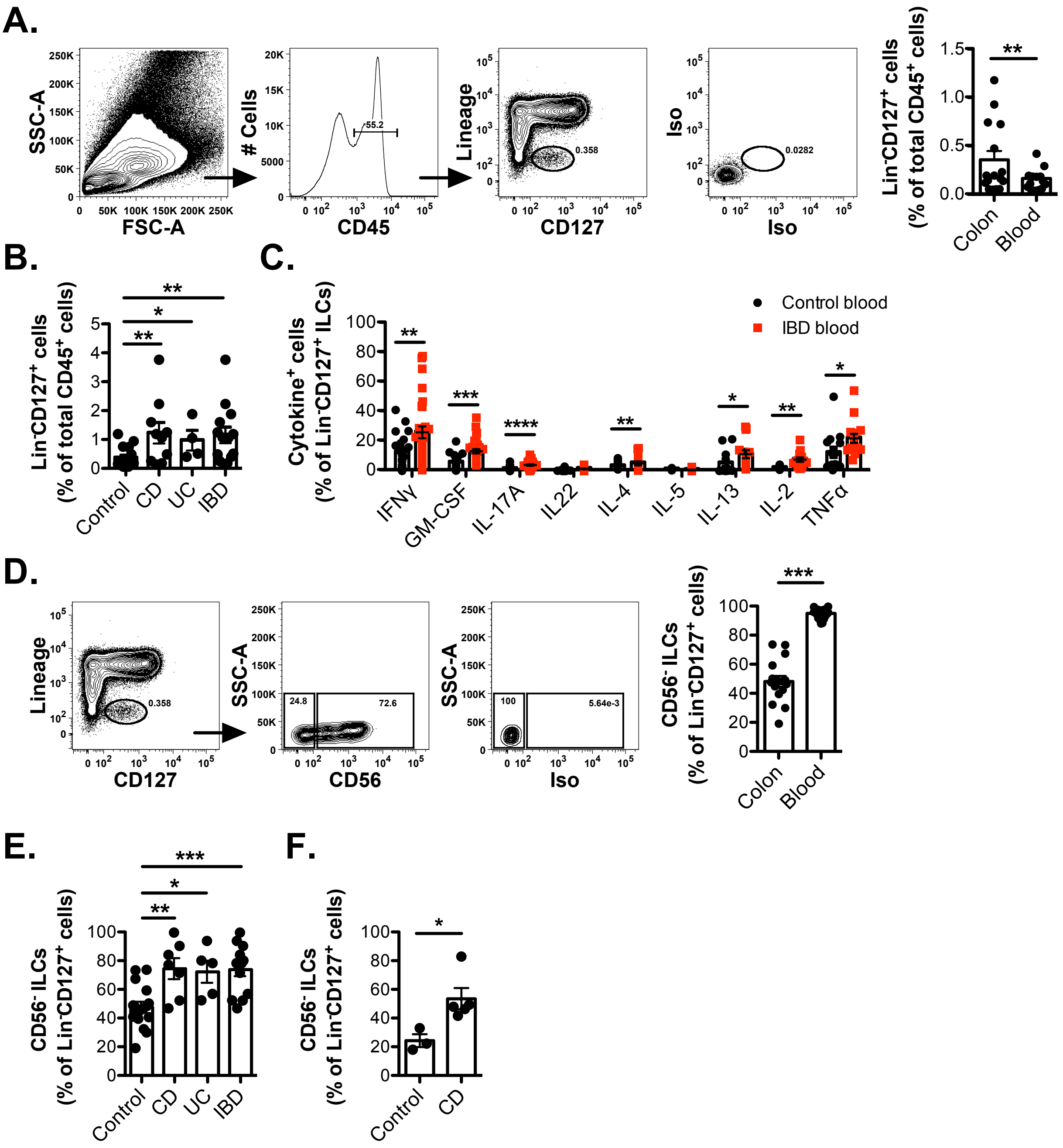

Figure 3.1: ILCs are enriched in the intestinal lamina propria and produce pro-inflammatory cytokines. (A) Representative gating strategy for total Lin^{-}CD127^{+} ILCs among LPMCs isolated from uninflamed colon (left) and quantification of total ILCs frrequency among CD45^{+} cells in the intestinal lamina propria and blood (right). **(B)** Quantification of Lin^{-}CD127^{+} ILCs in uninflamed and inflamed intestinal lamina propria. (**C**) Quantification of the proportion of cytokine expressing ILCs in control and IBD blood. **(D)** Representative FACS plot (left) and quantification (right) of CD56 expression on Lin^{-}CD127^{+} ILCs. **(E + F)** Quantification of CD56^{-} ILCs among total ILCs in uninflamed and inflamed colonic (E) and ileal (F) lamina propria. Each dot in the plots represents an individual donor. Statistical significance was determined by means of Mann-Whitney U tests. Bars represent mean ± SEM. $^{*}p \leq 0.05$. $^{**}p \leq 0.01$. $^{***}p \leq 0.001$. $^{****}p \leq 0.0001$.

3.2.4 CD56$^-$ ILCs are enriched in production of IL-17A, IFNγ, GM-CSF and IL-13 in IBD

Compared to cNK cells, both CD56$^+$ and CD56$^-$ ILCs expressed more RORγt and GATA3, and lower levels of T-bet (Figure 3.2A). No significant differences were detected between CD56$^+$ and CD56$^-$ ILCs with respect to RORγt and T-bet expression, but CD56$^-$ ILCs expressed significantly higher levels of GATA3. No significant differences in cytokine production could be detected between CD56$^+$ and CD56$^-$ ILC subsets under uninflamed conditions, although there was a trend towards increased expression of IL-17A, IFNγ and IL-13 in the CD56$^-$ ILCs, while CD56$^+$ ILCs tended towards greater expression of IL-22 (Figure 3.2B). While both CD56$^+$ and CD56$^-$ ILCs upregulated production of IL-17A, IL-22 and GM-CSF under inflamed conditions, only CD56$^-$ ILCs increased production of IFNγ, TNFα and IL-13 (Figure 3.2C and D). Furthermore, the above described trends towards differences in cytokine profiles between CD56$^+$ and CD56$^-$ ILCs became statistically significant under inflammatory conditions. Compared to CD56$^+$ ILCs, CD56$^-$ ILCs were enriched in production of IL-17A, IFNγ, GM-CSF and IL-13, whereas a greater proportion of CD56$^+$ ILCs produced IL-22 (Figure 3.2C). Thus, CD56 expression defines functionally distinct ILC subsets, with CD56$^-$ ILCs enriched for IL-17A, IFNγ and IL-13 expression and CD56$^+$ ILCs enriched for IL-22 expression.

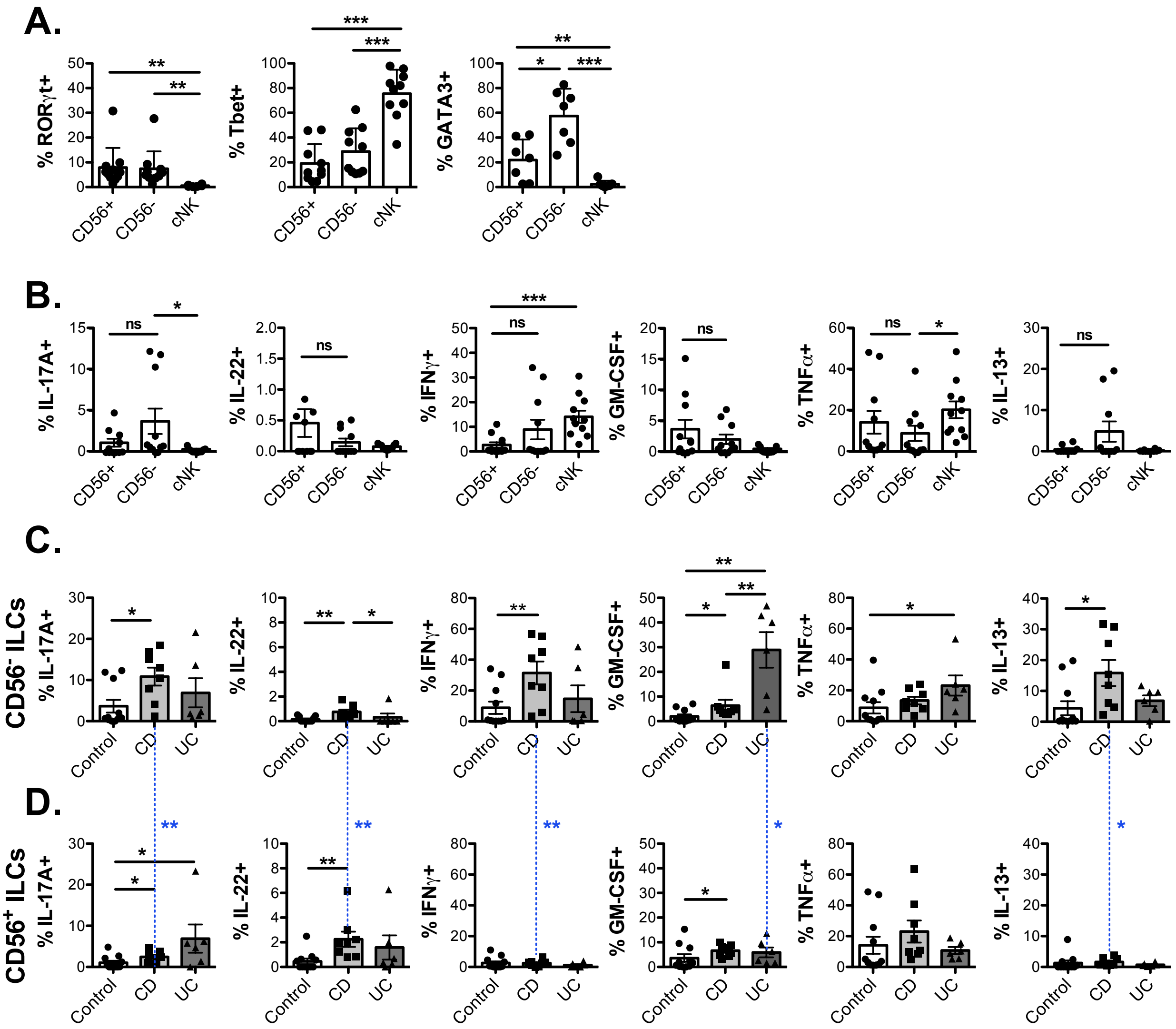

Figure 3.2: CD56$^-$ ILCs are enriched for expression of IBD-associated cytokines in blood from CD patients. (A + B) Quantified flow cytometry data of (A) TF and (B) cytokine expression by CD56$^-$ ILCs, CD56$^+$ ILCs and cNK cell in healthy control blood. **(C + D)** Quantified flow cytometry data of cytokine expression by (C**)** CD56$^-$ ILCs and (D) CD56$^+$ ILCs in control and IBD blood. Each dot in the plots represents an individual donor. Blue dotted lines indicate comparison of data between CD56$^-$ and CD56$^+$ ILCs. Statistical significance was determined by means of Mann-Whitney U tests. Bars represent mean ± SEM. *$p \leq 0.05$. **$p \leq 0.01$. ***$p \leq 0.001$.

3.2.5 Lin$^-$CD127$^+$ ILCs show increased *in situ* proliferation in the inflamed lamina propria

We next sought to determine the mechanism behind the accumulation of Lin$^-$CD127$^+$ ILCs in the inflamed lamina propria of IBD patients. Possible explanations include inflammation-induced increase in proliferation of tissue-resident ILCs and recruitment of circulating ILCs from the blood.

In order to test whether there might be increased *in situ* proliferation of resident ILC populations, freshly isolated LPMCs from control and IBD patients were analysed for intracellular expression of the proliferation-associated marker Ki67. The proportion of proliferating ILCs was compared with total CD3$^+$ T cells and cNK cells. As expected (343), the proportion of proliferating T cells in the uninflamed colonic lamina propria was low, with a significant increase observed in IBD tissue. cNK cells and ILCs closely mirrored this trend (Figure 3.3A and B). Due to low numbers of Ki67$^+$ cells in the ILC gate, it was impossible to determine whether CD56$^-$ ILCs displayed comparatively higher proliferation rates, accounting for their selective enrichment. However, these findings clearly indicated that increased ILC *in situ* proliferation can contribute to their accumulation in the inflamed intestinal lamina propria of IBD patients.

3.2.6 CD56$^-$ ILCs show increased expression of CD25 and may accumulate preferentially in response to IL-2 derived signals

FACS analysis of blood and tissue-resident ILCs revealed high expression levels of the IL-2Rα chain CD25 (Figure 3.3C). CD56$^-$ ILCs in both peripheral blood and intestinal lamina propria were enriched for CD25 expression compared to CD56$^+$

ILCs (Figure 3.3C). Stimulation of bulk LPMC populations with IL-2 revealed that this could indeed provide proliferative signals to ILCs, as indicated by increased Ki67 expression and absolute numbers of ILCs following stimulation with IL-2 (Figure 3.3D). Elevated levels of IL-2 have been reported in inflammatory lesions of IBD patients (344) and our data indicate that ILCs themselves upregulate IL-2 production during inflammation (Figure 3.1C). Paracrine or autocrine IL-2 signals may thus contribute to the increase in ILC proliferation observed in the inflamed tissue.

3.2.7 CD56$^-$ ILCs highly express CCR6 and may be recruited to the inflamed lamina propria from the blood

We next sought to investigate whether chemokine-mediated recruitment of blood ILCs may in addition be involved in the accumulation of ILCs in the inflamed intestinal lamina propria. Flow cytometry analysis on peripheral blood samples revealed a decrease in the frequency of total Lin$^-$CD127$^+$ ILCs in IBD patients compared to healthy controls, suggesting that ILCs may indeed be recruited from the blood to the inflamed tissue (Figure 3.3E). To assess the migratory potential of ILCs in peripheral blood, we examined their CCR expression using flow cytometry. In contrast to total CD3$^+$ T cells, Lin$^-$ CD127$^+$ ILCs did not express CCR7, nor did they express CCR9 (data not shown). However, we observed high CCR6 expression on total Lin$^-$CD127$^+$ ILCs (Figure 3.3F). This confirmed previous findings regarding CCR6 expression by ILC populations in human tonsil and gut (183,185).

Interestingly, CCR6 expression did not seem to be evenly distributed between CD56$^+$ and CD56$^-$ ILC subsets in peripheral blood, with a significant enrichment observed within the CD56$^-$ ILCs subset (Figure 3.3G). Differential expression of this homing marker could account for the preferential intestinal accumulation of CD56$^-$ ILCs during inflammation. Supporting the idea of specific recruitment to the intestine, a relative decrease in CD56$^-$ ILCs was observed in the peripheral blood of IBD patients, while the frequency of CD56$^+$ ILCs remained unchanged compared to control blood (Figure 3.3H). Thus, preferential CCR6-mediated recruitment of CD56$^-$ ILCs from blood may contribute to their selective accumulation in the inflamed intestinal lamina propria.

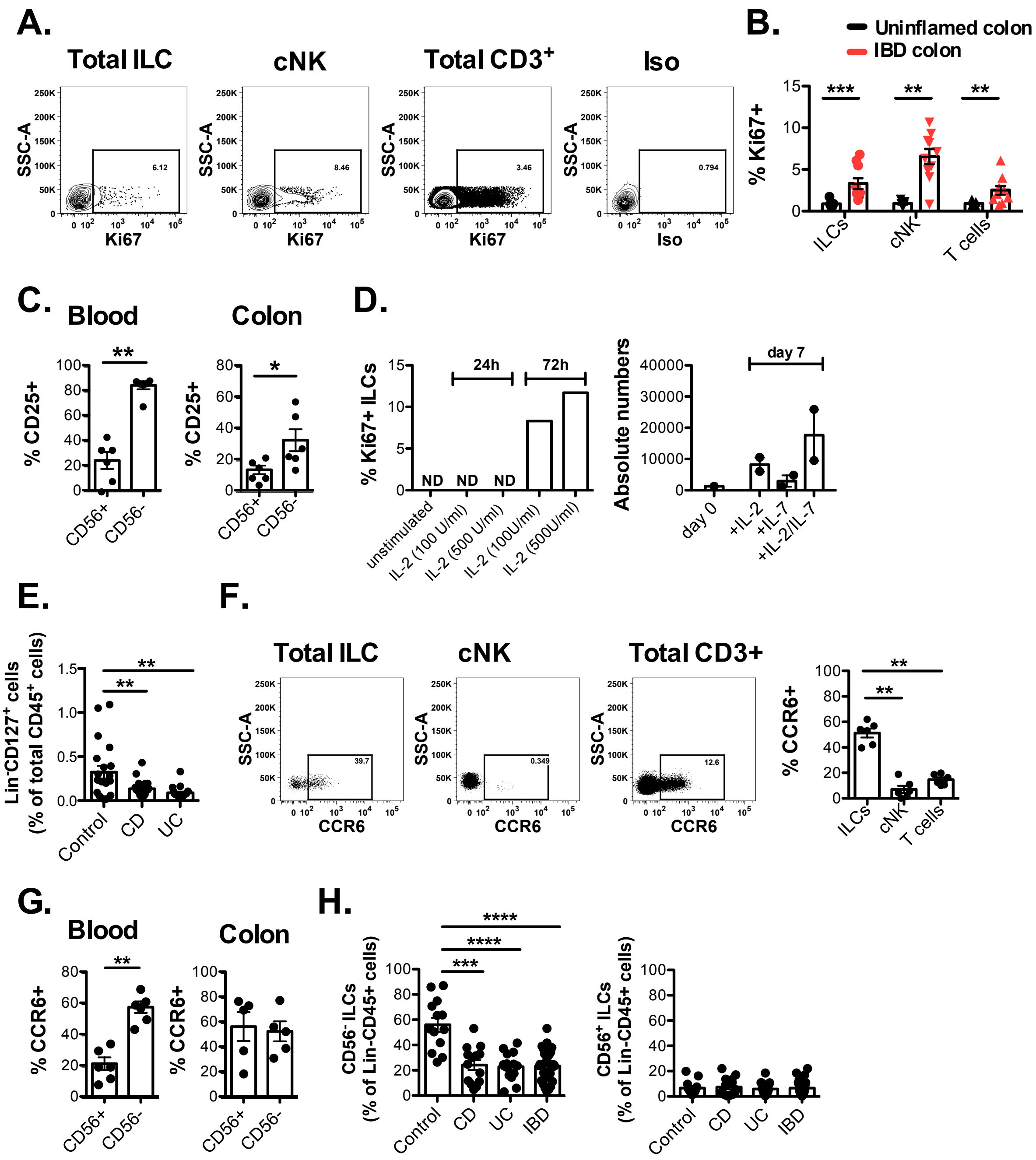

Figure 3.3: Accumulation and proliferation of Lin$^-$CD127$^+$ ILCs in the intestinal lamina propria of IBD patients. (A) Representative FACS plots of Ki67 expression in total Lin$^-$CD127$^+$ ILCs, cNK cells and total CD3$^+$ T cells in inflamed IBD colon. **(B)** Quantification of flow cytometry data of Ki67 expression in ILCs, cNK cells and T cells in uninflamed and IBD colonic lamina propria. **(C)** Quantification of flow cytometry data of CD25 expression by blood and colonic CD56$^+$ and CD56$^-$ ILCs. **(D)** Quantification of Ki67 expressing ILCs (left) and absolute number of ILCs (right) following stimulation of total control LPMCs with IL-2. **(E)** Quantification of total Lin$^-$CD127$^+$ ILC frequency among CD45$^+$ cells in control and IBD blood. **(F)** Representative FACS plots (left) and quantification (right) of CCR6 expression by total ILCs, cNK cells and total CD3$^+$ T cells in control blood. **(G)** Quantification of CCR6 expression by CD56$^+$ and CD56$^-$ ILCs in blood (left) and colon (right) of control patients. **(H)** Quantification of the frequency of CD56$^-$ (left) and CD56$^+$ (right) ILCs among Lin$^-$CD45$^+$ cells in control and IBD blood. Each dot in the plots represents an individual donor. Statistical significance was determined by means of Mann-Whitney U tests. Bars represent mean ± SEM. $^*p \leq 0.05$. $^{**}p \leq 0.01$. $^{***}p \leq 0.001$. $^{****}p \leq 0.0001$.

3.2.8 CRTH2$^+$ ILC2 are present in peripheral blood and intestinal tissues

Our findings of a population of GATA3 and IL-13-expressing cells within the CD56$^-$ ILC subset suggested that similar to published data from the mouse (11,13), there could be ILCs specialized for type 2 cytokine production in the human system as well. Indeed, Mjösberg et al. soon reported identification of such an ILC lineage in the human tonsil and foetal gut, which could be identified based on surface expression of the prostaglandin D2 receptor CRTH2 and which they termed ILC2 (16). Thus, we decided to investigate the frequency of ILC2 in the intestinal lamina propria and blood of controls and IBD patients on the basis of CRTH2 expression.

As shown in Figure 3.4A, a clear population of CRTH2$^+$ ILC2 cells could be identified within the Lin$^-$CD127$^+$ ILC fraction. These ILC2 did not express the NK marker CD56, but in accordance with the published findings of Mjösberg et al. expressed high levels of CD161 and CD45 (16). CRTH2$^+$ ILCs in control blood constituted approximately 13.2% of Lin$^-$CD127$^+$ cells in control blood, which was a significantly larger proportion than in the uninflamed colonic lamina propria, where only approximately 2.8% of Lin$^-$CD127$^+$ ILCs expressed CRTH2 (Figure 3.4B). Based on the original identification of GATA3-expressing ILCs in murine adipose tissue (13), we examined the frequency of CRTH2$^+$ ILC2 in gut-associated visceral fat and could indeed detect a population of ILC2 that were significantly enriched compared to the colonic lamina propria (Figure 3.4B). The frequency of CRTH2$^+$ ILC2 amongst Lin$^-$CD127$^+$ cells was significantly increased in both CD and UC blood compared to healthy controls. However, contrary to our initial hypothesis, no changes in CRTH2$^+$ ILC2 frequency were detected in the inflamed compared to the uninflamed colonic lamina propria (Figure 3.4C). Using *in vitro* stimulation of whole PBMCs with PMA/ionomycin followed by intracellular cytokine staining (ICS) and flow cytometry, we confirmed that Lin$^-$CD127$^+$CRTH2$^+$ cells were indeed functional ILC2. Gating on Lin$^-$CD127$^+$CD56$^-$ cells revealed that the CRTH2$^+$ cells within this population were the predominant producers of IL-13, while CRTH2$^-$ ILCs were enriched for IFNγ and IL-17A (Figure 3.4D).

Thus, human IL-13-producing CRTH2$^+$ ILC2 are present in peripheral blood, intestinal lamina propria and visceral adipose tissue of uninflamed controls and are enriched in the blood of IBD patients.

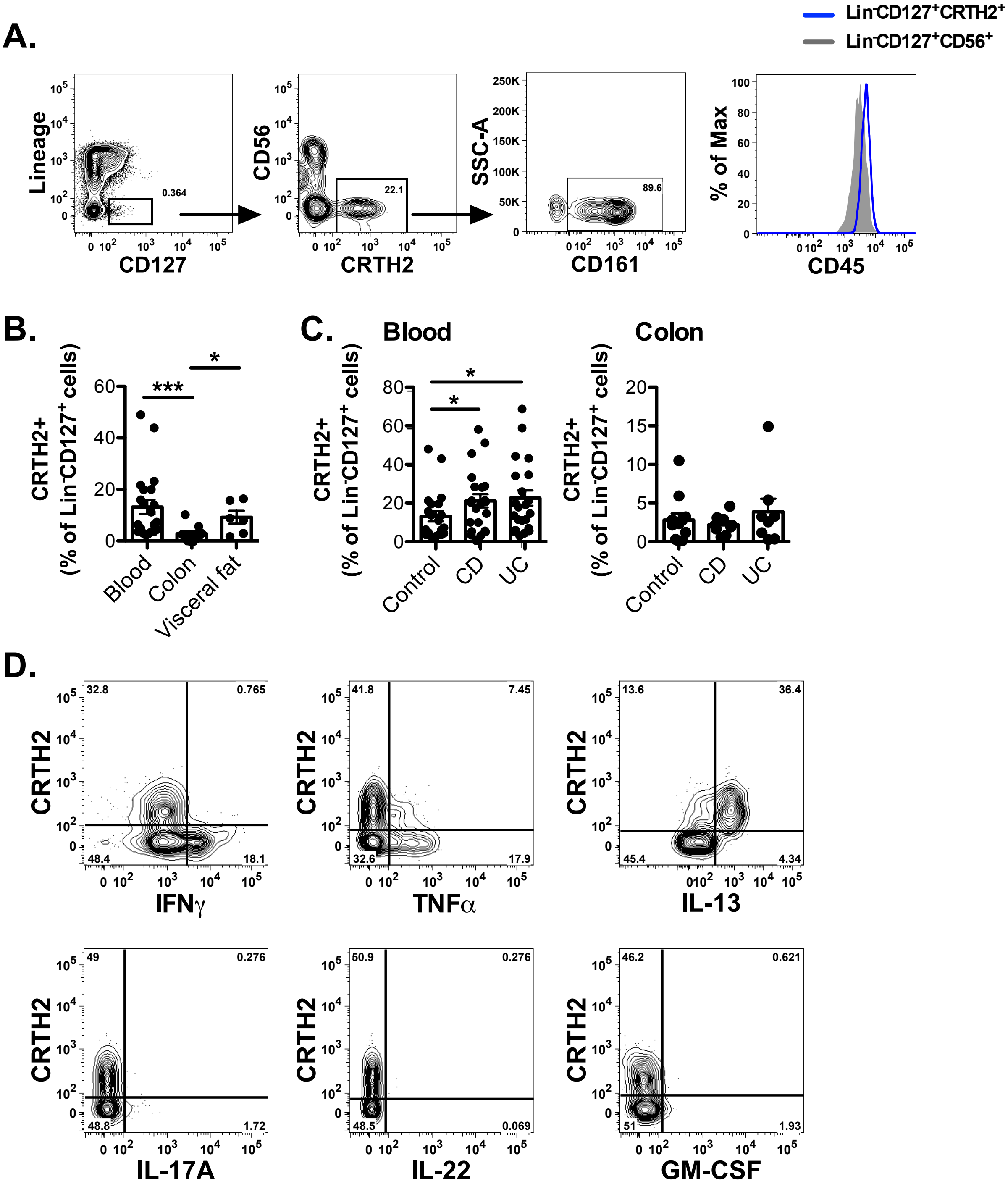

Figure 3.4: CRTH2$^+$ ILC2 enriched for IL-13 production are present in blood, colon and mesenteric fat and are enriched in the blood of IBD patients. (A) Representative FACS plots showing identification of CRTH2+ ILCs in human blood. **(B)** Quantification of ILC2 frequency among total Lin-CD127+ ILCs in blood, colon and mesenteric fat from control patients. **(C)** Quantification of ILC2 frequency among total Lin-CD127+ ILCs in blood (left) and colon (right) of control and IBD patients. **(D** Representative FACS plots of cytokine expression in ILC2 following stimulation of whole PBMCs with PMA/ionomycin for 4h in the presence of Golgistop and Golgiplug. Each dot in the plots represents an individual donor. Statistical significance was determined by means of Mann-Whitney U tests. Bars represent mean ± SEM. $^*p \leq 0.05$. $^{**}p \leq 0.01$. $^{***}p \leq 0.001$.

3.2.9 *In situ* visualization of RORγ^{+} ILC3 using immunofluorescence

In order to examine the *in situ* localization characteristics of RORγ^{+} ILC3 in the human gut lamina propria, we performed immunofluorescence analysis on colonic and ileal tissue sections. The strategy for visualization of RORγ^{+} ILCs involved a double staining approach, using antibodies against CD3 and RORγ, with ILCs expected to be CD3^{-}RORγ^{+}. Using this method, CD3^{+}RORγ^{-} T cells, CD3^{+}RORγ^{+} T cells and CD3^{-}RORγ^{+} ILCs could be clearly identified in the images obtained (Figure 3.5A).

Confirming our earlier findings obtained using flow cytometry analysis, quantification of anti-CD3/anti-RORγ stained tissue sections revealed increases in the frequency and density of CD3^{-}RORγ^{+} in CD colon and ileum compared to control colon (Figure 3.5B). As expected based on published data, the frequency of CD3^{+}RORγ^{+} cells was similarly increased (341). Interestingly, RORγ^{+} T cells and RORγ^{+} ILCs were present at similar frequencies and absolute numbers within the uninflamed lamina propria.

To validate that this approach correctly identified ILCs, we performed triple stainings using anti-CD3, anti-RORγ and anti-CD127 antibodies, with ILC3 expected to be CD3^{-}RORγ^{+}CD127^{+}. Indeed, the vast majority of CD3^{-}RORγ^{+} cells expressed CD127, confirming that they were indeed ILCs (Figure 3.5C and D). In addition, rare CD3^{-}RORγ^{-}CD127^{+} cells were found scattered throughout the lamina propria. CRTH2^{+} ILC2 and ILC1 in adult tissue express CD127 but no or low levels of RORγ (16) (189), suggesting that these rare CD3^{-}RORγ^{-}CD127^{+} cells may be representative of other ILC lineages. Taken together, this staining approach allowed us to determine ILC3 localization *in situ*.

Examining their localization within the different tissues, it was noticeable that CD3$^-$ RORγ$^+$ ILCs were not distributed homogeneously, but rather seemed to occur focally, co-localizing with aggregates of CD3$^+$ T cells (Figure 3.5E). As a result of the close co-localization of CD3$^+$ T cells and RORγ$^+$ ILCs, we were interested in examining the potential functional interactions between these cell types. In order to investigate the different ILC populations functionally, we needed to establish an *in vitro* culture system allowing for the expansion of these extremely rare cell populations.

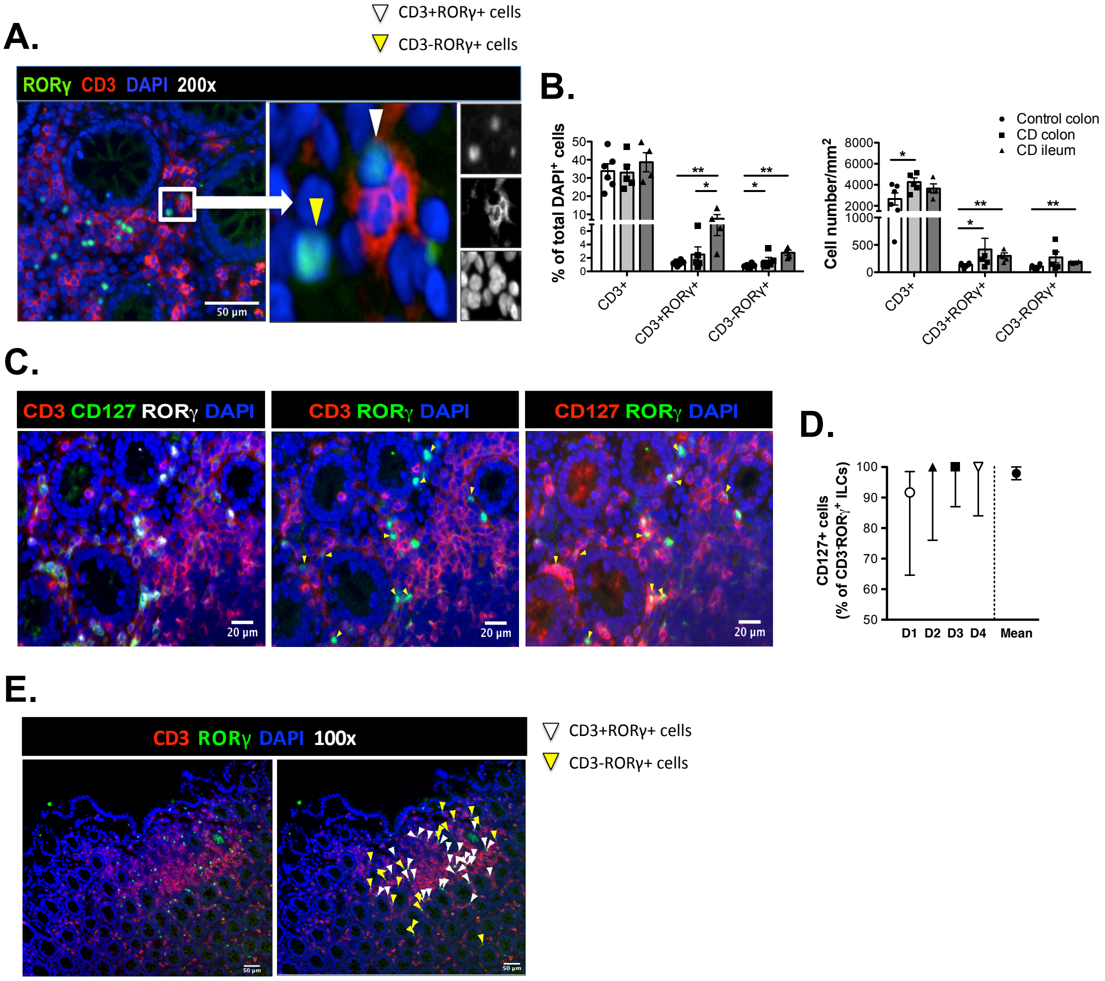

Figure 3.5: RORγ$^+$ ILCs can be visualized in frozen intestinal tissue sections and localize in close proximity to CD3$^+$ T cells. (A) Representative image showing CD3$^-$RORγ$^+$ ILCs and CD3$^+$RORγ$^+$ T cells in a frozen tissue section from normal colon. **(B)** Quantification of relative and absolute numbers of CD3$^+$ T cells, CD3$^+$RORγ$^+$ T cells and CD3$^-$RORγ$^+$ ILCs in frozen tissue sections obtained from uninflamed CRC colon and inflamed CD colon and ileum. **(C)** Representative image of a triple staining approach to visualize CD127 expression by CD3$^-$RORγ$^+$ ILCs. **(D)** Quantification of CD127 expression by CD3$^-$RORγ$^+$ cells. **(E)** Representative image of the close co-localization of CD3$^-$RORγ$^+$ ILCs and CD3$^+$ T cells. Each dot in the plots represents an individual donor. In (B) statistical significance was determined by means of Mann-Whitney U tests. Bars represent mean ± SEM. $^*p \leq 0.05$. $^{**}p \leq 0.01$. For individual specimens in (D) the 95% confidence intervals for a single proportion were calculated using the Wald equation.

3.2.10 Revised phenotypic definition of ILC3, ILC2 and ILC1 populations

In the course of our study, using a refined panel of cell surface markers that included CD117, Bernink et al. identified T-bet- and IFNγ-expressing ILC1 that were phenotypically distinct from the known ILC3 and ILC2 populations and accumulated in the inflamed lamina propria of CD patients. Furthermore, the group identified an ILC subset intermediate between ILC3 and ILC1 based on transcription factor and cytokine profiles, which they termed ILC0 (189). Within the Lin^{-}CD127^{+} population of immune cells, these ILC1 are now defined as CRTH2^{-}CD117^{-}NKp44^{-} cells, while ILC3 are CRTH2^{-}CD117^{+}NKp44^{+} cells, ILC2 are CRTH2^{+}CD117$^{+/-}$NKp44^{-} cells and ILC0 are CRTH2^{-}CD117^{+}NKp44^{+} cells (6).

We repeated our analysis of the frequency of ILC subsets in uninflamed and inflamed intestinal lamina propria based on these revised definitions (Figure 3.6A). In the uninflamed colon, ILC3 and ILC0 constituted the highest proportion of Lin^{-}CD127^{+} cells, while ILC2 and ILC1 were much less frequent (Figure 3.6B). No significant differences were observed in the frequency of ILC2 or ILC3 subsets, while ILC0 were significantly reduced in UC colon. However, in the inflamed mucosa of CD patients there was an accumulation of CD117^{-}NKp44^{-} ILC1, confirming the above-mentioned findings by Bernink et al. (Figure 3.6C-F). The frequency of ILC1 among total Lin^{-}CD127^{+} ILCs was unchanged in control compared to IBD blood, suggesting that *in situ* proliferation and/or differentiation rather than recruitment from the blood may contribute to the observed accumulation of ILC1 (Figure 3.6G).

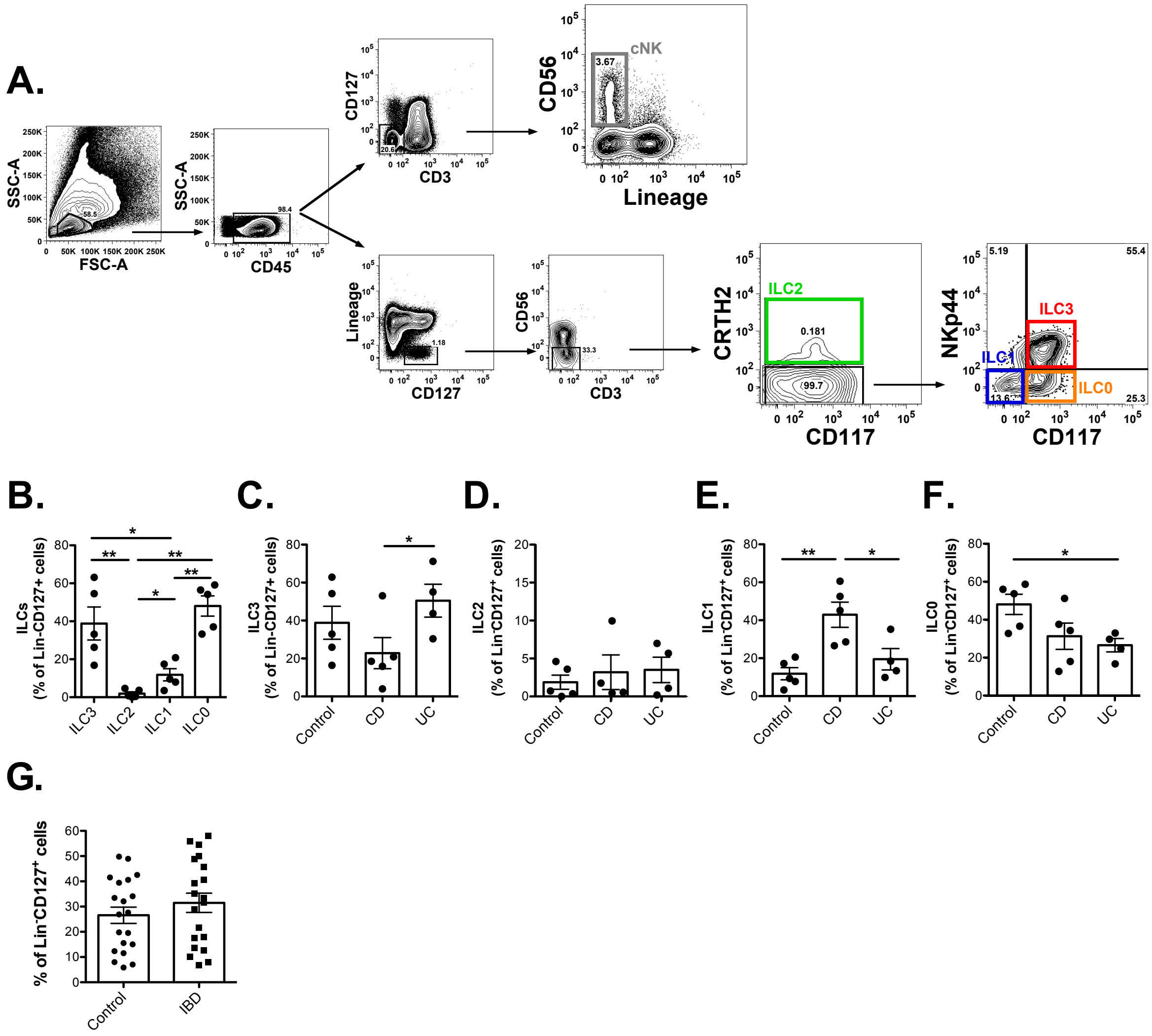

Figure 3.6: The frequency of ILC1 is increased in intestinal lamina popria of CD patients. (A) Representative FACS plots for a revised gating strategy for ILC1, ILC2, ILC3 and ILC0 subsets in LPMCs isolated from uninflamed control colon. (**B)** Quantification of the frequencies of the different ILC subsets in control intestinal lamina propria. (**C - F)** Quantification of the frequencies of ILC3 (C), ILC2 (D), ILC1 (E) and ILC0 (F) among total Lin$^-$CD127$^+$ ILCs in control and IBD intestinal lamina propria. **(G)** Quantification of ILC1 frequency among total Lin$^-$CD127$^+$ ILCs in control and IBD blood. Each dot in the plots represents an individual donor. Statistical significance was determined by means of Mann-Whitney U tests. Bars represent mean ± SEM. $^*p \leq 0.05$. $^{**}p \leq 0.01$.

3.2.11 Sorting strategy of ILC3, ILC2 and ILC1 populations for *in vitro* cultures

We next sought to develop a tractable human system for ILC expansion to use in functional experiments and we decided to purify individual ILC subsets from human peripheral blood according to the revised ILC nomenclature outlined above. As blood ILCs do not express NKp44 under homeostatic conditions, we defined the different ILC populations on the basis of CRTH2 and CD117 expression. Thus, within the $CD45^+Lin^-CD127^+CD56^-$ population, ILC1 were sorted as $CRTH2^-CD117^-$ cells, ILC2 as $CRTH2^+CD117^{+/-}$ and ILC3 as $CRTH2^-CD117^+$ cells, while cNK cells were sorted as $CD45^+CD3^-CD127^-CD56^+$ cells (Figure 3.7A). To confirm that these populations indeed corresponded to the known ILC subsets, we performed flow cytometric and qRT-PCR analysis of transcription factor and cytokine profiles expressed by these cells directly *ex vivo*.

Both on protein and mRNA levels, ILC1 and cNK cells were enriched for expression of T-bet, while cNK cells preferentially expressed Eomes. ILC2 expressed highest levels of GATA3 and ILC3 contained the greatest proportion of RORγt-expressing cells (Figure 3.7B-D). Both ILC3 and ILC2 were enriched for *AHR* mRNA expression, while ILC2 expressed highest levels of *RORA* mRNA, a transcription factor that has been linked to ILC2 development (21) (Figure 3.7E). All ILC subsets expressed *ID2* transcript, a transcriptional regulator essential for the differentiation of ILCs from CLPs (5), albeit at different levels with ILC3 and cNK cells expressing highest levels, ILC2 intermediate levels and ILC1 lowest levels of *ID2* mRNA (Figure 3.7E).

Following stimulation with PMA/ionomycin, the different ILC subsets displayed distinct cytokine profiles (Figure 3.8A). ILC3 were enriched for production of T_H17-associated cytokines such as GM-CSF and IL-17A (Figure 3.8B). ILC2 predominantly produced the T_H2-associated cytokine IL-13 and a proportion also expressed IL-4 (Figure 3.8C). ILC1 mainly produced the T_H1-associated cytokine IFNγ, although some expression of IL-17A was also detected (Figure 3.8D). cNK cells were included as a control group, and as expected predominantly expressed IFNγ and TNFα (Figure 3.8E). All three ILC subsets produced TNFα and interestingly also IL-2 (Figure 3.8B-D). Thus, our sorting strategy allows us to reliably purify functionally distinct ILC subsets from human peripheral blood.

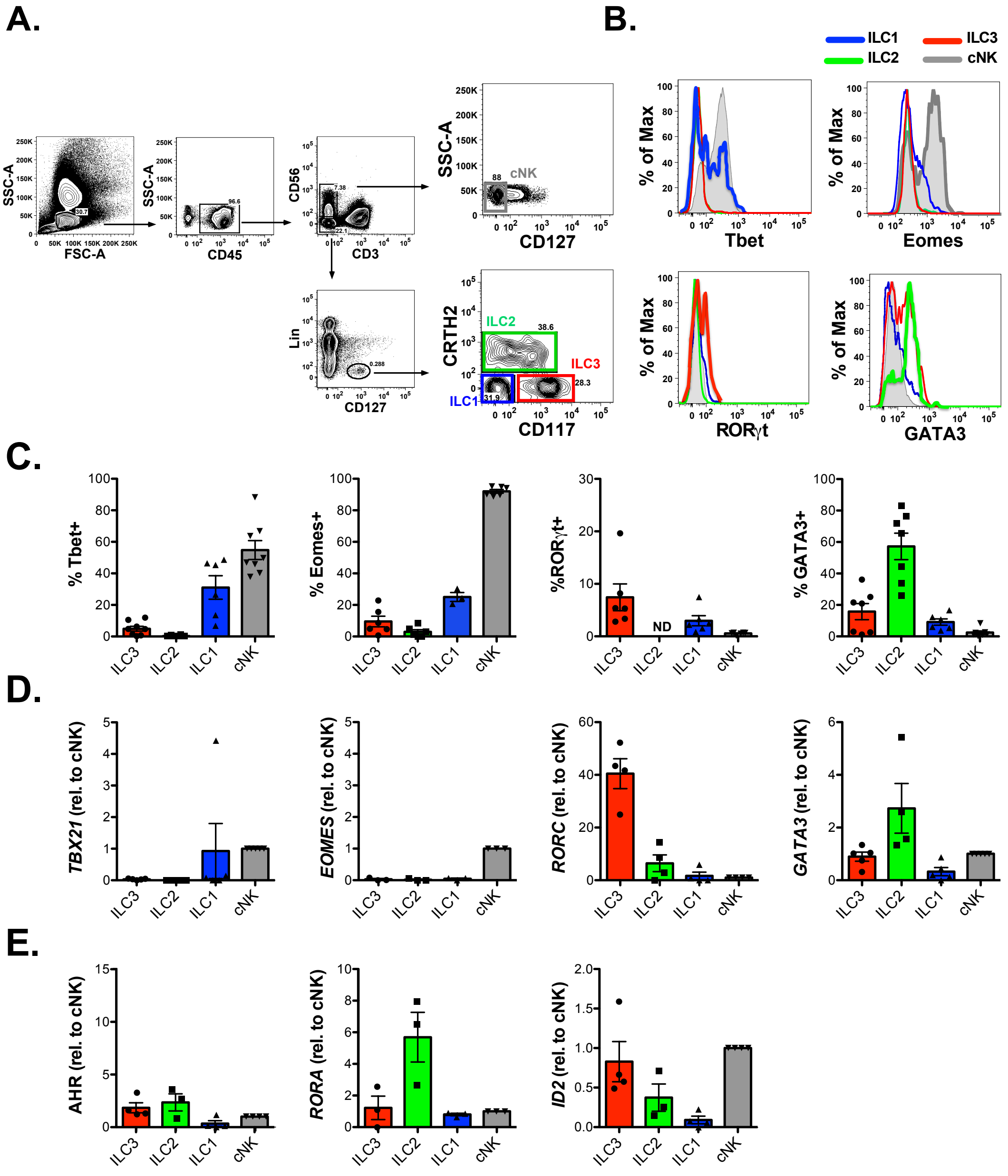

Figure 3.7: Characterisation of TF expression by blood ILC subsets. (A) Representative gating strategy for ILC1, ILC2 and ILC3 subsets in peripheral blood. **(B)** Representative FACS plots showing TF expression by blood ILC1, ILC2 and ILC3 subsets. Quantification of the frequencies of the different ILC subsets in control intestinal lamina propria. **(C)** Quantification of the proportion of Tbet-, Eomes-, RORγt- and GATA3-expressing cells among blood ILC1, ILC2 and ILC3. **(D)** qRT-PCR analysis of *TBX21*, *EOMES*, *RORC* and *GATA3* expression by FACS sorted blood ILC subsets (normalized to cNK expression levels). **(E)** qRT-PCR analysis of *AHR*, *RORA* and *ID2* expression by FACS sorted blood ILC subsets (normalized to cNK expression levels). Each dot in the plots represents an individual donor. Statistical significance was determined by means of Mann-Whitney U tests. Bars represent mean ± SEM.

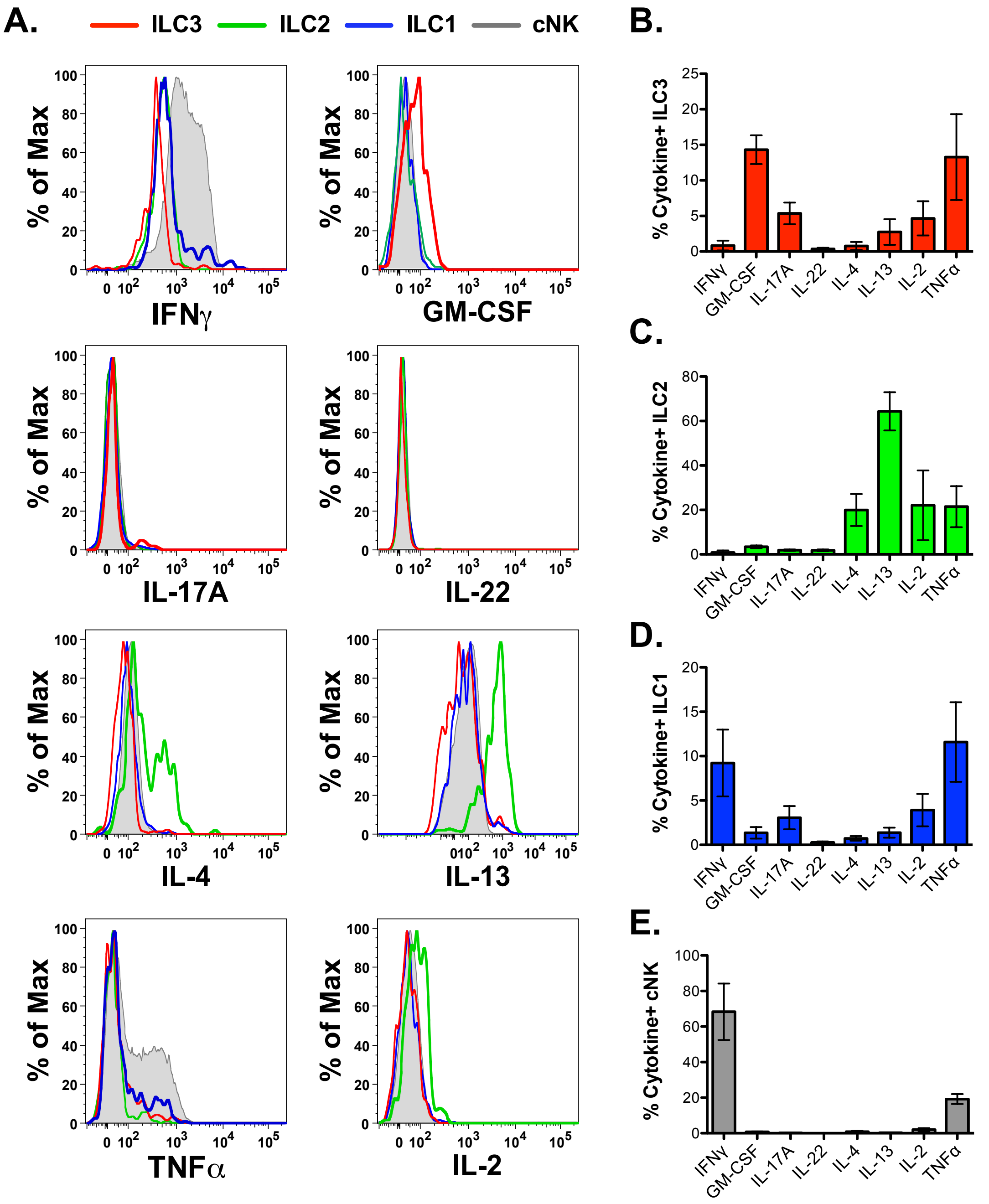

Figure 3.8: Analysis of cytokine expression by blood ILC subsets. Whole PBMCs from healthy donors were stimulated with PMA/ionomycin for 4h in the presence of Golgistop/Golgiplug followed by ICS and flow cytometry analysis. **(A)** Representative FACS plots of cyokine expression by ILC1, ILC2, ILC3 and cNK cells. ILC subsets were gated as in Figure 3.7. **(B - E)** Quantification of cytokine-expressing cells amongst ILC3 (B), ILC2 (C), ILC1 (D) and cNK cells (E). Data are representative of n = 3 - 6 individual donors.Bars represent mean ± SEM.

3.2.12 ILC subsets can be expanded in presence of exogenous IL-2 and IL-7

We next sought to establish a method for the *in vitro* expansion of ILC subsets purified from human peripheral blood. From each leukocyte cone, we obtained between 1 and 5 x 10^4 ILCs per subset, emphasizing that ILCs are indeed an extremely rare population of immune cells. The culture strategy we adopted was based on published data from the Spits lab and involved expansion of FACS sorted ILC populations on a feeder layer of irradiated PBMCs mixed from three allogeneic donors in the presence of IL-2 and/or IL-7 (188). At the beginning of each culture, an initial PHA stimulus was given, following which fresh growth medium containing IL-2 and/or IL-7 was administered every second day (Figure 3.9A).

Using this approach, we initially compared the expansion of the different FACS sorted blood ILC subsets cultured with IL-2 and IL-7 alone or in combination. After three weeks of culture, all three ILC subsets expanded robustly when cultured with either IL-2 or IL-7 or a combination of both cytokines, whereas no growth was observed in the absence of exogenous cytokines (Figure 3.9B). For all three ILC subsets, the greatest expansion was achieved using a combination of IL-2 and IL-7. Therefore, this was a suitable culture system for the *in vitro* expansion of human ILC subsets.

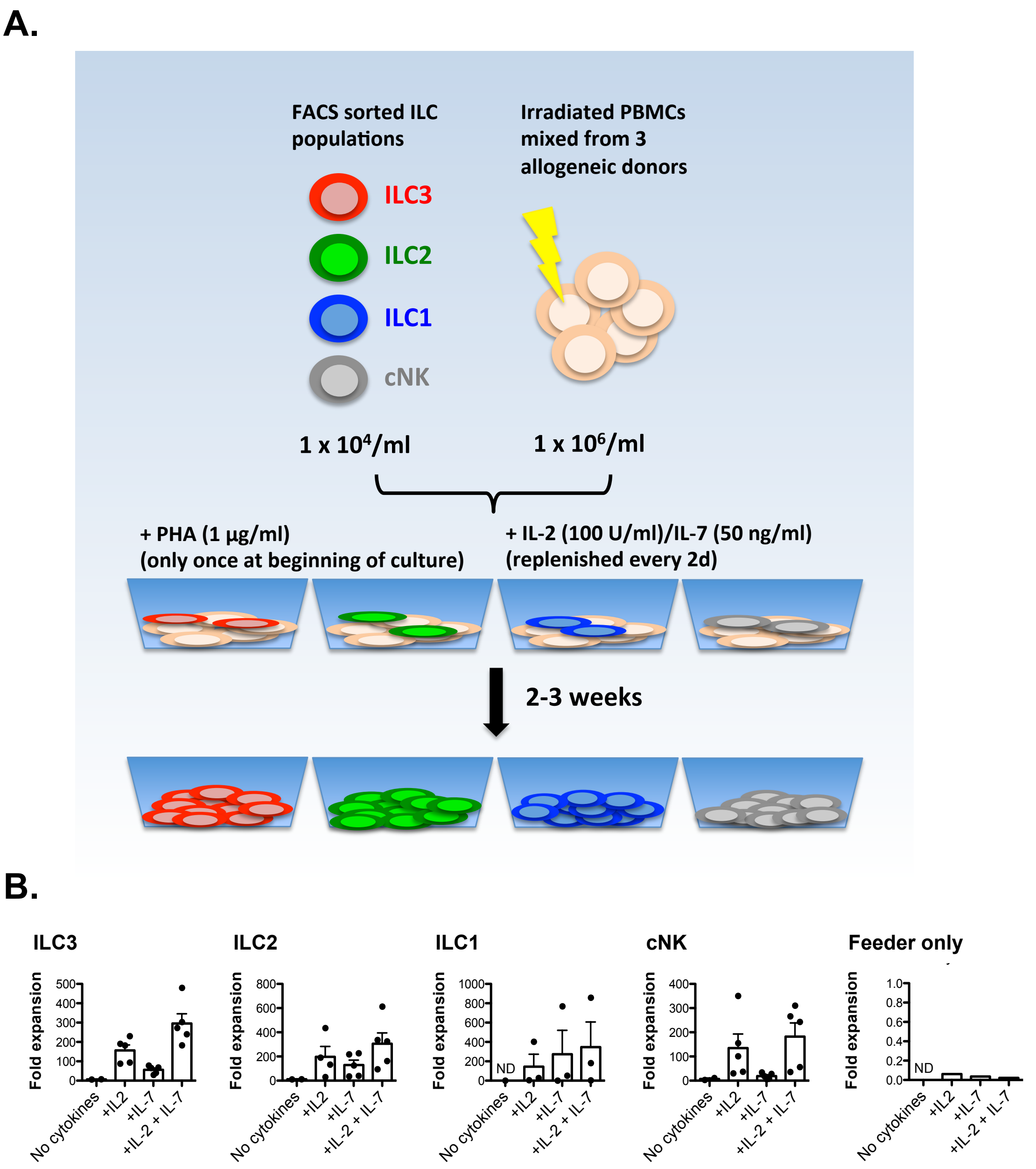

Figure 3.9: Establishment of culture conditions for *in vitro* expansion of FACS sorted blood ILC subsets. (A) Schematic depiction of culture strategy. FACS sorted ILC1, ILC2, ILC3 and cNK populations were plated in round-bottom 96-well plates (1 x 10^4 cells/ml) on a feeder layer of mixed irradiated PBMCs (45 Gy) from three allogeneic donors (1 x 10^6 cell/ml). The cells were cultured in complete growth medium supplemented with IL-2 (100 U/ml) and/or IL-7 (50 ng/ml) (see Materials & Methods). PHA (1µg/ml) was added once at the beginning of the cultures. IL-2 and IL-7 were replenished every three days. ILCs greatly expanded within 2-3 weeks of culture and were cultured for up to 6 weeks before being used in experiments. **(B)** Fold expansion of FACS sorted ILC subsets cultured for 3 weeks in IL-2 (100 U/ml) and/or IL-7 (50 ng/ml). Each dot in the plots represents an individual donor. Bars represent mean ± SEM.

3.2.13 Characterisation of *in vitro* expanded ILC subsets

We next examined phenotypic and functional characteristics of the *in vitro* cultured ILCs in order to determine whether FACS sorted blood ILC subsets could be expanded stably *in vitro* without loss of their defining features.

First we analysed ILC surface marker expression (Figure 3.10A). Similar to *ex vivo* blood ILC subsets, *in vitro* expanded ILC3 had highest expression of CD117 compared to heterogeneous expression in ILC2 and significantly lower expression in ILC1 (Figure 3.10B). *In vitro* expanded ILC3 upregulated NKp44 and CD56 expression, whereas no NKR expression was observed on cultured ILC2 or ILC1 in line with previous reports (16,188,189) (Figure 3.10C and D). Compared to ILC2 or ILC1, cultured ILC3 were enriched for CCR6 expression, which again reflected *ex vivo* expression patterns (Figure 3.10E). Furthermore, *in vitro* expanded ILC3 maintained high expression of CD25 and CD161 (Figure 3.10F and G). Cultured ILC2 retained high expression of their defining lineage marker CRTH2 compared to ILC2 or ILC1 subsets (Figure 3.10H) and highly expressed CD25 and CD161. *In vitro* expanded ILC1 showed high expression of CD25 (Figure 3.10F). All three ILC populations had low expression of the cNK-specific marker CD94, but highly expressed ICOS (Figure 3.10I and J). Therefore, based on surface expression, ILCs expanded in the culture system resembled *ex vivo* ILC populations.

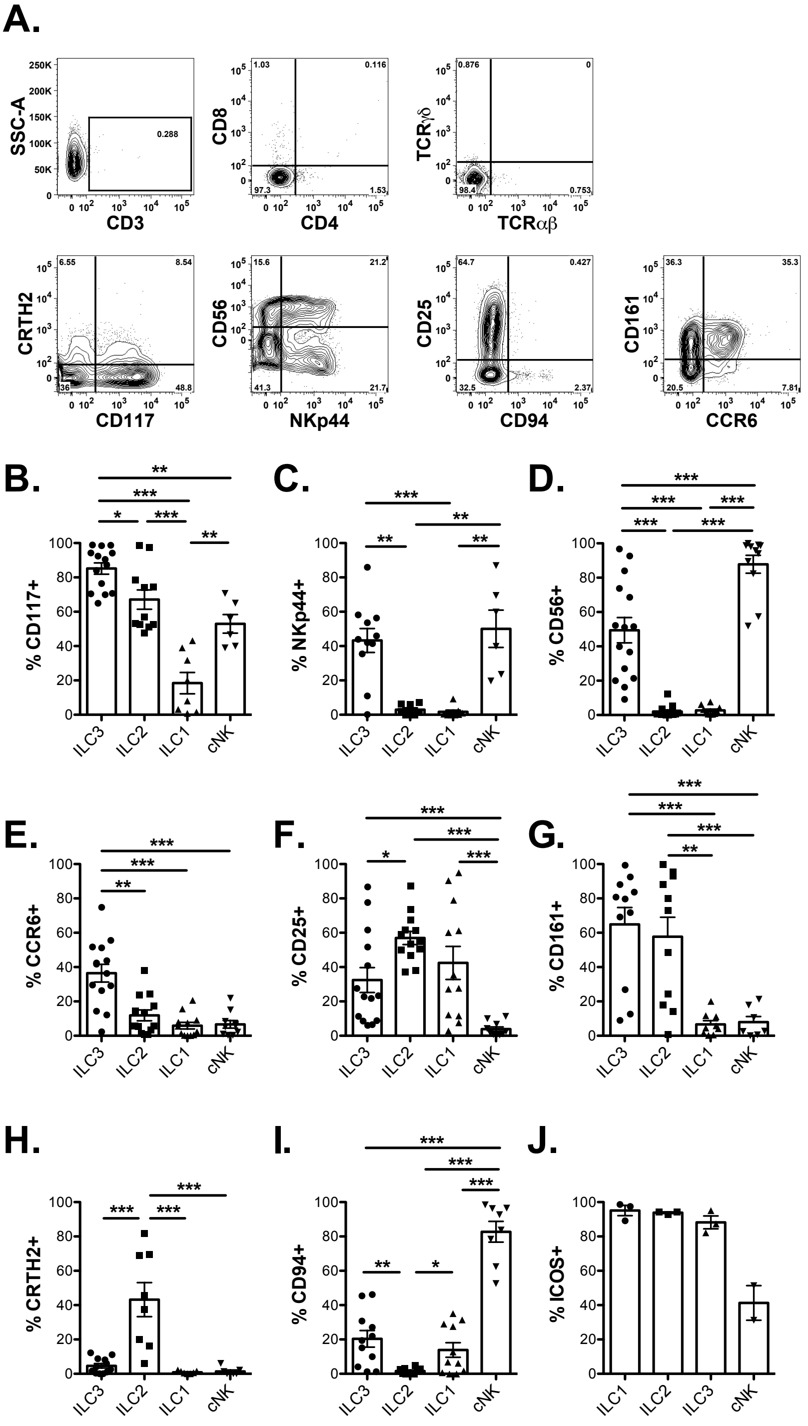

Figure 3.10: Characterisation of surface marker expression by *in vitro* expanded blood ILC subsets. FACS sorted ILC subsets were cultured in IL-2 (100 U/ml) and IL-7 (50 ng/ml) for 3-5 weeks followed by flow cytometry analysis of surface marker expression. **(A)** Representative FACS plots showing expression of surface markers by ILC3. **(B - J)** Quantification of the proportion of cells among cultured ILC1, ILC2, ILC3 and cNK that express CD117 (B), NKp44 (C), CD56 (D), CCR6 (E), CD25(F), CD161 (G), CRTH2 (H), CD94 (I) and ICOS (J). Each dot in the plots represents an individual donor. Statistical significance was determined by means of Mann-Whitney U tests. Bars represent mean ± SEM. *p ≤ 0.05. **p ≤ 0.01. ***p ≤ 0.001.

We next examined functional characteristics of *in vitro* expanded ILCs. Following stimulation with PMA/ionomycin, the cytokine profiles of *in vitro* cultured ILC populations were assessed. As expected from the *ex vivo* cytokine expression patterns, ILC3 were enriched for expression of T_H17-type cytokines IL-17A, IL-22 and GM-CSF (Figure 3.11A and D). ILC2 showed highest expression of the T_H2-associated cytokines IL-4, IL-5 and IL-13 (Figure 11B and E) and ILC1 were enriched for production of IFNγ (Figure 3.11C and 11F). All three ILC subsets retained high expression of TNFα, with a trend towards highest expression in ILC1 (Figure 3.11C and F). Similar to the *ex vivo* cytokine expression data presented in Figure 3.8, all ILC subsets were capable of producing IL-2, with highest expression in ILC2 (Figure 3.11F). Thus, *in vitro* expanded ILCs had cytokine profiles similar to *ex vivo* ILC populations.

Finally, analysis of transcription factor expression by *in vitro* expanded ILC populations indicated that cultured ILCs expressed key lineage-associated transcription factors. Highest expression of RORγt was found in the ILC3 subset (Figure 3.12A and B), while GATA3 expression was enriched in ILC2 (Figure 3.12A and C). ILC1 showed high expression of T-bet, comparable to expression levels in cNK cells (Figure 3.12A and D), while cNK cells expressed highest levels of Eomes (Figure 3.12A and E).

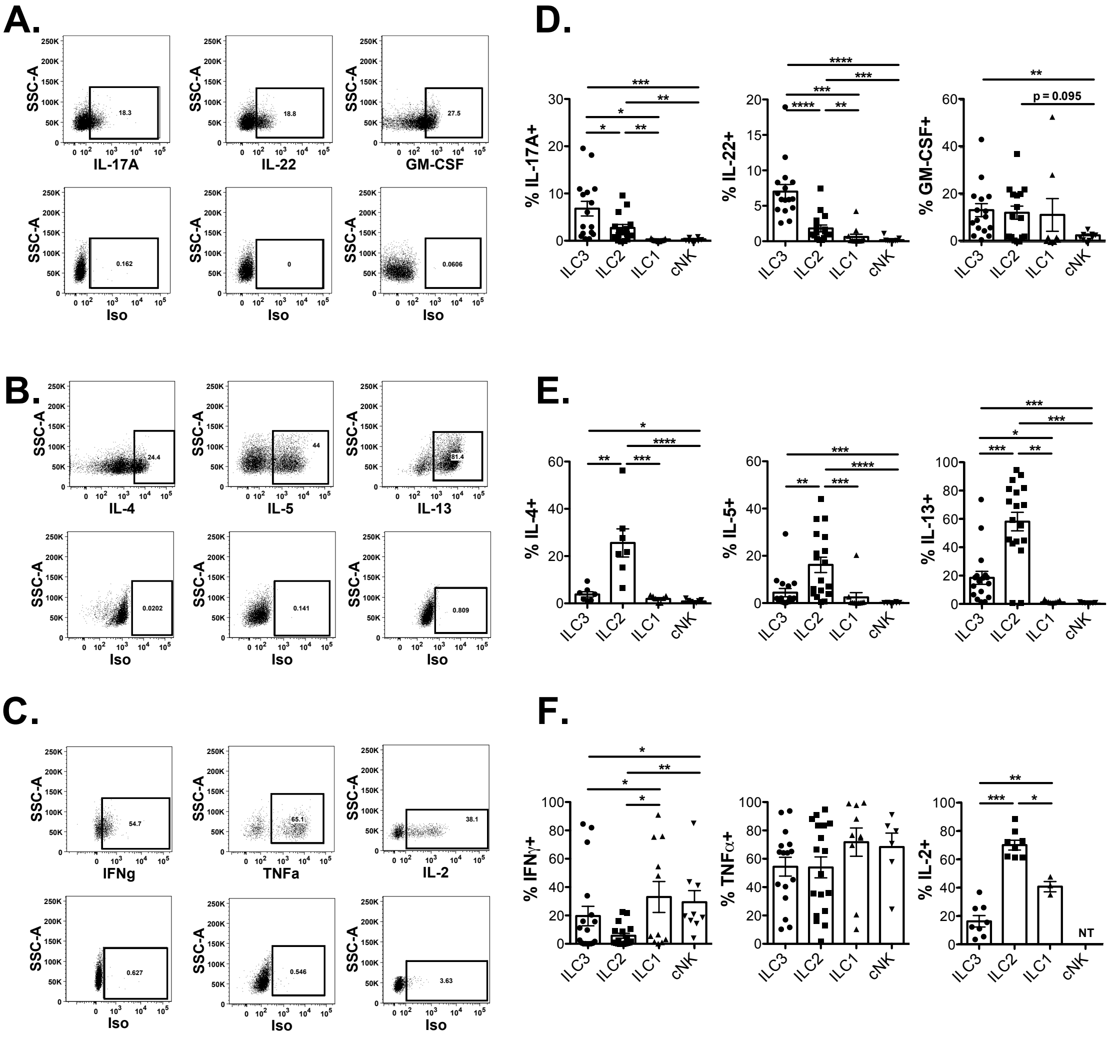

Figure 3.11: Characterisation of cytokine expression by *in vitro* expanded blood ILC subsets. FACS sorted ILC subsets were cultured in IL-2 (100 U/ml) and IL-7 (50 ng/ml) for 3-5 weeks and then stimulated for 4h with PMA/ionomycin in the presence of Golgistop. This was followed by ICS and flow cytometry analysis. **(A-C)** Representative FACS plots of cytokine expression by cultured ILC3 (A), ILC2 (B) and ILC1 (C). **(D)** Quantification of IL-17A, IL-22 and GM-CSF expression by the different ILC subsets. **(E)** Quantification of IL-4, IL-5 and IL-13 expression by the different ILC subsets. **(F)** Quantification of IFNγ, TNFα and IL-2 expression by the different ILC subsets. Each dot in the plots represents an individual donor. Statistical significance was determined by means of Mann-Whitney U tests. Bars represent mean ± SEM. *$p \leq 0.05$. **$p \leq 0.01$. ***$p \leq 0.001$. ****$p \leq 0.0001$.

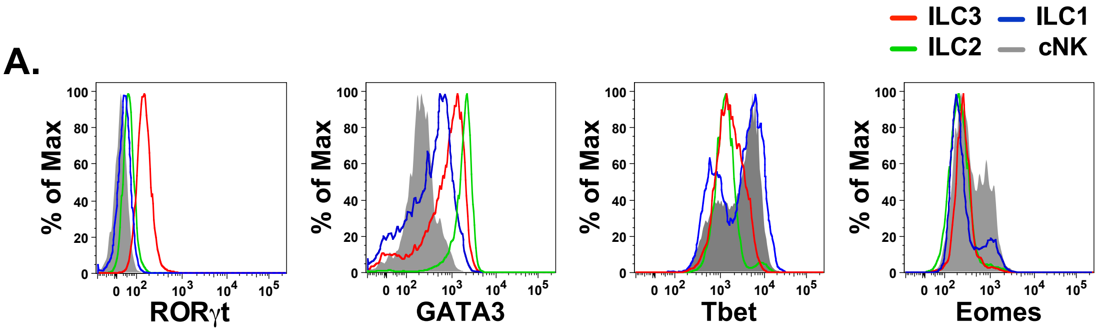

Figure 3.12: Characterisation of TF expression by *in vitro* expanded blood ILC subsets. FACS sorted ILC subsets were cultured in IL-2 (100 U/ml) and IL-7 (50 ng/ml) for 3-5 weeks followed by flow cytometry analysis. Representative FACS plots of TF expression by cultured ILC subsets are shown.

Comparison of cytokine expression patterns of ILC1, ILC2 and ILC3 expanded with IL-2 or IL-7 alone or with a combination of both IL-2 and IL-7 indicated that these different cytokine combinations did not induce significant changes in ILC cytokine profiles (Figure 3.13A-C). The data shown are representative for ILC3, but equivalent results were observed for ILC2 and ILC1.

Collectively, these data indicate that ILC3, ILC2 and ILC1 populations FACS sorted from human blood can be stably expanded *in vitro* in the presence of exogenous IL-2 and IL-7 while retaining their defining surface marker, cytokine and transcription factor expression patterns. The ILC populations used in all subsequent experiments were expanded using IL-2 and IL-7.

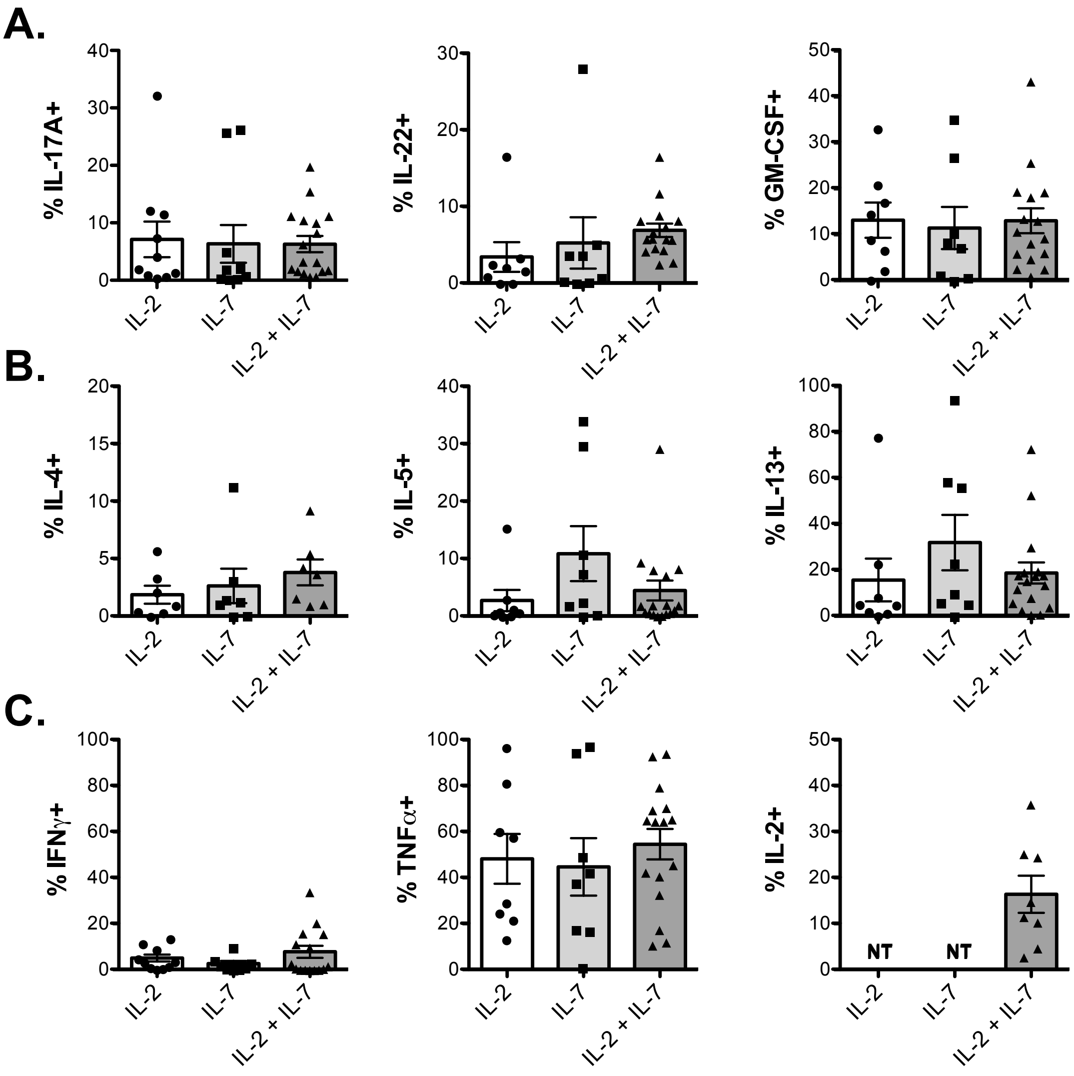

Figure 3.13: The cytokine expression profiles of ILC3 cultured IL-2, IL-7 or IL2 + IL-7 are not significantly different. FACS sorted blood ILC3 were cultured in IL-2 (100 U/ml), IL-7 (50 ng/ml) or a combination of both cytokines for 3-5 weeks. This was followed by stimulation with PMA/ionomycin for 4h in the presence of Golgistop/ Golgiplug, ICS and flow cytometry analysis. **(A - C)** Quantification of IL-17A, IL-22 and GM-CSF (A), IL-4, IL-5 and IL-13 (B) and IFNγ, TNFα and IL-2 (C) expression by ILC3 cultured with the different cytokine combinations. Each dot in the plots represents an individual donor. Statistical significance was determined by means of Mann-Whitney U tests. Bars represent mean ± SEM.

3.2.14 ILC3 express LTi-associated markers and activate intestinal stromal cells

In the mouse, adult RORγt+ ILC3 were initially identified based on their phenotypic similarities to foetal LTi cells, which, in conjunction with stromal cells, are responsible for the induction of organised secondary lymphoid tissues in the developing embryo (56,64,89,345). Using co-cultures with mesenchymal stromal cells (MSCs), human Lin$^-$CD127$^+$ ILCs isolated from foetal lymph nodes and tonsil have been shown to have a similar inducer potential. *In vitro* human LT$\alpha_1\beta_2^+$ ILCs promoted upregulation of ICAM-1 and VCAM-1 expression by LTβR$^+$ MSCs, mimicking the LTi cell-mediated induction of lymphocyte-retaining adhesion molecules on LN anlagen-resident stromal cells that is thought to occur *in vivo* during foetal development (182,188). We wanted to examine the inducer potential of the different adult ILC populations expanded *in vitro* from blood.

ILC3, but not ILC2 or ILC1 expressed the LTi-associated markers *TNFSF14* (*LIGHT*), *LTA* and *LTB* at mRNA level (Figure 3.14A-C). Co-culture of the different ILC subsets with the intestinal stromal cell line (iSC) CCD18co was then used to functionally validate whether ILCs were capable of inducing ICAM-1 expression on the iSCs. Stimulation of iSCs with TNFα, IL-17A and recombinant human LTα were used as positive controls for induction of adhesion molecule expression (87,182,346,347).

Stimulation with TNFα, IL-17A and LTα induced significant upregulation of ICAM-1 expression on the iSCs (Figure 3.14D). Co-culture with ILC3 but not ILC1 induced robust upregulation of ICAM-1 expression at levels equivalent to LTα stimulation. Interestingly, despite their lack of LIGHT or LT expression, ILC2 were equivalent to ILC3 in their capacity to induce ICAM-1 expression on iSCs. Although cultured ILC2 produce TNFα, this mechanism seems to be TNFα-independent, since *in vitro* expanded ILC1 can produce TNFα and yet fail to induce iSC activation (Figure 3.11D). However, ILC2 produce large quantities of IL-4 and IL-13, cytokines that have been implicated in stromal cell activation (348,349). Thus, adult human ILC3 and ILC2, but not ILC1, displayed inducer potential. Different mechanisms likely underlie the capacity of ILC3 and ILC2 to activate iSCs.

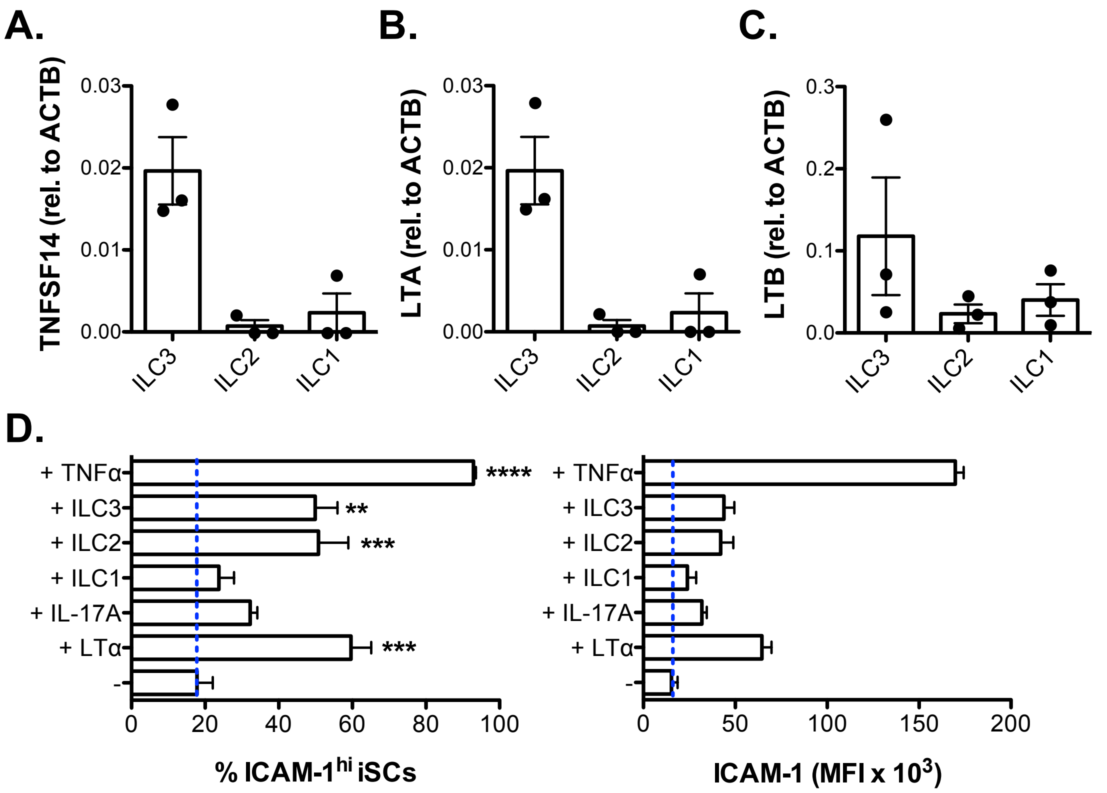

Figure 3.14: ILC3 and ILC2 induce ICAM-1 upregulation on intestinal stromal cells. (A - C) Quantification of *TNFSF14* (A), *LTA* (B) and *LTB* (C) mRNA expression by *ex vivo* sorted blood ILC populations. Each dot in the plots represents an individual donor. **(D)** CCD18co colonic stromal cells were co-cultured with *in vitro* expanded ILC1, ILC2 or ILC3 for 3 days followed by flow cytometry analysis. ILCs were derived from n = 3 - 5 individual donors. Stimulation of CCD18co cells with recombinant human TNFα, IL-17A or LTα was used as a positive control for induction of ICAM-1 expression. The plots represent quantification of the percentage (left) and MFI (right) of ICAM-1 expression by CCD18co cells following co-culture with ILC3, ILC2, ILC1 or following cytokine stimulation. Statistical significance was determined for each co-culture conditions with respect to untreated CCD18co cells by means of Mann-Whitney U tests. Bars represent mean ± SEM. *$p \leq 0.05$. **$p \leq 0.01$. ***$p \leq 0.001$. ****$p \leq 0.0001$.

3.3 Discussion

By examining ILCs *ex* vivo from human tissue and blood, we show here that Lin$^-$ CD127$^+$ ILCs are enriched in the human intestinal lamina propria compared to peripheral blood and further accumulate in the inflamed lamina propria of CD and UC patients compared to uninflamed controls. Based on ILC nomenclature at the time, we investigated the relative frequencies of CD56$^+$ and CD56$^-$ ILC subsets and could confirm a previous report (185) of a selective increase in lamina propria-resident CD56$^-$ ILC frequency not only in CD but also in UC patients. No significant differences in terms of cytokine and transcription factor expression were detected between CD56$^-$ and CD56$^+$ ILCs in healthy control blood (except for GATA3 expression, which was significantly higher in the CD56$^-$ ILCs). However under inflammatory conditions CD56$^-$ ILCs showed significantly increased expression of pro-inflammatory cytokines implicated in IBD pathogenesis such as IL-17A, IFNγ, GM-CSF and IL-13, while CD56$^+$ ILCs were enriched for IL-22 expression.

The relative decrease of CD56$^+$ ILCs in the intestinal lamina propria of IBD patients suggests a decrease in ILC-derived IL-22 in the lamina propria of IBD patients. While IL-22 can exert pro-inflammatory effects in several mouse models of chronic inflammatory disorders including rheumatoid arthritis and psoriasis (350-353), the majority of reports to date have demonstrated a protective role for IL-22 in mouse models of colitis (311). Specifically, ILC-mediated expression of IL-22, regulated via RA and the tyrosine kinase Lyn, has been shown to protect mice from DSS-induced colitis (354,355). It is conceivable that a reduction in ILC-derived IL-22 could contribute to impaired epithelial barrier function, including reduced secretion of antimicrobial peptides, epithelial fucosylation and epithelial repair, all of which are features of both CD and UC patients. This may lead increased translocation of commensal antigens into the intestinal lamina propria, promoting inflammatory immune responses and secondary activation of commensal-specific CD4$^+$ T cells.

Analysis of *in situ* localization characteristics of RORγ$^+$ ILCs confirmed inflammation-associated accumulation of these cells in the colonic and ileal lamina propria of CD patients and furthermore revealed that RORγ$^+$ ILCs localize in proximity of CD3$^+$ T cells. This suggests that RORγ$^+$ ILCs and T cells may functionally interact in the intestinal lamina propria. In support of this idea, evidence suggests that in mouse spleen, RORγt$^+$ ILC3 may support survival and activation of CD4$^+$ memory T cells through provision of OX40L and CD30L signals (356-358). We investigate potential functional interactions between ILCs and T cells in Chapter 4.

Examining potential mechanisms of accumulation, we found for the first time that there was increased *in situ* proliferation among total ILCs in the inflamed human lamina propria. We furthermore showed that ILCs proliferate in response to IL-2, which is increased in inflamed IBD lesions (344). CD56$^-$ ILCs expressed higher levels of CD25 in both peripheral blood and colonic lamina propria, suggesting that differential sensitivity to IL-2 may result in the preferential accumulation of CD56$^-$ ILCs under conditions of inflammation. Our findings indicate that ILCs themselves are producers of IL-2, with increased production observed in IBD patients compared to control individuals, and it is conceivable that ILC-derived IL-2 may act in an autocrine manner to stimulate proliferation of these cells. Furthermore, activated CD4$^+$ T cells are major producers of IL-2 (359-361). In light of our finding that ILCs and T cells closely co-localize in the intestinal lamina propria, this presents the interesting possibility that activated CD4$^+$ T cells may regulate ILCs through IL-2. Recent published evidence that arose in the course of this study indeed suggests that this may be the case. Oliphant et al. reported that ILC2 were induced to proliferate and to upregulate expression of IL-5 and IL-13 in the presence of activated $CD4^+$ T cells *in vitro*. Neutralization of IL-2 prohibited ILC2 activation (146).

Analysis of CCR expression by blood ILCs revealed that $CD56^-$ ILCs had higher expression of the gut-homing receptor CCR6 compared to $CD56^+$ ILCs. Preferential recruitment to the intestinal lamina propria under conditions of inflammation may contribute to the observed selective accumulation of $CD56^-$ ILCs in CD and UC patients. CCL20-dependent recruitment of pro-inflammatory CCR6-expressing effector cells has been implicated in the pathogenesis of several animal models of chronic inflammatory diseases, including EAE, RA and colitis (362-366). In humans, increased expression of the CCR6 ligand CCL20 by activated epithelial and stromal cells is found in IBD lesions and has been correlated with the severity of inflammation in paediatric UC patients (367-369). Furthermore, SNPs in the gene encoding CCR6 are associated with increased susceptibility to CD (370). Thus, CCR6-dependent recruitment of pro-inflammatory $CD56^-$ ILCs may contribute to disease pathogenesis in IBD patients.

In contrast to an earlier report of CCR7 expression on human LTi cells isolated from the foetal MLN (182), we did not detect CCR7 expression by blood ILCs. This indicates that CCR7 expression may be limited to the foetal LTi subset, which seed the foetal mesentery early during development (182). Alternatively, it is possible that blood ILCs do not directly home to LNs, but first migrate into peripheral tissue sites, for example in a CCR6-dependent manner, followed by upregulation of CCR7 and migration to the draining MLN. A recent publication revealed that in the murine system $ROR\gamma t^+$ ILCs migrate from the small intestinal lamina propria to the draining MLN in a CCR7-dependent manner (371). Examination of CCR7 expression on lamina propria-resident ILC populations would be required to assess this possibility in a human setting.

While our data suggest that increased proliferation and preferential recruitment may contribute to the selective accumulation of CD56$^-$ ILCs in the inflamed intestinal lamina propria, downregulation of CD56 expression by CD56$^+$ ILCs under inflammatory conditions cannot be excluded. *In vitro* a plastic relationship between human NKR$^-$ and NKR$^+$ ILCs has been demonstrated (189,196). Stimulation of NKp44$^+$ ILC3 with IL-12 can lead to downregulation of NKp44 and RORγt expression and upregulation of T-bet and IFNγ expression (189). It is conceivable that in an environment enriched for pro-inflammatory cytokines such as IL-12, IL-23 and TNFα as is found in the inflamed intestinal lesions of IBD patients, CD56$^+$ ILCs may differentiate into inflammatory CD56$^-$ ILCs. However, this hypothesis would require further examination *in vitro*. Evidence indicates that TGF-β may drive a loss in IL-22 expression by T_H17 cells in UC patients and promote the generation of IL-17 single producers (293). It would be interesting to test whether a similar regulatory mechanism may be at play in the ILC compartment.

Following identification of a CRTH2$^+$ ILC subset enriched for GATA3 expression and type 2 cytokine production in the human foetal gut and tonsil (16) and based on our finding of high GATA3 and IL-13 expression among the CD56$^-$ ILC subset, we investigated the presence of CRTH2$^+$ ILC2 in the adult human blood and gut. In view of their role in Type 2 immunity and allergic inflammation in both mice and humans (10,16,338), we hypothesized that an increased frequency of these cells might be found in UC colon. Increased levels of IL-33 are present in UC lesions (372-374), and it is conceivable that IL-33-mediated expansion and activation of IL-5 and IL-13-

producing CRTH2$^+$ ILC2 cells could contribute to disease pathogenesis (11,317,338,375).

A clear CRTH2$^+$ ILC population that expressed IL-13 but not IFNγ or T_H17-related cytokines was present in blood and intestinal lamina propria, albeit at much lower frequency in the latter. While ILC2 frequency in the blood of CD and UC patients was increased, no significant difference was found in IBD compared to uninflamed gut. Wojno et al. recently reported reduced expression of CRTH2 on IL-33R$^+$ ILC2 in human and mouse lung compared to peripheral blood (140). The group suggested that ligation of CRTH2 by PGD2 in the blood induces downregulation of CRTH2 and migration of ILC2 into the lung. It is conceivable that a similar mechanism could account for the reduced proportion of CRTH2$^+$ cells amongst the Lin$^-$CD127$^+$ ILC population observed in the colon compared to peripheral blood. A different staining approach based on definition of ILC2 according to GATA3 and IL-33R expression could help to clarify open questions regarding the size of the ILC2 population in both the steady-state and inflamed intestinal lamina propria.

Our finding that ILC2 are present in human mesenteric adipose tissue opens up an interesting hypothesis for future investigation. Hypertrophy of mesenteric fat ('creeping fat') overlying inflammatory intestinal lesions is a phenomenon closely associated with CD, although its role in disease pathogenesis is not well understood (376). In CD patients, increased bacterial translocation across the inflamed and leaky intestinal epithelial barrier into mesenteric fat has been described (377). Recent evidence indicates that creeping fat is infiltrated by alternatively activated macrophages. It was suggested that these cells, in conjunction with adipocytes, aid in the establishment of an immunoregulatory environment that prevents systemic inflammation due to bacterial translocation, but allows for development of effective local immunity to bacterial antigens (378). Murine ILC2 have been identified in fat-associated lymphoid structures where they contribute to metabolic homeostasis by maintaining adipose tissue-associated eosinophils and alternatively activated macrophages as well as through direct IL-4- and IL-13-mediated effects on adipocyte progenitors (13,171,180,181). Based on our finding that ILC2 are present in mesenteric adipose tissue it would be interesting to examine a potential role for ILC2 in the generation and functionality of CD-associated creeping fat.

Using a revised panel of surface markers according to a proposal for a unified ILC nomenclature that arose in the course of this study (6), we could confirm a previous report of increased ILC1 frequency in the inflamed intestinal lamina propria of CD compared to control patients (189). Flow cytometry analysis of transcription factor and cytokine expression by blood ILC subsets gated on the basis of CD56, CD117 and CRTH2 expression confirmed that these subsets were indeed enriched for functional markers associated with known ILC1, ILC2 and ILC3 subsets.

However, while the cytokine and transcription factor profiles of these populations indicate that they correspond to the equivalent populations identified in the mouse, it is unclear how human ILC3, ILC0 and ILC1 interrelate and whether ILC1 constitute an independent *bona fide* ILC1 lineage or rather differentiate from ILC3 or ILC0. Both ILC3 and ILC0 populations have been shown to differentiate into ILC1 in response to IL-12 (189). Increased levels of IL-12 are present in the inflamed lamina propria of CD patients (292) and may induce the preferential differentiation of ILC1, resulting in an accumulation of these cells in the intestinal lamina propria. In line with this hypothesis, we observed a trend towards reduced intestinal ILC3 and ILC0 frequencies in CD patients. Further investigations into the plasticity of ILC1 populations will be required to determine the relationship between ILC1, ILC3 and ILC0 more conclusively. Our data indicate that CD56$^-$ ILCs express both RORγt and T-bet. Furthermore, while ILC3 populations are heterogeneous for CD56 expression, ILC1 *ex vivo* do not express CD56 (189). It is therefore likely that the CD-associated IFNγ and IL-17A-producing CD56$^-$ ILC population identified in our lab is comprised of a mixture of ILC3 and *bona fide* and ILC3-derived ILC1.

The functional investigation of human ILC subsets is hampered by their low frequency and compounded by the challenges of obtaining human tissue specimens. Based on knowledge of the developmental dependence of ILCs on common γ chain cytokines from mouse and human studies (379) as well as previous reports of *in vitro* culture of human ILCs (188,196), we describe the establishment of an *in vitro* culture system using IL-2 and IL-7 allowing for the robust expansion of FACS purified ILC1, ILC2 and ILC3 subsets from human peripheral blood. After up to 6 weeks in culture, these ILC populations maintained stable expression of their characteristic surface markers, cytokines and transcription factors. Thus, we successfully established a method to investigate human ILCs functionally *in vitro*.

Co-culture experiments with iSCs indicate that ILC3, ILC2 and ILC1 have a differential capacity to induce stromal cell adhesion molecule expression. ILC3 appear to be most closely related to foetal LTi cells and seem to share their inducer capacity, while ILC1 do not exert an effect on ICAM-1 expression by iSC. The formation of aberrant tertiary lymphoid organs (TLOs) is associated with a range of autoimmune and chronic inflammatory diseases, including IBD. TLOs are thought to arise through LT-dependent mechanisms that recapitulate SLO formation during foetal development and contribute to disease pathogenesis by facilitating the priming and expansion of pathogenic T and B cell responses. TLOs are characterised by the presence of activated stromal cells that highly express adhesion molecules such as ICAM-1 and VCAM-1, and chemokines such as CXCL13, CCL21, CCL19, and CXCL12, helping them to attract and retain infiltrating immune effector cells (380,381).

Our data indicate that, similar to the reported function of foetal LTi cells, ILC3 may contribute to the activation of stromal cells and thus potentially to TLO formation. Future work would aim to investigate more closely the molecular pathways responsible for ILC3-mediated iSC activation and examine whether ILC3 conditioned by the inflammatory environment of IBD lesions are more effective at driving iSC activation. Surprisingly, ILC2 had an inducer capacity equivalent to ILC3. The mechanisms behind ILC3- and ILC2-mediated inducer function most likely engage distinct signalling pathways. LTi/ILC3-mediated inducer capacity has been shown to occur through TNFSF members such as $LT\alpha_1\beta_2$ and LIGHT, as well as through IL-17A (87,182,346,347). ILC2 do not express these LTi-associated markers, but in contrast express high levels of IL-4 and IL-13. Further experiments would be required to elucidate a potential role for these cytokines in ILC2-mediated inducer capacity.

It has been suggested that both physiological and inflammatory TLOs can form in an ILC3-and LT-independent manner. For example, it has recently been proposed that adipose tissue-resident ILC2 may be responsible for the induction of fat-associated lymphoid clusters (95,381). Our data indicate that perhaps ILC2, through IL-4- and IL-13-dependent mechanisms, may also contribute to the induction of TLOs during intestinal inflammation.

In summary, we have identified phenotypically and functionally distinct ILC populations in the human intestinal lamina propria and peripheral blood. Our data indicate that dynamic changes occur in the relative frequencies of ILC subsets in the lamina propria and blood of IBD patients, with ILCs enriched for expression of pro-inflammatory cytokines such as IL-17A and IFNγ accumulating in the inflamed intestine. Potential mechanisms of ILC accumulation include increased *in situ* proliferation and chemokine-mediated recruitment from blood. Examination of the *in situ* localization characteristics of RORγ$^+$ ILC3 revealed that in the intestinal lamina propria, ILC3 closely co-localize with aggregates of T cells. In order to further investigate potential functional interactions between ILCs and T cells, we developed a reliable culture system allowing for the stable expansion of rare ILC subsets purified from human peripheral blood.

Chapter 4: ILCs – unconventional antigen-presenting cells?

4.1 Introduction

In light of our finding that ILCs localize in close proximity to CD3$^+$ T cells in the intestinal lamina propria, we next wanted to investigate the potential functional interactions between these two cell types.

Evidence from murine studies has described direct ILC-derived effects on CD4$^+$ T cell responses that are dependent on expression of MHC class II and co-stimulatory ligands by ILCs. In the initial characterisation of CD4$^+$CD3$^-$ LTi cells in the mesenteric lymph nodes of neonatal mice, Mebius et al. (64) found that, in addition to mediators of lymphoid tissue formation, approximately 50% of cells also express MHC class II *ex vivo*, in the absence of CD40, CD80 or CD86 expression. Nevertheless, co-culture of antigen-specific CD4$^+$ T cells with antigen-pulsed LTi cells induced IL-2 production by the T cells, although at lower levels than following stimulation with lipopolysaccharide (LPS)-activated antigen-pulsed B cells (64). These data suggest the intriguing possibility that LTi cells may regulate antigen-specific CD4$^+$ T cell activation. Further analysis by Eberl et al. revealed that LTi cells resident in LN and PP anlagen at ED16.5 already express MHC class II. However, the functional relevance of this remains unclear since at this time point T cells have not yet started to emigrate from the thymus (56).

Another indication for the potential regulation of CD4$^+$ T cells by LTi-like ILCs comes from their localization characteristics in the murine spleen. While CD11c$^+$ DCs are found mainly in the T cell zones, CD4$^+$CD3$^-$ LTi-like cells are located in the B cell areas and the B:T interface, the site of interaction between activated T helper cells and B cells (382). Following transfer of $CD45.1^+$ OTII-transgenic T cells into congenic $CD45.2^+$ mice and challenge with alum-precipitated ovalbumin (OVA), $CD4^+$ T cells show an early association with $CD11c^+$ DCs, but by day 5 the majority of antigen-specific $CD4^+$ T cells can be found in association with $CD4^+CD3^-$ LTi-like cells at the B:T zone border. Thus, it appears that following priming by DCs in the T cell zones of the spleen, antigen-specific $CD4^+$ T cells migrate to and associate with $CD4^+CD3^-$ LTi-like cells located at the B:T interface. Analysis of purified splenic $CD4^+CD3^-$ LTi-like cells revealed that they express lower levels of MHCII, CD40, CD80 and CD86 than $CD11c^+$ DCs and are unable to directly present antigen to T cells (382).

However, LTi-like ILCs highly express the co-stimulatory ligands OX40L (TNF superfamily 4 (TNFSF4)) and CD30L (TNFSF8) (382). The complementary receptors, OX40 and CD30, are upregulated on $CD4^+$ T cells following antigenic stimulation and deliver essential anti-apoptotic signals required for the sustained survival of memory T cells (383). Mice deficient for OX40 and/or CD30 have intact primary expansion of antigen-specific $CD4^+$ T cells in response to antigenic stimulation, but severely reduced memory $CD4^+$ T cell populations resulting in defective immunity (357,358,382,384). $CD4^+CD3^-$ LTi-like cells purified from mouse spleen can support the survival of memory $CD4^+$ T cells in an OX40-dependent manner *in vitro* (357,382,385). While multiple immune cell types can express OX40L/CD30L after activation *in vivo,* expression of these TNFSF ligands by adult LTi-like cells occurs constitutively and in the absence of antigenic stimulation (357,385). Thus, ILC-mediated OX40L/CD30L signalling may play an important role in the maintenance of memory $CD4^+$ T cell populations in the absence of persistent antigenic stimulation.

In addition to MHC class II expression by foetal LTi cells and adult ILC3, expression of MHC class II transcripts and protein by MLN-resident ILC2 has been reported (11).

Thus ILCs are capable of constitutive MHC class II expression and can mediate functional interactions with $CD4^+$ T cells. In light of the paucity of data regarding the potential modulation of adaptive T cell function by ILCs in humans, we sought to (i) undertake a systematic analysis of MHC class II and co-stimulatory molecule expression by blood- and tissue-resident human ILC populations in control and IBD patients; (ii) examine how MHC class II and co-stimulatory molecule expression by human ILC populations is regulated and (iii) ascertain the functional effects of MHC class II and co-stimulatory molecule expression by ILCs on human antigen-specific T cell responses.

4.2 Results

4.2.1 *Ex vivo* human ILC populations in blood and colon express HLA-DR

Evidence regarding HLA-DR expression by human ILCs is limited. We first wanted to examine HLA-DR expression by ILC subsets in human blood and the intestinal lamina propria.

Flow cytometric analysis showed that a clear population of HLA-DR expressing cells could be identified amongst Lin^-CD127^+ ILCs in peripheral blood and colonic lamina propria of uninflamed control patients (Figure 4.1A). Lin^-CD127^+ ILCs were significantly enriched for HLA-DR expression compared to cNK cells (Figure 4.1B). Further analysis revealed that ILC1, ILC2 and ILC3 subsets showed differential expression of HLA-DR. In blood, approximately 12.8 ± 5.2% of ILC1 expressed HLA-DR, while only 2.7 ± 1.0% of ILC2 and 6.4 ± 1.2% of ILC3 showed HLA-DR expression (Figure 4.1C). In the colon, a different trend was observed with ILC3 containing the highest proportion of HLA-DR expressing cells (50.3 ± 13.0%) (Figure 4.1C). Comparison of blood and colonic ILC subsets revealed that tissue-resident ILCs were significantly enriched for HLA-DR expression, a difference which was most pronounced for ILC3 (Figure 4.1D). qRT-PCR analysis of *ex vivo* FACS sorted ILC subsets confirmed expression on mRNA level of *HLA-DRA* and revealed expression of *HLA-DMA*, *HLA-DMB* and the invariant chain *CD74,* additional markers involved in the antigen presentation pathway. In comparison to $CD14^+$ monocytes ILCs expressed considerably lower levels of *HLA-DR* and related transcripts, suggesting that their potential to present antigen is likely reduced relative to professional antigen-presenting cells (APCs) (Figure 4.1E). However, levels of class II-related genes were higher in ILCs than in iSCs.

4.2.2 *Ex vivo* blood and intestinal ILCs express co-stimulatory ligands

Flow cytometric analysis of ILC populations in blood and colonic lamina propria from uninflamed control patients indicated that a proportion of Lin$^-$CD127$^+$ ILCs express the co-stimulatory ligands CD80, CD86, OX40L and programmed death-ligand 1 (PD-L1) in addition to HLA-DR (Figure 4.2A). Only a very small percentage of Lin$^-$CD127$^+$ ILCs expressed CD80 (0.58 ± 0.25%) and CD86 (2.75 ± 0.91%), at levels equivalent to cNK cells (Figure 4.2B). However, a substantial proportion of ILCs expressed OX40L (17.2 ± 3.6%) and the inhibitory ligand PD-L1 (21.8 ± 3.3%). Compared to cNK cells, ILCs were enriched for expression of OX40L and showed equivalent expression of PD-L1 (Figure 4.2B). Comparison of the different ILC subsets indicated that in the blood ILC1 were enriched for expression of CD86, OX40L and PD-L1 compared to ILC3 and ILC2 (Figure 4.2C). Analysis of colonic ILC subsets did not reveal significant differences in co-stimulatory ligand expression between ILC1, ILC2 and ILC3 (Figure 4.2D). In contrast to HLA-DR expression, which was enriched in colonic ILCs, no significant differences in co-stimulatory ligand expression were detected between blood and colonic ILC subsets (Figure 4.2E).

Taken together, our findings indicate that *ex vivo* human ILC populations in blood and intestinal lamina propria express HLA-DR and co-stimulatory ligands. A larger proportion of ILCs express HLA-DR in the colon compared to blood. In the blood, ILC1 are enriched for HLA-DR and co-stimulatory ligand expression, while in the colon, ILC3 are enriched for HLA-DR expression.

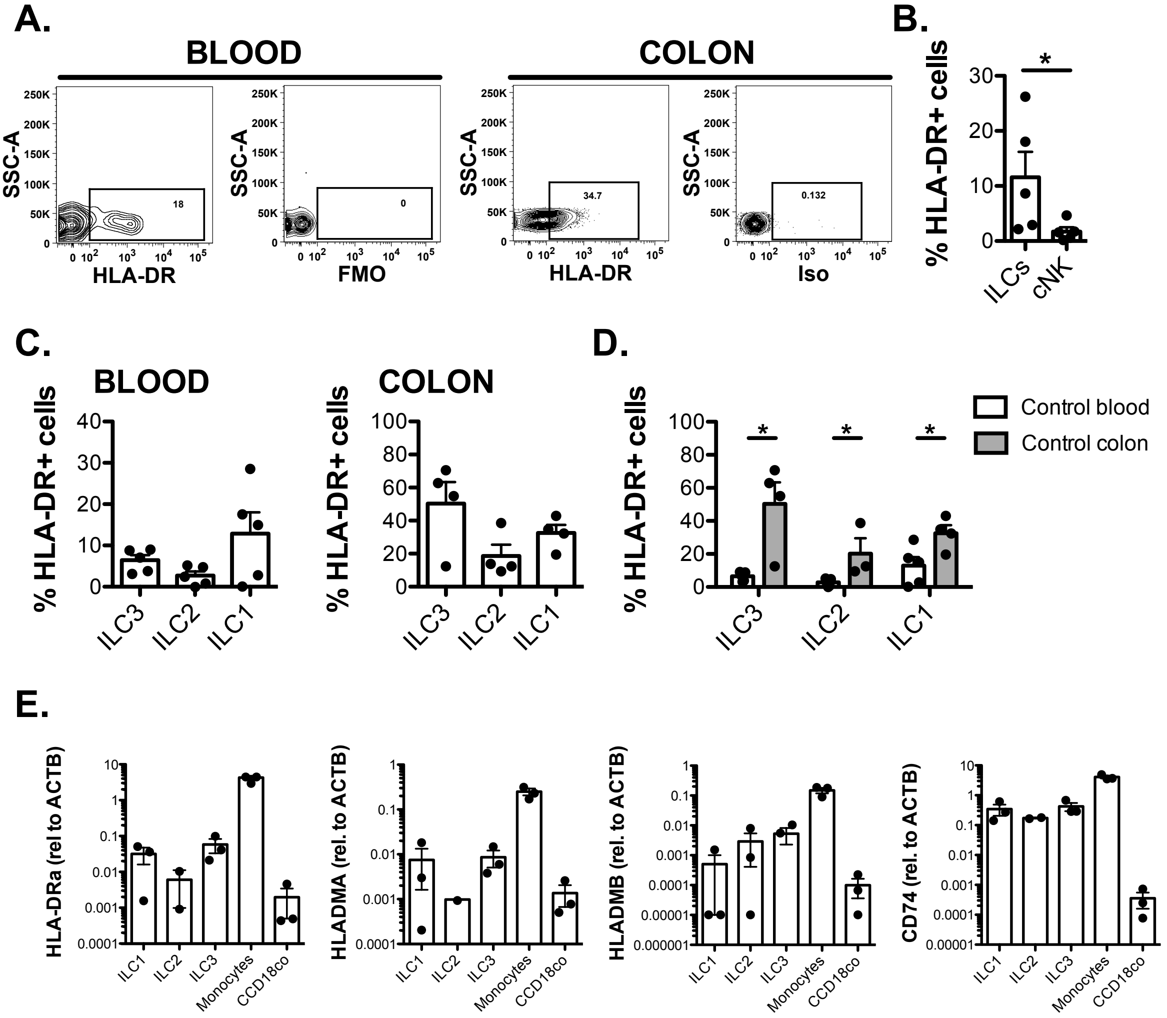

Figure 4.1: Human *ex vivo* ILC subsets in blood and intestinal lamina propria express HLA-DR. PBMCs or LPMCs were isolated and stained for flow cytometry analysis. ILCs were gated as described in Chapter 3. **(A)** Representative FACS plots depicting HLA-DR expression by *ex vivo* Lin$^-$CD127$^+$ ILCs in blood and control from uninflamed controls. **(B)** Quantification of HLA-DR expression by total Lin$^-$CD127$^+$ ILCs and cNK cells in blood from healthy controls. **(C)** Quantification of HLA-DR expression by *ex vivo* ILC subsets in control blood and colon intestinal lamina propria. **(D)** Comparison of HLA-DR expression by blood and colonic ILCs from control patients. **(E)** qPCR analysis of expression of HLA-DR-related markers in *ex vivo* FACS sorted blood ILC subsets. Each dot in the plots represents an individual donor. Statistical significance was determined by means of Mann-Whitney U tests. Bars represent mean ± SEM. *$p \leq 0.05$.

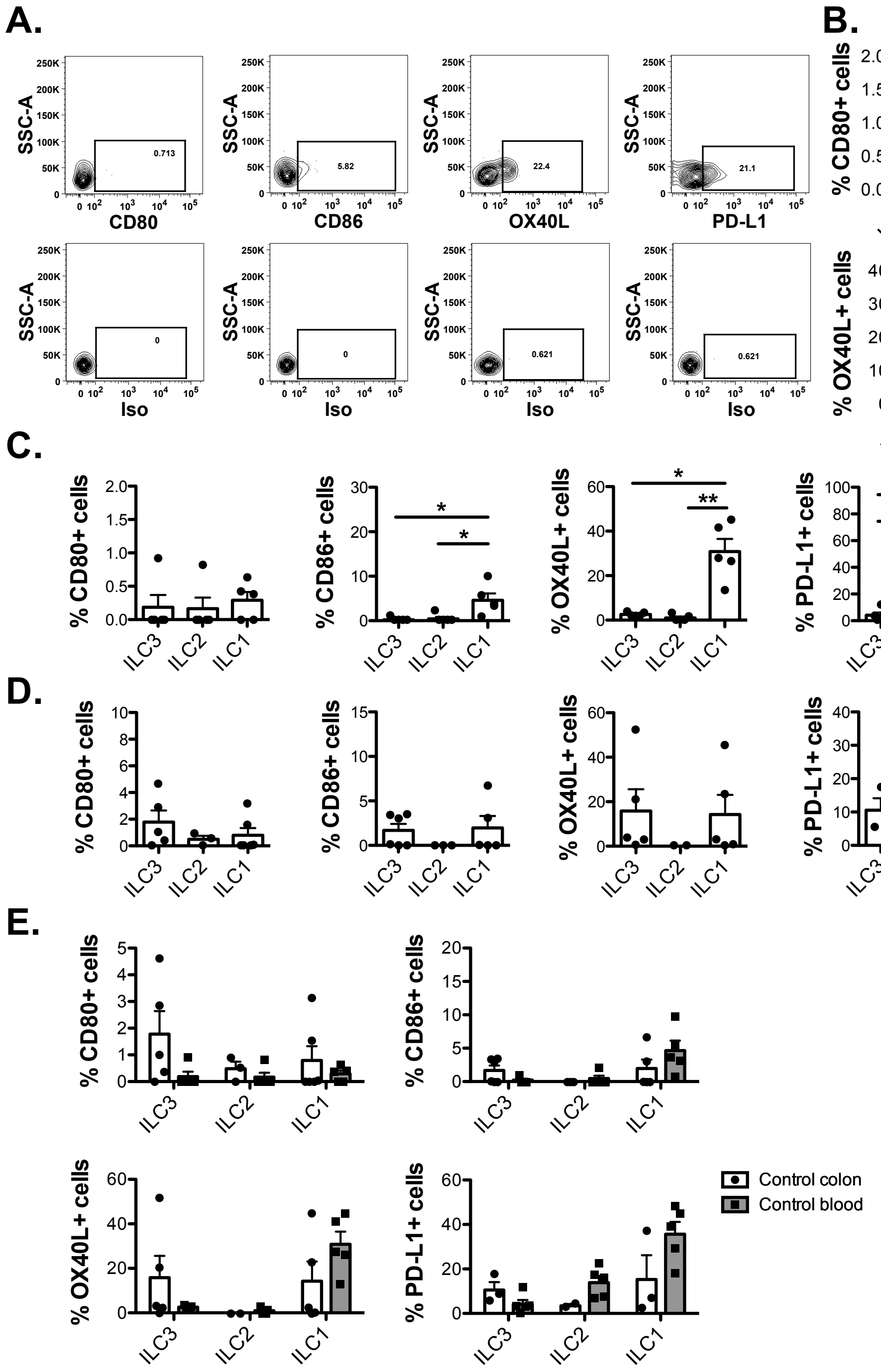

Figure 4.2: Human ILC subsets in blood and intestinal lamina propria express express co-stimulatory ligands. (A) Representative FACS plots showing co-stimulatory ligand expression by total Lin$^-$CD127$^+$ ILCs. **(B)** Comparison of co-stimulatory ligand expression between total Lin$^-$CD127$^+$ ILCs and cNK cells in control blood. **(C + D)** Quantification of co-stimulatory ligand expression by individual ILC subsets in blood (C) and colonic lamina propria (D) of control patients. **(E)** Comparison of HLA-DR and co-stimulatory ligand expression by colonic and blood ILC subsets. Each dot in the plots represents an individual donor. Statistical significance was determined by means of Mann-Whitney U tests. Bars represent mean ± SEM. *$p \leq 0.05$. **$p \leq 0.01$.

4.2.3 *In vitro* expanded ILCs express HLA-DR and co-stimulatory ligands

Next we examined whether *in vitro* expanded blood ILC populations expressed HLA-DR and co-stimulatory ligands. ILC subsets were sort purified from control blood and expanded using a mixture of IL-2 (100 U/ml) and IL-7 (50 ng/ml) as described in Chapter 3. HLA-DR and co-stimulatory ligand expression was assessed by flow cytometry after 3-5 weeks of culture.

All three ILC subsets expressed high levels of HLA-DR following *in vitro* culture. 39.6 ± 4.8% of ILC3, 56.8 ± 6.2% of ILC2 and 59.7 ± 8.3% of ILC1 expressed HLA-DR (Figure 4.3A). We detected expression of co-stimulatory ligands CD80, CD86, OX40L and PD-L1 as observed in *ex vivo* ILC subsets (Figure 4.3B-D). Furthermore, we observed expression of CD83, CD40 and CD70 by *in vitro* expanded ILC subsets (Figure 4.3C and E). Comparison of *ex vivo* and *in vitro* cultured blood ILC subsets revealed modulation of HLA-DR and co-stimulatory ligand expression following culture. Compared to *ex vivo* blood ILC subsets, cultured ILC1, ILC2 and ILC3 expressed significantly higher levels of HLA-DR, CD80 and CD86. In contrast, OX40L expression was reduced on *in vitro* expanded compared to *ex vivo* ILC1, while no significant differences were observed between *in vitro* cultured and *ex vivo* ILC2 and ILC3. PD-L1 expression was significantly reduced on all *in vitro* cultured ILC subsets compared to *ex vivo* ILCs (Figure 4.3F). Thus, *in vitro* cultured ILCs expressed higher levels of class II-related genes compared to *ex vivo* ILC subsets.

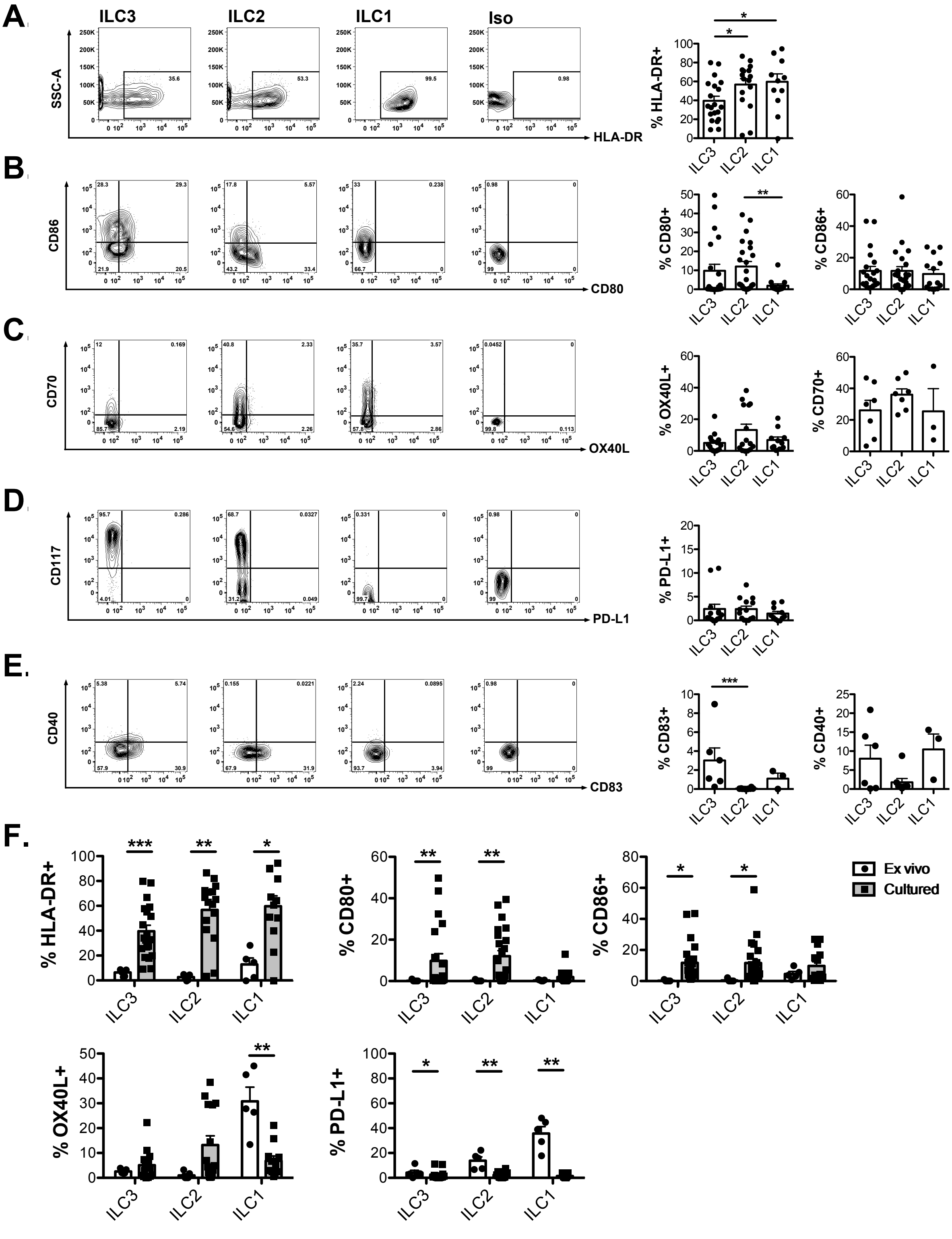

Figure 4.3: *In vitro* expanded blood ILCs express HLA-DR and co-stimulatory ligands. (A - E) Representative FACS plots (left) and quantification (right) of HLA-DR and co-stimnulatory ligand expression by blood ILC subsets expanded in vitro for 3-5 weeks with IL-2 (100 U/ml) and IL-7 (50 ng/ml). **(F)** Comparison of HLA-DR and co-stimulatory ligand expression between *ex vivo* and *in vitro* expanded blood ILC subsets. Each dot in the plots represents an individual donor. Statistical significance was determined by means of Mann-Whitney U tests. Bars represent mean ± SEM. *p ≤ 0.05. **p ≤ 0.01. ***p ≤ 0.001.

4.2.4 ILC1 show increased expression of HLA-DR in IBD compared to control blood

Next we examined HLA-DR expression by blood and intestinal ILC subsets in control and IBD patients. As shown in Figure 4.4A, there was higher expression of HLA-DR amongst Lin^-CD127^+ ILCs in IBD compared to control blood. Quantification of HLA-DR expression by ILC subsets showed that HLA-DR expression amongst ILC1 was significantly increased in blood from CD (48.1 ± 6.6% $HLA\text{-}DR^+$) and UC patients (45.2 ± 4.6% $HLA\text{-}DR^+$) compared to healthy controls (12.8 ± 5.2%). While there was a trend towards increased HLA-DR expression by ILC2 and ILC3 in IBD blood this difference did not reach statistical significance (Figure 4.4B).

In the intestinal lamina propria no significant differences in HLA-DR expression by ILC subsets were observed between IBD and control patients. However, in contrast to our findings in blood, there was a trend towards decreased HLA-DR expression by colonic ILC3 in both CD and UC patients, but these differences were not statistically significant (Figure 4.4C). Thus, our data point towards differences in HLA-DR expression by ILC populations in IBD patients compared to uninflamed controls, with potentially different regulation in peripheral blood compared to the intestinal lamina propria.

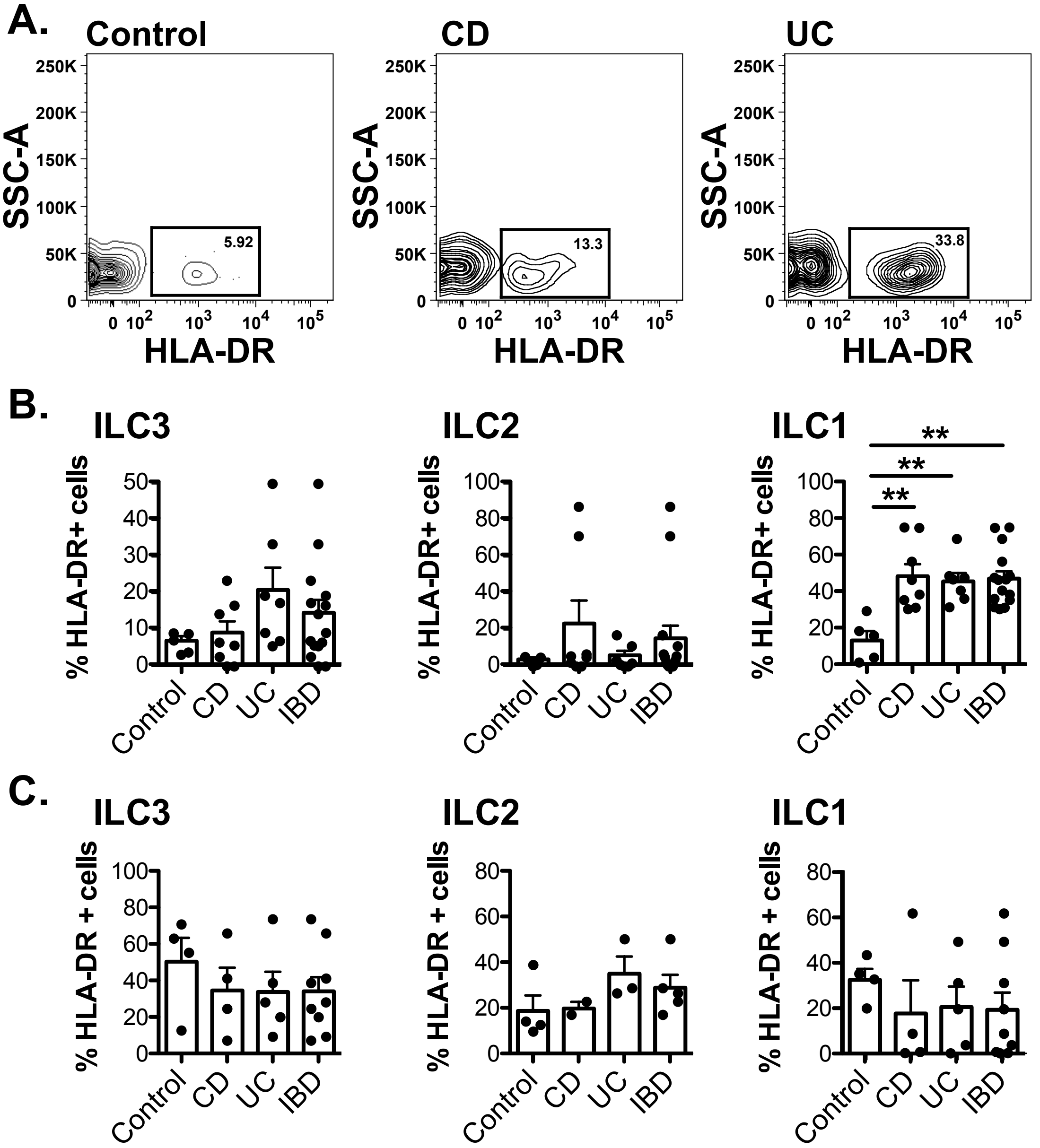

Figure 4.4: ILC1 have increased HLA-DR expression in IBD blood. FACS analysis of HLA-DR expression by *ex vivo* blood and colonic ILCs from control compared to IBD patients. **(A)** Representative FACS plots showing HLA-DR expression by total Lin$^-$CD127$^+$ ILCs from control and IBD blood. **(B + C)** Quantification of HLA-DR expression by ILC subsets from blood (B) and colon (C) of control and IBD patients. Each dot in the plots represents an individual donor. Statistical significance was determined by means of Mann-Whitney U tests. Bars represent mean ± SEM. $^{**}p \leq 0.01$.

4.2.5 HLA-DR expression by ILCs is not regulated by IFNγ

In view of the differential HLA-DR expression by *ex vivo* ILCs depending on tissue environment (blood versus colon) and inflammation state (uninflamed versus IBD) as well as the increased HLA-DR expression induced by *in vitro* culture, we wanted to examine how HLA-DR expression by ILCs was regulated.

Due to its well-documented role as an inducer of MHC class II expression, we initially wanted to examine whether IFNγ was involved in the regulation of HLA-DR expression by human ILC subsets (386,387). *In vitro* expanded ILC subsets were stimulated with IFNγ (1ng/ml) for 24h, followed by flow cytometric analysis. No significant differences in HLA-DR expression could be detected in IFNγ-stimulated ILC1, ILC2 or ILC3 compared to unstimulated controls (Figure 4.5A-C). Similarly, expression of the co-stimulatory ligands CD80 and CD86 by ILC subsets was unaffected following stimulation with IFNγ (Figure 4.5D-I). Stimulation of total PBMCs with varying doses of IFNγ (0.1 ng/ml; 1 ng/ml; and 10 ng/ml) for 24h confirmed that the cytokine used was bioactive. We observed upregulation of CD86 expression both by bulk PBMCs as well as CD14$^+$ monocytes in response to IFNγ stimulation (Figure 4.5J). Thus, HLA-DR and co-stimulatory ligand expression by ILCs appear to be regulated in an IFNγ-independent manner.

4.2.6 Cytokine-dependent regulation of HLA-DR expression by ILCs

We next wanted to examine whether other cytokines may play a role in the modulation of HLA-DR and co-stimulatory ligand expression by ILCs. Published data indicate that ILC1 are highly responsive to stimulation with IL-12, IL-15 or IL-18, while ILC2 are activated by IL-25 and IL-33 and ILC3 are responsive to stimulation with IL-1β and IL-23 (16,185,189,196). qRT-PCR analysis of cytokine receptor expression by *ex vivo* sorted ILC populations confirmed enrichment of *IL23R* and *IL1R1* expression by ILC3, while ILC2 expressed highest levels of *IL1RL1*, the gene encoding IL-33R/ST2 (Figure 4.6A). All three ILC subsets expressed *IL12RB1*, although ILC2 expressed lower levels compared to ILC1 and ILC3. Similarly, expression of *IL6R* transcripts was detected in all three ILC subsets.

We stimulated *in vitro* expanded blood ILC1, ILC2 and ILC3 overnight with combinations of IL-1β, IL-23, IL-6 as well as with IL-33, IL-12, IL-15 and TNFα, followed by flow cytometric analysis of HLA-DR expression. We detected upregulation of HLA-DR expression by ILC3 stimulated with IL-1β, IL-23, IL-1β + IL-23 as well as TNFα (Figure 4.6B). *In vitro* expanded ILC2 expressed increased levels of HLA-DR following stimulation with IL-33 and TNFα (Figure 4.6C). Finally, stimulation of ILC1 with IL-15 resulted in increased expression of HLA-DR (Figure 4.6D). Furthermore, *ex vivo* blood ILC3 stimulated overnight with IL-1β, IL-6 and IL-23 alone or in combination resulted in increased expression on mRNA level of *HLA-DRA* and *HLA-DMA* as well as of the co-stimulatory ligands *CD80* and *TNFSF4* (encoding OX40L) (Figure 4.6E). Similarly, overnight stimulation of *in vitro* expanded colonic ILC3 with IL-1β and IL-23 resulted in upregulation of HLA-DR expression as assessed by flow cytometry (Figure 4.6F).

Taken together, these results indicate HLA-DR and co-stimulatory ligand expression by human ILCs may be regulated by different cytokines specific for each ILC subset, but not by IFNγ.

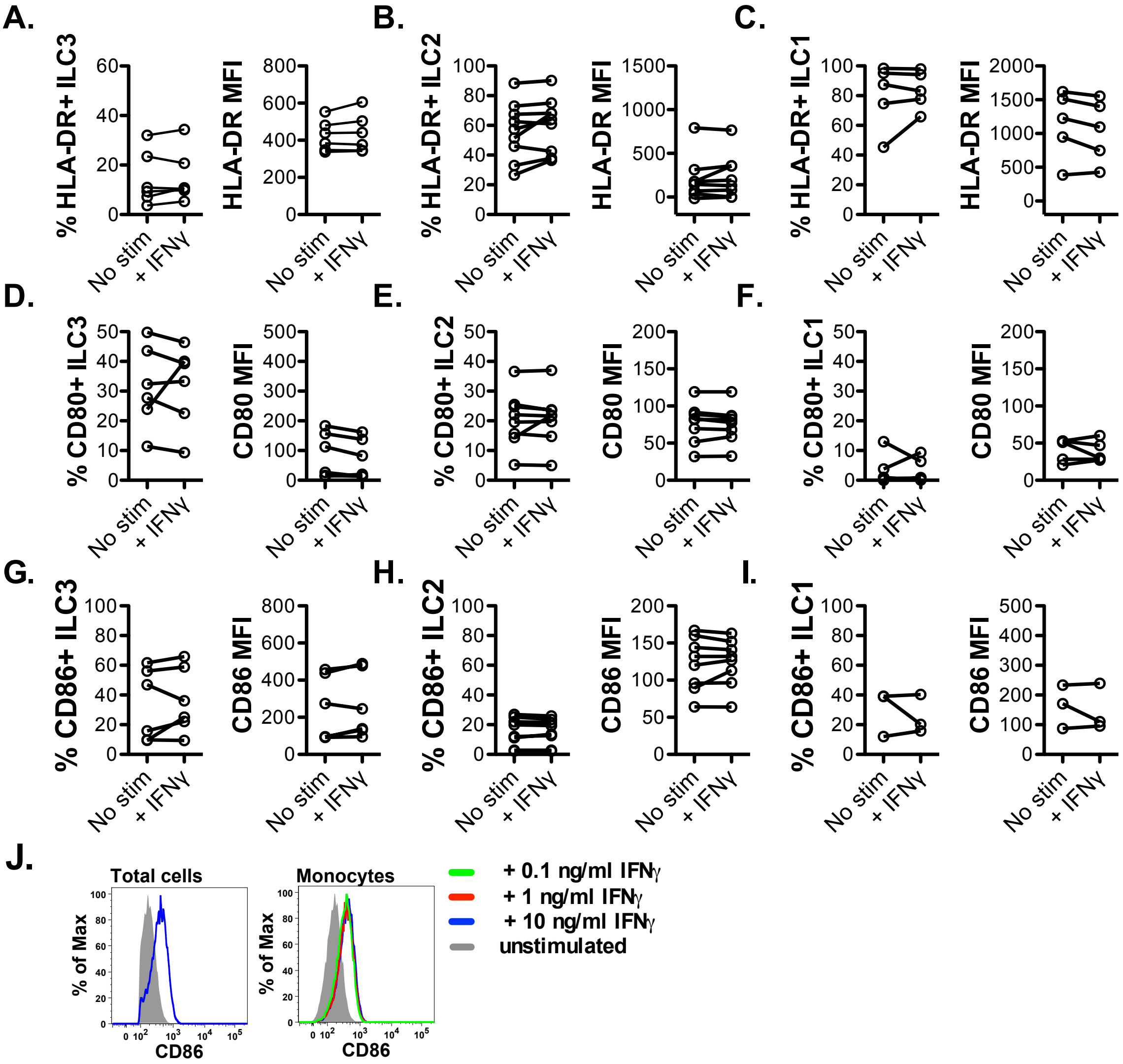

Figure 4.5. IFNγ-independent regulation of ILC MHC class II and co-stimulatory ligand expression. (A - I) Flow cytometry analysis of HLA-DR (A-C), CD80 (D-F) and CD86 (G-I) expression by *in vitro* expanded blood ILC subsets stimulated with IFNγ (1 ng/ml) for 24h. **(J)** Whole PBMCs were stimulated with IFNγ (0.1, 1 and 10 ng/ml) for 24h. Representative FACS plot depiciting CD86 expression by whole PBMCs or gated on CD14+ monocytes. Each dot in the plots represents an individual donor. Statistical significance was determined by means of Wilcoxon matched-pairs signed rank tests.

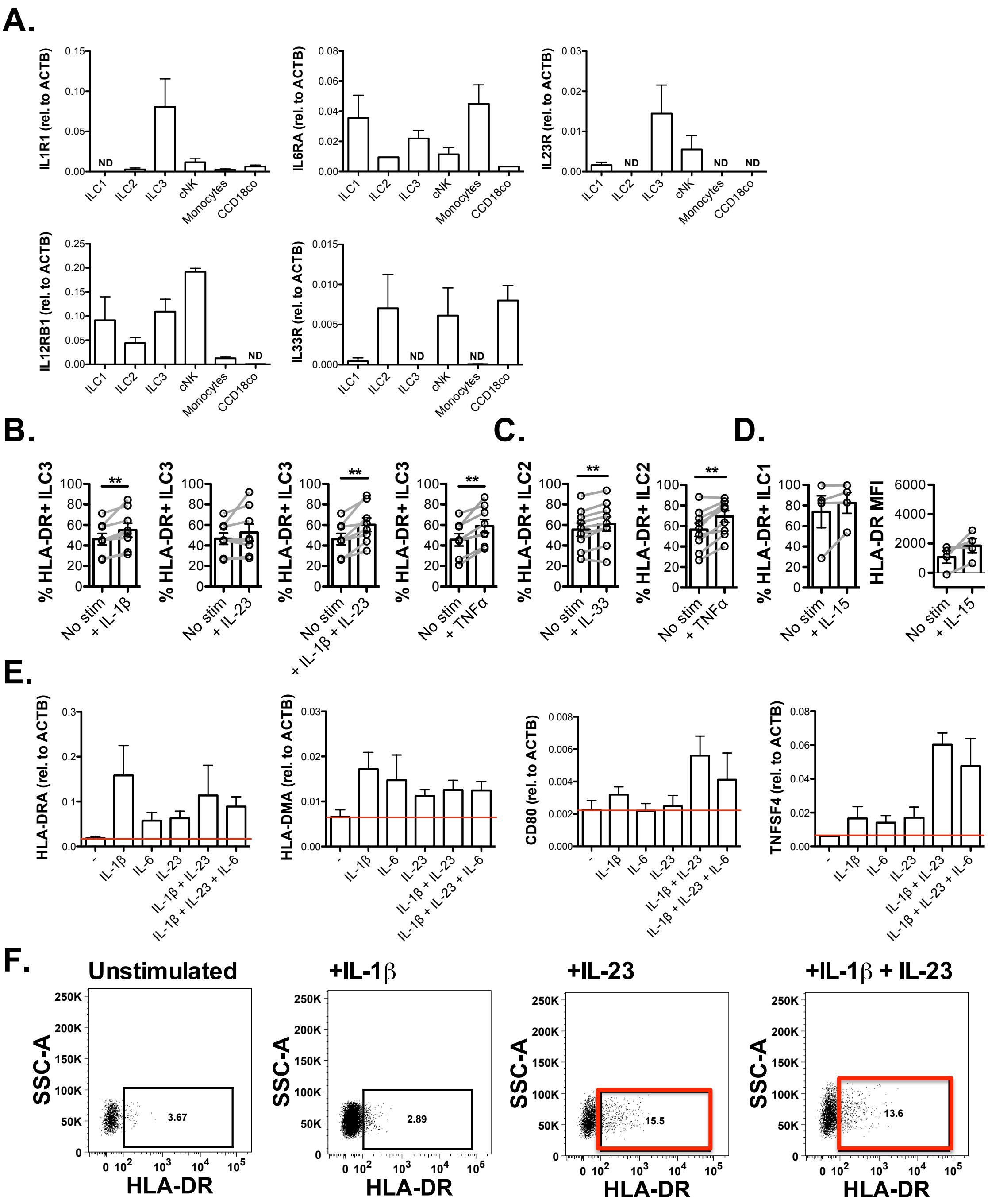

Figure 4.6: Cytokine signals but not direct bacterial stimulation regulate HLA-DR expression by ILCs. (A) qRT-PCR analysis of *ex vivo* cytokine receptor expression by FACS sorted blood ILCs subsets from n = 2-5 individual donors. **(B)** Quantification of HLA-DR expression by *in vitro* expanded ILC3 stimulated overnight with IL-1β and/or IL-23 or TNFα. **(C)** Quantification of HLA-DR expression by *in vitro* expanded ILC2 stimulated with IL-33 or TNFα. **(D)** Quantification of HLA-DR expression by *in vitro* expanded ILC1 stimulated with IL-15. **(E)** qRT-PCR analysis of *in vitro* expanded ILC3 stimulated with individual cytokines or combinations of IL-1β, IL-6 and IL-23. **(F)** Representative FACS plots of *in vitro* expanded colonic ILC3 stimulated with IL-1β and IL-23 alone or in combination. In (E) qRT-PCR analysis was performed on ILC subsets from n = 3 individuals donors. Each dot in the plots represents an individual donor. Statistical significance was determined by means of Mann-Whitney U tests. $^{**}p \leq 0.01$.

4.2.7 ILCs take up and process exogenous protein antigen

Due to their expression of HLA-DR and co-stimulatory ligands, we next investigated whether ILCs were capable of taking up and processing exogenous antigen. DQ-OVA is a self-quenching protein that, upon cellular uptake and proteolytic digestion in the endosomal pathway, becomes fluorescent and detectable by flow cytometry, thus allowing quantification of protein antigen uptake and processing (Figure 4.7A). *In vitro* expanded blood ILC1, ILC2 or ILC3 were incubated with DQ-OVA for 4h at 37°C to allow proteolysis or on ice in order to quench phagocytic and proteolytic activity. Monocytes and B cells were used as positive antigen-processing control populations, total CD3$^+$ T cells and cNK cells as negative control populations.

Incubation of ILC3, ILC2, ILC1, monocytes and B cells with DQ-OVA at 37°C resulted in a clear shift in fluorescein isothiocyanide (FITC) fluorescence, whereas only a small shift was observed for cNK cells and T cells (Figure 4.7B). Quantification of FITC fluorescence (normalized to FITC signal on ice) indicated that the capacity of ILCs to take up and process DQ-OVA was lower than that of monocytes, but similar to that of B cells and significantly increased compared to T cells and cNK cells (Figure 4.7C). Similar results were obtained in an experiment using *in vitro* expanded colonic ILC3 and ILC1 (Figure 4.7D).

Finally, we confirmed these findings by means of a phagocytosis assay using FITC-coated latex beads. Similar to the DQ-OVA assay, *in vitro* expanded blood ILCs had a capacity to take up phagocytosis beads that was intermediate between monocytes and T cells (Figure 4.7E). Therefore, these data suggest that ILCs can take up and process protein antigen.

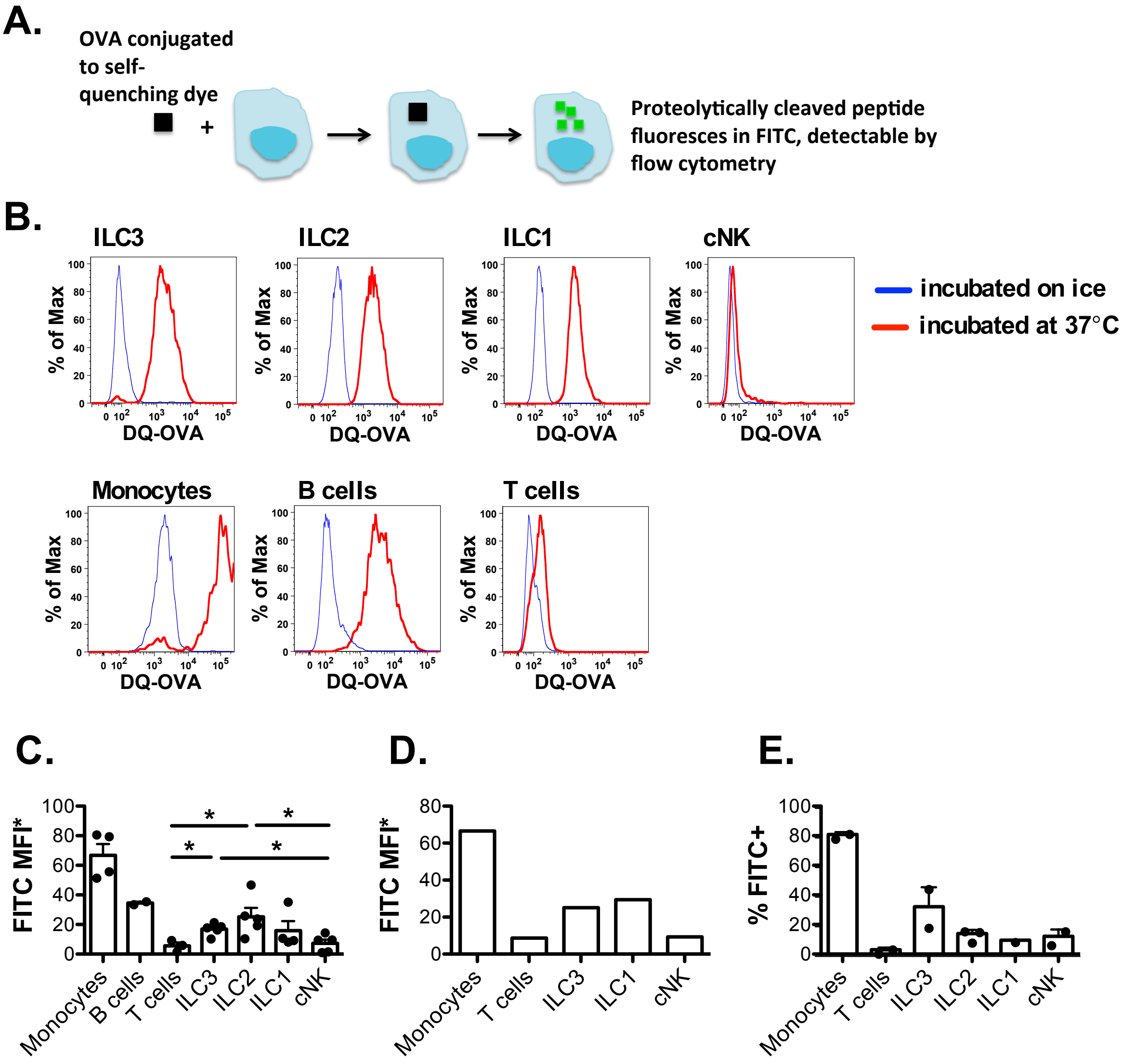

Figure 4.7. ILCs can take up and proteolytically process protein antigen. (A) Schematic representation of the principle underlying the DQ-OVA assay. DQ-OVA is a self-quenching OVA-conjugate that, upon cellular uptake and proteolytic digestion in the endosomal pathway, becomes fluoerescent and detectable by flow cytometry, thus allowing quantification of protein antigen uptake and processing. **(B)** Representative FACS plots depicting FITC fluorescence of DQ-OVA in *in vitro* expanded ILCs or control populations incubated on ice or at 37°C. **(C)** Quantification of FITC fluorescence in ILCs and control populations from human blood. **(D)** Quantification of FITC fluorescence in *in vitro* expanded ILCs and control populations from human intestinal lamina propria. **(E)** ILCs and control populations were incubated overnight with FITC-coated phagocytosis beads followed by flow cytometry analysis. Quantification of percentage of FITC-expressing cells. Each dot in the plots represents an individual donor. Statistical significance was determined by means of Mann-Whitney U tests. Bars represent mean ± SEM. $*p \leq 0.05$.

4.2.8 Establishment of antigen-specific memory CD4$^+$ T cell lines

Thus far our data have shown that human ILC populations localize in proximity to CD3$^+$ T cell aggregates in the intestinal lamina propria (Chapter 3), express HLA-DR and co-stimulatory ligands and can take up and process model antigens. We next wished to investigate the potential functional effects of HLA-DR-mediated antigen presentation by ILCs to CD4$^+$ T cells.

As a large proportion of CD4$^+$ T cells resident in the intestinal lamina propria are memory cells that have already encountered cognate antigen (388), we aimed to model a situation of ILC-mediated antigen presentation to memory CD4$^+$ T cells. Non-typhoidal *Salmonella enterica* infections are a leading cause of human gastroenteritis, accounting for an estimated 93.8 x 10^6 cases world-wide annually (389). CD4$^+$ T cells undergo a drastic expansion following *Salmonella* infection and production of Th1 and Th17 effector cytokines is thought to play an important role in the resolution of infection (390). As a result of wide exposure, we reasoned that *Salmonella*-specific memory CD4$^+$ T cells would be present in a high proportion of individuals.

Our strategy for isolation and expansion of *Salmonella*-specific memory CD4$^+$ T cells is outlined in Figures 4.8 and 4.9. In order to avoid HLA mismatch and allogenicity-dependent T cell proliferation, we isolated autologous memory CD4$^+$ T cells, ILC subsets and monocytes from the same donors. ILC subsets were sort purified and expanded with a mixture of IL-2 (100 U/ml) and IL-7 (50 ng/ml) as described in Chapter 3. Memory CD4$^+$ T cells in human peripheral blood were defined phenotypically as CD45$^+$CD8$^-$CD4$^+$CD45RA$^-$CD45RO$^+$ cells and FACS sorted to purities ≥99.9% (Figure 4.9A). Monocytes were isolated using an adherence method in combination with MACS purification, yielding purities ≥95.0% (Figure 4.9B). Monocytes were irradiated (45 Gy) and pulsed with *Salmonella* lysate for 6-8 hours to allow for antigen uptake and processing. Memory CD4$^+$ T cells and antigen-pulsed monocytes were then combined into co-cultures, allowing *Salmonella*-responsive CD4$^+$ T cells to expand. Co-cultures without addition of bacterial antigen were used as negative controls for CD4$^+$ T cell proliferation (Figure 4.8A). After 10 days, the co-cultures were terminated and *Salmonella*-responsive CD4$^+$ T cells were FACS sorted as CFSE$^-$CD8$^-$CD14$^-$CD4$^+$Inducible T-cell co-stimulator (ICOS)^{high} cells (Figure 4.9C). Sorted cells were expanded further by means of stimulation with CD3/CD28 dynabeads beads and IL-2 (200 U/ml). After 5-7 days of culture, the expanded *Salmonella*-specific CD4$^+$ T cells were recovered and flow cytometry analysis indicated that they had retained a pure CD3$^+$CD8$^-$CD4$^+$ phenotype (Figure 4.9D). The *Salmonella*-specific CD4$^+$ T cells were starved overnight in order to reduce background proliferation induced by the expansion protocol and re-labelled with CFSE.

In order to assess the ability of ILC subsets to activate antigen-specific CD4$^+$ memory T cells, autologous *in vitro* expanded ILC1, ILC2 or ILC3 were irradiated (45Gy), pulsed with *Salmonella* lysate for 6-8 hours and co-cultured with the expanded CFSE-labelled *Salmonella*-responsive CD4$^+$ T cells for 5 days. Read-outs for CD4$^+$ T cell activation included proliferation as assessed by CFSE dilution, expression of surface activation markers (ICOS, CD25, OX40, PD-1, CD127), transcription factors (T-bet, Eomes, GATA3, Foxp3) and cytokines (IL-2, IL-17A, IL-22, GM-CSF, IFNγ, IL-4, IL-5, TNFα, IL-10). Irradiated antigen-pulsed autologous monocytes were used as positive controls for the induction of *Salmonella*-specific CD4$^+$ T cell activation. ILCs or monocytes pulsed with *Bifidobacteria* lysate (an unrelated bacterial species) were used to control for the specificity of CD4$^+$ T cell responses, while stimulation of co-cultures with SEB served as a positive control for the induction of CD4$^+$ T cell proliferation (Figure 4.8B).

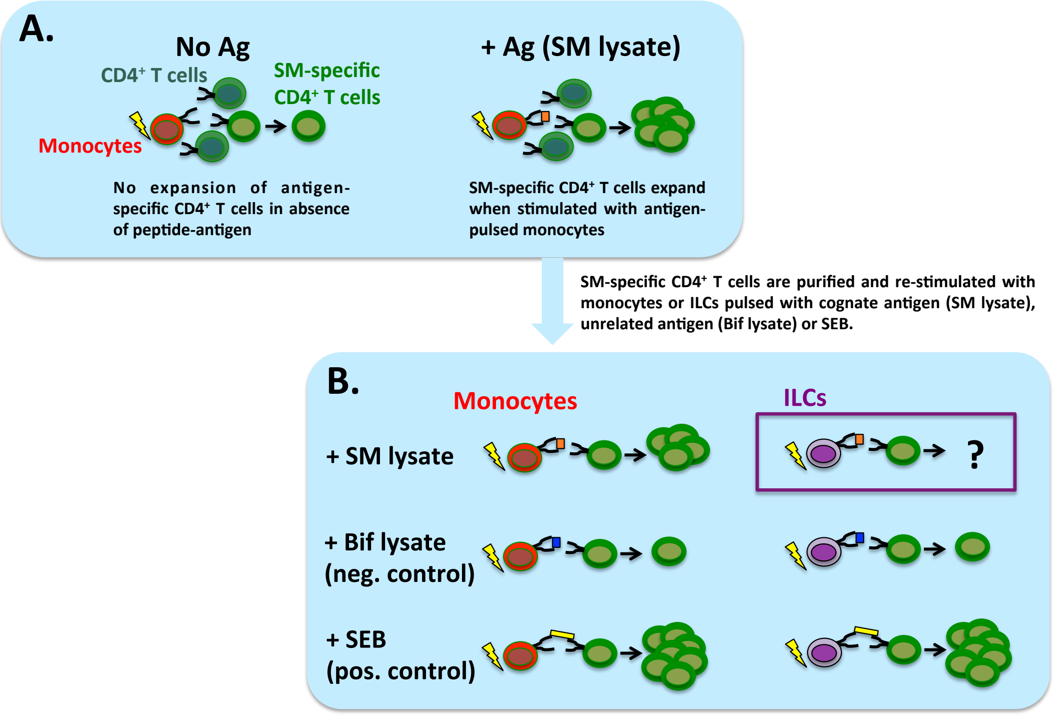

No expansion of antigen-specific CD4$^+$ T cells in absence of peptide-antigen

SM-specific CD4$^+$ T cells expand when stimulated with antigen-pulsed monocytes

SM-specific CD4$^+$ T cells are purified and re-stimulated with monocytes or ILCs pulsed with cognate antigen (SM lysate), unrelated antigen (Bif lysate) or SEB.

Figure 4.8: Establishment of antigen-specific CD4$^+$ T cell assays. (A) Schematic representation of primary expansion of antigen-specific memory CD4$^+$ T cells isolated from peripheral blood. FACS sorted CD4$^+$CD45RO$^+$ memory T cells were labelled with CFSE and stimulated *in vitro* for 10 days with irradiated autologous monocytes pulsed with *Salmonella (SM)* lysate antigen. In the presence of *SM* antigen, rare *SM*-specific CD4$^+$ T cells become activated and undergo clonal expansion, which is detectable as dilution of CFSE signal by flow cytometry (right). In the absence of antigen, no CD4$^+$ T cell proliferation is observed (left). *SM*-responsive (CFSE^{negative}) CD4$^+$ T cells were re-sorted using FACS and expanded further *in vitro* using CD3/CD28 activator beads. **(B)** Schematic representation of re-stimulation of *in vitro* epanded *SM*-specific memory CD4$^+$ T cells. The capacity of ILCs to activate *SM*-responsive CD4$^+$ T cells was tested in direct comparison to monocytes. Read-outs for CD4$^+$ T cell activation included proliferation as measured by CFSE dilution, expression of surface activation markers, cytokine production and TF expression. *In vitro* expanded *SM*-specific CD4$^+$ T cells were again labelled with CFSE and co-cultured for 5 days with irradiated monocytes or ILCs pulsed with *SM* lysate. Monocytes/ILCs pulsed with the unrelated antigen *Bifidobacterium (Bif)* lysate were used as controls for the specificity of CD4$^+$ T cell responses. Monocytes/ILCs pulsed with SEB were used as positive controls for the induction of T cell proliferation.

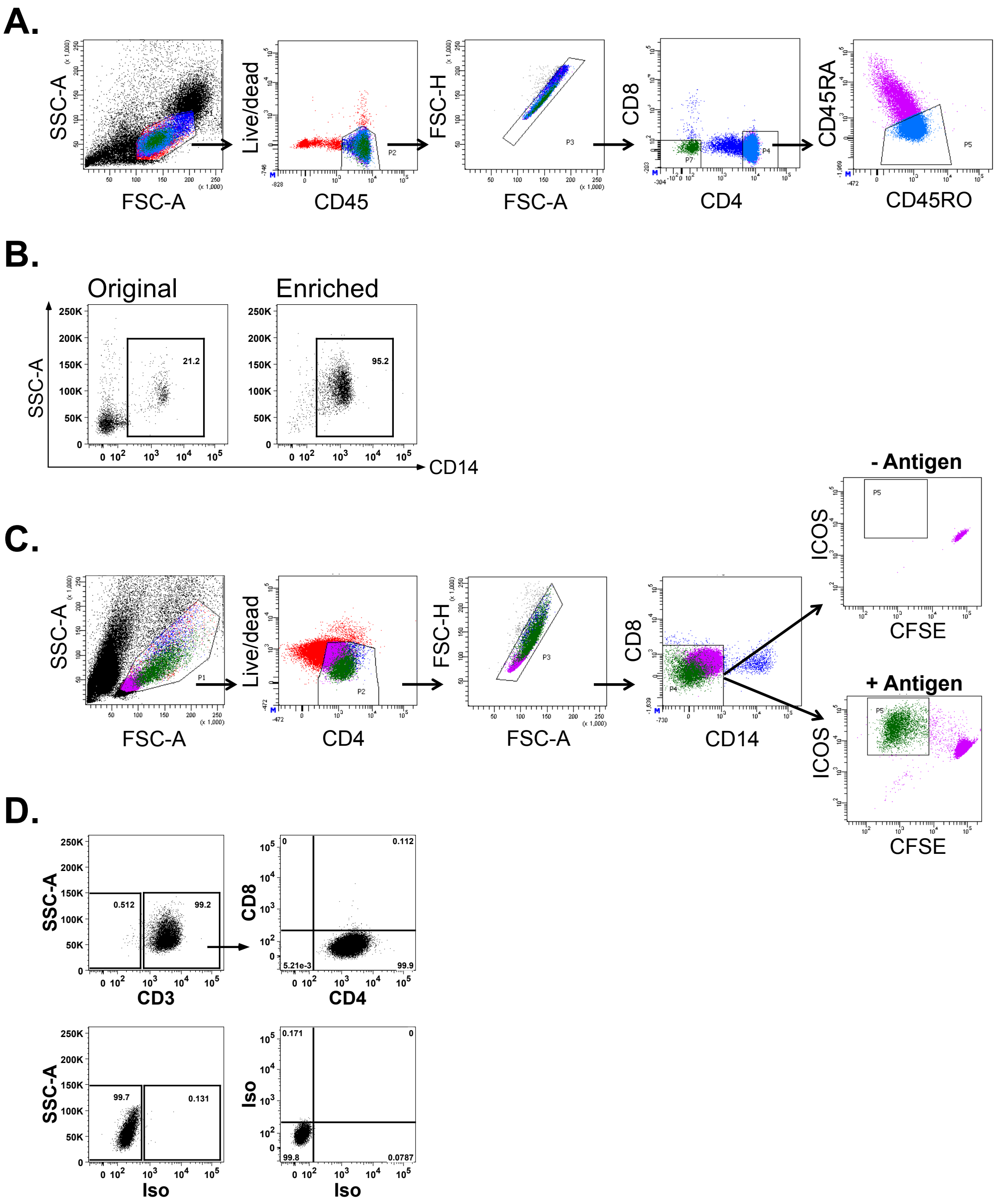

Figure 4.9: Expansion of *Salmonella*-responsive memory CD4$^+$ T cells. (A) Representative FACS plots showing sort strategy for blood memory CD4$^+$ T cells pre-enriched using MACS. **(B)** Representative FACS plots showing monocyte purity following MACS enrichment. **(C)** Representative FACS plots showing re-sort of *Salmonella (SM)*-responsive CD4$^+$ T cells based on CFSE dilution following expansion with *SM* lysate-pulsed autologous monocytes. **(D)** Representative FACS plots showing surface characterisation of *SM*-specific CD4$^+$ T cells following further expansion using CD3/CD28 activator beads and IL-2 (200 U/ml).

4.2.9 ILCs pulsed with *Salmonella* lysate do not directly activate *Salmonella*-specific memory CD4$^+$ T cells

Flow cytometry analysis showed that co-culture of *Salmonella*-specific CD4$^+$ T cells with SEB-pulsed ILCs or monocytes induced vigorous proliferation as measured by CFSE dilution and upregulation of the cell surface activation markers ICOS, CD25 and OX40. In contrast, *Salmonella*-specific CD4$^+$ T cells co-cultured with monocytes or ILCs pulsed with *Bifidobacterium* lysate did not proliferate or display an activated surface phenotype (Figure 4.10A-F). These results indicated that the CD4$^+$ T cells were capable of proliferation in response to stimulation with superantigen, but showed restricted antigen specificity due to unresponsiveness to stimulation with an unrelated antigen. Confirming the specificity of the CD4$^+$ T cell lines, co-culture with *Salmonella* lysate-pulsed monocytes induced T cell proliferation at levels equivalent to SEB stimulation as well as upregulation of activation marker expression. In contrast, no increase in CD4$^+$ T cell proliferation or expression of activation markers was detected following co-culture with ILCs that had been pulsed with *Salmonella* lysate.

Examination of transcription factor expression by *Salmonella*-specific CD4$^+$ T cells in the different co-culture conditions yielded similar results. As expected, stimulation of CD4$^+$ T cells with SEB-pulsed ILCs or monocytes induced upregulation of T-bet, Eomes, GATA3 and Foxp3 expression (Figure 4.11A and B). In contrast, transcription factor expression by CD4$^+$ T cells remained low following co-culture with ILCs or monocytes pulsed with *Bifidobacterium* lysate. Stimulation of CD4$^+$ T cells with *Salmonella* lysate-pulsed monocytes induced clear upregulation of T-bet and Foxp3 expression, however, in contrast stimulation of CD4$^+$ T cells with *Salmonella* lysate-pulsed ILCs did not yield detectable upregulation of transcription factor expression (Figure 4.11C-F).

Finally, we analysed expression of CD4$^+$ T cell-derived cytokines following PMA/ionomycin stimulation and ICS at the end of the co-cultures. *Salmonella*-specific CD4$^+$ T cells stimulated with SEB-pulsed ILCs or monocytes showed clear upregulation of several cytokines, including GM-CSF, IL-5, IL-2 and TNFα (Figure 4.12A-C). In contrast, CD4$^+$ T cells stimulated with ILCs or monocytes pulsed with *Bifidobacterium* lysate expressed lower levels of these cytokines. Co-culture of CD4$^+$ T cells with *Salmonella* lysate-pulsed monocytes induced robust upregulation of cytokine production (Figure 4.12D-G). However, no increase in cytokine expression compared to unrelated antigen control was detected when CD4$^+$ T cells were stimulated with *Salmonella* lysate-pulsed ILCs.

Flow cytometry analysis of the *in vitro* expanded ILC subsets showed that they expressed high levels of HLA-DR and CD86, whereas there was no detectable expression of the inhibitory ligands PD-L1 or PD-L2 (Figure 4.13A). However, direct comparison of HLA-DR expression by *in vitro* expanded blood ILC subsets in comparison to CD14$^+$ monocytes indicated that ILCs expressed much lower levels of HLA-DR than professional APCs (Figure 4.13B). Thus, while ILCs clearly expressed HLA-DR, perhaps the density of surface HLA-DR molecules on ILCs may not be sufficiently high to enable efficient presentation of antigen to CD4$^+$ T cells.

Thus, our findings indicate that in contrast to monocytes, *in vitro* expanded blood ILC populations pulsed with protein antigen do not functionally operate as APCs and do not stimulate antigen-specific memory CD4$^+$ T cell responses.

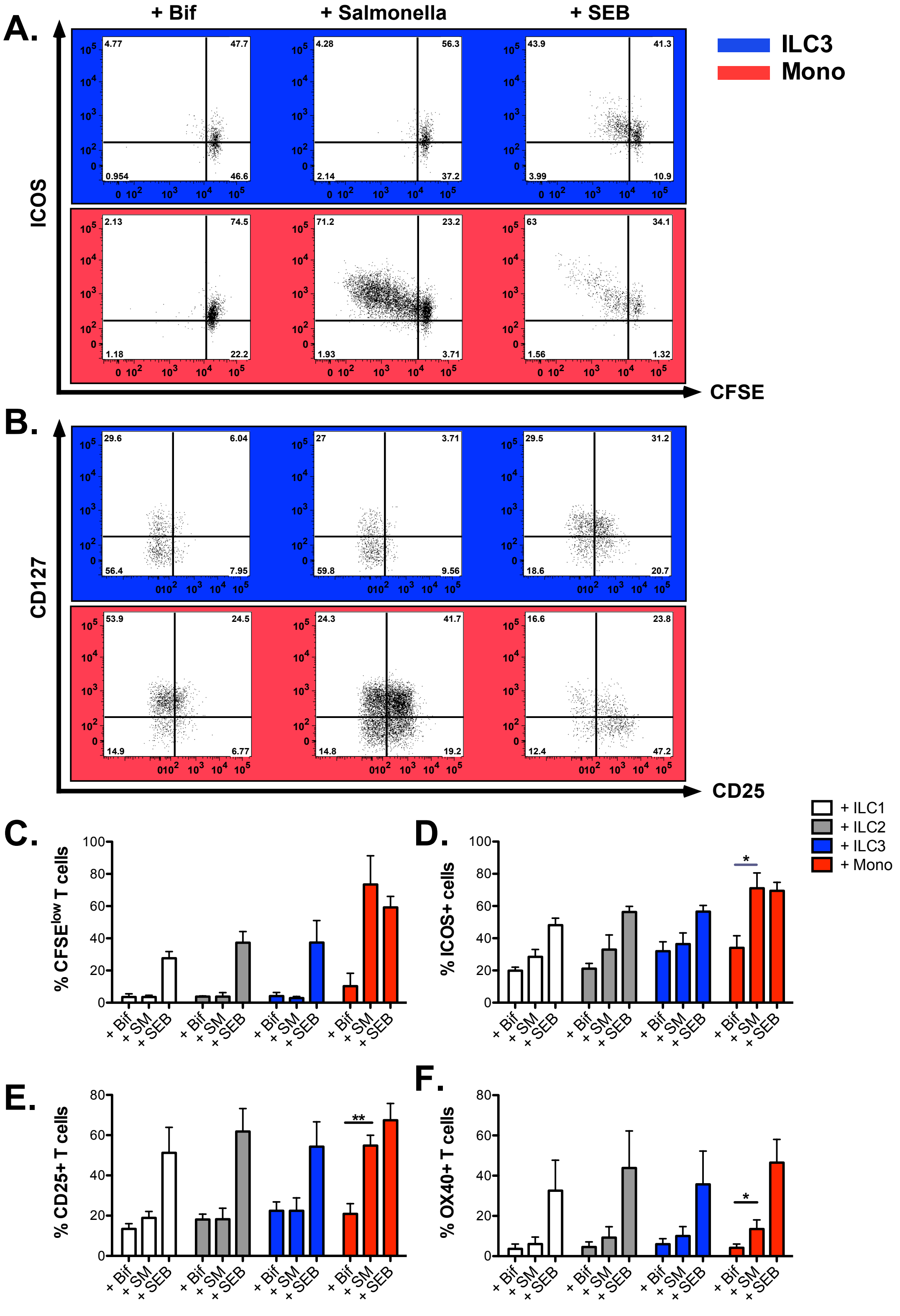

Figure 4.10: ILCs do not mediate antigen-specific memory CD4^{+} T cell activation. CD14^{+} monocyte or *in vitro* expanded ILC subsets were pulsed with *Salmonella (SM)* lysate, *Bifidobacterium (Bif)* lysate (negative control) or SEB (positive control) for 6-8 hours before co-culture with CFSE-labelled *SM*-specific CD4^{+} T cells for 5d. **(A + B)** Representative FACS plots showing CFSE dilution and expression of ICOS, CD25 and CD127 by T cells co-cultured with *SM*-lysate pulsed ILC3 (blue) or monocytes (red). **(C - F)** Quantification of T cell expression of CFSE (C), ICOS (D), CD25 (E) and OX40 (F) following re-stimulation with ILC subsets or monocytes pusled with *SM* lysate, *Bif* lysate or SEB. Data are derived from n = 2 - 5 donors. Statistical significance was determined by means of Mann-Whitney U tests. Bars represent mean ± SEM. *$p \leq 0.05$. **$p \leq 0.01$.

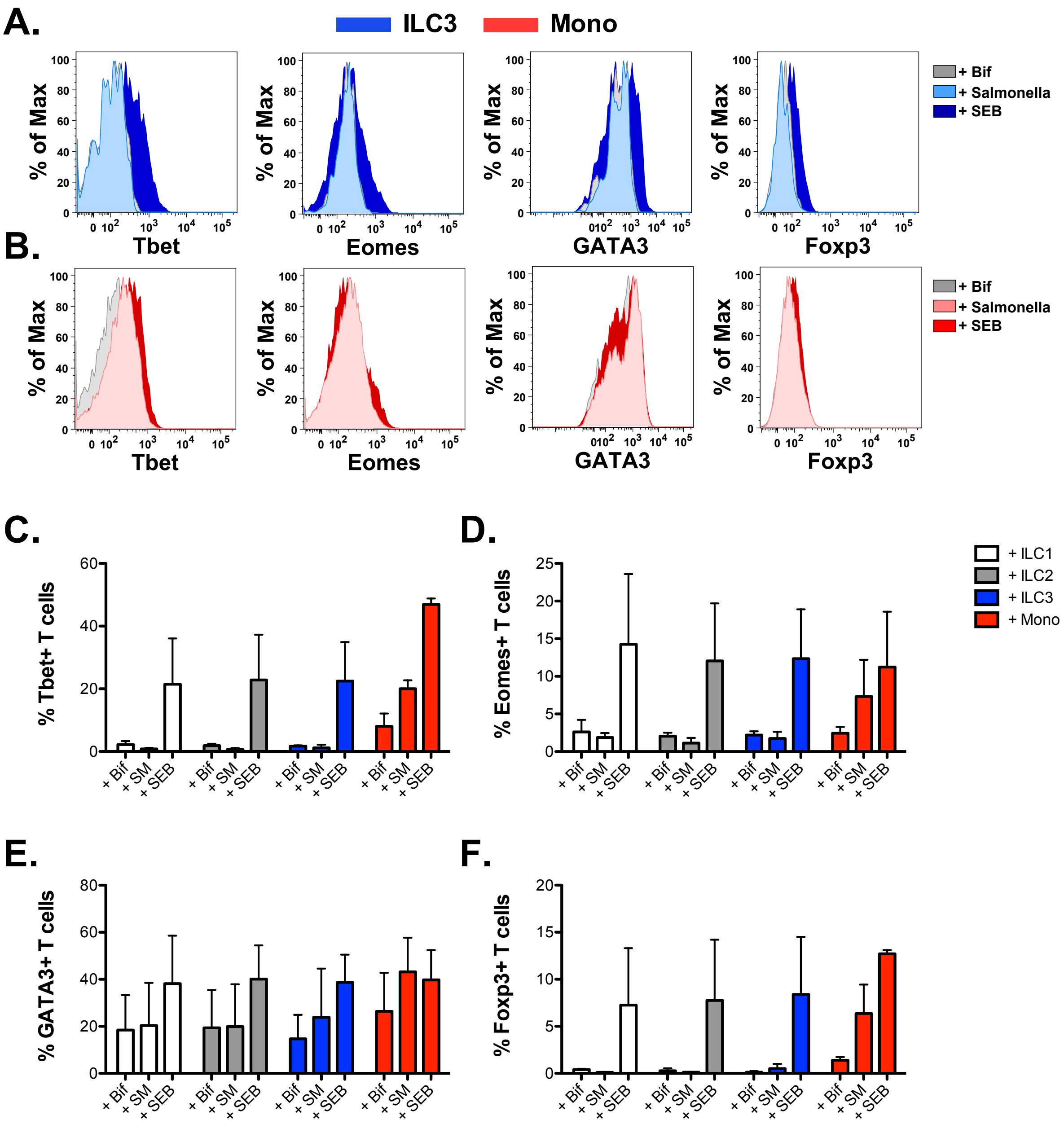

Figure 4.11: ILCs do not enhance TF expression by antigen-specific memory CD4$^+$ T cell. CD14$^+$ monocyte or *in vitro* expanded ILC subsets were pulsed with *Salmonella (SM)* lysate, *Bifidobacteria* (*Bif*) lysate (negative control) or SEB (positive control) for 6-8 hours before co-culture with CFSE-labelled *SM*-specific CD4$^+$ T cells for 5d. **(A + B)** Representative FACS plots showing TF expression by T cells co-cultured with *SM*-lysate pulsed ILC3 (blue) or monocytes (red). **(C - F)** Quantification of T cell expression of Tbet (C), Eomes (D), GATA3 (E) and Foxp3 (F) following re-stimulation with ILC subsets or monocytes pusled with *SM* lysate, *Bif* lysate or SEB. Data represent n = 2 donors. Bars represent mean ± SEM.

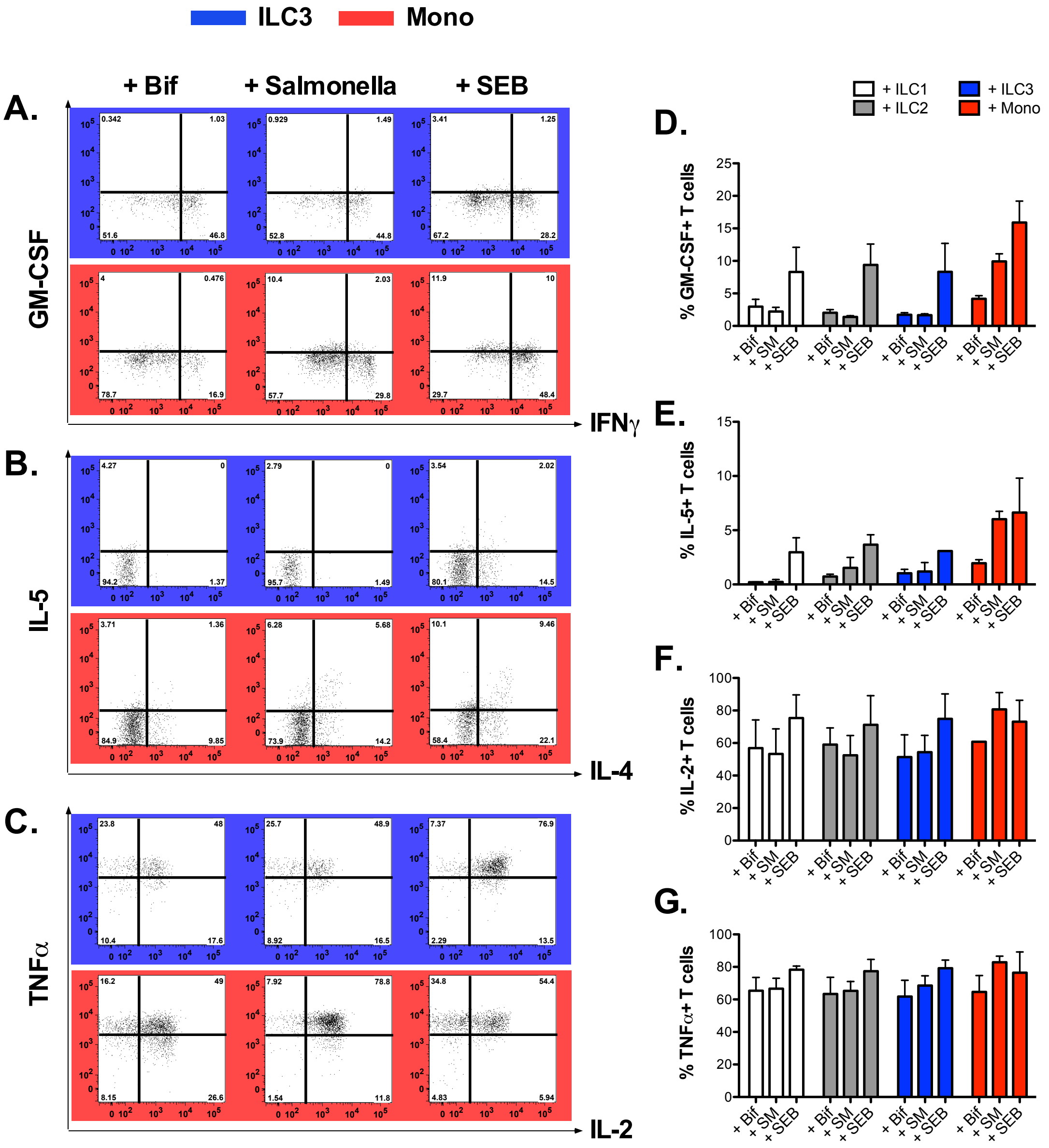

Figure 4.12: ILCs do not induce cytokine production in antigen-specific memory CD4$^+$ T cells. CD14$^+$ monocyte or *in vitro* expanded ILC subsets were pulsed with *Salmonella (SM)* lysate, *Bifidobacteria (Bif)* lysate (negative control) or SEB (positive control) for 6-8 hours before co-culture with CFSE-labelled *SM*-specific CD4$^+$ T cells for 5d. **(A - C)** Representative FACS plots showing cytokine expression by T cells co-cultured with *SM*-lysate pulsed ILC3 (blue) or monocytes (red). **(D - G)** Following co-culture, cells were retrieved and stimulated with PMA/ ionomycin for 4h in the presence of Golgistop/Golgiplug. This was followed by ICS and flow cytometry analysis. Quantification of CD4$^+$ T cell expression of GM-CSF (D), IL-5 (E), IL-2 (F) and TNFα (G). Each dot in the plots represents an individual donor. Data obtained from n = 2 donors. Bars represent mean ± SEM.

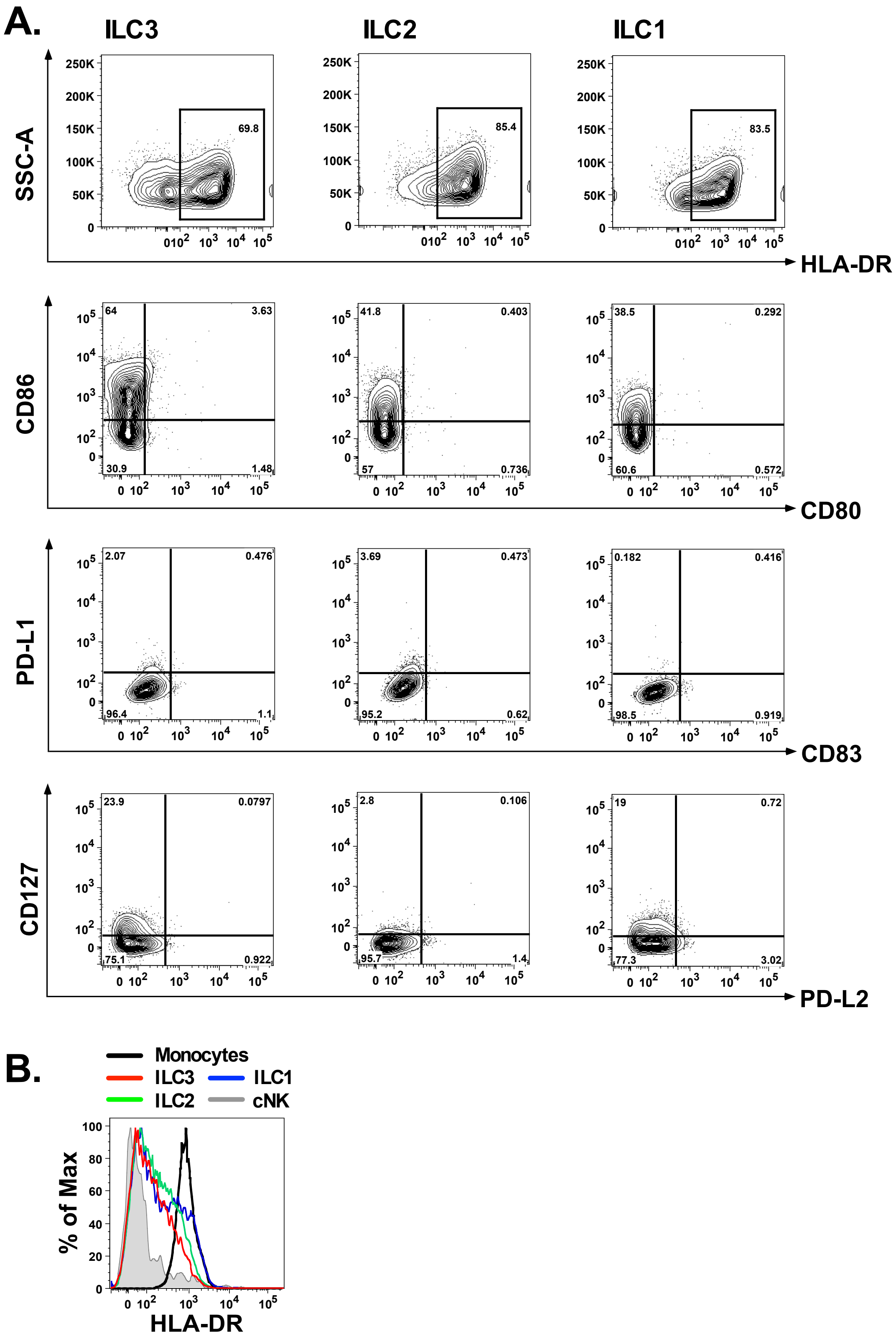

Figure 4.13: ILCs used in T cell assays express high levels of HLA-DR and CD86. (A) Representative FACS plots indicating HLA-DR and co-stimulatory ligand expression by *in vitro* expanded blood ILC subsets. Gates were set according to unstained controls. **(B)** Representative FACS plot of HLA-DR expression by *in vitro* cultured blood ILC subsets and MACS purified blood monocytes used in T cell assays.

4.3 Discussion

Our results indicate that *ex vivo* ILC populations in human blood and the intestinal lamina propria as well *in vitro* expanded blood ILC subsets express HLA-DR and co-stimulatory ligands. In the colon, ILC3 were found to contain the highest proportion of HLA-DR expressing cells, with intermediate expression by ILC1 and lowest expression by ILC2. A similar distribution of HLA-DR expression among mouse ILC subsets has been reported by Hepworth et al., with small intestinal (SI) RORγt^{+}T-bet^{-} and RORγt^{+}T-bet^{+} ILC3 populations containing a significantly higher percentage of HLA-DR^{+} cells compared to ILC2 or RORγt^{-} ILC1 (164). Confirming the potential for ILC expression of MHC class II, during the course of this study several reports examining the function of MHC class II expression by murine ILCs were published (145,146,164,165,391). Our data reveal novel features of human ILC biology relating to HLA-DR and co-stimulatory ligand expression.

Compared to blood ILCs, HLA-DR expression was enriched in intestinal lamina propria-resident ILCs. In line with this finding, a potential role for tissue environment-dependent factors in the regulation of MHC class II expression by murine ILCs has been highlighted in recent reports (146,164). Approximately 80% of ILC2 in the MLN and PP of naïve C57Bl/6 mice express MHC class II, while only approximately 60% of splenic and lung ILC2 and 30% of peritoneal ILC2 express MHC class II, indicating that ILC2 have a relatively wide range of MHC class II expression depending on their tissue residency (146). A similar tissue-dependence of MHC class II expression seems to apply to murine ILC3. While approximately 72% of ILC3 in MLNs express MHC class II, only approximately 3-36% of ILC3 in spleen, PP, SI, lung and thymus express MHC class II (164). It is unclear what drives these differences in ILC MHC class II expression in different tissue sites. Our data indicate that cytokines can regulate HLA-DR expression by human ILCs (see below) and it is conceivable that local differences in the cytokine environment may contribute to tissue-dependent differences in MHC class II expression by ILCs.

Our data indicate that HLA-DR expression amongst ILC1 is significantly increased in the blood of both CD and UC patients compared to healthy controls. While there was a trend towards increased expression of HLA-DR by ILC3 and ILC2 in IBD blood, this did not reach statistical significance. In contrast to the blood compartment, no significant differences in HLA-DR expression by intestinal ILCs were observed between uninflamed controls and IBD patients. However, there was a possible trend towards decreased HLA-DR expression in IBD. It is conceivable that the selective upregulation of HLA-DR expression by ILC1 in IBD blood may result from a pro-inflammatory cytokine environment in human blood that favours ILC1 activation. For example, increased serum levels of IL-15 have been reported in both CD and UC patients (392) and our data have demonstrated a direct effect of IL-15 in driving HLA-DR upregulation by ILC1. In addition, we and others have shown that ILC1 accumulate in the inflamed intestinal lamina propria of CD patients (Chapter 3). An increased redistribution of HLA-DR$^+$ ILC1 from tissue to blood through lymph under inflammatory conditions may occur and could also contribute the observed increase in HLA-DR expressing ILC1 in CD blood.

The decreased expression of HLA-DR by intestinal ILCs in an inflammatory setting seems somewhat counterintuitive and would need to be confirmed by means of a larger sample size. However, in line with our findings recently published data showed lower HLA-DR expression by ILC3 in the inflamed colon of early-onset paediatric IBD patients compared to uninflamed controls (165).

Stimulation of *in vitro* expanded ILCs with IFNγ did not induce upregulation of HLA-DR or co-stimulatory ligand expression by *in vitro* cultured ILCs, suggesting that HLA-DR expression in this cell type may be regulated in an IFNγ-independent manner. However, our results indicate that other cytokines can regulate HLA-DR expression by ILC subsets. ILC3 upregulated HLA-DR expression following overnight stimulation with IL-1β, IL-6, IL-23 and TNFα, while ILC2 expressed higher levels of HLA-DR following stimulation with IL-33 and TNFα, and ILC1 upregulated HLA-DR expression following stimulation with IL-15. It is conceivable that differences in the expression levels of these cytokines between tissue sites (blood, intestinal lamina propria) and inflammation states (control, CD, UC) may account for the above-discussed differences in HLA-DR expression between colonic and blood ILCs and between ILCs from IBD patients compared to uninflamed controls.

In line with our observations, recently published evidence points towards an IFNγ-independent regulation of MHC class II expression in colonic and MLN-resident ILC3 in the mouse (165). Expression of MHC class II, CD80 or CD86 by ILC3 was shown to be unaffected following *in vitro* stimulation of whole LPMC suspensions with IFNγ. Furthermore, in mice deficient for IFNγ, IFNγR1 or STAT1 *in vivo* MHC class II expression by ILC3 is unchanged compared to wildtype mice. Moreover, a recent study identified a role for IL-1β in the regulation of MHC class II and co-stimulatory ligand expression in *ex vivo* and *in vitro* generated mouse ILC3 (391), similar to our finding for human ILC3. However, it is unclear from this report whether IL-1β directly drives MHC class II upregulation by ILC3, since IL-1β stimulation also elicits production of other pro-inflammatory cytokines (TNFα, GM-CSF) by ILC3 (391), which may affect MHC class II expression. Similarly, it is unclear whether the observed cytokine-mediated enhancement of ILC HLA-DR expression observed in our experiments is a direct effect or potentially mediated indirectly via induction of (an)other key cytokine(s) capable of modulating HLA-DR expression in an autocrine manner. This highlights the need for further investigation into the mechanistic details of how MHC class II expression is regulated in ILCs. A requirement for class II transactivator (CIITA), a master transcriptional regulator of MHC class II expression, in driving MHC class II expression by ILC3 has been demonstrated (165). However, in contrast to MHC class II expression in professional APCs such as DCs and B cells, which is dependent on the pIII promoter of the *Ciita* gene, ILC3 rely on the pIV promoter of *Ciita* (165). Future work would aim to elucidate whether the cytokines we identified as regulators of HLA-DR expression by human ILC3 exert their function through pIV and CIITA, and whether similar mechanisms also apply to ILC2 and ILC1 populations.

Our findings indicated that, following *in vitro* expansion, a higher proportion of ILCs appeared to express HLA-DR and co-stimulatory ligands CD80 and CD86 compared to *ex vivo* ILCs. It is unclear from our experiments whether the observed increase in HLA-DR expression by *in vitro* cultured ILCs is the result of a dynamic regulation of HLA-DR expression, for example mediated by cytokines present in the cultures, or whether it represents selective outgrowth of a population of HLA-DR$^+$ ILCs distinct from HLA-DR$^-$ ILCs. Murine ILC2 have been shown to acquire MHC class II from professional APCs by means of trogocytosis (146). However, it is unlikely that the increase in HLA-DR expression we observed can be explained by trogocytosis-mediated acquisition of HLA-DR from APCs present in the mix of feeder cells used for the cultures. Experiments using CFSE-labelled irradiated feeders indicated that these cells usually disappeared from the cultures by week 2 (data not shown). In view of the high proliferation rates of IL-2/IL-7-fed ILCs *in vitro*, membrane turnover would be too high to allow detection of significant increases in HLA-DR expression due to trogocytosis at the later analysis time points of week 3-5 that we used in this study.

Investigating the functional effects of HLA-DR expression by human ILCs, our experiments using DQ-OVA and phagocytosis assays showed that *in vitro* expanded ILC populations could take up and process protein antigen, at levels equivalent to B cells but significantly lower than professional APCs such as monocytes. These data are in agreement with recent reports of uptake and processing of DQ-OVA and phagocytosis beads by murine ILC2 and ILC3 (146,164,391). Furthermore, two independent murine studies have investigated the capacity of ILC2 and ILC3 to successfully load peptides from exogenous protein antigen onto MHC class II (146,164). ILC2 and ILC3 pulsed with the GFP-labelled protein Eα were stained with Y-Ae antibody, which is specific for the Eα-derived peptide $E\alpha_{52-68}$ bound to MHC class II. A clear GFP/Y-Ae double positive population of cells was detectable using flow cytometry (146,164). This supports the idea that ILC2 and ILC3 are indeed capable of processing ingested protein antigens and load them onto MHC class II for presentation to $CD4^+$ T cells, although the efficiency at which ILCs were shown to do this is much lower than that of professional APCs.

Testing the functional effects of ILC-mediated antigen presentation, we found that, unlike monocytes, *in vitro* expanded ILC1, ILC2 and ILC3 pulsed with *Salmonella* lysate were unable to effectively activate *Salmonella*-specific memory $CD4^+$ T cells as assessed through examination of T cell proliferation and expression of surface activation markers, cytokines and transcription factors. Our data indicate that this effect occurred in spite of high expression of HLA-DR and co-stimulatory ligands by the ILC subsets used in the assays. Our results contradict a recent report of activatory ILC2-mediated antigen presentation to CD4$^+$ T cells (146). Human ILC2 pulsed with the house dust mite-derived peptide DRB15 were shown to induce IL-4, IL-13 and IFNγ expression in house dust mite-specific CD4$^+$ T cell lines *in vitro*. Potential effects of ILC2-mediated antigen presentation on CD4$^+$ T cell proliferation were not discussed in this study (146).

Similarly opposing findings have been made regarding the capacity of murine ILCs to drive MHC class II-dependent activation of antigen-specific CD4$^+$ T cells (summarized in Table 4.1). ILC3 from the mouse small intestine have been reported to successfully take up and process OVA antigen, yet they fail to induce proliferation of antigen-specific OTII-transgenic CD4$^+$ T cells in co-cultures *in vitro* (164). These data are in direct contrast to a publication in which MHC class II-dependent presentation of OVA peptide by splenic RORγt$^+$ NKR$^-$ ILC3 resulted in OTII-transgenic splenic CD4$^+$ T cell activation and proliferation *in vitro* (391). Furthermore, murine ILC2 have been shown to present OVA-derived peptide to OVA-specific CD4$^+$ T cells *in vitro*, resulting in T cell proliferation and induction of Type 2 cytokine production (145,146).

Table 4.1: Overview of murine *in vitro* and *in vivo* experiments testing the capacity of ILCs to activate antigen-specific CD4$^+$ T cells

ILC population	ILC origin	Type of antigen	Tissue environment from which ILCs are derived for *in vitro* experiments	Tissue environment during *in vivo* experiments	CD4$^+$ T cell activation	References
ILC3	SI	Protein	Steady-state	--------	✖	(164)
ILC3	SI	Peptide	--------	Steady-state	✖	(164)
ILC3	Spleen	Peptide	Steady-state	Inflammatory (alum-precipitated OVA + CpG)	✔	(391)
ILC3	Spleen	Protein	Steady-state	--------	✖	(391)
ILC2	Lung	Peptide	Inflammatory (IL-33 injected)	Inflammatory (*N. brasiliensis* infected or IL-33 injected)	✔	(145,146)
ILC2	Lung	Protein	Inflammatory (IL-33 injected)	--------	✖	(145,146)

It is unclear why such contradictory findings have been made regarding the outcome of ILC-mediated antigen presentation to CD4$^+$ T cells. One possible explanation may be a differential capacity of ILCs to present peptide versus protein antigens. While mouse ILC2 can take up and process protein antigens, only ILC2 pulsed with OVA peptide but not with whole OVA protein are capable of efficiently inducing proliferation in OVA-specific CD4$^+$ T cells *in vitro* (145,146). It has been suggested that antigen processing by ILC2 may not occur at sufficiently high levels to effectively induce T cell proliferation. Instead, *in vivo* ILC2 may mainly present peptide antigens acquired through direct binding to MHC class II as well as through trogocytosis from professional APCs (146). Similarly, *in vitro* splenic ILC3 have been shown to induce proliferation and cytokine production in OTII-transgenic CD4$^+$ T cells efficiently when pulsed with OVA peptide but not OVA protein (391). Thus, the discrepancy between our results and the above-mentioned report by Oliphant et al. of human ILC2-mediated activation of antigen-specific CD4$^+$ T cells may be the consequence of differences in the respective experimental set-ups. While the *Salmonella* lysates we used in our assays consist mainly of whole protein antigens, Oliphant et al. used house dust mite-derived peptide in their experiments. Future work would aim to clarify the role of protein versus peptide antigen in our experimental system.

However, this may be too simplistic an explanation as *in vivo* experiments using only peptide-pulsed ILCs have reported discrepant outcomes regarding the ability of ILCs to mediate CD4$^+$ T cell activation (164,165). Hepworth et al. have shown that MHC class II-mediated presentation of the commensal-derived CBir1 peptide by intestinal ILC3 suppresses the activation of CBir1-specific CD4$^+$ T cells *in vivo* (164,165). In contrast to our finding of co-stimulatory ligand expression on human ILC3, no co-stimulatory ligand expression was observed on small intestinal murine ILC3. Antigen-presentation in the absence of co-stimulation may lead to the induction of CD4$^+$ T cell anergy. Indeed, MHC class II-mediated presentation of CBir1 peptide to CD4$^+$ T cells by ILC3 in the MLN results in expression of the pro-apoptotic molecule Bim in CD4$^+$ T cells and induction of apoptosis (165). Thus, these findings suggest a tolerogenic role for intestinal ILC3 in the suppression of CD4$^+$ T cell responses to commensal antigens. In line with this idea, ILC3-specific deletion of MHCII expression in *H2-Ab1*$^{fl/fl}$ x *Rorc*^{cre} mice results in immune hyperactivation under steady-state conditions, characterised by an increased frequency of proliferating CD4$^+$ T cells and elevated levels of commensal bacteria-specific serum IgG (164). In contrast, MHC class II-mediated presentation of OVA peptide by *splenic* ILC3 induces

$CD4^+$ T cell proliferation and cytokine secretion (391). Thus, at least in the case of ILC3, a second possibility is that the observed experimental discrepancies are the result of tissue-dependent differences in the capacity of ILCs to mediate $CD4^+$ T cell activation. While intestinal ILC3 may preferentially limit $CD4^+$ T cell responses to the commensal microbiota, antigen presentation by peripheral ILC3 may induce $CD4^+$ T cell activation. In support of this hypothesis, peripheral ILC3 have been reported to express higher levels of co-stimulatory ligands than intestinal ILC3 following activation by IL-1β (391).

Future work would aim to systematically examine MHC class II and co-stimulatory ligand expression by ILC populations in distinct tissue sites and to clarify whether the proposed gut-specific tolerogenic function of ILC3 also applies to ILC2 and ILC1 populations. In contrast to ILC3, intestinal ILC2 have been shown to drive MHC class II-dependent activation of antigen-specific $CD4^+$ T cells *in vivo*. Specific depletion of ILC2 in *N. brasiliensis* infected mice results in a higher worm burden and delayed worm clearance, which correlates with a decrease in IL-5 and IL-13-producing $CD4^+$ T cells. Whilst adoptive transfer of wild-type ILC2 into recipient mice restores efficient worm expulsion, transfer of MHC class II-deficient ILC2 does not (146). It is thus conceivable that ILC2 may be differentially regulated than ILC3 and ILC1 in the gut. While a role for ILC2 in promoting $CD4^+$ T cell activation may be beneficial in response to intestinal helminth infections, an activatory function of ILC3 and ILC1 in driving commensal-specific $CD4^+$ T cell responses could potentially lead to a breakdown of host-commensal homeostasis and inflammatory pathology.

Analysis of the published mouse studies indicates a third possibility to explain the observed discrepancies in the outcomes of ILC-mediated antigen-presentation to $CD4^+$ T cells *in vivo*. In the case of ILC2, *in vivo* experiments were performed in the context of *N. brasiliensis* infection, i.e. in an inflammatory setting characterised by high expression of ILC2-activating cytokines such as IL-33 and IL-25 (146). Similarly, the capacity of splenic ILC3 to activate antigen-specific $CD4^+$ T cells was tested in an inflammatory context following adjuvant administration. In contrast, intestinal ILC3 antigen-presentation function was analysed under steady-state conditions (164,165). It is conceivable that the capacity of ILCs to inhibit or activate $CD4^+$ T cells through MHC class II-dependent presentation of peptide antigen may be modulated by inflammatory signals, in particular in light of our observation that pro-inflammatory cytokines can induce expression of HLA-DR by ILCs. It would be interesting to investigate in the future whether in an inflammatory environment, as is found in the intestine of IBD patients, the ability of ILCs to elicit antigen-specific $CD4^+$ T cell activation is altered.

In summary, our data suggest that, while ILCs express HLA-DR and co-stimulatory ligands and are capable of taking up and proteolytically processing protein antigen, they do not act as professional antigen presenting cells and fail to induce proliferation, transcription factor expression or cytokine secretion in antigen-specific memory $CD4^+$ T cells. Thus these data suggest that ILCs are unlikely to contribute to the initiation of intestinal inflammation in IBD through direct activation of pathogenic memory $CD4^+$ T cell responses.

The seemingly contradictory findings in the literature regarding the capacity of MHC class II-expressing ILCs to activate antigen-specific CD4$^+$ T cells may result from

(i) differences in how ILCs handle peptide versus protein antigens (in some settings, ILCs can efficiently present peptide but not protein antigens)

(ii) tissue-dependent differences in the capacity of ILCs to elicit antigen-specific CD4$^+$ T cell activation (splenic ILC3 promote CD4$^+$ T cell activation, while intestinal ILC3 do not)

(iii) inflammation-dependent differences in ILC functionality ('inflammatory' ILC2 drive antigen-specific CD4$^+$ T cell activation, while 'steady-state' ILC3 do not) and

(iv) potential inherent differences between ILC subsets (intestinal ILC2 elicit antigen-specific CD4$^+$ T cell activation, while ILC3 promote CD4$^+$ T cell tolerance).

Therefore further work is required to unravel the complexities of ILC and CD4$^+$ T cell interactions in human IBD.

Chapter 5: Reciprocal activation between ILCs and monocytes

5.1 Introduction

ILCs are known to respond rapidly to myeloid- and epithelial-derived signals (147). However, less is known about whether ILCs in turn can modulate activation and effector functions of myeloid cells, with potential downstream effects also on developing adaptive immune responses.

Early murine evidence suggested that direct bidirectional interactions between intestinal ILC3 and DCs are required for clearance of *C. rodentium* infection in mice (113). Protective immunity to *C. rodentium* infection is critically dependent on early IL-22 production by intestinal ILC3 (100,115). ILC3-derived IL-22 is induced via IL-23 secreted by CX3CR1$^+$ inflammatory macrophages and CD11b$^+$ DCs (110-112). *In vivo* depletion of CX3CR1$^+$ macrophages leads to increased intestinal pathology and increased mortality in response to *C. rodentium* infection, which is associated with decreased IL-22 production by intestinal ILC3 and reduced downstream production of the AMPs RegIIIβ and RegIIIγ by IECs (110,111). Moreover, CXCL16 secreted by intestinal CD11b$^+$ DCs has been implicated in the recruitment of IL-22 producing CXCR6$^+$ ILC3 to the villus epithelium following *C. rodentium* infection. Ablation of CXCL16-CXCR6 signalling in *Rag1*$^{-/-}$ mice leads to selective loss of IL-22-producing ILC3 in the villus lamina propria, associated with increased susceptibility to *C.rodentium* infection (112). A positive feedback loop dependent on direct interactions between LT$\alpha_1\beta_2^+$ ILC3 and LTβR$^+$ DCs in intestinal lymphoid follicles is thought to be required for optimal IL-23-driven IL-22 production by ILC3 following *C. rodentium* infection. Blockade of LT-LTβR-signalling by means of LTβR-Ig fusion protein treatment or ILC3-specific ablation of LT expression in RORγt-*Ltb*$^{-/-}$ mice is associated with reduced expression of DC-derived IL-23 and ILC3-derived IL-22 and increased susceptibility to *C. rodentium* infection (113). Thus, bidirectional interactions between ILC3 and macrophages/DCs are critical for defence against *C. rodentium* infection.

Furthermore, it has been shown that crosstalk between intestinal RORγt$^+$ ILC3 and DCs/macrophages is important for the maintenance of intestinal T_{Reg} and tolerance to food antigens in the mouse (166). In steady-state colon RORγt$^+$ ILC3 are the main producers of GM-CSF in response to IL-1β secreted by lamina propria-resident macrophages. ILC3-derived GM-CSF in turn acts on colonic DCs and macrophages to promote expression of tolerogenic modules required for the induction and maintenance of T_{Reg}. Accordingly, colonic DCs and macrophages from ILC-deficient *Rag2*$^{-/-}$*Il2rg*$^{-/-}$ mice show reduced expression of IL-10, TGF-β and Aldh1, associated with a reduced number of CD4$^+$Foxp3$^+$ T_{Reg} in the colonic lamina propria and impaired establishment of oral tolerance to OVA. This phenotype can be rescued through adoptive transfer of RORγt$^+$ ILC3 from *Cfs2*$^{+/+}$ but not *Cfs2*$^{-/-}$ mice (166).

In the case of ILC2, interactions between ILC2 and DCs were shown to be required for optimal induction of T_H2 responses in a model of papain-induced allergic lung inflammation. ILC2-derived IL-13 induces CD11c$^+$ DCs to upregulate CD40 and migrate to the mediastinal lymph node in a CCR7-dependent manner for the effective induction of antigen-specific T_H2 responses. *Rora*$^{sg/sg}$ 'staggerer' mice with selective deficiency of ILC2 have decreased counts of T_H2 cells in the mediastinal LN and lung and reduced production of T_H2-cytokines following papain challenge, a phenotype which can be rescued through adoptive transfer of wild-type but not IL-13-deficient

ILC2 (144). Furthermore, it has been reported that ILC2-derived IL-13 contribute to the maintenance of AAM in the lung, which are required for protective immunity in a mouse model of secondary infection with the helminth *N. brasiliensis* (393).

Like their murine counterparts, human ILCs are responsive to stimulation with myeloid-derived cytokines such as IL-1β, IL-12, IL-23, IL-15, IL-18, IL-25 and IL-33 (16,183,185,188,189,196,219). However, only one publication has shown direct functional interactions between human ILCs and myeloid cells. Using *in vitro* co-cultures of NKp44^{+} ILC3 and TLR-activated monocytes, Cella et al. have demonstrated a direct role for myeloid cell-derived factors in the regulation of IL-22 production by human RORγt^{+} ILC3 (183). A reciprocal role for human ILCs in the regulation of myeloid cells has not been identified.

One of the major functions of myeloid populations is activation of antigen-specific naïve and memory CD4^{+} T cell responses via the presentation of peptide antigen in the context of MHC class II molecules and provision of co-stimulatory signals. Here, we examined whether human ILCs play a role in the modulation of these functions. Using *in vitro* co-culture of human ILC populations and CD14^{+} blood monocytes in absence or presence of lipopolysaccharide (LPS) stimulation, we modelled the early interactions that may occur between lamina propria-resident ILCs and infiltrating monocytes and examine potential effects on monocyte HLA-DR and co-stimulatory ligand expression as well as direct bactericidal activity. In a second step, we investigated the functional effects of such ILC-monocyte interactions on CD4^{+} T cell activation using a system of soluble anti-CD3-mediated polyclonal T cell activation in the presence of monocytes and/or ILC populations.

5.2 Results

5.2.1 ILCs act directly and in synergy with LPS to induce monocyte activation

In order to assess whether ILCs exerted an effect on antigen-presentation function by monocytes, $CD14^+$ monocytes were co-cultured with *in vitro* expanded ILC1, ILC2 and ILC3 at a 1:1 ratio for 48h in the presence of exogenous IL-2 (100 U/ml) to promote ILC survival. LPS (1μg/ml) was added as a comparative activator of monocytes. LPS is a major cell wall constituent of gram-negative bacteria and, via ligation of the TLR4-MD2 complex, induces NF-κB-dependent pro-inflammatory modules in monocytes, including secretion of cytokines of the IL-1 and IL-12 families, IL-6, IL-15, GM-CSF and TNFα, and upregulation of the antigen-presentation machinery (394). ILCs lack expression of CD14 and thus were unresponsive to direct stimulation with LPS.

Flow cytometric analysis was used to examine expression of HLA-DR and co-stimulatory ligands on monocytes following co-culture with ILCs (Figure 5.1A-C). No significant change in the percentage of HLA-DR-expressing monocytes was detected when monocytes were co-cultured with ILC3 alone. Monocyte-activation with LPS induced a slight reduction in the proportion of HLA-DR-expressing monocytes, which was not observed when ILC3 were also present (Figure 5.1D). Assessment of HLA-DR mean fluorescence intensity (MFI) revealed that co-culture with ILC3 induced significant upregulation of HLA-DR expression on the monocytes. As observed at the population level, LPS stimulation resulted in a downregulation of HLA-DR. However, this was not seen in the presence of ILC3. Downregulation of HLA-DR expression following LPS priming may seem surprising; however, published analysis of the kinetics of HLA-DR expression by human monocytes that were primed *in vitro* with LPS for 24h showed that an initial upregulation of HLA-DR expression within the first 12h post-priming was followed by prolonged downregulation of HLA-DR expression (395).

Co-culture with ILC3 alone induced robust downregulation of CD14 expression on the monocytes (Figure 5.1E). Stimulation with LPS alone induced upregulation of monocyte CD14 expression to levels significantly higher than the baseline as has been reported previously (396,397). This LPS-induced upregulation of CD14 was observed also in the presence of ILC3.

Examination of monocyte proliferation using Ki67 staining indicated that co-culture with ILC3 resulted in an increase in the percentage of Ki67-expressing cells. While LPS stimulation alone did not significantly change monocyte proliferation compared to baseline levels, stimulation with LPS in the presence of ILC3 led to significant upregulation of Ki67 expression (Figure 5.1F).

Next, we assessed monocyte expression of the co-stimulatory ligands CD80, CD86, OX40L and CD70 (Figure 5.1G-J). Co-culture with ILC3 significantly increased the percentage of CD80-expressing monocytes and CD80 MFI (Figure 5.1G). In LPS-treated monocytes there was a trend towards increased CD80 expression, although this did not reach significance. However, a robust increase of CD80 expression by monocytes was observed upon stimulation with LPS in the presence of ILC3, with a trend towards a greater increase in expression compared to co-culture with ILC3 alone. This suggests that there may be a synergistic effect of ILC3-derived factors and LPS in the induction of CD80 expression on monocytes. While no change in the percentage of CD86-expressing monocytes was detected across the different culture conditions, comparison of CD86 MFI showed significant upregulation of CD86 expression by monocytes following co-culture with ILC3 (Figure 5.1H). No change in CD86 expression was detected following stimulation with LPS. LPS stimulation in the presence of ILC3 did not result in further upregulation of CD86 expression, contrary to the synergistic effect observed for regulation of CD80 expression. OX40L expression by monocytes showed no significant change following co-culture with ILC3 alone (Figure 5.1I). However, OX40L expression was increased by LPS stimulation and upregulated even more robustly when ILC3 were additionally present, again suggesting a synergistic role for ILC3-derived factors and LPS in the regulation of OX40L expression by monocytes. CD70 expression by monocytes was increased following co-culture with ILC3 on population level as well as on individual cell basis (Figure 5.1J). LPS stimulation alone did not affect CD70 expression and did not further increase ILC3-mediated upregulation of CD70 expression.

We obtained similar findings when monocytes were co-cultured with *in vitro* expanded ILC2 and ILC1 (Figures 5.2 and 5.3). However, a direct comparison indicated that the different ILC subsets exerted distinct effects on the monocytes (Figure 5.4A-G). Under co-culture conditions in the presence of LPS, ILC3 were the most potent drivers of monocyte proliferation and OX40L and CD80 expression, while ILC2 seemed to preferentially induce upregulation of CD86 and CD70 expression and downregulation of CD14 expression. ILC1-driven monocyte activation was generally lower compared to the effects observed for ILC3 and ILC2, however, ILC1 alone in the absence of LPS stimulation induced significantly higher HLA-DR upregulation compared to the other ILC subsets.

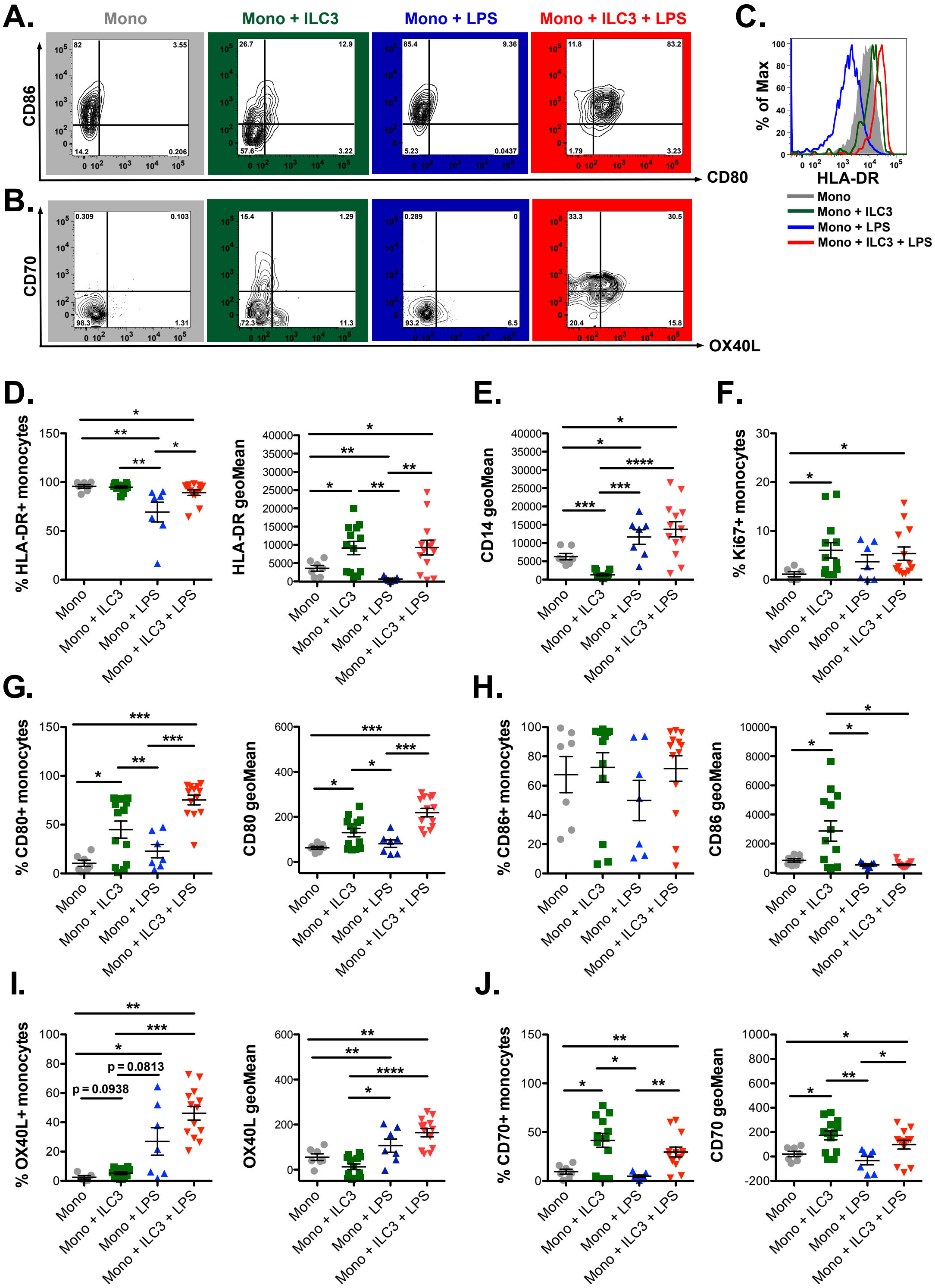

Figure 5.1: Co-culture with ILC3 drives monocyte activation. MACS purified monocytes and *in vitro* expanded FACS purified ILC3 were co-cultured for 2 days in absence or presence of LPS (1µg/ml) followed by flow cytometry analysis. **(A - C).** Representative FACS plots depicting monocyte expression of CD80 and CD80 **(A)**, OX40L and CD70 **(B)** and HLA-DR **(C)**. **(D)** Quantification of percentage (left) and MFI (right) of HLA-DR expression by monocytes. **(E)** Quantified MFI of CD14 expression by monocytes. **(F)** Quantification of percentage of Ki67 expressing monocytes. **(G-J)** Quantification of percentage (left) and MFI (right) of CD80 **(G)**, CD86 **(H)**, OX40 **(I)** and CD70 **(J)** expressing monocytes. Monocytes from n = 7 donors and ILCs from n = 7 donors were incubated in an autologous or allogeneic system. No significant differences were observed between autologous or allogeneic co-cultures. Data are pooled from two separate experiments. Statistical significance was determined by means of Mann-Whitney U tests. Bars represent mean ± SEM. $^{*}p \leq 0.05$. $^{**}p \leq 0.01$. $^{***}p \leq 0.001$. $^{****}p \leq 0.0001$.

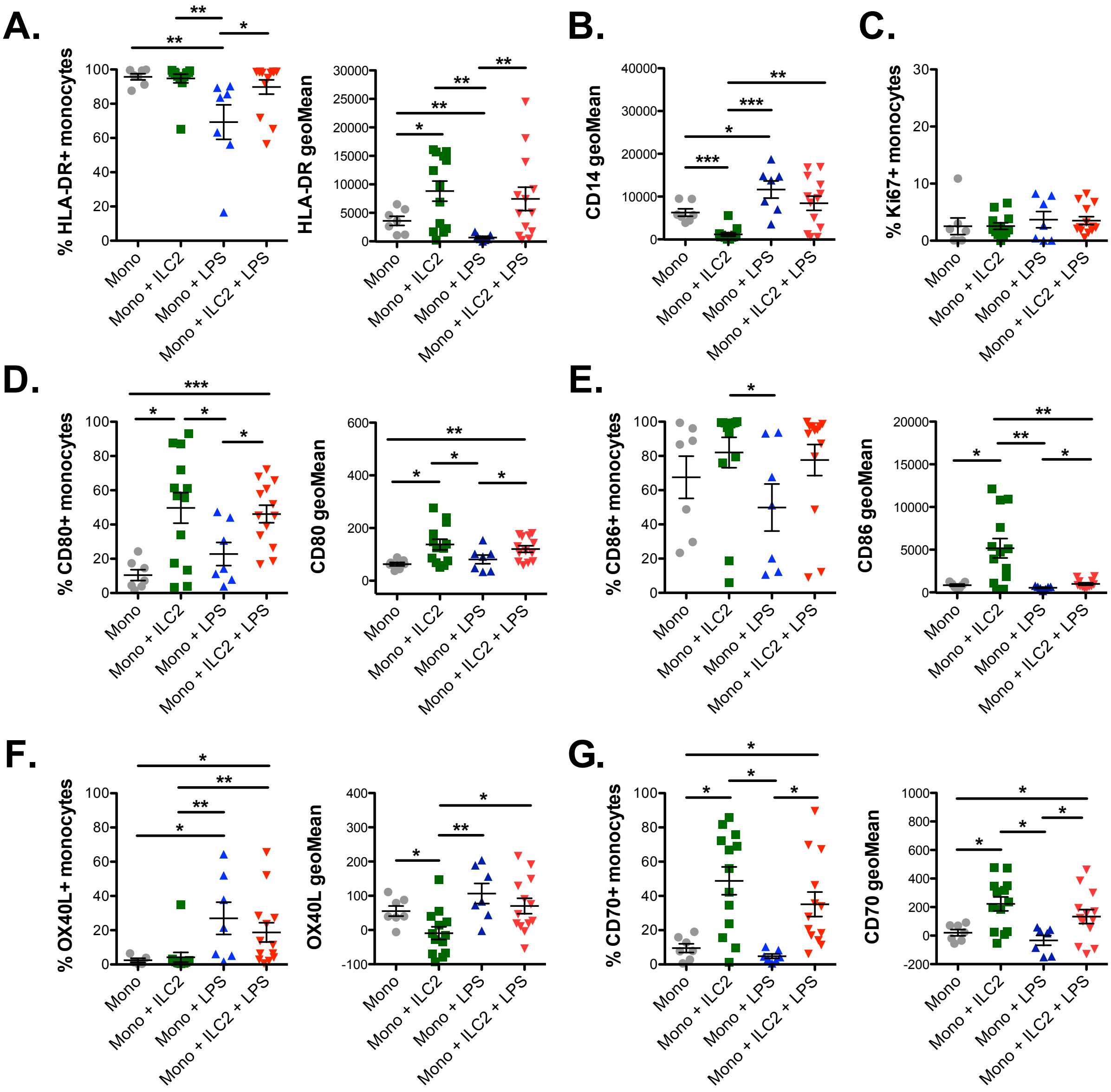

Figure 5.2: Co-culture with ILC2 drives monocyte activation. MACS purified monocytes and *in vitro* expanded FACS purified ILC2 were co-cultured as described before. **(A)** Quantification of percentage (left) and MFI (right) of HLA-DR expression by monocytes. **(B)** Quantification of MFI of monocyte CD14 expression. **(C)** Quantification of percentage of Ki67 expressing monocytes. **(D)** Quantification of percentage (left) and MFI (right) of CD80 expressing monocytes. **(E)** Quantification of percentage (left) and MFI (right) of CD86 expressing monocytes. **(F)** Quantification of percentage (left) and MFI (right) of OX40L expressing monocytes. **(G)** Quantification of percentage (left) and MFI (right) of CD70 expressing monocytes. Monocytes from n = 7 donors and ILCs from n = 7 donors were incubated in an autologous or allogeneic system. No significant differences were observed between autologous or allogeneic co-cultures. Data are pooled from two separate experiments. Statistical significance was determined by means of Mann-Whitney U tests. Bars represent mean ± SEM. $^*p \leq 0.05$. $^{**}p \leq 0.01$. $^{***}p \leq 0.001$.

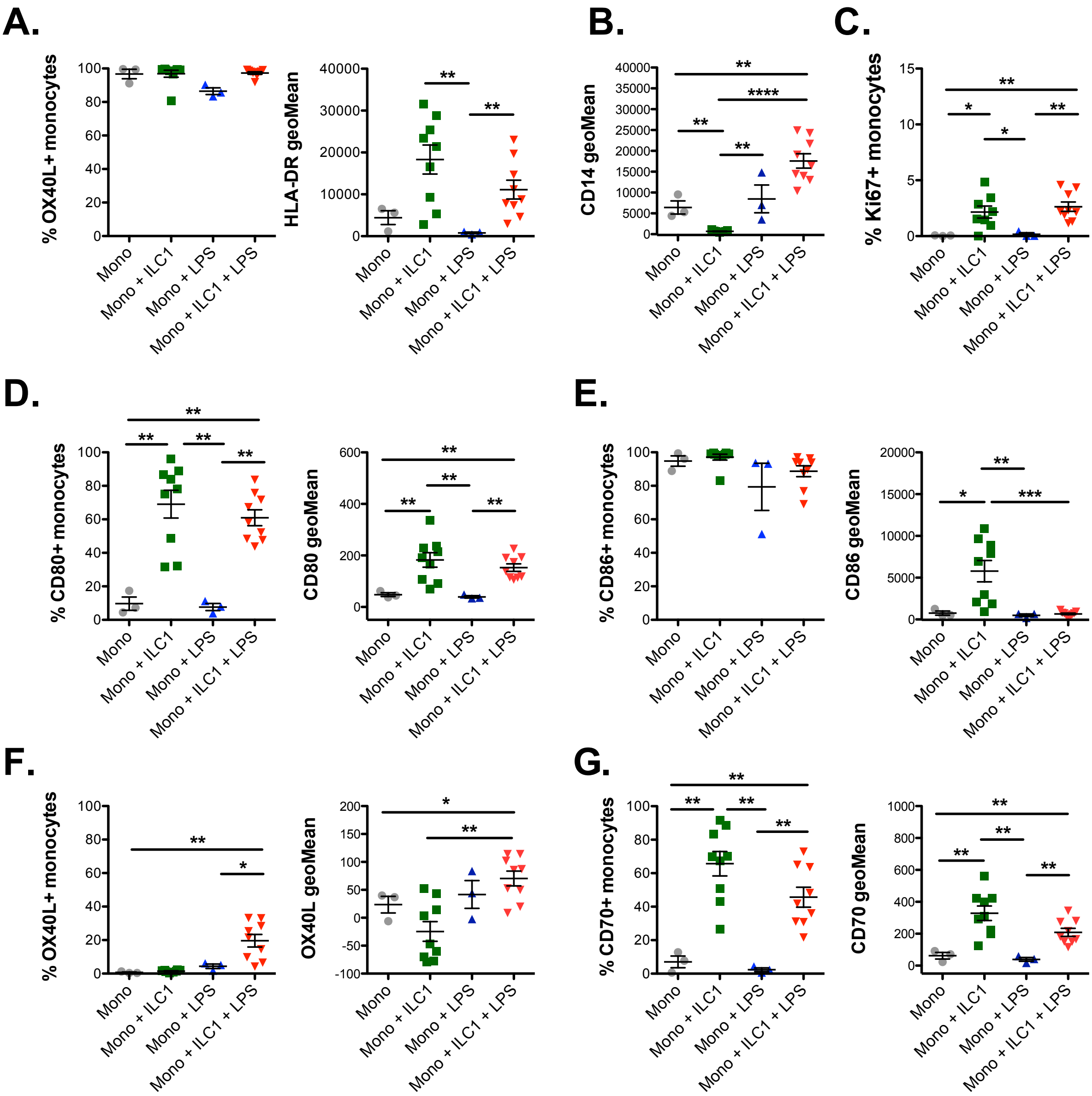

Figure 5.3: Co-culture with ILC1 drives monocyte activation. MACS purified monocytes and *in vitro* expanded FACS purified ILCs were co-cultured as described before. **(A)** Quantification of HLA-DR geoMean on monocytes. **(B)** Quantification of CD14 geoMean on monocytes. **(C)** Percentage of Ki67 expressing monocytes. **(D)** Percentage (left) and MFI (right) of CD80 expressing monocytes. **(E)** Percentage (left) and MFI (right) of CD86 expressing monocytes. **(F)** Percentage (left) and MFI (right) of CD70 expressing monocytes. **(G)** Percentage (left) and MFI (right) of OX40L expressing monocytes. Monocytes from n = 3 donors and ILCs from n = 3 donors were incubated in an autologous or allogeneic system. No significant differences were observed between autologous or allogeneic co-cultures. Statistical significance was determined by means of Mann-Whitney U tests. Bars represent mean ± SEM. *$p \leq 0.05$. **$p \leq 0.01$. ***$p \leq 0.001$. ****$p \leq 0.0001$.

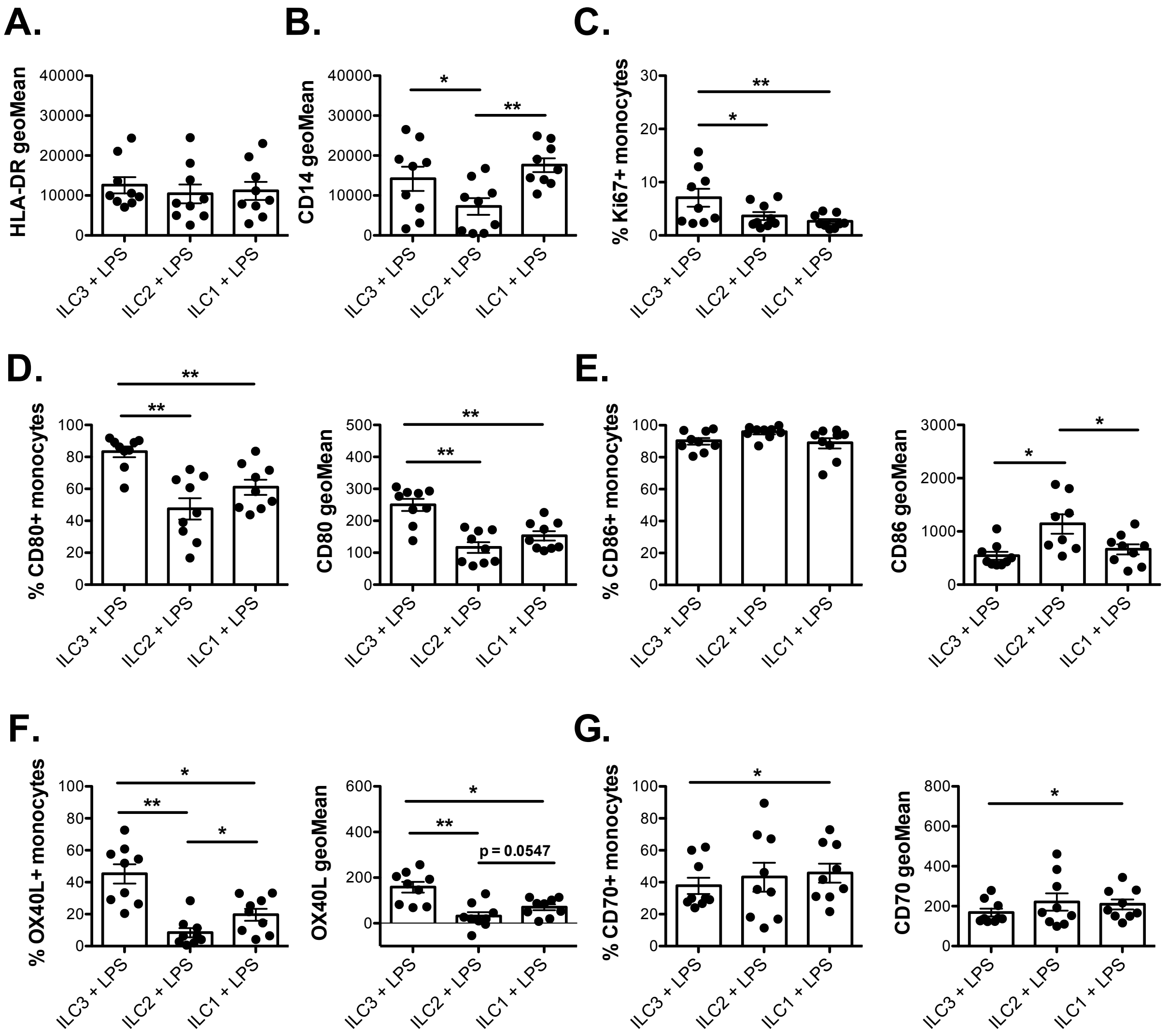

Figure 5.4: Different ILC subsets have distinct effects on monocyte activation. MACS purified monocytes and *in vitro* expanded FACS purified ILCs were co-cultured in the presence of LPS as described before. Comparison of **(A)** monocyte HLA-DR (MFI) **(B)** percentage of Ki67-expressing monocytes **(C)** percentage (left) and MFI (right) of monocyte CD80 expression **(D)** percentage (left) and MFI (right) of monocyte CD86 expresssion **(E)** percentage (left) and MFI (right) of monocyte OX40L expression **(F)** percentage (left) and MFI (right) of monocyte CD70 expression folllowing co-culture with ILC3, ILC2 or ILC1 in presence of LPS (1μg/ml). Monocytes from n = 3 donors and ILCs from n = 3 donors were incubated in an autologous or allogeneic system. No significant differences were observed between autologous or allogeneic co-cultures. Statistical significance was determined by means of Mann-Whitney U tests. Bars represent mean ± SEM. $^*p \leq 0.05$. $^{**}p \leq 0.01$.

In summary, these observations suggest that ILCs, in synergy with LPS, can promote the proliferation and maturation of CD14^{+} monocytes into CD14^{low} antigen-presenting cells characterised by high expression of HLA-DR and co-stimulatory molecules CD80, CD86, OX40L and CD70. The different ILC subsets vary in their capacity to induce monocyte proliferation and expression of individual co-stimulatory ligands (Table 5.1).

Table 5.1: Different ILC subsets have distinct effects on monocyte activation

Monocyte expression of	***- LPS***			***+ LPS***		
	+ ILC3	+ ILC2	+ ILC1	+ ILC3	+ ILC2	+ ILC1
HLA-DR	↑	↑	↑↑	↑↑	↑	↑↑
CD14	↓	↓↓	↓	↑↑	↑	↑↑
Proliferation	↑↑	—	↑	↑↑	↑	↑
CD80	↑	↑	↑	↑↑	↑	↑
CD86	↑	↑↑	↑	↑	↑↑	↑
OX40L	↑	—	—	↑↑	↑	↑
CD70	↑	↑	↑↑	↑	↑	↑↑

↑/↓ indicates statistically significant difference
↑↑/↓↓ indicates relatively increased upregulation
— indicates no change compared to baseline expression level

5.2.2 ILC-induced monocyte activation can be partially reduced by blockade of pro-inflammatory cytokines

We next wished to elucidate the mechanism(s) by which ILCs can induce monocyte activation and maturation. Signalling by the pro-inflammatory mediators IL-1β, TNFα, IL-6 and GM-CSF was abrogated by high-dose treatment (10 μg/ml) with blocking antibodies. Clinically utilized antibodies, anti-TNFα (Infliximab) and anti-IL-6R (Tocilizumab) as well as commercially available purified anti-human IL-1β and anti-human GM-CSF antibodies, were used in these experiments. Very similar results were obtained in monocyte-ILC3 and monocyte-ILC2 co-cultures. Due to low cell numbers, we were not able to perform these experiments with ILC1. Therefore, only monocyte-ILC3 co-cultures will be discussed below.

In the absence of additional LPS stimulation, monocyte expression of HLA-DR was significantly reduced by blockade of TNFα and GM-CSF signalling to levels similar to the baseline expression level by untreated monocytes. In contrast, addition of anti-IL-1β and anti-IL-6R antibodies showed no effect (Figure 5.5A). Treatment with infliximab reversed the downregulation of CD14 induced by co-culture with ILC3, resulting in CD14 expression that was even higher than baseline (Figure 5.5B). Neutralization of all four cytokines led to reduced monocyte proliferation as indicated by lower Ki67 expression, however, the strongest effects were observed when IL-1β and GM-CSF signalling were blocked (Figure 5.5C). CD80 expression was unaffected by addition of anti-IL-1β and anti-IL-6R antibodies. While a trend towards upregulation of CD80 expression was seen following neutralization of GM-CSF, this did not reach statistical significance. However, treatment with infliximab led to a significant increase in CD80 expression (Figure 5.5D). Blockade of TNFα and GM-CSF signalling lowered CD86 expression to levels similar to baseline expression by untreated monocytes. No effect was seen following neutralization of IL-1β or IL-

6R (Figure 5.5E). Similar to CD80, OX40L expression was increased in the presence of anti-TNFα and anti-GM-CSF antibodies, while blockade of IL-1β or IL-6 again had no effect (Figure 5.5F). Finally, CD70 expression was reduced when infliximab was present in the cultures, and increased following neutralization of IL-1β, whereas anti-GM-CSF and anti-IL-6R treatment did not induce any changes (Figure 5.5G).

Very similar effects were observed when IL-1β, TNFα, IL-6R and GM-CSF signalling were blocked in co-cultures in which LPS was additionally present. Monocyte HLA-DR expression was significantly lowered following administration of infliximab (Figure 5.5H) and monocyte proliferation was reduced following neutralization of TNFα, IL-1β and IL-6R (Figure 5.5J). Furthermore, expression of the co-stimulatory ligands CD86 and CD70 was reduced in the presence of anti-TNFα and anti-GM-CSF antibodies (Figure 5.5L and N). However, in contrast to co-culture conditions without LPS, cytokine blockade generally only resulted in partial reduction of surface marker expression that did not return to baseline expression levels, except in the case of HLA-DR and Ki67 expression following TNFα blockade (Figure 5.5H). Furthermore, in the presence of LPS, blockade of TNFα and GM-CSF signalling appeared to have the opposite effect on expression of CD80 and OX40L compared to co-cultures in which LPS was not present, with a reduction seen in both CD80 and OX40L expression (Figure 5.5K and M).

Thus, blocking experiments indicate that the augmentation of monocyte activation observed in co-cultures with ILCs can be partially reversed through inhibition of pro-inflammatory cytokine signalling.

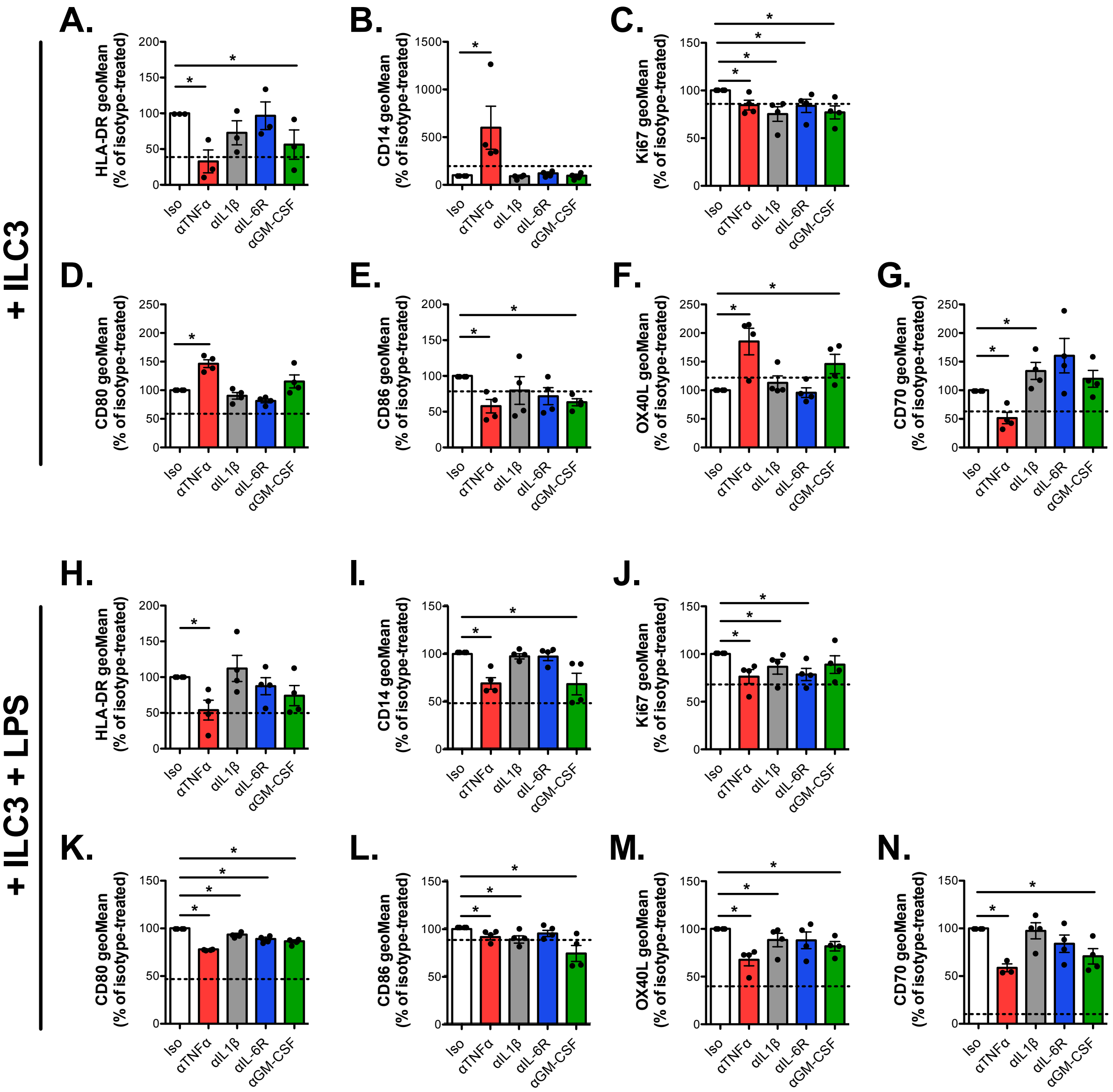

Figure 5.5: ILC-mediated augmentation of monocyte activation is reduced by blockade of cytokine signaling. CD14^{+} monocytes were co-cultured with *In vitro* expanded ILC3 **(A - G)** or ILC3 + LPS **(H - N)** as described previously. Blocking antibodies directed against IL-1β, TNFα, IL-6R and GM-CSF or an isotype control were added at the beginning of the culture. After 2 days of culture, flow cytometry analysis was used to determine monocyte expression of HLA-DR, CD80, CD86, OX40L, CD70, CD14 and Ki67. Isotype-treated controls were defined as 100% activation and the blocking antibody-treated conditions were expressed as a percentage of this. The dotted lines represent mean expression by untreated monocytes cultured without ILCs, shown also as a percentage of the isotype treated controls. Monocytes from n = 4 donors and ILCs from n = 4 donors were incubated in an autologous system. Statistical significance was determined by means of Wilcoxon matched-pairs signed rank tests. Bars represent mean ± SEM. $^{*}p \leq 0.05$.

5.2.3 ILC3 enhance macrophage-mediated bacterial killing

In order to examine the functional implications of ILC-mediated monocyte maturation, we assessed the microbicidal effector functions of monocyte-derived macrophages (MDM) in an *in vitro* model of *Salmonella typhimurium (S. typhimurium)* infection following stimulation with ILC-derived supernatants. *S. typhimurium* is a gram-negative bacterium that causes a self-limiting gastroenteritis in humans and depends on intracellular colonisation of macrophages, dendritic cells, epithelial cells and fibroblasts for its replication and survival. Macrophages respond to *S. typhimurium* infection by increasing their production of reactive oxygen and nitrogen species, which leads to enhanced bacterial killing and eventually clearance of the infection (398,399).

MDM were cultured overnight with supernatants derived from unstimulated ILC3 or IL-23-stimulated ILC3, as well as unstimulated ILC2 or ILC1. Fibroblast and B cell supernatants were included in comparison. This was followed by infection with *S. typhimurium* at a multiplicity of infection (MOI) of 10. After 1h, extracellular bacteria were killed by gentamicin treatment, MDM lysed and plated onto agar plates. The number of colony forming units (CFU) recovered from the lysates was determined the next day.

Pre-treatment with ILC3-derived supernatants increased the ability of MDM to control *S. typhimurium*, as indicated by a decrease in the number of CFU recovered per well. No further increase in killing capacity was observed following MDM treatment with the IL-23-stimulated ILC3 supernatants. A similar augmentation of macrophage bactericidal capacity was observed following overnight stimulation with ILC1 supernatants and fibroblast supernatants. In contrast, ILC2 supernatants did not enhance macrophage-dependent bacterial killing, which was equivalent to B cells (Figure 5.6A and B).

Thus, soluble factors secreted by ILC3 and ILC1 are able to enhance the capacity of macrophages to kill ingested bacteria, which may play a role in limiting bacterial infections.

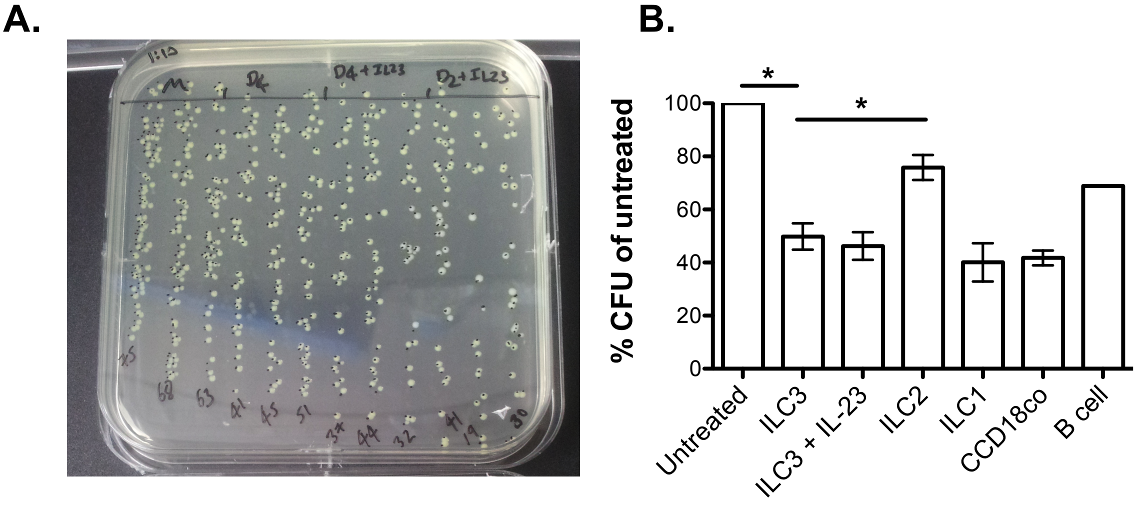

Figure 5.6: ILC3 enhance macrophage-mediated bacterial killing. (A) Representative image of bacterial colonies retrieved from Triton-X lysed macrophages. **(B)** Quantification of recovered bacterial colonies/well. ILC3 supernatants were derived from n = 7 donors, EBV B cell supernatant from n =1 donor and all other supernatants from n = 3 donors. Data are pooled from two separate experiments. Statistical significance was determined by means of Mann-Whitney U tests. Bars represent mean ± SEM. *$p \leq 0.05$.

5.2.4 Reciprocal activation of ILCs by monocytes

As discussed in Chapter 4, *ex vivo* ILCs from the blood and colon and *in vitro* expanded blood ILCs can express co-stimulatory molecules such as CD80, CD86 and OX40, whose expression on ILCs was regulated by cytokines such as IL-1β, IL-15, IL-23 and TNFα. Since activated monocytes are major producers of these cytokines, we wanted to examine whether co-culture of monocytes and ILCs can influence ILC co-stimulatory ligand expression.

In vitro expanded blood ILC1, ILC2 and ILC3 were labelled with CellTrace Violet and co-cultured at a 1:1 ratio with MACS purified CD14$^+$ monocytes (± LPS) in the presence of exogenous IL-2 (100 U/ml) to promote ILC survival. This was followed by flow cytometry analysis after two days of culture (Figure 5.7A).

Co-culture of ILC3 and monocytes led to an increase in the percentage of ILC3 expressing CD80 and CD86, which were further increased by addition of LPS (Figure 5.7B and C). ILC3 alone were unresponsive to LPS stimulation, suggesting that the LPS-mediated enhancement of ILC activation is an indirect effect that occurs via LPS-induced activation of monocytes. ILC3 expression of both OX40L and CD70 showed a trend towards increase in co-cultures with monocytes, but neither difference was statistically significant (Figure 5.7D and E). However, addition of LPS to the co-cultures induced significant upregulation of OX40L on ILC3. ILC3 CD70 expression was similarly increased, but still did not reach statistical significance. Interestingly, LPS-activated monocytes also promoted enhanced expression of CD25, the high-affinity IL-2 receptor α chain, by ILC3, potentially rendering them more susceptible to stimulation with IL-2, which is a potent proliferative factor for ILCs (Figure 5.7F). Indeed, examination of ILC3 proliferation by means of CellTrace Violet dilution showed that ILC3 proliferated more vigorously in the presence of monocytes, which was increased further following activation of the monocytes with LPS (Figure 5.7G). This was reflected by increased absolute numbers of ILC3 (Figure 5.7H). In addition, co-culture with both untreated and LPS-activated monocytes significantly reduced the proportion of CD117-expressing ILC3 (Figure 5.7I).

Co-culture of ILC2 and monocytes under conditions of LPS stimulation resulted in a significant increase in the proportion of ILC2 that expressed CD86, CD70 and CD25 (Figure 5.8A-C, E and F), as well as a trend towards increased OX40L expression and ILC2 proliferation and absolute numbers (Figure 5.8D, G and H). No changes in ILC2 CD117 expression were detected (Figure 5.8I). Similarly, co-culture of ILC1 with monocytes under conditions of LPS stimulation induced an increase in the proportion of ILC1 expressing CD86, OX40L and CD25, but not CD80 or CD70 (Figure 5.9).

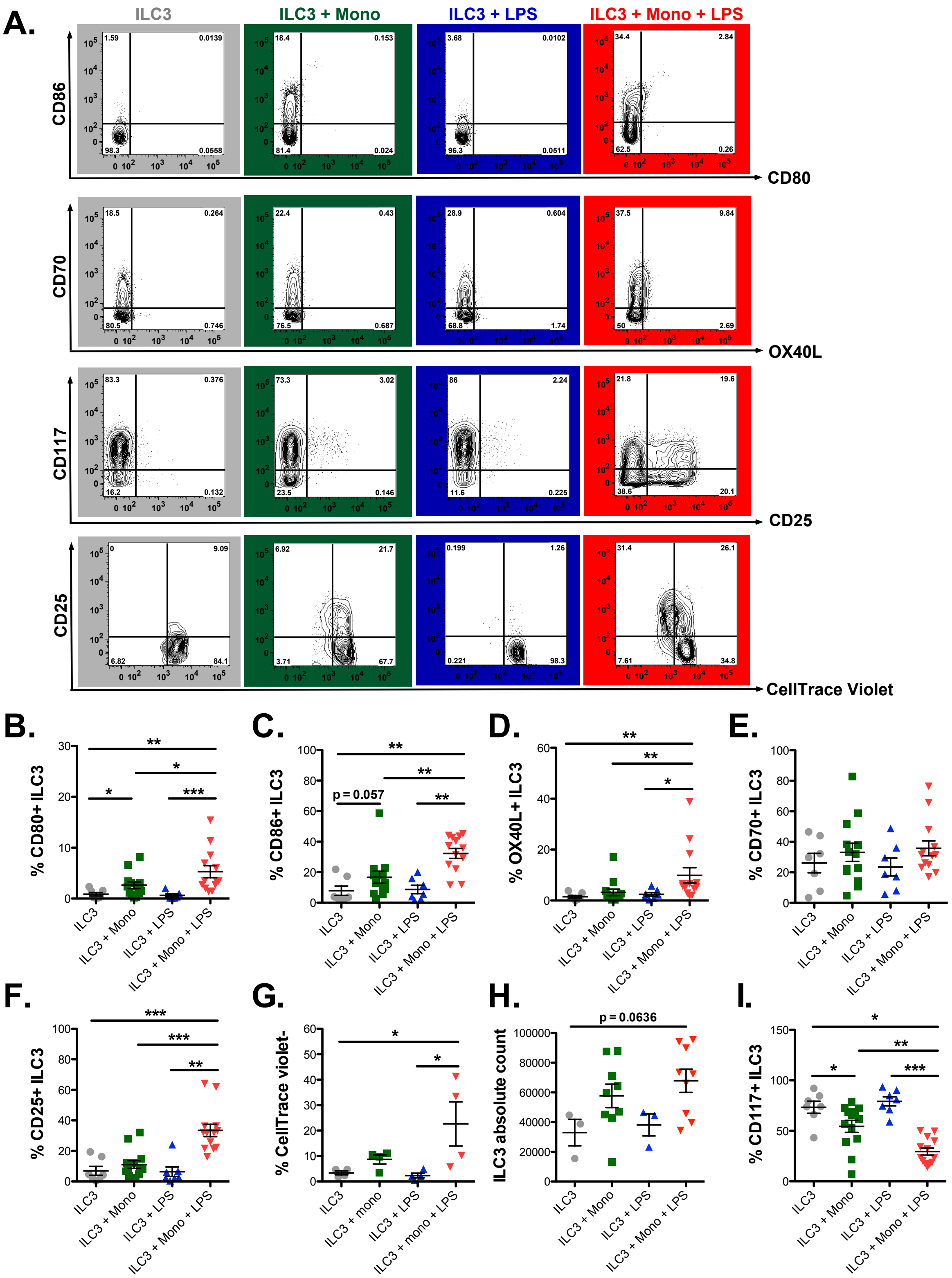

Figure 5.7: Co-culture of monocytes and ILC3 increases ILC3 activation and proliferation. *In vitro* expanded CellTrace violet-labelled ILC3 and MACS purified CD14$^+$ monocytes were co-cultured in absence or presence of LPS (1μg/ml) for 2 days, followed by flow cytometry analysis. **(A)** Representative FACS plots of ILC3 surface marker expression and CellTrace Violet dilution. **(B - I)** Quantification of ILC3 expressing CD80 **(B)**, CD86 **(C)**, OX40L **(D)**, CD70 **(E)**, CD25 **(F)**, CellTrace Violet **(G)**, absolute counts **(H)** and CD117 **(I)**. In (B-E), (F) and (I) ILCs from n = 7 donors and monocytes from n = 7 donors were incubated in an autologous or allogeneic manner. No significant differences were observed between autologous or allogeneic co-cultures. Data are pooled from two separate experiments. In (G), ILCs from n = 4 donors and monocytes from n = 4 donors were incubated in an allogeneic system. In (H), ILCs from n = 3 donors and monocytes from n =3 donors were incubated in an autologous or allogeneic manner. Statistical significance was determined by means of Mann-Whitney U tests. Bars represent mean ± SEM. *$p \leq 0.05$. **$p \leq 0.01$. ***$p \leq 0.001$.

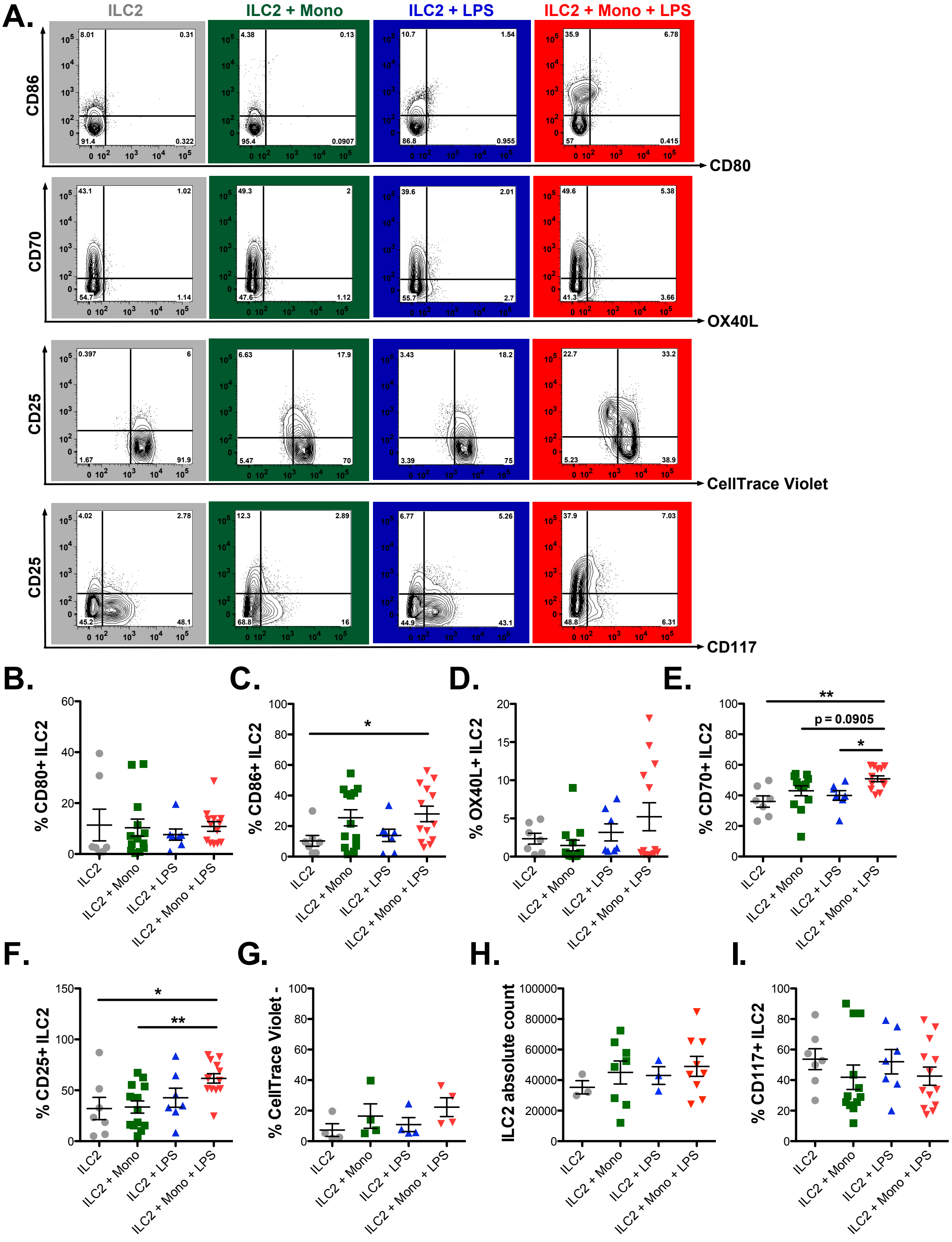

Figure 5.8: Co-culture of monocytes and ILC2 increases ILC2 activation. *In vitro* expanded CellTrace violet-labelled ILC2 and MACS purified CD14^{+} monocytes were co-cultured in absence or presence of LPS for 2 days, followed by flow cytometry analysis. **(A)** Representative FACS plots of surface marker expression and CellTrace Violet dilution. **(B - I)** Quantification of ILC3 expressing CD80 **(B)**, CD86 **(C)**, OX40L **(D)**, CD70 **(E)**, CD25 **(F),** CellTrace violet **(G)**, absolute ILC2 count **(H)** and CD117 **(I)**. In (B-E), (F) and (I) ILCs from n = 7 donors and monocytes from n = 7 donors were incubated in an autologous or allogeneic manner. No significant differences were observed between autologous or allogeneic co-cultures. Data are pooled from two separate experiments. In (G), ILCs from n = 4 donors and monocytes from n = 4 donors were incubated in an allogeneic system. In (H), ILCs from n = 3 donors and monocytes from n =3 donors were incubated in an autologous or allogeneic manner. Statistical significance was determined by means of Mann-Whitney U tests. Bars represent mean ± SEM. $^{*}p \leq 0.05$. $^{**}p \leq 0.01$.

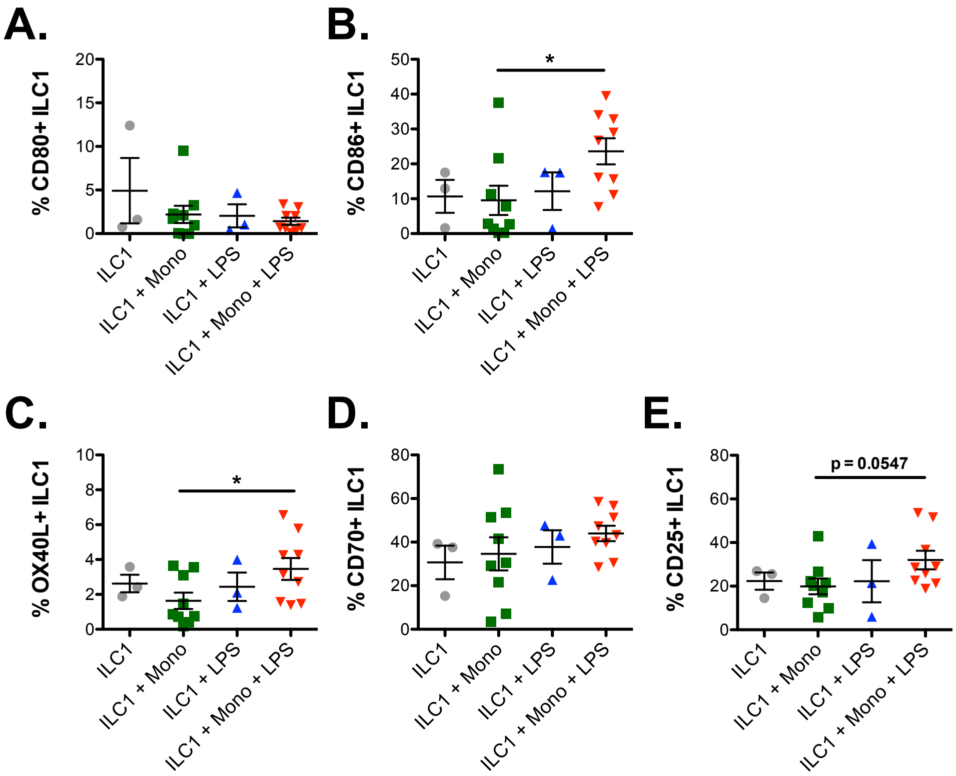

Figure 5.9: Co-culture of monocytes and ILC1 induces ILC1 activation. *In vitro* expanded ILC1 and MACS purified CD14+ monocytes were co-cultured in absence or presence of LPS for 2 days, followed by flow cytometry analysis. Quantification of percentage of ILC1 expressing CD80 **(A)**, CD86 **(B)**, OX40L **(C)**, CD70 **(D)** and CD25 **(E)**. ILCs from n = 3 donors and monocytes from n = 3 donors were incubated in an autologous or allogeneic manner. No significant differences were observed between autologous or allogeneic co-cultures. Statistical significance was determined by means of Mann-Whitney U tests. Bars represent mean ± SEM. $^*p \leq 0.05$.

Thus, as summarized in Table 5.2, our findings indicate that monocytes, and in particular LPS-stimulated monocytes, can induce a state of enhanced co-stimulatory ligand expression on the different ILC subsets, increase their expression of CD25 and augment their proliferative behaviour.

Table 5.2: (LPS-activated) monocytes drive ILC activation

	+ Mono - LPS			***+ Mono + LPS***		
ILC expression of	ILC3	ILC2	ILC1	+ ILC3	+ ILC2	+ ILC1
CD25	↑	—	—	↑↑	↑↑	↑
Proliferation	↑	—	NT	↑↑	↑	NT
CD80	↑↑	—	—	↑↑	—	—
CD86	↑	↑	↑	↑↑	↑↑	↑↑
OX40L	—	—	—	↑↑	↑	↑↑
CD70	—	↑	—	↑	↑↑	↑

↑	indicates trend towards upregulation
↑↑	indicates statistically significant upregulation
—	indicates no change compared to baseline expression level

5.2.5 Monocyte-dependent activation of ILCs is partially mediated by TNFα, IL-1β and IL-6R signalling

In order to examine a potential mechanism by which monocytes induced ILC activation, blocking antibodies directed against TNFα, IL-1β, IL-6R and GM-CSF were added to co-cultures of monocytes and CellTrace Violet-labelled ILC2 or ILC3 in the presence of LPS.

As with monocytes (Figure 5.5), neutralization of TNFα strongly decreased expression of CD80, OX40L, CD70 and CD25 by ILC3, while treatment with anti-IL-1β antibody reduced ILC3 expression of CD80, OX40L and CD70 and blockade of IL6R decreased expression of OX40L and CD25 (Figure 5.10A-D). Furthermore, ILC3 proliferation was partially inhibited by treatment with any of the four blocking antibodies (Figure 5.10E). However, these effects were relatively mild and ILC3 activation remained considerably above baseline following antibody treatment. In contrast, addition of blocking antibodies in co-cultures of ILC2 with monocytes had much clearer effects. Blockade of TNFα and IL-6R significantly reduced ILC2 expression of OX40L to levels comparable to baseline, and similar trends were observed for CD80 and CD70 (Figure 5.10F-H). Furthermore, anti-TNFα and anti-IL-6R treatment both decreased CD25 expression and proliferation by ILC2 (Figure 5.10I and J). In contrast to ILC3, ILC2 were completely unaffected by treatment with anti-IL1β antibody, which is consistent with their lower expression of *IL1R1* transcript (see Chapter 4).

Thus, our findings indicate that monocyte-dependent activation of ILCs appears to be at least partially driven by the pro-inflammatory cytokines TNFα, IL-1β and IL-6, as blockade of these signalling pathways reduced expression of co-stimulatory ligands and CD25 as well as proliferation by ILCs.

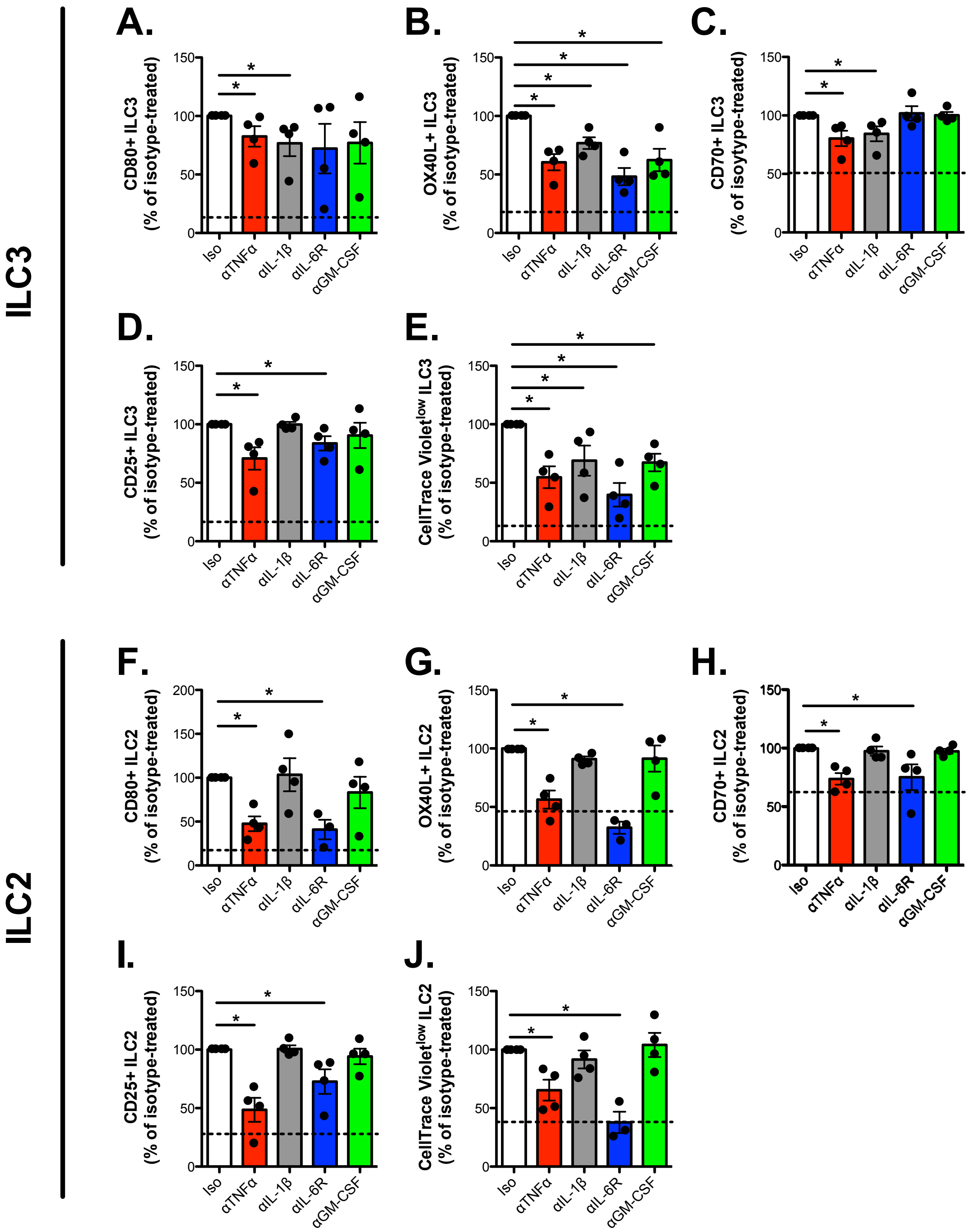

Figure 5.10: Monocyte-mediated activation of ILC2 and ILC3 is reduced by blockade of TNFα, IL−1β and IL-6R signalling. *In vitro* expanded ILC3 **(A-E)** and ILC2 **(F-J)** were co-cultured with monocytes and LPS for two days as described previously. Blocking antibodies directed against IL-1β, TNFα, IL-6R and GM-CSF and isotype control were added at the beginning of the culture. Flow cytometry analysis was used to determine ILC expression of CD80, OX40L and CD70. The data shown depict the conditions of maximum ILC activation (ILCs + Monocytes + LPS). Isotype-treated controls were defined as 100% activation and the blocking antibody-treated conditions were expressed as a percentage of this. The dotted lines represent mean expression by untreated ILCs in culture without monocytes, shown also as a percentage of the isotype treated controls. ILCs from n = 4 donors and monocytes from n = 4 donors were co-cultured in an autologous manner. Statistical significance was determined by means of Wilcoxon matched-paris signed rank tests. Bars represent mean ± SEM. *$p \leq 0.05$.

5.2.6 *Ex vivo* total Lin$^-$ CD127$^+$ ILCs enhance CD4$^+$ T cell proliferation and activation following stimulation with soluble anti-CD3 antibody and monocytes

The paradigm of T cell activation posits that two signals are required for full induction of a T cell response. The first signal is delivered when complexes of MHC and cognate antigen peptide bind to the TCR, providing specificity to the response. However, TCR ligation alone is insufficient for full T cell activation and a second signal is required, provided by the binding of co-stimulatory molecules expressed by activated APCs to receptors on the T cell surface. TCR ligation in the absence of co-stimulatory signals induces a state of T cell anergy (400). We hypothesized that the increased co-stimulatory molecule expression resulting from the bi-directional activation loop between ILCs and monocytes may lead to an augmentation of CD4$^+$ T cell activation when CD4$^+$ T cells are stimulated in the presence of both cell types. We decided to use a system of polyclonal CD4$^+$ T cell activation with soluble anti-CD3 antibody and monocytes. Effective CD4$^+$ T cell activation in this system is dependent on the additional provision of co-stimulatory signals, rendering it a useful tool to test the functional effects of enhanced co-stimulatory ligand expression.

As schematically represented in Figure 5.11A, our pilot experiment involved activation of CD4$^+$ CD45RO$^+$ memory T cells with soluble anti-CD3 antibody and autologous CD14$^+$ monocytes in the absence or presence of bulk autologous Lin$^-$ CD127$^+$ ILCs. All cells were used directly *ex vivo* following FACS (ILCs, T cells) or MACS (monocytes) purification. The co-cultures were terminated after five days and the cells harvested for flow cytometric analysis. The read-outs for T cell activation included T cell proliferation and activation as assessed by expression of the proliferation-associated marker Ki67, and expression of cell surface activation markers CD25, ICOS and OX40.

As expected, co-culture with monocytes and soluble anti-CD3 antibody elicited robust proliferation of $CD4^+$ T cells as indicated by increased expression of Ki67 (Figure 5.11B and C). This was accompanied by upregulation of the T cell activation markers CD25, ICOS and OX40 on a per cell and population level (Figure 5.11D-F). In contrast to monocytes, ILCs do not express Fc receptors, and accordingly did not promote anti-CD3-mediated activation of $CD4^+$ T cells on their own. No increase in $CD4^+$ T cell proliferation was observed following addition of anti-CD3 antibody to ILC-T cell co-cultures in the absence of monocytes (Figure 5.11B and C). Similarly, no change in the expression of the surface markers ICOS, CD25 and OX40 was detected following activation of T cells in the presence of ILCs alone (Figure 5.11D-F).

However, when $CD4^+$ T cells were activated with anti-CD3 antibody in the presence of both ILCs and monocytes, ILCs seemed to enhance the ability of monocytes to induce anti-CD3-mediated T cell proliferation. While approximately 13.6% of $CD4^+$ T cells expressed Ki67 following anti-CD3 mediated activation in the presence of monocytes, this was further increased to approximately 26.3% when ILCs were additionally present (Figure 5.11C). This increase in $CD4^+$ T cell proliferation was associated with increased expression of the activation markers ICOS, CD25 and OX40 (Figure 5.11D-F).

5.2.7 ILC2 and ILC3 enhance monocyte- and anti-CD3-mediated activation of CD4$^+$ T cells

Repeat experiments aimed to further subdivide total Lin$^-$ CD127$^+$ ILCs into CRTH2$^+$ ILC2 and CD117$^+$ CRTH2$^-$ ILC3 subsets in order to examine whether ILC3 and ILC2 populations were similar in their ability to enhance CD4$^+$ T cell activation and proliferation in this system. Due to technical issues during *in vitro* expansion, ILC1 could not be included in this analysis. In order to obtain sufficient numbers of ILC2 and ILC3 autologous to the CD4$^+$ T cells and monocytes, the two ILC subsets were FACS sorted from 30ml of human peripheral blood and expanded *in vitro* using the culture system described in Chapter 3. After 2-3 weeks of expansion, the same donors provided another 20ml of blood, which was then used to purify CD14$^+$ monocytes by MACS and CD4$^+$CD45RO$^+$ memory T cells by FACS. The CD4$^+$ T cells were labelled with CFSE and plated at a density of 4 x 10^4 cells/well together with 2 x 10^4 monocytes and/or 2 x 10^4 ILC2 or ILC3. As before, no exogenous cytokines were added to the cultures and anti-CD3 antibody was used at a concentration of 10 μg/ml.

Similar to the observations described above for co-cultures with bulk ILCs, CD4$^+$ T cells proliferated more vigorously when activated in the presence of both monocytes and ILC2 or ILC3 compared to stimulation in presence of monocytes alone, resulting in recovery of increased numbers of T cells (Figure 5.12A-C). Furthermore, the CD4$^+$ T cells stimulated in the presence of ILCs displayed a more highly activated phenotype with significantly increased expression of the cell surface activation markers CD25, OX40 and ICOS (Figure 5.13A-D).

In the absence of the activatory stimulus provided by the anti-CD3 signal, the additional presence of ILC2 or ILC3 in monocyte-T cell cultures did not affect the inherent baseline activation state of $CD4^+$ T cells. No significant differences in $CD4^+$ T cell activation or proliferation were observed between T cell-monocyte and T cell-monocyte-ILC co-cultures in the absence of soluble anti-CD3 antibody (Figures 5.12 and 5.13).

Thus, our results indicate that in the context of polyclonal $CD4^+$ T cell activation mediated by monocytes and soluble anti-CD3 antibody, the additional presence of ILCs can augment $CD4^+$ T cell activation.

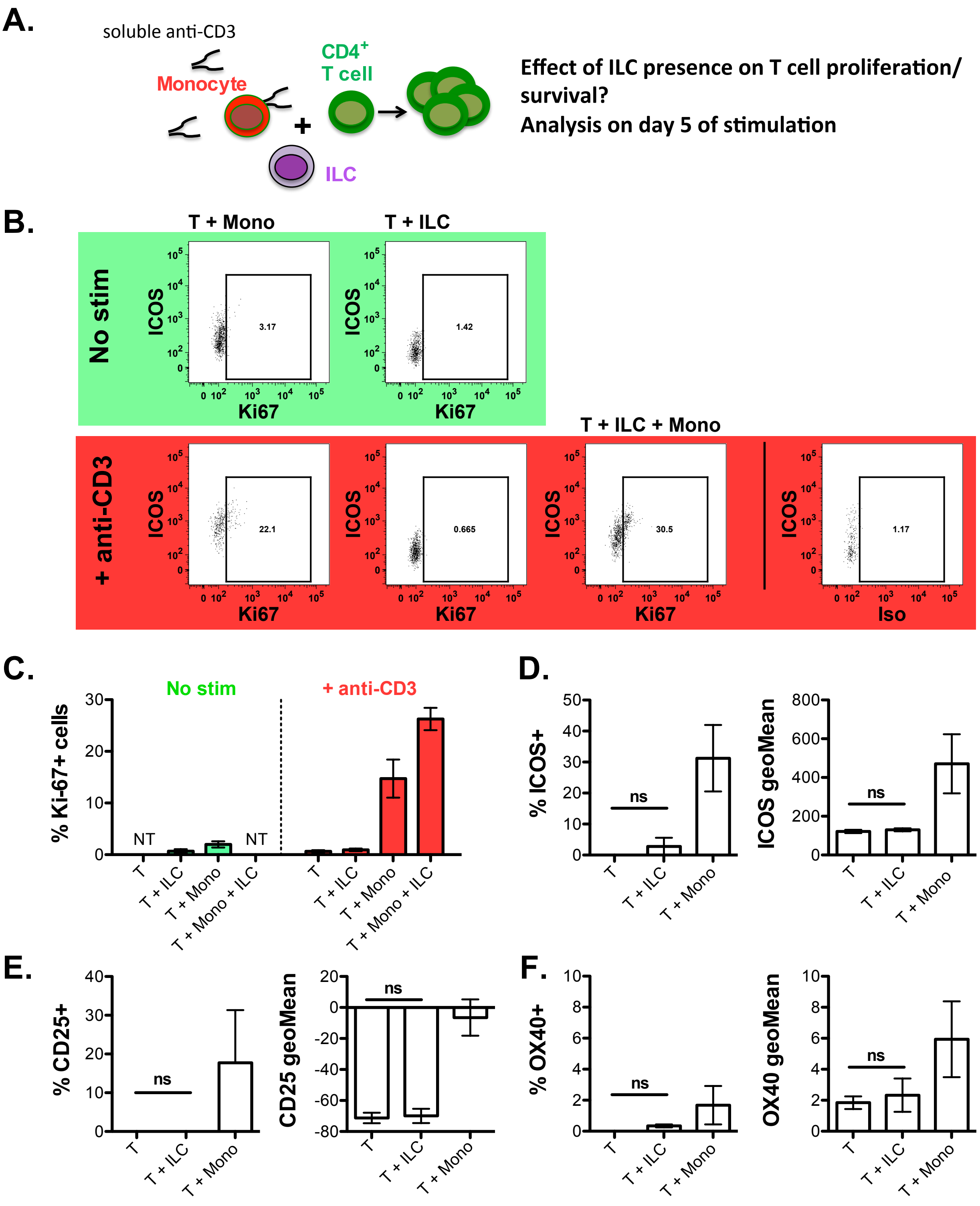

Figure 5.11: ILCs do not support soluble anti-CD3 mediated T cell expansion, but enhance T cell proliferation following stimulation with soluble anti-CD3 in presence of monocytes. (A) Schematic depicting experimental set-up. FACS sorted CD4$^+$CD45RO$^+$ memory T cells were co-cultured with autologous MACS sorted CD14$^+$ monocytes in absence or presence of autologous FACS sorted *ex vivo* bulk ILCs (Lin$^-$ CD127$^+$CD117$^+$) ILCs. Soluble anti-CD3 antibody was added to polyclonally activate the T cells. T cell proliferation and expression of surface activation markers were assessed using flow cytometric analysis after 7 days of culture. **(B)** Representative FACS plots of T cell Ki67 expression. Cells were pre-gated as Live CD3$^+$CD4$^+$CD14$^-$CD117$^-$ cells. **(C)** Quantification of T cell proliferation as assessed by Ki67 staining and flow cytometry analysis. **(D)** Percentage (left) and MFI (right) of ICOS expression by CD4$^+$ T cells. **(E)** Percentage (left) and MFI (right) of CD25 expression by CD4$^+$ T cells. **(F)** Percentage (left) and MFI (right) of OX40 expression by CD4$^+$ T cells. Autologous T cells, ILCs and monocytes were obtained from n = 3 donors. Statistical significance was determined by means of Wilcoxon matched-pairs signed rank tests. Bars represent mean ± SEM.

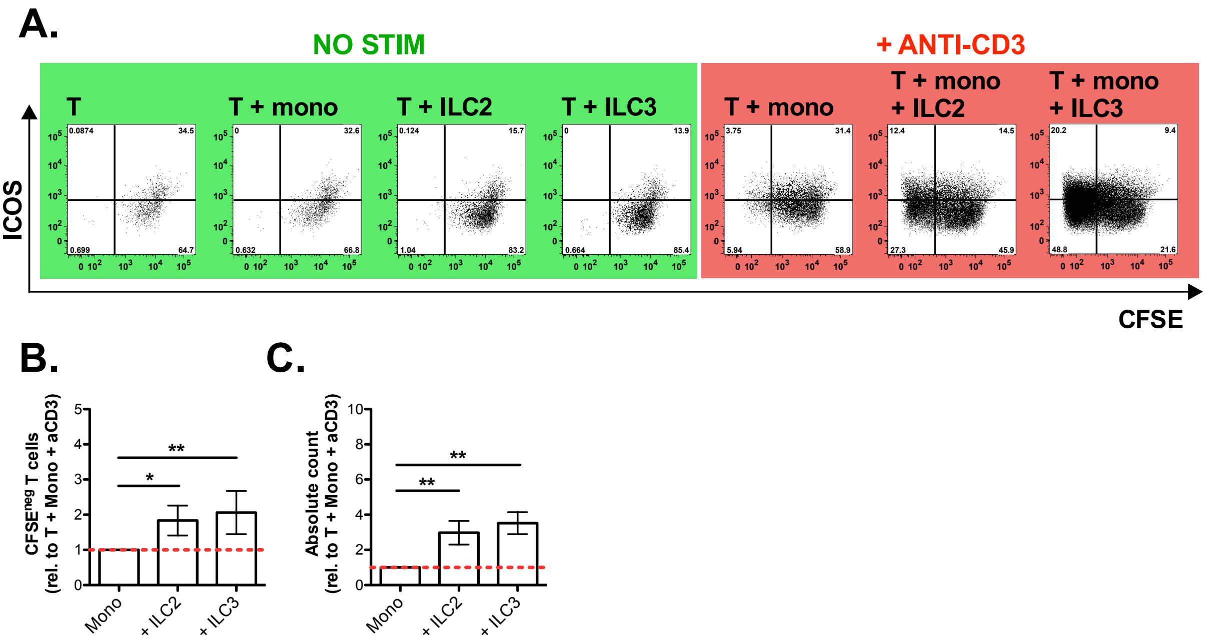

Figure 5.12: ILC3 enhance T cell proliferation following stimulation with soluble anti-CD3 in presence of monocytes. FACS sorted CD4$^+$CD45RO$^+$ memory T cells were co-cultured for 7 days with autologous MACS purified monocytes in absence or presence of autologous *in vitro* expanded ILC2 or ILC3. T cells were labelled with CFSE and were polyclonally activated with soluble anti-CD3 antibody. T cell proliferation was assessed via CFSE dilution as determined by flow cytometry analysis. Absolute cell counts were obtained using CountBright beads for flow cytometry. **(A)** Representative FACS plots gated on CD3$^+$CD4$^+$ cells showing CFSE dilution across different culture conditions. **(B)** Quantification of total CFSE^{negative} T cells. **(C)** Quantification of absolute numbers of T cells recovered from each condition. Autologous T cells, ILCs and monocytes were obtained from n = 12 donors in (B) and n = 8 donors in (C). Data were pooled from three separate experiments in (B) or two separate experiments in (C). Statistical significance was determined by means of Wilcoxon matched-pairs signed rank tests. Bars represent mean ± SEM. *$p \leq 0.05$. **$p \leq 0.01$.

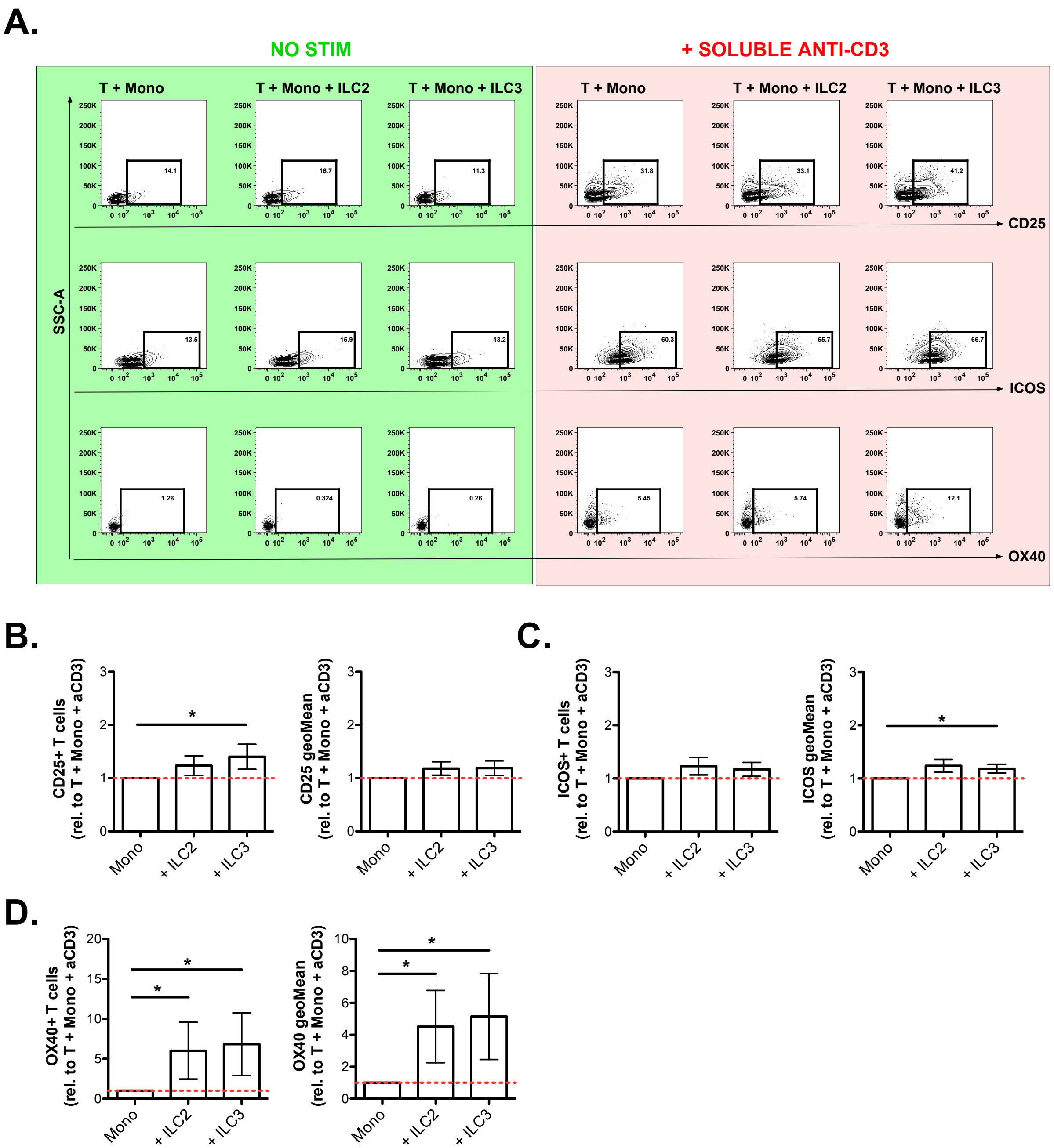

Figure 5.13: Expression of surface activation markers on memory CD4$^+$ T cells following soluble anti-CD3-mediated activation in absence or presence of ILC2 or ILC3. (A) Representative FACS plots depicting expression of CD25, ICOS and OX40 on CD4$^+$ T cells across the different culture conditions. **(B)** Percentage (right) and MFI (left) of CD25 expression. **(C)** Percentage (right) and MFI (left) of ICOS expression. **(D)** Percentage (right) and MFI (left) of OX40 expression. Autologous T cells, ILCs and monocytes were obtained from n = 8 donors. Data were pooled from two separate experiments. Statistical significance was determined by means of Wilcoxon matched-pairs signed rank tests. Bars represent mean ± SEM. *$p \leq 0.05$.

5.2.8 ILC-mediated effects on CD4$^+$ T cell proliferation and activation are partially dependent on direct cell-cell contact between ILCs and monocytes and/or T cells

Next we wanted to examine whether direct cellular interactions between ILCs and CD4$^+$ T cells and/or monocytes were required to achieve the observed enhancement in T cell proliferation and activation. CD4$^+$ T cell activation cultures in which ILCs were separated from the monocytes and T cells via 0.4μm polycarbonate transwell inserts prior to addition of soluble anti-CD3 antibody were set up in parallel to cultures without inserts (Figure 5.14A).

In order to exclude technical variability between the different experiments, all values in our analysis were expressed relative to T cells activated by monocytes and soluble anti-CD3. Separation of ILCs from monocytes and CD4$^+$ T cells reduced the ILC-mediated boost of T cell expansion observed in cultures without a transwell insert (Figure 5.14B and C). Furthermore, reduced CD4$^+$ T cell expansion in the transwell system was accompanied by lower expression of cell surface activation markers ICOS and OX40, although CD25 expression was unchanged (Figure 5.14D-F). Nonetheless, in the transwell cultures, stimulation in the presence of ILCs still resulted in increased proliferation and absolute numbers of CD4$^+$ T cells compared to stimulation with monocytes alone (Figure 5.14B and C). This suggests that ILCs exert their effect on CD4$^+$ T cell proliferation through a mixture of contact-dependent signals and soluble factors such as cytokines.

Thus, the enhanced CD4$^+$ T cell activation observed in the presence of ILCs partially depends on direct cell-cell contact between ILCs and CD4$^+$ T cells or ILCs and monocytes. In addition, soluble factors likely play a role.

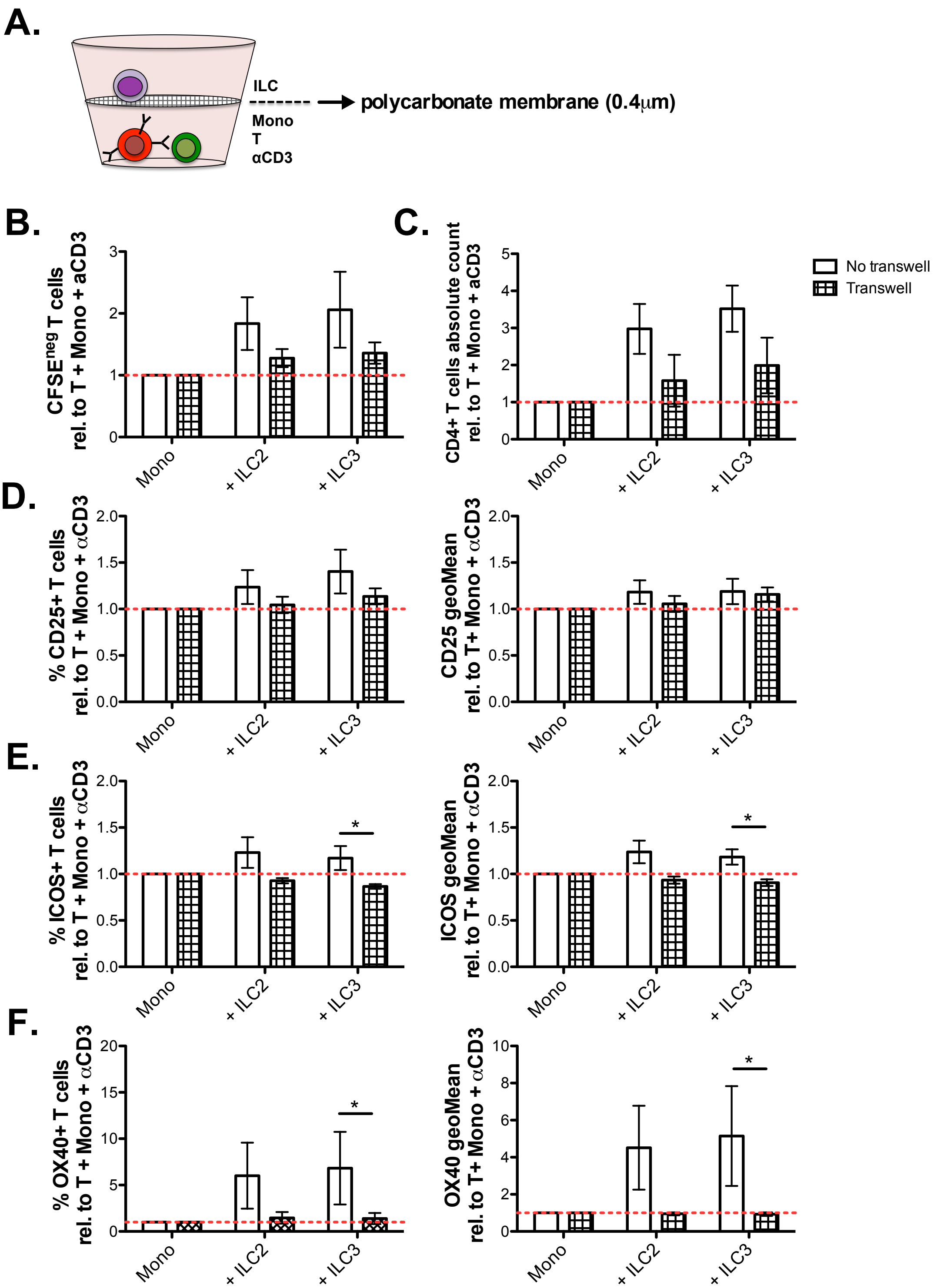

Figure 5.14: Comparison of ILC-mediated effects on $CD4^+$ memory T cell expansion in a non-transwell vs transwell setting. (A) Schematic representation of experimental set-up. (**B**) Comparison of $CFSE^{negative}$ $CD4^+$ memory T cells between non-transwell and transwell settings. (**C**) Comparison of absolute numbers of $CD4^+$ memory T cells between non-transwell and transwell settings. (**D**) Comparison of percentage (left) and MFI (right) of CD25 expression by $CD4^+$ memory T cells in non-transwell vs transwell settings. (**E**) Comparison of percentage (left) and MFI (right) of ICOS expression by $CD4^+$ memory T cells in non-transwell vs transwell settings. (**F**) Comparison of percentage (left) and MFI (right) of OX40 expression by $CD4^+$ memory T cells in non-transwell vs transwell settings. Data were normalized to T cells in cultures with monocytes and soluble αCD3-activated T cells. Autologous T cells, ILCs and monocytes were obtained from n = 6 donors. Data were pooled from two separate experiments. Statistical significance was determined by means of Wilcoxon matched-pairs signed rank testss. Bars represent mean ± SEM. $^*p \leq 0.05$.

5.2.9 Altered spatial interactions between monocytes and CD4$^+$ T cells do not account for the enhanced T cell activation observed in the presence of ILCs

The additional presence of ILCs in our culture system could modify spatial interactions between monocytes and CD4$^+$ T cells, leading to changes in accessibility of T cells to anti-CD3 and/or co-stimulatory signals provided by monocytes and ultimately lead to changes in the levels of T cell proliferation/activation. In order to distinguish such a generic effect from a specific ILC-dependent effect on CD4$^+$ T cell activation, we performed a repeat experiment in which ILCs were substituted with inert, lymphocyte-sized polystyrene beads (10μm bead diameter).

The additional presence of beads did not change the levels of CD4$^+$ T cell proliferation induced by stimulation with soluble anti-CD3 and monocytes compared to cultures in which only CD4$^+$ T cells and monocytes were present (Figure 5.15A and B). This suggests that the enhanced CD4$^+$ T cell activation observed in the presence of ILCs and its partial reversal in the transwell system is not the result of altered spatial interactions between CD4$^+$ T cells and monocytes. Instead, ILCs actively boost T cell proliferation through expression of immunologically active surface-bound and soluble mediators.

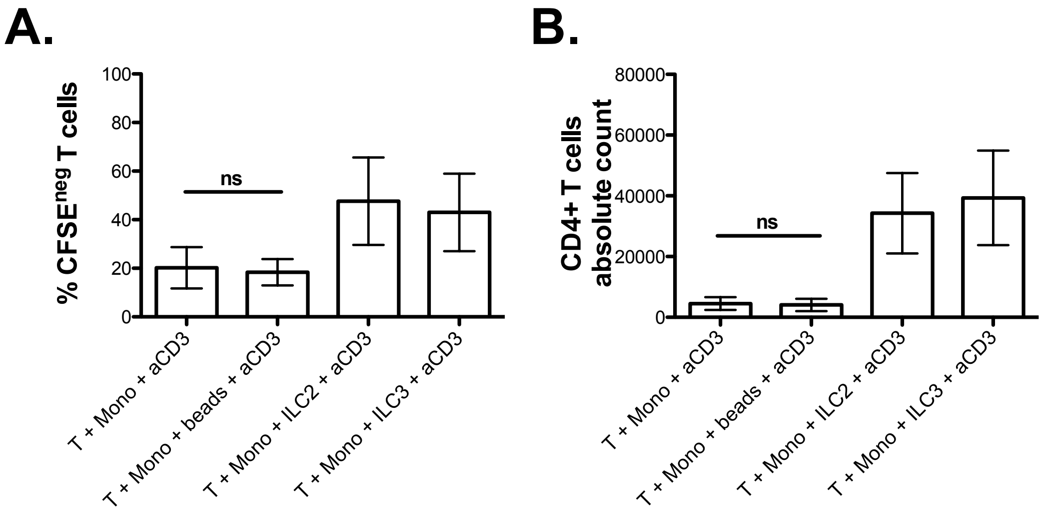

Figure 5.15: T cell activation by monocytes + soluble anti-CD3 is not changed in the presence of inert lymphocyte-sized filler beads. **(A)** Quantification of CFSE^{low} CD4^{+} memory T cells. (**B)** Quantification of CFSE^{negative} CD4^{+} memory T cells. (**C)** Absolute numbers of CD4^{+} memory T cells recovered. Autologous T cells, ILCs and monocytes were obtained from n = 3 donors. Statistical significance was determined by means of Wilcoxon matched-paris signed rank tests. Bars represent mean ± SEM.

5.2.10 ILCs upregulate CD25 expression following co-culture with activated CD4$^+$ T cells and monocytes

In addition to ILC-mediated effects on CD4$^+$ T cells, CD4$^+$ T cell-dependent activation of ILCs has been described in the murine system (146,401). In particular, the T cell-derived cytokine IL-2 has been shown to promote *in vivo* ILC survival and proliferation as well as cytokine production (146,402). We hypothesised that human ILCs may be similarly regulated by CD4$^+$ T cells and examined ILC expression of the high-affinity IL-2 receptor α chain (CD25) and proliferation in our co-culture system (Figure 5.16A).

Co-culture of ILC3 with unstimulated CD4$^+$ memory T cells led to an increase in the percentage of CD25-expressing ILC3 and an increase in CD25 MFI (Figure 5.16B). No further increase was observed when ILC3 were co-cultured with monocytes in addition to CD4$^+$ T cells. However, when anti-CD3 antibody was added in order to activate the CD4$^+$ T cells, CD25 expression by the ILC3 was further increased compared to co-culture with unstimulated CD4$^+$ T cells alone or in combination with monocytes.

Higher expression of CD25 may render ILC3 more susceptible to autologous or T cell-derived IL-2, which, in conjunction with IL-7, is an important proliferative and/or survival factor for ILC3 (see Chapter 3). Indeed, ILC3 displayed an increase in proliferative behaviour when co-cultured with unactivated CD4$^+$ T cells alone or with CD4$^+$ T cells and monocytes, which was boosted further following activation of CD4$^+$ T cells by addition of soluble anti-CD3 antibody (Figure 5.16C). This induction of ILC3 proliferation was reflected in an increased ILC3 count following co-culture with unstimulated CD4$^+$ T cells alone (2.8-fold expansion) and in particular with anti-CD3-activated CD4⁺ T cells (5.0-fold expansion) (Figure 5.16D). Based on a FACS-based purity check at the start of the experiment, the ILC2 and ILC3 used showed no expression of T cell-associated markers CD3, CD4, CD8, TCRαβ and TCRγδ, and furthermore expressed high levels of CD117 (data not shown). Therefore, a potential contamination of the ILC populations with T cells is highly unlikely.

Co-cultures of ILC2 with CD4⁺ T cells and monocytes yielded very similar results. CD25 expression by ILC2 was increased following co-culture with CD4⁺ T cells, with no further changes induced when monocytes were also present (Figure 5.16E). However, CD25 expression was further enhanced following anti-CD3-mediated activation of CD4⁺ T cells. As for ILC3, this upregulation of CD25 expression was accompanied by increased proliferation and increased numbers of ILC2 (Figure 5.16F and G).

Thus, it appears that CD4⁺ T cells, perhaps in conjunction with monocytes, can influence CD25 expression levels and increase the proliferative behaviour of both ILC2 and ILC3, potentially through increasing ILC responsiveness to IL-2.

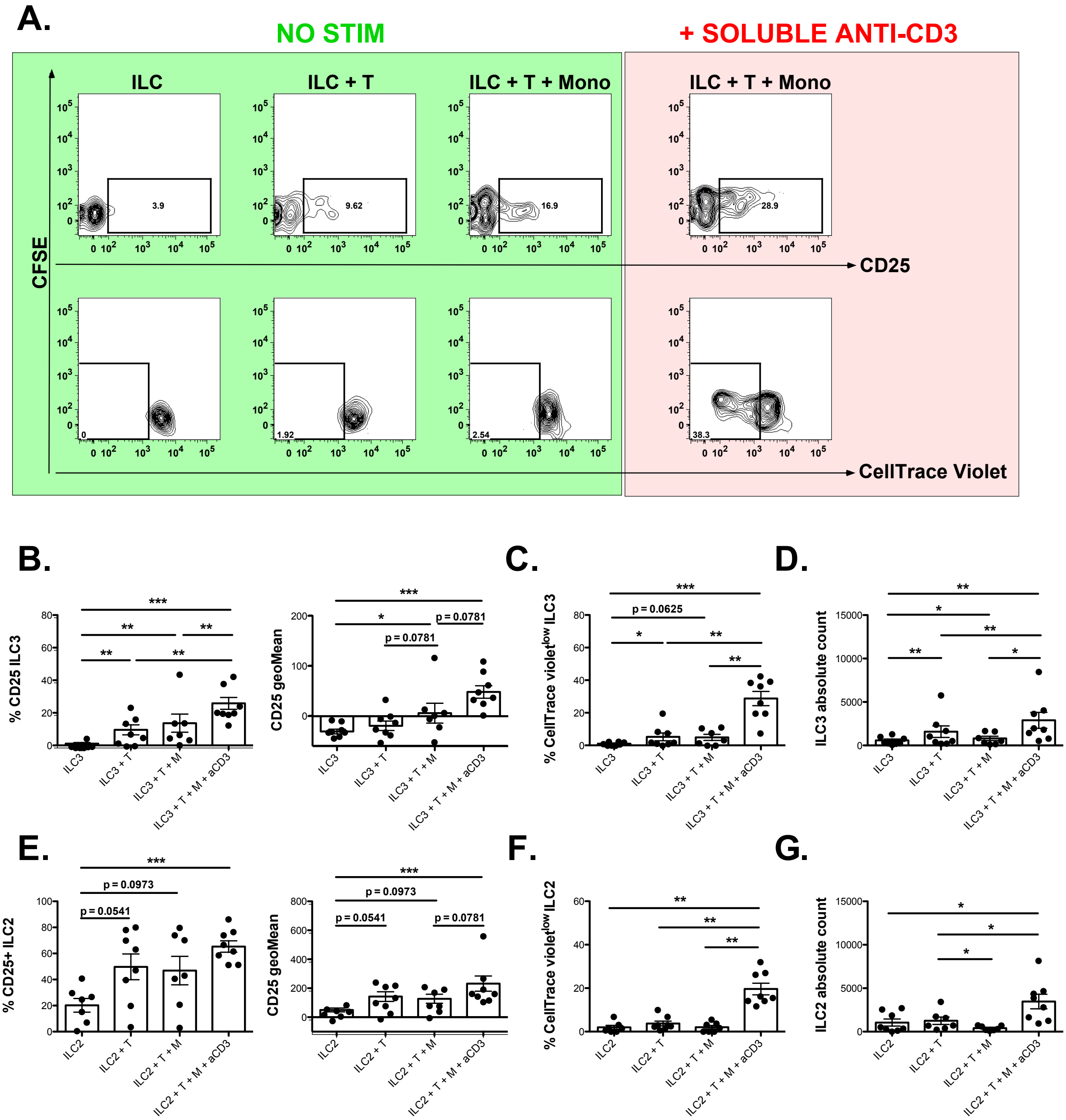

Figure 5.16: Co-culture with CD4$^+$ memory T cells increases the proportion of CD25 expressing ILC2 and ILC3. *In vitro* expanded ILC2 and ILC3 were labelled with CellTrace Violet and were co-cultured with autologous CD4$^+$ memory T cells in absence or presence of autologous monocytes and in absence or presence of polyclonal T cell activation using soluble anti-CD3 administration. Flow cytometry analysis was performed at day 7 of culture. **(A)** Representative FACS plots showing CD25 expression and CellTrace Violet dilution by ILC3. **(B)** Percentage (left) and MFI (right) of CD25 expressing ILC3. **(C)** Proliferation of ILC3 as measured by CellTrace Violet dilution using flow cytometry. (**D)** Absolute numbers of ILC3 as determined using CountBright beads and flow cytometry analysis. (**E)** Percentage (left) and MFI (right) of CD25 expressing ILC2. (**F)** Proliferation of ILC2 as measured by CellTrace Violet dilution using flow cytometry. (**G)** Absolute numbers of ILC2 as determined using CountBright beads and flow cytometry analysis. Autologous T cells, ILCs and monocytes were obtained from n = 8 donors. Data were pooled from two separate experiments. Statistical significance was determined by means of Mann-Whitney U tests. Bars represent mean ± SEM. *$p \leq 0.05$. **$p \leq 0.01$. ***$p \leq 0.001$.

5.3 Discussion

Here, we describe a novel reciprocal relationship, mediated at least partially by inflammatory cytokines, between human ILCs and monocytes that modulates their activation. We have shown here for the first time that human ILCs act directly on monocytes to enhance their antigen-presentation and co-stimulation capacity. Following short-term co-culture for two days, ILCs alone and in synergy with LPS promoted monocyte proliferation, increased expression of HLA-DR and co-stimulatory ligands CD80, CD86, OX40L and CD70. Co-culture with ILCs, and in particular ILC2, furthermore induced robust downregulation of CD14 expression in the monocytes. Downregulation of CD14 in conjunction with upregulation of MHC class II molecules and co-stimulatory ligands are suggestive of monocyte differentiation into immature DCs, indicating that ILCs may promote a maturation of monocytes into monocyte-derived DCs (403,404). In contrast, stimulation of monocytes with LPS resulted in upregulation of CD14 expression compared to the baseline, in line with previous reports (396,397). This LPS-induced upregulation of CD14 was observed also in the presence of ILCs, perhaps in line with the idea that the ILC3-induced immature DCs become activated through the TLR4 stimulus and further differentiate into mature DCs.

Comparison of monocytes co-cultured with ILC3, ILC2 and ILC1 revealed that the different ILC subsets seem to induce distinct patterns of co-stimulatory ligand expression by monocytes. While ILC3 preferentially induced monocyte proliferation and expression of CD80 and OX40L, ILC2 promoted expression of CD86. ILC1 were generally weaker than ILC3 or ILC2 in inducing upregulation of HLA-DR and co-stimulatory ligand expression in monocytes, but in comparison preferentially induced CD70 expression. The induction of differential co-stimulatory molecule expression by different ILC subsets is interesting, as it has been suggested that the composition of co-stimulatory molecules can influence the quality of subsequent $CD4^+$ T cell responses (405). For example, delivery of CD70-CD27 dependent co-stimulatory signals has been reported to preferentially promote T_H1 differentiation in both human and mouse $CD4^+$ T cells (406-409). Since our data indicate that ILC1 preferentially induced CD70 expression in monocytes, this suggests a potential mechanism through which innate ILC subsets could promote the differentiation of $CD4^+$ T cells into functionally equivalent adaptive T helper subsets, i.e. ILC1 promote T_H1 differentiation, ILC2 promote T_H2 responses etc. In line with this hypothesis, CD86 co-stimulatory signals were reported to be essential for the differentiation of mouse T_H2 but not T_H1 cells *in vitro* and *in vivo* (410,411) and we observed preferential induction of CD86 expression in monocytes by ILC2. Furthermore, we detected highest levels of OX40L expression in monocytes co-cultured with ILC3. OX40 signalling in $CD4^+$ T cells has been shown to enhance IL-17A production and promote T_H17 responses under conditions of aberrant immune activation in mouse models of uveitis and arthritis (412,413) However, OX40L-OX40 signalling can also induce T_H2 and T_H9 differentiation (414-417), indicating that the regulation of T helper differentiation by co-stimulatory ligands is complex and requires further investigation, including examination of potential contributions by co-stimulatory ligand expressing ILCs .

Our results indicate that ILC-induced upregulation of monocyte HLA-DR and co-stimulatory ligand expression seems to be at least partially dependent on the soluble mediators TNFα and GM-CSF as revealed by experiments in which these cytokines were neutralized using blocking antibodies. Interestingly, blockade of TNFα and GM-CSF had different effects on monocyte CD80 and OX40L expression depending on whether LPS was present in the system or not. These differences could be due to a concentration-dependent effect of TNFα and GM-CSF. Perhaps a low concentration of these pro-inflammatory cytokines is representative of the low-grade inflammation found in a homeostatic gut environment in response to commensal antigens. A more tolerogenic monocyte phenotype with lower expression of the co-stimulatory ligands CD80 and OX40L would be desirable in this case. However, following breach of the intestinal barrier by a pathogenic organism as mimicked by LPS-mediated activation of the monocytes, increased levels of TNFα, GM-CSF and other pro-inflammatory cytokines would signal the need for an effective antigen-specific immune response, in which increased expression of co-stimulatory molecules would be desirable for the effective activation and sustenance of $CD4^+$ T cell responses. Alternatively, maturation stage-dependent differences in monocyte responsiveness to TNFα and GM-CSF could explain the differential outcomes of cytokine neutralization under conditions of additional LPS stimulation.

From our experiments it is not clear whether TNFα and GM-CSF in this system are ILC or monocyte-derived. Both ILC2 and ILC3 populations can produce TNFα and GM-CSF (see Chapter 3). However, monocytes, especially after stimulation with LPS, are potent producers of these cytokines as well (418,419). Intracellular cytokine staining and flow cytometry analysis would be required to examine which population is the main producer in the different co-culture conditions. Furthermore, since monocyte activation was only partially abrogated following neutralization of TNFα and GM-CSF in this co-culture system, it would be interesting to examine whether additional ILC-derived cytokines (IL-17A, IFNγ, IL-5, IL-13) as well as cell contact-dependent interactions play a role in driving monocyte activation in this context.

Our experiments showed that soluble factors secreted by ILC3 and ILC1 potently increased the capacity of monocyte-derived macrophages to kill the pathogenic bacterium *S. typhimurium*. In contrast, incubation with ILC2 supernatants had only a mild effect comparable to B cell supernatants. Classical macrophage activation in the context of bacterial infection is thought to depend on two signals, namely the sensing of microbial PAMPs through TLRs (signal 1) in the presence of TNFα and IFNγ (signal 2) (398,420,421). IFNγ is a potent activator of macrophages and has been shown to directly regulate macrophage bactericidal activity as well as antigen-presentation function (420). IFNγ acts synergistically with autocrine or paracrine TNFα in the activation of macrophages. TNFα-induced NFκB activation is enhanced in the presence of IFNγ via a STAT1-dependent mechanism (422). In turn, TNFα signalling leads to upregulation of IFNγR and enhances IFNγ-induced effects on antigen-presentation machinery (423). All three ILC subsets can produce TNFα and thus may contribute to TNFα-mediated macrophage activation. IFNγ has been suggested to be produced mainly by NK cells, NKT cells and potentially macrophages themselves early during infection, and by T_H1 cells during the adaptive phase of an immune response (420,421,424-426). Our own and published data show that human ILC3 and ILC1 are producers of IFNγ, identifying them as another potential source of early IFNγ (see Chapter 3) (185,189,196). In contrast, ILC2 do not express IFNγ (see Chapter 3) (16). This difference in IFNγ expression may contribute to the differential capacity of ILC3/ILC1 and ILC2 to enhance macrophage-mediated bacterial killing. Neutralization experiments could provide more conclusive evidence for a role of these cytokines in mediating the observed ILC-driven increase in macrophage bactericidal activity.

In addition to ILC-dependent effects on monocyte activation, our data suggest a reciprocal regulation of ILC activation by monocytes. We found that co-culture with monocytes in the presence of LPS induced ILCs to upregulate expression of the co-stimulatory molecules CD80, CD86 and OX40L. Furthermore, ILCs increased their expression of CD25 and showed increased levels of proliferation. Future experiments would examine in detail the role of IL-2 signalling in driving ILC proliferation in this system, in particular whether ILCs co-cultured with LPS-activated monocytes are rendered more sensitive to IL-2 (e.g. express increased levels of phosphorylated STAT5) and whether addition of anti-CD25 blocking antibodies could abrogate the induction of ILC proliferation. Blockade of TNFα and IL-6R signalling in particular significantly reduced co-stimulatory ligand expression, proliferation and CD25 expression by ILC3 and ILC2. Repeat experiments would also test the effects of combined blockade of the previously assessed pro-inflammatory cytokines as well as that of IL-23, a key activator of ILC3. Another interesting candidate here is the TNFSF member TL1A, which, in conjunction with IL-1β and IL-23, has been shown to induce upregulation of CD25 in human RORγt$^+$ ILC3 differentiated *in vitro* from HSCs (427).

Furthermore, our data indicated that co-culture with monocytes reduced the expression of CD117 by ILC3, which was further reduced following addition of LPS. High CD117 expression is a hallmark of ILC3 that differentiates them from both ILC2, which show heterogeneous expression of CD117, and ILC1, which do not express CD117. Similar to findings in the murine system, considerable plasticity exists between human ILC3 and ILC1 populations. *In vitro* culture of CD117^{high} NKp44$^+$ RORγt$^+$ foetal gut ILC3 with IL-2 and IL-12 leads to acquisition of an ILC1-like phenotype, including downregulation of CD117, NKp44 and RORγt expression and acquisition of T-bet and IFNγ expression. CD117^{low}NKp44^{-} ILC1 accumulate in the intestinal lamina propria of CD patients and can drive intestinal inflammation in a DSS colitis model in humanized mice through production of IFNγ (189). However, it is unclear whether these pathogenic ILC1 are *bona fide* ILC1 or 'ex-ILC3' that have downregulated expression of CD117, NKp44 and RORγt. Our data suggest that (LPS-activated) monocytes may drive ILC3 to adopt a more ILC1-like phenotype. However, this would need to be tested functionally by examining transcription factor and cytokine profiles in CD117^{low} ILC3 that have been co-cultured with monocytes.

Testing the functional effects of the bi-directional activation loop between ILCs and monocytes, we observed a significant increase in memory CD4^{+} T cell proliferation and absolute counts when CD4^{+} T cell were activated with monocytes and soluble anti-CD3 antibody in the presence of ILC3 or ILC2. The CD4^{+} T cells furthermore displayed a more highly activated phenotype based on expression of cell surface activation markers OX40 and ICOS. When ILCs were separated from monocytes and CD4^{+} T cells using a transwell insert, CD4^{+} T cell activation and cell counts were reduced, but did not return fully to the levels observed when CD4^{+} T cells were stimulated with monocytes alone in the absence of ILCs, indicating a role for both soluble and cell contact-dependent mediators. We have shown that ILC-mediated activation of monocytes is at least partially dependent on the soluble mediators TNFα and GM-CSF, a mechanism that would remain intact in a transwell system and could potentially account for the remnant augmentation of CD4^{+} T cell activation. Pre-activation of monocytes with ILC-derived supernatants in absence or presence of blocking antibodies followed by assessment of their capacity to drive enhanced CD4^{+} T cell activation would provide evidence regarding a functional role for cytokine-mediated activation of monocytes by ILCs in this system.

While direct cell-cell contact is clearly important in driving enhanced $CD4^+$ T cell activation based on data from the transwell experiments, it is unclear whether this needs to occur between ILC3 and monocytes or ILC3 and $CD4^+$ T cells. ILC3 express the co-stimulatory molecules CD80, CD86, OX40L and CD70, which furthermore may be subject to TNFα- and IL-6-dependent upregulation following co-culture with activated monocytes. The reduced $CD4^+$ T cell activation observed in the transwell system may result from an abrogation of the co-stimulation provided to $CD4^+$ T cells directly by ILCs. Indeed, provision of co-stimulatory OX40L and CD30L signals by $ROR\gamma t^+$ LTi-like ILC3 cells has been suggested to be important in supporting memory $CD4^+$ T cell differentiation and survival in the mouse spleen (356-358). However, a direct functional role for this in enhancing $CD4^+$ T cell activation remains to be proven. Co-culture experiments in which co-stimulatory molecule expression is knocked down using small interfering RNA (siRNA) in ILCs but not monocytes would help to elucidate whether direct co-stimulatory signals provided to $CD4^+$ T cells by ILCs play a role in our system.

Alternatively, abrogation of cell contact-dependent activatory interactions between ILC3 and monocytes may also account for the reduced $CD4^+$ T cell activation in the transwell system. TL1A is a member of the TNFSF expressed in membrane-bound or soluble form by activated cells of the myeloid lineage (428). Single-nucleotide polymorphisms in the TL1A gene have been associated with an increased risk for IBD (429). Recent publications suggest that DR3 is highly expressed by mouse and human ILC2 and ILC3, and stimulation with TL1A enhances IL-23- and IL-1β-induced production of IL-22 and GM-CSF by human and mouse ILC3 (110,337,427). It is conceivable that in the transwell system abrogation of signalling between membrane-bound TL1A on monocytes and death receptor 3 (DR3) on ILC3 could lead to reduced GM-CSF production by ILC3, resulting in reduced monocyte activation and ultimately in reduced CD4$^+$ activation.

Another open question relates to the qualitative functional implications of the described ILC-mediated effects on CD4$^+$ T cell activation, in particular whether ILCs can influence the functional polarisation of T helper responses, either via direct effects on CD4$^+$ T cells or indirect effects on myeloid cells. In the mouse, ILC2-derived IL-13 can induce upregulation of the co-stimulatory molecule CD40 on lung CD11c$^+$ DCs. Following CCR7-dependent migration to the mediastinal lymph nodes, these CD40^{high} DCs induce the clonal expansion and differentiation of antigen-specific T$_H$2 cells (144). IFNγ produced by cNK cells has been reported to promote T$_H$1 differentiation and inhibit the development of T$_H$2 and T$_H$17 responses following DC-mediated priming of CD4+ T cells in secondary lymphoid tissues (430,431). Similarly, early production of IL-17A by γδ$^+$ T cells has been reported to amplify T$_H$17 responses in several murine models (432-434). Furthermore, our own data indicate that the different ILC subsets drive different patterns of co-stimulatory ligand expression on monocytes, although the potential functional effects of this on the polarization of CD4$^+$ T cell responses remain to be tested. Further work would aim to elucidate the role of ILC subset specific cytokines (IL-17A, IL22, IL-5, IL-13, IFNγ) and surface markers in influencing the quality of CD4$^+$ T helper responses either directly or indirectly via myeloid cells.

Finally, our observation of increased CD25 expression and proliferation by ILCs co-cultured with LPS-activated monocytes or anti-CD3 activated CD4$^+$ T cells may represent an interesting mechanism through which CD4$^+$ T cells can shape the size of ILC responses. Activated CD4$^+$ T cells may provide a local source of IL-2, which could drive CD25$^+$ ILCs to proliferate. Our findings are in line with several recent publications that have highlighted a role for CD4$^+$ T cell-derived IL-2 in the regulation of ILC function in the mouse. Murine ILC2 have been shown to proliferate and secrete Type 2 cytokines following *in vitro* co-culture with activated CD4$^+$ T cells (145). *In* vivo IL-9 expression by murine ILC2 was reported to depend on IL-2 signals from adaptive immune cells in a model of papain-induced airway inflammation (14). Furthermore, in a mouse model of *N. brasiliensis* infection ILC2 and CD4$^+$ T cells were shown to engage in an MHC class II-dependent crosstalk, whereby MHC class II-expressing ILC2 activated antigen-specific CD4$^+$ T cells to proliferate and upregulate expression of IL-5, IL-13 and IL-2. CD4$^+$ T cell-derived IL-2 then fed back on ILC2 to induce proliferation and Type 2 cytokine induction. This reciprocal amplification loop is required for successful parasite expulsion, since both ILC2-deficient mice and *Rag2*$^{-/-}$ mice lacking T cells show reduced worm clearance, which can be rescued by adoptive transfer of MHC class II-sufficient ILC2 or administration of IL-2, respectively (146).

As summarized in Figure 5.17, our data show that human ILCs and monocytes engage in a bi-directional activation loop resulting in proliferation and increased expression of co-stimulatory ligands by both ILCs and monocytes, enhanced bactericidal activity in monocyte-derived macrophages and increased sensitivity to IL-2 derived signals in ILCs. Furthermore, we highlight a role for ILC3 in the augmentation of memory CD4$^+$ T cell activation by monocytes and soluble anti-CD3 *in vitro*. Several open questions remain regarding mechanisms of interactions between ILCs and monocytes or ILCs and CD4$^+$ T cells, in particular with respect to the role of different ILC subsets in driving CD4$^+$ T cell polarization. We propose that this amplification loop between ILCs and monocytes occurs early during an immune response and may contribute to the potentiation of CD4$^+$ T cell responses. In turn, activated CD4$^+$ T cells can feed back into this activation loop by driving further ILC activation through IL-2-dependent signals. ILC1, ILC2 and ILC3 populations have been shown to reside in close proximity to CD11c$^+$ myeloid cells and CD4$^+$ T cells in the intestinal lamina propria and mesenteric lymph nodes, indicating that interactions between all three of cell types are indeed likely to occur *in vivo* (113,357,371). Under conditions of aberrant immune activation as is the case in IBD, such activatory interactions between ILCs and monocytes may contribute to the potentiation and perhaps polarization of pathogenic CD4$^+$ T cell responses, which could further perpetuate this activation loop through IL-2-mediated effects on ILCs.

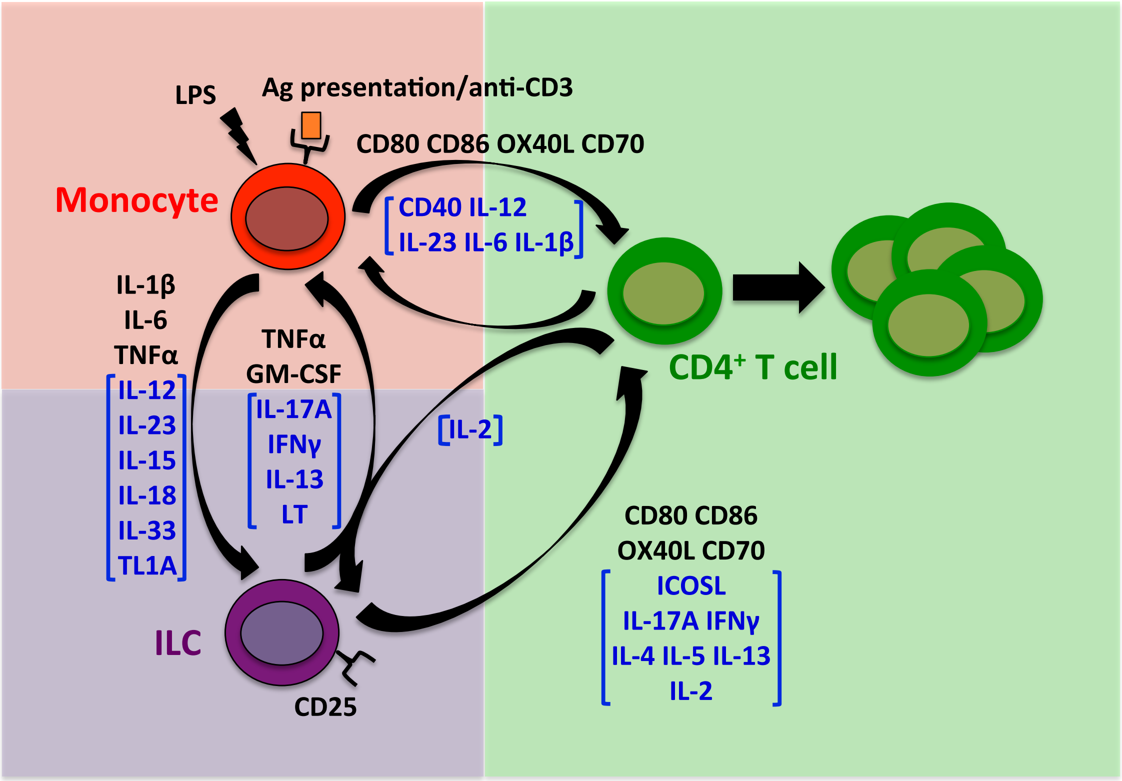

Figure 17: Monocyte and soluble anti-CD3-mediated expansion of CD4+ memory T cells is enhanced in the presence of ILCs. Bidirectional interactions between ILCs and monocytes and also between ILCs and CD4$^+$ T cells may contribute to this effect. Pathways of interest for future investigation are highlighted in blue.

Chapter 6: Conclusion

6.1 Summary and discussion

Despite a wealth of knowledge regarding ILC biology obtained from the study of murine models, data on human ILC biology remains more limited, particularly with respect to functional pathways and mechanisms. This thesis aimed to investigate potential mechanisms by which human ILCs can contribute to intestinal inflammation in IBD.

Confirming previous data from our laboratory (185), we detected an increased frequency of Lin$^-$CD127$^+$ ILCs in the inflamed intestinal lamina propria of IBD patients compared to uninflamed controls. We extended these findings by describing possible mechanisms of ILC accumulation in the inflamed intestine. Our data indicate that the frequency of ILCs in the blood of IBD patients was decreased compared to healthy controls, suggesting that recruitment of ILCs from blood to the intestinal lamina propria may contribute to their accumulation. ILCs expressed high levels of CCR6 and it is conceivable that the high levels of the CCR6 ligand CCL20 produced by activated epithelial and stromal cells in IBD lesions may mediate their recruitment (367-369).

We found for the first time that intestinal ILCs in IBD patients showed greater expression of Ki67, suggesting that increased *in situ* proliferation in an inflammatory environment may contribute to their accumulation. ILCs express high levels of CD25 and stimulation of whole LPMCs with IL-2 induced potent ILC proliferation *in vitro*, indicating that IL-2 may drive the increased ILC proliferation observed in the inflamed intestinal lamina propria. Likely local sources of IL-2 include ILCs themselves and activated CD4$^+$ T cells (359-361). In support of the latter, we showed that co-culture of ILCs with polyclonally activated memory CD4$^+$ T cells stimulates ILC proliferation. In addition, we found that co-culture of ILCs with LPS-activated monocytes also drives ILC proliferation. This was abrogated partially through blockade of TNFα, IL-1β and IL-6 signalling, indicating that these pro-inflammatory cytokines may also contribute to the proliferation and accumulation of ILCs in the inflamed intestinal lamina propria. Thus, our results suggest that the increased frequency of ILCs observed in the intestinal lamina propria of IBD patients may result from increased recruitment of blood ILCs to the intestine as well as from increased *in situ* proliferation of intestinal ILCs.

Functionally, ILCs in the peripheral blood of IBD patients were characterised by increased production of IL-17A, IFNγ, GM-CSF, TNFα, IL-2 and IL-13. ILC populations producing IL-17A and IFNγ selectively accumulated in the intestinal lamina propria of IBD patients. This suggests that pro-inflammatory cytokine production by ILCs may contribute to inflammation in IBD. Furthermore, our data indicate that ILCs may contribute to IBD pathogenesis through the ability to activate adhesion molecule expression by intestinal stromal cells. *In vitro* expanded ILC3 and ILC2, but not ILC1, induced upregulation of ICAM-1 expression on colonic stromal cells, equivalent to the levels induced by treatment with recombinant lymphotoxin. In the context of IBD, increased stromal cell adhesion molecule expression may engender the formation of TLOs in the inflamed colon, which may contribute to the chronicity of inflammatory processes by facilitating the efficient induction of pathogenic adaptive immune responses.

Using immunofluorescence, we examined the localisation characteristics of CD3^{-} RORγ^{+} ILCs in colonic and ileal tissue sections obtained from uninflamed controls and IBD patients. ILCs were not distributed homogeneously throughout the tissue, but seemed to occur focally, in cluster-like aggregates that co-localized with T cell aggregates. The spatial association of ILCs and T cells in human colonic tissue raises questions about their potential interactions that may have relevance for IBD pathophysiology. Early studies on LTi cells in mice revealed that the majority of these cells in the foetal and adult intestine express MHC class II (56,64). On the basis of these observations, we investigated the capacity of human ILCs to present antigen to CD4^{+} T cells.

Human ILC populations expressed HLA-DR and co-stimulatory ligands, although at lower levels compared to monocytes, and showed a comparatively reduced capacity to take up and process the model antigen DQ-OVA. Furthermore, in contrast to monocytes, ILCs pulsed with whole protein antigen failed to activate antigen-specific CD4^{+} memory T cells in an *in vitro* T cell stimulation assay. While there are open questions regarding the differential capacity of ILCs to present protein versus peptide antigens, based on our experiments we can conclude that, in spite of their expression of HLA-DR and co-stimulatory ligands, *in vitro* expanded human ILCs do not act as professional APCs.

In light of our finding that HLA-DR and co-stimulatory ligand expression by ILCs may be subject to modulation by pro-inflammatory cytokines and LPS-activated monocytes, future work would examine whether the *in vitro* antigen-presentation capacity of human ILCs may be altered by their prior activation through these stimuli. Perhaps in an inflammatory microenvironment, as is found in the inflamed intestinal lamina propria of IBD patients, ILCs could successfully promote the expansion of pathogenic CD4$^+$ T cell responses through MHC class II-mediated presentation of commensal antigens. Yet, in an inflammatory context with concomitant accumulation of professional APCs such as monocytes and DCs in the intestinal lamina propria (435-438), it is an open question whether ILC-mediated direct antigen presentation to CD4$^+$ T cells would significantly contribute to the induction of pathogenic T cell responses. A report by Oliphant et al. has shown that in a mouse model of *N. brasiliensis* infection the deletion specifically of ILC2 leads to impaired T_H2 responses, associated with higher worm burden at day 5 post-infection and delayed worm clearance. Effective worm clearance can be re-established by transfer of MHC class II sufficient but not MHC class II deficient ILC2 (146). While these findings may indeed point towards a contribution of direct ILC2-mediated antigen presentation to the induction of CD4$^+$ T cell responses, there may be another possibility.

The study by Oliphant et al. has highlighted a role for CD4$^+$ T cell-derived IL-2 in driving the optimal activation of ILC2, including their proliferation and secretion of Type 2 cytokines (146). Analysis of the serum half-life of IL-2 following *in vivo* administration has shown that it is an extremely short-lived cytokine, with a half-life of approximately 3.7 mins (439). Therefore, close proximity between effector CD4$^+$ T cells and ILC2 may be beneficial to ensure effective IL-2 signalling between these cells. Perhaps MHC class II-TCR interactions function as a tether to bring into close contact activated antigen-specific CD4$^+$ T cells and ILC2. Following disruption of this interaction through ILC2-specific deletion of MHC class II, ILC2 proliferate less and show reduced secretion of IL-13. In turn, ILC2-derived IL-13 has been shown to drive differentiation of T_H2 responses through indirect effects of DCs (144). Thus, according to this model, the function of MHC class II expression by ILC2 would not lie in the primary activation of antigen-specific naïve CD4$^+$ T cells, i.e. a function that is fulfilled effectively by professional APCs. Instead, MHC class II expression by ILC2 would promote the close spatial interactions between ILC2 and IL-2-producing activated effector CD4$^+$ T cells that are in turn required for optimal activation of ILC2 and the subsequent potentiation of T$_H$2 responses via IL-13-conditioned DCs. It is conceivable that intestinal ILC3 or ILC1 could contribute to the augmentation of effector CD4$^+$ T cell responses in a similar manner in the pathogenic context of IBD.

Hepworth et al. have shown in the mouse that under steady-state conditions MHC class II-dependent interactions between intestinal ILC3 and effector CD4$^+$ T cells can also inhibit CD4$^+$ T cell responses, partly mediated through withdrawal of local IL-2 from CD4$^+$ T cells by CD25$^+$ ILC3 (164,165). However, in IBD an increase in the availability of IL-2 (344,359-361) due to widespread immune activation could mean that IL-2 consumption by ILC3 may no longer be a limiting factor for effector CD4$^+$ T cells. In this context, activated T cell-derived IL-2 in conjunction with other pro-inflammatory cytokines (IL-1β, IL-6, IL-12, IL-23) could further drive inflammatory ILC3 activation, in a manner similar to CD4$^+$ T cell-mediated ILC2 activation in infection-induced inflammation. ILC3-derived effector cytokines (IL-17A, IFNγ, TNFα, GM-CSF) could then feed back to potentiate pathogenic effector CD4$^+$ T cell responses, either directly or indirectly via APCs.

In the mouse, intestinal OX40L/CD30L-expressing LTi-like cells have also been proposed to deliver a secondary co-stimulatory impulse to CD4$^+$ T cells following their priming by DCs, which may play a role in the optimal activation of effector CD4$^+$ T cell responses and their differentiation into memory CD4$^+$ T cells (357,382,385).

The increased co-stimulatory ligand expression by ILCs we have observed following their stimulation with pro-inflammatory cytokines and LPS-activated monocytes suggests the possibility that ILCs may also potentiate pathogenic CD4$^+$ T cell activation through this additional mechanism in IBD.

Thus, we conclude that ILCs do not act as professional APCs and *in vivo* most likely do not drive primary CD4$^+$ T cell activation through direct MHC class II-mediated antigen presentation. However, the above discussion highlights that MHCII-TCR-dependent interactions between ILCs and activated effector CD4$^+$ T cells may nonetheless regulate both CD4$^+$ T cell and ILC function. We hypothesize that these interactions may allow close co-localization of both cell types, leading to reciprocal activation of both ILCs and CD4$^+$ T cells. In an inflammatory context, this activation loop may contribute to the augmentation of pathogenic immune effector responses.

While ILCs may not effectively function as professional APCs, we wanted to examine whether ILCs could modulate *bona fide* professional APCs, whose key functions lie in the uptake and processing of antigen and the subsequent activation of antigen-specific T cell responses. ILCs induced increased expression of HLA-DR and co-stimulatory ligands in monocytes in co-cultures *in vitro*. This was at least partially dependent on the pro-inflammatory cytokines TNFα, IL-1β, IL-6 and GM-CSF as indicated by blocking experiments. Furthermore, soluble factors secreted by ILC3 and ILC1, but not by ILC2, enhanced the ability of monocyte-derived macrophages to kill engulfed bacteria. In reverse, monocytes, and in particular LPS-stimulated monocytes, promoted proliferation and increased co-stimulatory ligand expression by ILCs through a mechanism partially dependent on the pro-inflammatory cytokines TNFα, IL-1β and IL-6.

These novel findings indicate that human ILCs and monocytes may engage in a bidirectional activation loop that enhances innate bactericidal activity and drives increased expression of functional markers intimately linked to $CD4^+$ T cell activation. We speculated that this innate activation loop could in turn potentiate the activation of $CD4^+$ T cells. When memory $CD4^+$ T cells were polyclonally activated *in vitro* using monocytes and soluble anti-CD3 antibody, the additional presence of ILCs in the co-cultures augmented $CD4^+$ T cell proliferation, expression of surface activation markers and higher absolute numbers of $CD4^+$ T cells could be recovered. This effect was partially abrogated when ILCs were separated from monocytes and $CD4^+$ T cells through a transwell insert, indicating that both direct cell contact-dependent interactions between the different cell types and soluble factors may play a role in driving the observed augmentation of $CD4^+$ T cell activation. However, whether direct interactions are required mainly between monocytes and ILCs or $CD4^+$ T cells and ILCs remains to be elucidated.

Thus, our data suggest that activatory interactions between ILCs and professional APCs may drive enhanced activation of $CD4^+$ T cell responses. In the context of a protective immune response, this would mean that ILCs may contribute to the optimal activation of myeloid cell function (bacterial killing, antigen presentation function) and induction of $CD4^+$ T cell responses. However, we speculate that through increased net provision of co-stimulatory signals this innate activation loop could also contribute to the dysregulation of pathogenic $CD4^+$ T cell responses in the chronic inflammatory context of IBD. Future work would aim to characterise more closely the functional pathways mediating the reciprocal activation loop between ILCs and monocytes and to examine the potential qualitative effects of these ILC-monocyte interactions on $CD4^+$ T cell responses. Halim et al. have shown that ILC2-

derived IL-13 promotes the induction of DCs that preferentially polarize CD4$^+$ T cells towards a T$_H$2 phenotype. It would be interesting to investigate whether ILC3 and ILC1 may have similar effects on the induction of T$_H$17 and T$_H$1 responses, respectively. Furthermore, we would need to test the validity of our observations in a more physiologically relevant, antigen-specific setting of CD4$^+$ T cell activation, for example using our system of *Salmonella*-specific CD4$^+$ T cells.

Our findings place human ILC function in the context of other immune effector cells, namely CD4$^+$ T cells and professional APCs, and provide novel insights into how human ILCs as a rare immune cell subset could functionally contribute to the pathogenesis of IBD. ILCs lack expression of antigen-specific T and B cell receptors and are not reliant on clonal expansion following their activation. We hypothesize that ILCs are therefore equipped to act early in a developing immune response and through their production of cytokines and interactions with professional APCs and CD4$^+$ T cells could contribute to the shaping of later, quantitatively much larger adaptive responses. Accordingly, rare ILCs could have immunological effects that go beyond what would be expected on the basis of their population size alone. In the context of IBD, aberrant reciprocal activation of ILCs and professional APCs (caused for example by dysregulated CD25, IL-23R, STAT3 or CCR6 signalling in ILCs or NOD2 or ATG16L1 signalling in APCs as a result of genetic risk variants (234)), could contribute to disease flare-ups and the subsequent potentiation and shaping of pathogenic CD4$^+$ T cell responses. Activated CD4$^+$ T cells may then feed into this amplification loop through production of IL-2 (additional risk variants in *IL2* have been identified (234)), resulting in the further activation of ILCs.

6.2 Functional analysis of human ILCs

The functional investigation of *ex vivo* human ILCs *in vitro* is challenging, as ILCs are an exceedingly rare subset of immune effector cells and the availability of enough tissue for the isolation of sufficient numbers of ILCs is limited. Circumventing these issues, we have demonstrated that ILCs purified from human peripheral blood can be expanded *in vitro* using feeder cells of mixed, irradiated PBMCs from three allogeneic donors and exogenous IL-2 and IL-7. The ILC populations expanded using this method maintained stable expression of subset-specific surface markers and functional markers such as cytokines and transcription factors even after 6 weeks of culture. The robust expansion of ILCs in this manner allowed us to obtain high enough cell numbers to perform *in vitro* analyses of human ILC function as outlined in Chapters 3-5.

However, more physiologically relevant experimental systems would be desirable in order to more closely approximate the *in vivo* functions of human ILCs and their interactions with other immune cells. Exciting future possibilities for this are emerging. Elaborate three-dimensional (3D) organotypic *in vitro* cultures replicating the tissue-specific morphology and function of the parental tissue from which they are derived, can be successfully established from a variety of tissues, including the gut. There are a variety of methods to establish 3D cultures, including spontaneous aggregation of cells in suspension cultures, implantation of cells into matrix scaffolds, stacking of confluent cell sheets. Primary cells, cultured cells or established cell lines can be used. In addition, induction of a 3D gut model from induced pluripotent stem cells has been described (440,441). 3D cultures can range from inclusion of a single cell type to multiple cell types, mimicking the complexity of *in vivo* tissue environments. This allows for the selective functional analysis and manipulation of a cell type of interest and its interactions with other cells types in different environmental conditions.

An interesting method for the establishment of gut-specific 3D cultures that closely resemble intestinal tissue structures has been described. Intestinal Caco2 epithelial cells were layered onto a matrix of collagen and matrigel-embedded CCD18co intestinal stromal cells. The resulting 3D culture was characterised by a columnar, polarized epithelial layer and an underlying connective tissue layer enriched in stroma-derived extracellular matrix (ECM) components such as fibronectin (442). Inclusion of ILCs and additional cells such as monocytes and CD4$^+$ T cells in this model would allow an examination of human ILC function in the context of other immune cells (eg. monocytes and CD4$^+$ T cells), stromal cells and intestinal epithelial cells that more closely resembles an *in vivo* intestinal environment. Stimulation of these cultures with microbial-derived factors (e.g. TLR agonists) or colonization with specific commensal or pathogenic bacteria could be used to model influences by the intestinal commensal flora and/or invading pathogens. Furthermore, generation of gut 3D cultures using primary cells derived from IBD patients compared to uninflamed controls could provide better insight into how ILCs integrate with other intestinal immune cells or epithelial cells during chronic intestinal inflammation.

In addition to more complex 3D tissue culture models, mice that harbour a human haemato-lymphoid system (HHLS mice) could provide an opportunity to investigate human ILC function in a true *in vivo* context. HHLS mice with a full complement of human immune cells can be generated through xenotransplantation of CD34$^+$ human HSCs into irradiated NOD Scid Gamma (NSG) mice (*NOD.Cg-Prkdc*^{scid} *Il2rg*^{tm1Wjl}*/SzJ*). NSG mice are severely immunodeficient, lacking T cells, B cells and NK cells, and as a result do not reject human HSC grafts. Furthermore, a polymorphism in the *Sirpa* gene associated with the NOD background is thought to aid in graft acceptance by promoting phagocytic tolerance (443).

A first use of HHLS mice in the investigation of human ILCs has been reported. Bernink et al. reconstituted NSG mice with human foetal liver-derived $CD34^{+}CD38^{-}$ HSCs. Two months after injection of HSCs, ILC1, ILC2 and ILC3 subsets could be detected in the intestinal lamina propria at frequencies equivalent to those observed in the uninflamed human gut (189). These findings demonstrate that ILCs reconstitute well in HHLS mice, supporting the future use of these mice in the investigation of human ILCs *in vivo*. Induction of DSS colitis in HHLS mice triggered an expansion of intestinal human $CD45^{+}$ cells and a selective expansion of IFNγ-producing ILC1, but not ILC3 or ILC2 (189). These observations are very similar to the finding that intestinal ILC1 frequencies are selectively increased in human IBD and indicate that ILC1 can accumulate in the intestinal lamina propria in direct response to the intestinal barrier breach and acute inflammation induced by DSS treatment. This suggests that ILCs are recruited early during intestinal inflammation and may contribute to the shaping of later immune responses, rather than accumulating passively in response to chronic inflammatory signals. In the context of our above-described *in vitro* findings, it would be interesting to examine in this model whether ILCs can indeed augment pathogenic $CD4^{+}$ T cell activation *in vivo*. A comparative assessment of the activation state and quality of $CD4^{+}$ T helper responses following induction of DSS colitis in HHLS mice sufficient or deficient of ILCs could provide insight into whether and how human ILCs may impact $CD4^{+}$ T cell responses in IBD.

The functional investigation of human cells in HHLS mice is still difficult since many signals involved in the activation of immune responses have a non-haematopoietic origin (e.g. epithelial cells or stromal cells) and are therefore mouse- rather than human-derived, which may lead to impaired signalling in human cells. However, the development of NSG mice with human gene knock-ins to replace mouse genes may circumvent these issues. For example, NSG mice with knock-ins of human *IL3*, *CSF1*, *CFS2* and *TPO* have recently been generated (444).

6.3 Therapeutic targeting of ILCs in IBD

Several recent studies have reported that ILC frequency or activation can be modulated by treatments currently in use for IBD patients (187,206). A study in psoriasis patients has shown that treatment with adalimumab, an anti-TNFα monoclonal antibody that is also used to treat CD and UC patients, results in amelioration of inflammation associated with a reduction in the frequency of an unusual pro-inflammatory ILC3 population in the blood (206). Furthermore, cyclosporin A, which can be used to manage severe forms of UC unresponsive to other treatments, was found to suppress IL-22 and TNFα production by ILC3 *in vitro* following their activation using an agonistic anti-NKp44 antibody (187). By extension, these observations suggest that broadly acting immunosuppressants and biologics that are currently used in IBD therapy may likely modulate human ILC function in IBD patients *in vivo*. However, as discussed in Chapter 1, these drugs are associated with a range of adverse side effects. The therapeutic goal lies in the development of drugs that more selectively inhibit the pathogenic immune pathways active in IBD patients without inducing broad immunosuppression and impairing host-protective immune responses to infectious agents or tumour cells.

Several of the pathway-specific monoclonal antibodies and small molecule inhibitors currently in development for CD or UC will likely impact the function of ILCs. The roles of IL-23, IL-6 and IL-1β in the recruitment and activation of disease-driving, IL-17A- and IFNγ-producing ILC populations have been highlighted in several mouse models of colitis (198,288,290,331,332). Similarly, these cytokines can induce pro-inflammatory cytokine production by human ILCs (185,196,198). In addition, IL-23, in conjunction with IL-12, regulates the plasticity of human ILC3 populations, with IL-23 preferentially promoting IL-17A and IL-22 production and IL-12 promoting

IFNγ production (189). These findings suggest that intestinal ILC accumulation and function in IBD patients would likely be modulated by monoclonal antibodies inhibiting IL-23p19, IL-12p40 and IL-6(R) that are currently being trialled for use in IBD or, in the case of IL-1β antagonists, have shown effectiveness in other chronic inflammatory diseases (445-453). Furthermore, monoclonal antibodies that neutralize pro-inflammatory effector cytokines produced by ILCs, including IL-17A, IFNγ and IL-13, are in clinical development for IBD (330,454-456).

In addition, inhibitors of JAK signalling have been shown to inhibit cytokine production by human ILCs *in vitro* and it is conceivable that ILC activation may be modulated through STAT inhibitors since IL-23 and IL-7 have been shown to induce STAT3 and STAT5 activation, respectively, in ILCs (187,219). Thus, the therapeutic targeting of intracellular signalling pathways in IBD patients through JAK/STAT inhibitors may also affect ILC activation (457,458).

While these drugs may in part inhibit pro-inflammatory functions of ILCs, they are not specific to ILCs and will also simultaneously target other immune effector populations involved in IBD pathogenesis. For example, neutralization of IL-23p19 will affect IL-17-producing T cell populations, including T_H17 cells and γδ T cells, while inhibition of IL-12p40 will also inhibit T_H1 activation (446). The simultaneous inhibition of ILC and T cell-mediated effector pathways may indeed be therapeutically beneficial in order to eliminate both the innate and adaptive arms of particular pathogenic immune pathways. However, there may also be advantages associated with an independent targeting of ILCs or $CD4^+$ T cells: murine studies in which ILCs are selectively depleted in the presence of an otherwise fully functional immune system emphasize that these cells do have non-redundant functions during both homeostatic and pathogenic immune responses (115,144,146,164,165). These findings provide a rationale for attempting to target ILCs therapeutically in IBD, but potentially also in other chronic inflammatory diseases.

Problematically, ILCs share a plethora of phenotypic and functional markers with $CD4^+$ T_H cells and to date no ILC-specific markers have been identified, rendering it difficult to target them selectively without simultaneously affecting $CD4^+$ T cell function. We propose that whole-transcriptome single-cell analysis of intestinal and blood ILCs from uninflamed controls and IBD patients in direct comparison to $CD4^+$ T cells could lead to the identification of markers or pathways specifically expressed by ILC but not $CD4^+$ T cells or specifically activated in ILCs but not $CD4^+$ T cells in IBD patients. These ILC-specific markers or pathways could then be targeted through monoclonal antibodies, inhibitors or antibody-drug conjugates to directly modulate the function of or deplete individual ILC subsets. Alternatively, this approach would allow selective inhibition of pathogenic $CD4^+$ T cell responses while keeping intact ILC-dependent innate responses, which may help to reduce the risk of infection with opportunistic pathogens such as *Candida albicans*.

However, in order to effectively target ILC populations in IBD, their roles in host-protective and homeostatic immunity would have to be carefully balanced with their potential pathogenic functions in intestinal inflammation. Murine studies have indicated that under homeostatic conditions ILC3 are the main producers of IL-22 in the intestine. IL-22, through its effects on the intestinal epithelium, is critical in maintaining mucosal homeostasis in the context of the commensal microbiota (58,59,63,96,115,459) and has also been shown to mediate protective effects in several murine models of colitis (459,460). Our own and published data indicate that human ILC3 and ILC1 populations enriched in the intestinal lamina propria of IBD patients preferentially produce IL-17A and IFNγ, but not IL-22 (185,189). Thus, it is conceivable that insufficient levels of intestinal ILC3-derived IL-22 in IBD patients, resulting in impaired epithelial regeneration, innate anti-microbial defence and containment of commensal microbes, may contribute to disease pathogenesis. Selective boosting of IL-22 production by ILC3 in IBD patients may thus have protective effects, although this would have to be weighed against a potential increase in the risk of colorectal cancer (461). Alternatively, selective depletion of pathogenic ILC1 but not IL-22-producing ILC3 using monoclonal antibodies against ILC1-specific markers may be associated with beneficial outcomes in IBD patients. Pathogenic ILC functions could also be selectively targeted through antibody-drug conjugates. For example, delivery of STAT5 inhibitors specifically to ILC1 in IBD patients may lead to their selective reduction as a result of impaired IL-2 and IL-7 signalling without affecting potentially host-protective ILC3.

In addition, a better understanding of ILC3 plasticity will be helpful for the development of therapeutic agents that aim to selectively target pathogenic ILC functions. It is currently unclear whether a RORγt-independent *bona fide* ILC1 population exists in humans and whether the inflammatory IFNγ-producing ILC1 that accumulate in the intestinal lamina propria of CD patients have mainly differentiated from ILC3 in response to IL-12 or rather constitute an independent ILC1 lineage. Therapeutic strategies to inhibit ILC1 function may differ depending on this. Patients with bi-allelic loss-of-function mutations in the *RORC* gene have been described recently (462) and analysis of the ILC repertoire in these patients may help to clarify open questions regarding the pathways underlying ILC1 development.

Our results indicated that ILCs may engage in an early bidirectional interaction with monocytes, which in turn may contribute to the augmentation of CD4$^+$ T cell responses. It is conceivable that selective inhibition of this activatory crosstalk between ILCs and monocytes/CD4$^+$ T cells may result in reduced activation of CD4$^+$ T cells in IBD patients and could potentially decrease the frequency or intensity of disease flare-ups. However, further experiments will be required to gain a deeper understanding of the functional pathways mediating these interactions and whether they may be targets for therapeutic intervention.

Bibliography

1. Artis D. Epithelial-cell recognition of commensal bacteria and maintenance of immune homeostasis in the gut. Nat Rev Immunol. 2008 Jun;8(6):411–20.

2. Brown EM, Sadarangani M, Finlay BB. The role of the immune system in governing host-microbe interactions in the intestine (vol 14, pg 660, 2013). Nature Immunology. 2014 Feb;15(2):205–5.

3. Cadwell K. The Virome in Host Health and Disease. Immunity. Elsevier Inc; 2015 May 19;42(5):805–13.

4. Underhill DM, Iliev ID. The mycobiota: interactions between commensal fungi and the host immune system. Nat Rev Immunol. 2014 May 23;14(6):405–16.

5. Spits H, Cupedo T. Innate Lymphoid Cells: Emerging Insights in Development, Lineage Relationships, and Function. Annu Rev Immunol. Annual Reviews; 2011;30:647–75.

6. Spits H, Artis D, Colonna M, Diefenbach A, Di Santo JP, Eberl G, et al. Innate lymphoid cells - proposal for uniform nomenclature. Nat Rev Immunol. Nature Publishing Group; 2013 Feb 1;13(2):145–9.

7. Diefenbach A, Colonna M, Koyasu S. Development, Differentiation, and Diversity of Innate Lymphoid Cells. Immunity. Elsevier Inc; 2014 Sep 18;41(3):354–65.

8. Sawa S, Cherrier M, Lochner M, Satoh-Takayama N, Fehling HJ, Langa F, et al. Lineage relationship analysis of RORgammat+ innate lymphoid cells. Science. 2010 Oct 29;330(6004):665–9.

9. Klose CSN, Kiss EA, Schwierzeck V, Ebert K, Hoyler T, d'Hargues Y, et al. A T-bet gradient controls the fate and function of CCR6−RORγt+ innate lymphoid cells. Nature. Nature Publishing Group; 2013 Jan 16;:1–7.

10. Chang Y-J, Kim HY, Albacker LA, Baumgarth N, McKenzie ANJ, Smith DE, et al. Innate lymphoid cells mediate influenza-induced airway hyper-reactivity independently of adaptive immunity. Nature Publishing Group. Nature Publishing Group; 2011 May 29;12(7):631–8.

11. Neill DR, Wong SH, Bellosi A, Flynn RJ, Daly M, Langford TKA, et al. Nuocytes represent a new innate effector leukocyte that mediates type-2 immunity. Nature. Nature Publishing Group; 2010 Apr 19;464(7293):1367–70.

12. Price AE, Liang H-E, Sullivan BM, Reinhardt RL, Eisley CJ, Erle DJ, et al. Systemically dispersed innate IL-13-expressing cells in type 2 immunity. Proc Natl Acad Sci USA. 2010 Jun 22;107(25):11489–94.

13. Moro K, Yamada T, Tanabe M, Takeuchi T, Ikawa T, Kawamoto H, et al. Innate production of TH2 cytokines by adipose tissue-associated c-Kit+Sca-1+ lymphoid cells. Nature. Nature Publishing Group; 2010 Jan 18;463(7280):540–4.

14. Wilhelm C, Hirota K, Stieglitz B, Van Snick J, Tolaini M, Lahl K, et al. An IL-9 fate reporter demonstrates the induction of an innate IL-9 response in lung inflammation. Nature Publishing Group. 2011 Oct 9;12(11):1071–7.

15. Barlow JL, Bellosi A, Hardman CS, Drynan LF, Wong SH, Cruickshank JP, et al. Innate IL-13-producing nuocytes arise during allergic lung inflammation and contribute to airways hyperreactivity. J Allergy Clin Immunol. 2012 Jan;129(1):191–8.e1–4.

16. Mjösberg JM, Trifari S, Crellin NK, Peters CP, van Drunen CM, Piet B, et al. Human IL-25- and IL-33-responsive type 2 innate lymphoid cells are defined by expression of CRTH2 and CD161. Nature Immunology. Nature Publishing Group; 2011 Sep 11;:1–9.

17. Mjösberg J, Bernink J, Golebski K, Karrich JJ, Peters CP, Blom B, et al. The Transcription Factor GATA3 Is Essential for the Function of Human Type 2 Innate Lymphoid Cells. Immunity. Elsevier Inc; 2012 Oct 19;37(4):649–59.

18. Klose CSN, Flach M, Moehle L, Rogell L, Hoyler T, Ebert K, et al. Differentiation of Type 1 ILCs from a Common Progenitor to All Helper-like Innate Lymphoid Cell Lineages. Cell. 2014;157(2):340–56.

19. Mebius RE, Miyamoto T, Christensen J, Domen J, Cupedo T, Weissman IL, et al. The Foetal Liver Counterpart of Adult Common Lymphoid Progenitors Gives Rise to All Lymphoid Lineages, CD45+CD4+CD3- Cells, As Well As Macrophages. The Journal of Immunology. 2001 Jun 1;166(11):6593–601.

20. Possot C, Schmutz S, Chea S, Boucontet L, Louise A, Cumano A, et al. Notch signaling is necessary for adult, but not foetal, development of RORγt+ innate lymphoid cells. Nature Immunology. 2011 Sep 11;12(10):949–58.

21. Wong SH, Walker JA, Jolin HE, Drynan LF, Hams E, Camelo A, et al. Transcription factor RORα is critical for nuocyte development. Nature Immunology. 2012 Jan 22;13(3):229–36.

22. Yang Q, Saenz SA, Zlotoff DA, Artis D, Bhandoola A. Cutting Edge: Natural Helper Cells Derive from Lymphoid Progenitors. The Journal of Immunology. 2011 Nov 18;187(11):5505–9.

23. Cherrier M, Sawa S, Eberl G. Notch, Id2, and RORγt sequentially orchestrate the foetal development of lymphoid tissue inducer cells. Journal of Experimental Medicine. 2012 Apr 9;209(4):729–40.

24. Gentek R, Munneke JM, Helbig C, Blom B, Hazenberg MD, Spits H, et al. Modulation of Signal Strength Switches Notch from an Inducer of T Cells to an Inducer of ILC2. Front Immunol. 2013;4:334.

25. Hoyler T, Klose CSN, Souabni A, Turqueti-Neves A, Pfeifer D, Rawlins EL, et al. The Transcription Factor GATA-3 Controls Cell Fate and Maintenance of Type 2 Innate Lymphoid Cells. Immunity. Elsevier Inc; 2012 Oct 19;37(4):634–48.

26. Lee JS, Cella M, McDonald KG, Garlanda C, Kennedy GD, Nukaya M, et al. AHR drives the development of gut ILC22 cells and postnatal lymphoid tissues via pathways dependent on and independent of Notch. Nature Immunology. 2011 Nov 20;13(2):144–51.

27. Mielke LA, Groom JR, Rankin LC, Seillet C, Masson F, Putoczki T, et al. TCF-1 Controls ILC2 and NKp46+ROR t+ Innate Lymphocyte Differentiation and Protection in Intestinal Inflammation. The Journal of Immunology. 2013 Oct 4;191(8):4383–91.

28. Yang Q, Monticelli LA, Saenz SA, Chi AW-S, Sonnenberg GF, Tang J, et al. T Cell Factor 1 Is Required for Group 2 Innate Lymphoid Cell Generation. Immunity. 2013 Apr;38(4):694–704.

29. Seillet C, Rankin LC, Groom JR, Mielke LA, Tellier J, Chopin M, et al. Nfil3 is required for the development of all innate lymphoid cell subsets. Journal of Experimental Medicine. 2014 Aug 25;211(9):1733–40.

30. Geiger TL, Abt MC, Gasteiger G, Firth MA, O'Connor MH, Geary CD, et al. Nfil3 is crucial for development of innate lymphoid cells and host protection against intestinal pathogens. Journal of Experimental Medicine. 2014 Aug 25;211(9):1723–31.

31. Kobayashi T, Steinbach EC, Russo SM, Matsuoka K, Nochi T, Maharshak N, et al. NFIL3-Deficient Mice Develop Microbiota-Dependent, IL-12/23-Driven Spontaneous Colitis. The Journal of Immunology. 2014 Feb 7;192(4):1918–27.

32. Xu W, Domingues RG, Fonseca-Pereira D, Ferreira M, Ribeiro H, Lopez-Lastra S, et al. NFIL3 Orchestrates the Emergence of Common Helper Innate Lymphoid Cell Precursors. CellReports. The Authors; 2015 Mar 31;10(12):2043–54.

33. Kamizono S, Duncan GS, Seidel MG, Morimoto A, Hamada K, Grosveld G, et al. Nfil3/E4bp4 is required for the development and maturation of NK cells in vivo. Journal of Experimental Medicine. 2009 Dec 21;206(13):2977–86.

34. Gascoyne DM, Long E, Veiga-Fernandes H, de Boer J, Williams O, Seddon B, et al. The basic leucine zipper transcription factor E4BP4 is essential for natural killer cell development. Nature Immunology. 2009 Sep 13;10(10):1118–24.

35. Male V, Nisoli I, Kostrzewski T, Allan DSJ, Carlyle JR, Lord GM, et al. The transcription factor E4bp4/Nfil3 controls commitment to the NK lineage and directly regulates Eomes and Id2 expression. Journal of Experimental Medicine. 2014 Apr 7;211(4):635–42.

36. Yu X, Wang Y, Deng M, Li Y, Ruhn KA, Zhang CC, et al. The basic leucine zipper transcription factor NFIL3 directs the development of a common innate lymphoid cell precursor. Elife. 2014;3.

37. Aliahmad P, la Torre de B, Kaye J. Shared dependence on the DNA-binding factor TOX for the development of lymphoid tissue–inducer cell and NK cell lineages. Nature Immunology. 2010 Sep 5;11(10):945–52.

38. Seehus CR, Aliahmad P, la Torre de B, Iliev ID, Spurka L, Funari VA, et al. The development of innate lymphoid cells requires TOX-dependent generation of a common innate lymphoid cell progenitor. Nature Immunology. Nature Publishing Group; 2015 Apr 27;:1–12.

39. Spits H. Another Armament in Gut Immunity: Lymphotoxin-Mediated Crosstalk between Innate Lymphoid and Dendritic Cells. Cell Host and Microbe. Elsevier Inc; 2011 Jul 21;10(1):3–4.

40. Verykokakis M, Zook EC, Kee BL. ID'ing innate and innate-like lymphoid cells. Immunol Rev. 2014 Sep;261(1):177–97.

41. Nechanitzky R, Akbas D, Scherer S, Györy I, Hoyler T, Ramamoorthy S, et al. Transcription factor EBF1 is essential for the maintenance of B cell identity and prevention of alternative fates in committed cells. Nature Immunology. 2013 Jun 30;14(8):867–75.

42. Boos MD, Yokota Y, Eberl G, Kee BL. Mature natural killer cell and lymphoid tissue-inducing cell development requires Id2-mediated suppression of E protein activity. J Exp Med. 2007 May 14;204(5):1119–30.

43. Satoh-Takayama N, Lesjean-Pottier S, Vieira P, Sawa S, Eberl G, Vosshenrich CAJ, et al. IL-7 and IL-15 independently program the differentiation of intestinal CD3-NKp46+ cell subsets from Id2-dependent precursors. Journal of Experimental Medicine. 2010 Feb 15;207(2):273–80.

44. Yokota Y, Mansouri A, Mori S, Sugawara S, Adachi S, Nishikawa S, et al. Development of peripheral lymphoid organs and natural killer cells depends on the helix-loop-helix inhibitor Id2. Nature. 1999 Feb 25;397(6721):702–6.

45. Gordon SM, Chaix J, Rupp LJ, Wu J, Madera S, Sun JC, et al. The Transcription Factors T-bet and Eomes Control Key Checkpoints of Natural Killer Cell Maturation. Immunity. Elsevier Inc; 2012 Jan 27;36(1):55–67.

46. Townsend MJ, Weinmann AS, Matsuda JL, Salomon R, Farnham PJ, Biron CA, et al. T-bet regulates the terminal maturation and homeostasis of NK and Valpha14i NKT cells. Immunity. 2004 Apr;20(4):477–94.

47. Vonarbourg C, Mortha A, Bui VL, Hernandez PP, Kiss EA, Hoyler T, et al. Regulated expression of nuclear receptor RORγt confers distinct functional fates to NK cell receptor-expressing RORγt(+) innate lymphocytes. Immunity. 2010 Nov 24;33(5):736–51.

48. Samson SI, Richard O, Tavian M, Ranson T, Vosshenrich CAJ, Colucci F, et al. GATA-3 promotes maturation, IFN-gamma production, and liver-specific homing of NK cells. Immunity. 2003 Nov;19(5):701–11.

49. Vosshenrich CAJ, García-Ojeda ME, Samson-Villéger SI, Pasqualetto V, Enault L, Goff OR-L, et al. A thymic pathway of mouse natural killer cell development characterized by expression of GATA-3 and CD127. Nature Immunology. 2006 Oct 1;7(11):1217–24.

50. Yagi R, Zhong C, Northrup DL, Yu F, Bouladoux N, Spencer S, et al. The transcription factor GATA3 is critical for the development of all IL-7Rα-expressing innate lymphoid cells. Immunity. 2014 Mar 20;40(3):378–88.

51. Serafini N, Klein Wolterink RGJ, Satoh-Takayama N, Xu W, Vosshenrich CAJ, Hendriks RW, et al. Gata3 drives development of ROR t+ group 3 innate lymphoid cells. Journal of Experimental Medicine. 2014 Feb 10;211(2):199–208.

52. Constantinides MG, McDonald BD, Verhoef PA, Bendelac A. A committed precursor to innate lymphoid cells. Nature. Nature Publishing Group; 2014 Apr 9;508(7496):397–401.

53. Savage AK, Constantinides MG, Han J, Picard D, Martin E, Li B, et al. The transcription factor PLZF directs the effector program of the NKT cell lineage. Immunity. 2008 Sep 19;29(3):391–403.

54. Kovalovsky D, Uche OU, Eladad S, Hobbs RM, Yi W, Alonzo E, et al. The BTB-zinc finger transcriptional regulator PLZF controls the development of invariant natural killer T cell effector functions. Nature Immunology. 2008 Sep;9(9):1055–64.

55. Verykokakis M, Krishnamoorthy V, Iavarone A, Lasorella A, Sigvardsson M, Kee BL. Essential functions for ID proteins at multiple checkpoints in invariant NKT cell development. The Journal of Immunology. 2013 Dec 15;191(12):5973–83.

56. Eberl G, Marmon S, Sunshine MJ, Rennert PD, Choi Y, Littman DR. An essential function for the nuclear receptor RORγt in the generation of foetal lymphoid tissue inducer cells. Nature Immunology. Nature Publishing Group; 2003;5(1):64–73.

57. Sanos SL, Bui VL, Mortha A, Oberle K, Heners C, Johner C, et al. RORγt and commensal microflora are required for the differentiation of mucosal interleukin 22–producing NKp46+ cells. Nature Immunology. 2008 Nov 23;10(1):83–91.

58. Satoh-Takayama N, Vosshenrich CAJ, Lesjean-Pottier S, Sawa S, Lochner M, Rattis F, et al. Microbial Flora Drives Interleukin 22 Production in Intestinal NKp46+ Cells that Provide Innate Mucosal Immune Defense. Immunity. Elsevier Inc; 2008 Dec 19;29(6):958–70.

59. Sawa S, Lochner M, Satoh-Takayama N, Dulauroy S, Bérard M, Kleinschek M, et al. RORγt+ innate lymphoid cells regulate intestinal homeostasis by integrating negative signals from the symbiotic microbiota. Nature Immunology. Nature Publishing Group; 2011 Feb 20;12(4):320–6.

60. Sciume G, Hirahara K, Takahashi H, Laurence A, Villarino AV, Singleton KL, et al. Distinct requirements for T-bet in gut innate lymphoid cells. Journal of Experimental Medicine. 2012 Dec 3.

61. Rankin LC, Groom JR, Chopin M, Herold MJ, Walker JA, Mielke LA, et al. The transcription factor T-bet is essential for the development of NKp46+ innate lymphocytes via the Notch pathway. Nature Publishing Group. 2013 Mar 3;14(4):389–95.

62. Malhotra N, Narayan K, Cho OH, Sylvia KE, Yin C, Melichar H, et al. A Network of High-Mobility Group Box Transcription Factors Programs Innate Interleukin-17 Production. Immunity. Elsevier Inc; 2013 Apr 18;38(4):681–93.

63. Hanash AM, Dudakov JA, Hua G, O'Connor MH, Young LF, Singer NV, et al. Interleukin-22 protects intestinal stem cells from immune-mediated tissue damage and regulates sensitivity to graft versus host disease. Immunity. 2012 Aug 24;37(2):339–50.

64. Mebius RE, Rennert P, Weissman IL. Developing lymph nodes collect CD4+CD3- LTbeta+ cells that can differentiate to APC, NK cells, and follicular cells but not T or B cells. Immunity. 1997 Oct 20;7(4):493–504.

65. Kiss EA, Vonarbourg C, Kopfmann S, Hobeika E, Finke D, Esser C, et al. Natural Aryl Hydrocarbon Receptor Ligands Control Organogenesis of Intestinal Lymphoid Follicles. Science. 2011 Dec 15;334(6062):1561–5.

66. Qiu J, Heller JJ, Guo X, Chen Z-ME, Fish K, Fu Y-X, et al. The Aryl Hydrocarbon Receptor Regulates Gut Immunity through Modulation of Innate Lymphoid Cells. Immunity. Elsevier Inc; 2012 Jan 27;36(1):92–104.

67. Zelante T, Iannitti RG, Cunha C, De Luca A, Giovannini G, Pieraccini G, et al. Tryptophan catabolites from microbiota engage aryl hydrocarbon receptor and balance mucosal reactivity via interleukin-22. Immunity. 2013 Aug 22;39(2):372–85.

68. Walker JA, Oliphant CJ, Englezakis A, Yu Y, Clare S, Rodewald HR, et al. Bcl11b is essential for group 2 innate lymphoid cell development. Journal of Experimental Medicine. 2015 May 11;193(5):2059.

69. Yu Y, Wang C, Clare S, Wang J, Lee SC, Brandt C, et al. The transcription factor Bcl11b is specifically expressed in group 2 innate lymphoid cells and is essential for their development. Journal of Experimental Medicine. 2015 May 11;193(5):2059.

70. Halim TYF, Krauß RH, Sun AC, Takei F. Lung Natural Helper Cells Are a Critical Source of Th2 Cell-Type Cytokines in Protease Allergen-Induced Airway Inflammation. Immunity. 2012 Mar;36(3):451–63.

71. Halim TYF, MacLaren A, Romanish MT, Gold MJ, McNagny KM, Takei F. Retinoic-Acid-Receptor-Related Orphan Nuclear Receptor Alpha Is Required for Natural Helper Cell Development and Allergic Inflammation. Immunity. Elsevier Inc; 2012 Sep 21;37(3):463–74.

72. Yang XO, Pappu BP, Nurieva R, Akimzhanov A, Kang HS, Chung Y, et al. T Helper 17 Lineage Differentiation Is Programmed by Orphan Nuclear Receptors RORα and RORγ. Immunity. 2008 Jan;28(1):29–39.

73. Hamilton BA, Frankel WN, Kerrebrock AW, Hawkins TL, FitzHugh W, Kusumi K, et al. Disruption of the nuclear hormone receptor ROR alpha in staggerer mice. Nature. 1996;379(6567):736–9.

74. Klein Wolterink RGJ, Serafini N, van Nimwegen M, Vosshenrich CAJ, de Bruijn MJW, Fonseca-Pereira D, et al. Essential, dose-dependent role for the transcription factor Gata3 in the development of IL-5+ and IL-13+ type 2 innate lymphoid cells. Proc Natl Acad Sci USA. 2013 Jun 18;110(25):10240–5.

75. Zhang JA, Mortazavi A, Williams BA, Wold BJ, Rothenberg EV. Dynamic Transformations of Genome-wide Epigenetic Marking and Transcriptional Control Establish T Cell Identity. Cell. Elsevier; 2012 Apr 13;149(2):467–82.

76. Peng H, Jiang X, Chen Y, Sojka DK, Wei H, Gao X, et al. Liver-resident NK cells confer adaptive immunity in skin-contact inflammation. J Clin Invest. 2013 Mar 25;123(4):1444–56.

77. Daussy C, Faure F, Mayol K, Viel S, Gasteiger G, Charrier E, et al. T-bet and Eomes instruct the development of two distinct natural killer cell lineages in the liver and in the bone marrow. Journal of Experimental Medicine. 2014 Mar 10;211(3):563–77.

78. Di Santo JP, Kühn R, Müller W. Common cytokine receptor gamma chain (gamma c)-dependent cytokines: understanding in vivo functions by gene targeting. Immunol Rev. 1995 Dec;148:19–34.

79. Habib T, Senadheera S, Weinberg K, Kaushansky K. The Common γ Chain (γc) Is a Required Signaling Component of the IL-21 Receptor and Supports IL-21-Induced Cell Proliferation via JAK3. Biochemistry. 2002 Jul;41(27):8725–31.

80. Cao X, Shores EW, Hu-Li J, Anver MR, Kelsall BL, Russell SM, et al. Defective lymphoid development in mice lacking expression of the common cytokine receptor gamma chain. Immunity. 1995 Mar;2(3):223–38.

81. Roediger B, Kyle R, Yip KH, Sumaria N, Guy TV, Kim BS, et al. Cutaneous immunosurveillance and regulation of inflammation by group 2 innate lymphoid cells. Nature Publishing Group. 2013 Apr 21;14(6):564–73.

82. Maki K, Sunaga S, Komagata Y, Kodaira Y, Mabuchi A, Karasuyama H, et al. Interleukin 7 receptor-deficient mice lack gammadelta T cells. Proc Natl Acad Sci USA. 1996 Jul 9;93(14):7172–7.

83. Vosshenrich CAJ, Ranson T, Samson SI, Corcuff E, Colucci F, Rosmaraki EE, et al. Roles for common cytokine receptor gamma-chain-dependent cytokines in the generation, differentiation, and maturation of NK cell precursors and peripheral NK cells in vivo. J Immunol. 2005 Feb 1;174(3):1213–21.

84. Spooner CJ, Lesch J, Yan D, Khan AA, Abbas A, Ramirez-Carrozzi V, et al. Specification of type 2 innate lymphocytes by the transcriptional determinant Gfi1. Nature Immunology. Nature Publishing Group; 2013 Oct 20;14(12):1229–36.

85. Kennedy MK, Glaccum M, Brown SN, Butz EA, Viney JL, Embers M, et al. Reversible defects in natural killer and memory CD8 T cell lineages in interleukin 15-deficient mice. J Exp Med. 2000 Mar 6;191(5):771–80.

86. Mebius RE. Organogenesis of lymphoid tissues. Nat Rev Immunol. 2003 Apr;3(4):292–303.

87. van de Pavert SA, Mebius RE. New insights into the development of lymphoid tissues. Nat Rev Immunol. Nature Publishing Group; 2010 Aug 13;10(9):664–74.

88. van de Pavert SA, Olivier BJ, Goverse G, Vondenhoff MF, Greuter M, Beke P, et al. Chemokine CXCL13 is essential for lymph node initiation and is induced by retinoic acid and neuronal stimulation. Nature Publishing Group. 2009 Nov;10(11):1193–9.

89. van de Pavert SA, Ferreira M, Domingues RG, Ribeiro H, Molenaar R, Moreira-Santos L, et al. van de Pavert. Nature. Nature Publishing Group; 2014 Mar 19;:1–17.

90. Bouskra D, Brézillon C, Bérard M, Werts C, Varona R, Boneca IG, et al. Lymphoid tissue genesis induced by commensals through NOD1 regulates intestinal homeostasis. Nature. 2008 Nov 5;456(7221):507–10.

91. Hamada H, Hiroi T, Nishiyama Y, Takahashi H, Masunaga Y, Hachimura S, et al. Identification of multiple isolated lymphoid follicles on the antimesenteric wall of the mouse small intestine. J Immunol. 2002 Jan 1;168(1):57–64.

92. Eberl G. Thymic Origin of Intestinal T Cells Revealed by Fate Mapping of ROR t+ Cells. Science. 2004 Jul 9;305(5681):248–51.

93. Tsuji M, Suzuki K, Kitamura H, Maruya M, Kinoshita K, Ivanov II, et al. Requirement for Lymphoid Tissue-Inducer Cells in Isolated Follicle Formation and T Cell-Independent Immunoglobulin A Generation in the Gut. Immunity. 2008 Aug;29(2):261–71.

94. Kanamori Y, Ishimaru K, Nanno M, Maki K, Ikuta K, Nariuchi H, et al. Identification of novel lymphoid tissues in murine intestinal mucosa where clusters of c-kit+ IL-7R+ Thy1+ lympho-hemopoietic progenitors develop. J Exp Med. 1996 Oct 1;184(4):1449–59.

95. Lochner M, Ohnmacht C, Presley L, Bruhns P, Si-Tahar M, Sawa S, et al. Microbiota-induced tertiary lymphoid tissues aggravate inflammatory disease in the absence of ROR t and LTi cells. Journal of Experimental Medicine. 2011 Jan 17;208(1):125–34.

96. Sonnenberg GF, Monticelli LA, Alenghat T, Fung TC, Hutnick NA, Kunisawa J, et al. Innate lymphoid cells promote anatomical containment of lymphoid-resident commensal bacteria. Science. 2012 Jun 8;336(6086):1321–5.

97. Wolk K, Kunz S, Witte E, Friedrich M, Asadullah K, Sabat R. IL-22 Increases the Innate Immunity of Tissues. Immunity. 2004 Aug;21(2):241–54.

98. Wolk K, Witte E, Wallace E, Döcke W-D, Kunz S, Asadullah K, et al. IL-22 regulates the expression of genes responsible for antimicrobial defense, cellular differentiation, and mobility in keratinocytes: a potential role in psoriasis. Eur J Immunol. 2006 May;36(5):1309–23.

99. Liang SC, Tan XY, Luxenberg DP, Karim R, Dunussi-Joannopoulos K, Collins M, et al. Interleukin (IL)-22 and IL-17 are coexpressed by Th17 cells and cooperatively enhance expression of antimicrobial peptides. Journal of Experimental Medicine. 2006 Sep 21;203(10):2271–9.

100. Zheng Y, Valdez PA, Danilenko DM, Hu Y, Sa SM, Gong Q, et al. Interleukin-22 mediates early host defense against attaching and effacing bacterial pathogens. Nat Med. 2008 Mar;14(3):282–9.

101. Sabat R, Ouyang W, Wolk K. Therapeutic opportunities of the IL-22-IL-22R1 system. Nat Rev Drug Discov. 2014 Jan;13(1):21–38.

102. Brand S. IL-22 is increased in active Crohn's disease and promotes proinflammatory gene expression and intestinal epithelial cell migration. AJP: Gastrointestinal and Liver Physiology. 2006 Apr 1;290(4):G827–38.

103. Raffatellu M, George MD, Akiyama Y, Hornsby MJ, Nuccio S-P, Paixao TA, et al. Lipocalin-2 resistance confers an advantage to Salmonella enterica serotype Typhimurium for growth and survival in the inflamed intestine. Cell Host and Microbe. 2009 May 8;5(5):476–86.

104. Eyerich S, Eyerich K, Pennino D, Carbone T, Nasorri F, Pallotta S, et al. Th22 cells represent a distinct human T cell subset involved in epidermal immunity and remodeling. J Clin Invest. 2009 Nov 16.

105. Andoh A, Zhang Z, Inatomi O, Fujino S, Deguchi Y, Araki Y, et al. Interleukin-22, a Member of the IL-10 Subfamily, Induces Inflammatory Responses in Colonic Subepithelial Myofibroblasts. Gastroenterology. 2005 Sep;129(3):969–84.

106. Liang SC, Nickerson-Nutter C, Pittman DD, Carrier Y, Goodwin DG, Shields KM, et al. IL-22 Induces an Acute-Phase Response. The Journal of Immunology. 2010 Oct 20;185(9):5531–8.

107. Zheng Y, Danilenko DM, Valdez P, Kasman I, Eastham-Anderson J, Wu J, et al. Interleukin-22, a TH17 cytokine, mediates IL-23-induced dermal inflammation and acanthosis. Nature. 2006 Dec 24;445(7128):648–51.

108. Munoz M, Heimesaat MM, Danker K, Struck D, Lohmann U, Plickert R, et al. Interleukin (IL)-23 mediates Toxoplasma gondii-induced immunopathology in the gut via matrix metalloproteinase-2 and IL-22 but independent of IL-17. Journal of Experimental Medicine. 2009 Dec 21;206(13):3047–59.

109. Sonnenberg GF, Fouser LA, Artis D. Border patrol: regulation of immunity, inflammation and tissue homeostasis at barrier surfaces by IL-22. Nature Immunology. Nature Publishing Group; 2011 May 1;12(5):383–90.

110. Longman RS, Diehl GE, Victorio DA, Huh JR, Galan C, Miraldi ER, et al. CX3CR1+ mononuclear phagocytes support colitis-associated innate lymphoid cell production of IL-22. Journal of Experimental Medicine. 2014 Jul 28;211(8):1571–83.

111. Manta C, Heupel E, Radulovic K, Rossini V, Garbi N, Riedel CU, et al. CX3CR1+ macrophages support IL-22 production by innate lymphoid cells during infection with Citrobacter rodentium. Mucosal Immunology. 2012 Aug 1;6(1):177–88.

112. Satoh-Takayama N, Serafini N, Verrier T, Rekiki A, Renauld JC, Frankel G, et al. The Chemokine Receptor CXCR6 Controls the Functional Topography of Interleukin-22 Producing Intestinal Innate Lymphoid Cells. Immunity. Elsevier Inc; 2014 Nov 3;:1–22.

113. Tumanov AV, Koroleva EP, Guo X, Wang Y, Kruglov A, Nedospasov S, et al. Lymphotoxin Controls the IL-22 Protection Pathway in Gut Innate Lymphoid Cells during Mucosal Pathogen Challenge. Cell Host and Microbe. Elsevier Inc; 2011 Jul 21;10(1):44–53.

114. Shih VF-S, Cox J, Kljavin NM, Dengler HS, Reichelt M, Kumar P, et al. Homeostatic IL-23 receptor signaling limits Th17 response through IL-22-mediated containment of commensal microbiota. Proc Natl Acad Sci USA. 2014 Sep 23;111(38):13942–7.

115. Sonnenberg GF, Monticelli LA, Elloso MM, Fouser LA, Artis D. CD4+ Lymphoid Tissue-Inducer Cells Promote Innate Immunity in the Gut. Immunity. Elsevier Inc; 2011 Jan 28;34(1):122–34.

116. Van Maele L, Carnoy C, Cayet D, Ivanov S, Porte R, Deruy E, et al. Activation of Type 3 innate lymphoid cells and interleukin 22 secretion in the lungs during Streptococcus pneumoniae infection. J Infect Dis. 2014 Aug 1;210(3):493–503.

117. Chen VL, Surana NK, Duan J, Kasper DL. Role of Murine Intestinal Interleukin-1 Receptor 1-Expressing Lymphoid Tissue Inducer-Like Cells in Salmonella Infection. Mizoguchi E, editor. PLoS ONE. 2013 Jun 4;8(6):e65405.

118. Pitt JM, Stavropoulos E, Redford PS, Beebe AM, Bancroft GJ, Young DB, et al. Blockade of IL-10 Signaling during Bacillus Calmette-Guerin Vaccination Enhances and Sustains Th1, Th17, and Innate Lymphoid IFN-gamma and IL-17 Responses and Increases Protection to Mycobacterium tuberculosis Infection. J Immunol. 2012;189(8):4079–87.

119. Mear JB, Gosset P, Kipnis E, Faure E, Dessein R, Jawhara S, et al. Candida albicans Airway Exposure Primes the Lung Innate Immune Response against Pseudomonas aeruginosa Infection through Innate Lymphoid Cell Recruitment and Interleukin-22-Associated Mucosal Response. Infect Immun. 2013 Dec 18;82(1):306–15.

120. Gladiator A, Wangler N, Trautwein-Weidner K, LeibundGut-Landmann S. Cutting edge: IL-17-secreting innate lymphoid cells are essential for host defense against fungal infection. The Journal of Immunology. 2013 Jan 15;190(2):521–5.

121. Zhang B, Chassaing B, Shi Z, Uchiyama R, Zhang Z, Denning TL, et al. Prevention and cure of rotavirus infection via TLR5/NLRC4-mediated production of IL-22 and IL-18. Science. 2014;346(6211):861–5.

122. Hernandez PP, Mahlakõiv T, Yang I, Schwierzeck V, Nguyen N, Guendel F, et al. Interferon-λ and interleukin 22 act synergistically for the induction of interferon-stimulated genes and control of rotavirus infection. Nature Immunology. 2015 May 25.

123. Yasuda K, Muto T, Kawagoe T, Matsumoto M, Sasaki Y, Matsushita K, et al. Contribution of IL-33-activated type II innate lymphoid cells to pulmonary eosinophilia in intestinal nematode-infected mice. Proc Natl Acad Sci USA. 2012 Feb 28;109(9):3451–6.

124. Zaiss DM, Yang L, Shah PR, Kobie JJ, Urban JF, Mosmann TR. Amphiregulin, a TH2 Cytokine Enhancing Resistance to Nematodes. Science. 2006 Dec 15;314(5806):1746–6.

125. Fort MM, Cheung J, Yen D, LI J, Zurawski SM, Lo S, et al. IL-25 induces IL-4, IL-5, and IL-13 and Th2-associated pathologies in vivo. Immunity. 2001 Dec;15(6):985–95.

126. Pulendran B, Artis D. New paradigms in type 2 immunity. Science. 2012 Jul 27;337(6093):431–5.

127. Urban JF, Noben-Trauth N, Donaldson DD, Madden KB, Morris SC, Collins M, et al. IL-13, IL-4Ralpha, and Stat6 are required for the expulsion of the gastrointestinal nematode parasite Nippostrongylus brasiliensis. Immunity. 1998 Feb;8(2):255–64.

128. Fallon PG. Identification of an interleukin (IL)-25-dependent cell population that provides IL-4, IL-5, and IL-13 at the onset of helminth expulsion. Journal of Experimental Medicine. 2006 Apr 3;203(4):1105–16.

129. Turner JE, Morrison PJ, Wilhelm C, Wilson M, Ahlfors H, Renauld JC, et al. IL-9-mediated survival of type 2 innate lymphoid cells promotes damage control in helminth-induced lung inflammation. Journal of Experimental Medicine. 2013 Dec 16;210(13):2951–65.

130. Herbert DR, Yang J-Q, Hogan SP, Groschwitz K, Khodoun M, Munitz A, et al. Intestinal epithelial cell secretion of RELM-beta protects against gastrointestinal worm infection. Journal of Experimental Medicine. 2009 Dec 21;206(13):2947–57.

131. McSorley HJ, Blair NF, Smith KA, McKenzie ANJ, Maizels RM. Blockade of IL-33 release and suppression of type 2 innate lymphoid cell responses by helminth secreted products in airway allergy. Mucosal Immunology. 2014 Sep;7(5):1068–78.

132. Hsu C-L, Neilsen CV, Bryce PJ. IL-33 is produced by mast cells and regulates IgE-dependent inflammation. PLoS ONE. 2010;5(8):e11944.

133. Molofsky AB, Savage AK, Locksley RM. Interleukin-33 in Tissue Homeostasis, Injury, and Inflammation. Immunity. Elsevier Inc; 2015 Jun 16;42(6):1005–19.

134. Cayrol C, Girard J-P. IL-33: an alarmin cytokine with crucial roles in innate immunity, inflammation and allergy. Current Opinion in Immunology. 2014 Dec;31:31–7.

135. Gorski SA, Hahn YS, Braciale TJ. Group 2 Innate Lymphoid Cell Production of IL-5 Is Regulated by NKT Cells during Influenza Virus Infection. Wherry EJ, editor. PLoS Pathog. 2013 Sep 19;9(9):e1003615.

136. Palmer G, Talabot-Ayer D, Lamacchia C, Toy D, Seemayer CA, Viatte S, et al. Inhibition of interleukin-33 signaling attenuates the severity of experimental arthritis. Arthritis Rheum. 2009 Mar;60(3):738–49.

137. Palmer G, Gabay C. Interleukin-33 biology with potential insights into human diseases. Nat Rev Rheumatol. 2011 Jun;7(6):321–9.

138. Hung LY, Lewkowich IP, Dawson LA. IL-33 drives biphasic IL-13 production for noncanonical Type 2 immunity against hookworms. 2013.

139. Xue L, Salimi M, Panse I, Mjösberg JM, McKenzie ANJ, Spits H, et al. Prostaglandin D2 activates group 2 innate lymphoid cells through chemoattractant receptor-homologous molecule expressed on TH2 cells. J Allergy Clin Immunol. 2014 Apr;133(4):1184–94.

140. Wojno EDT, Monticelli LA, Tran SV, Alenghat T, Osborne LC, Thome JJ, et al. The prostaglandin D2 receptor CRTH2 regulates accumulation of group 2 innate lymphoid cells in the inflamed lung. Nature Publishing Group; 2015 Apr 8:1–11.

141. Lefrançais E, Duval A, Mirey E, Roga S, Espinosa E, Cayrol C, et al. Central domain of IL-33 is cleaved by mast cell proteases for potent activation of group-2 innate lymphoid cells. Proc Natl Acad Sci USA. 2014 Oct 28;111(43):15502–7.

142. Motomura Y, Morita H, Moro K, Nakae S, Artis D, Endo TA, et al. Basophil-derived interleukin-4 controls the function of natural helper cells, a member of ILC2s, in lung inflammation. Immunity. 2014 May 15;40(5):758–71.

143. Kim BS, Wang K, Siracusa MC, Saenz SA, Brestoff JR, Monticelli LA, et al. Basophils Promote Innate Lymphoid Cell Responses in Inflamed Skin. The Journal of Immunology. 2014 Sep 19;193(7):3717–25.

144. Halim TYF, Steer CA, Mathä L, Gold MJ, Martinez-Gonzalez I, McNagny KM, et al. Group 2 Innate Lymphoid Cells Are Critical for the Initiation of Adaptive T Helper 2 Cell-Mediated Allergic Lung Inflammation. Immunity. 2014 Mar;40(3):425–35.

145. Mirchandani AS, Besnard AG, Yip E, Scott C, Bain CC, Cerovic V, et al. Type 2 Innate Lymphoid Cells Drive CD4+ Th2 Cell Responses. The Journal of Immunology. 2014 Feb 21;192(5):2442–8.

146. Oliphant CJ, Hwang YY, Walker JA, Salimi M, Wong SH, Brewer JM, et al. MHCII-Mediated Dialog between Group 2 Innate Lymphoid Cells and CD4+ T Cells Potentiates Type 2 Immunity and Promotes Parasitic Helminth Expulsion. Immunity. 2014 Aug 21;41(2):283–95.

147. Artis D, Spits H. The biology of innate lymphoid cells. Nature. 2015 Jan 14;517(7534):293–301.

148. Brenchley JM, Douek DC. Microbial Translocation Across the GI Tract. Annu Rev Immunol. 2012 Apr 23;30(1):149–73.

149. Hill DA, Artis D. Intestinal Bacteria and the Regulation of Immune Cell Homeostasis. Annu Rev Immunol. 2010 Mar;28(1):623–67.

150. Hashiguchi M, Kashiwakura Y, Kojima H, Kobayashi A, Kanno Y, Kobata T. Peyer's patch innate lymphoid cells regulate commensal bacteria expansion. Immunology Letters. European Federation of Immunological Societies; 2015 May 1;165(1):1–9.

151. Hasegawa M, Yada S, Liu MZ, Kamada N, Munoz-Planillo R, Do N, et al. Interleukin-22 Regulates the Complement System to Promote Resistance against Pathobionts after Pathogen-Induced Intestinal Damage. Immunity. 2014;41(4):620–32.

152. Chen VL, Kasper DL. Interactions between the intestinal microbiota and innate lymphoid cells. Gut Microbes. 2014 Jan 29;5(1):129–40.

153. Guo X, Liang Y, Zhang Y, Lasorella A, Kee BL, Fu Y-X. Innate Lymphoid Cells Control Early Colonization Resistance against Intestinal Pathogens through ID2-Dependent Regulation of the Microbiota. Immunity. Elsevier Inc; 2015 Apr 21;42(4):731–43.

154. Ivanov II, Atarashi K, Manel N, Brodie EL, Shima T, Karaoz U, et al. Induction of Intestinal Th17 Cells by Segmented Filamentous Bacteria. Cell. 2009;139(3):485–98.

155. Qiu J, Guo X, Chen Z-ME, He L, Sonnenberg GF, Artis D, et al. Group 3 Innate Lymphoid Cells Inhibit T-Cell-Mediated Intestinal Inflammation through Aryl Hydrocarbon Receptor Signaling and Regulation of Microflora. Immunity. Elsevier Inc; 2013 Aug 22;39(2):386–99.

156. Hooper LV. Immunology. Innate lymphoid cells sweeten the pot. Science. 2014 Sep 12;345(6202):1248–9.

157. Goto Y, Obata T, Kunisawa J, Sato S, Ivanov II, Lamichhane A, et al. Innate lymphoid cells regulate intestinal epithelial cell glycosylation. Science. 2014 Sep 11;345(6202):1254009–9.

158. Pickard JM, Maurice CF, Kinnebrew MA, Abt MC, Schenten D, Golovkina TV, et al. Rapid fucosylation of intestinal epithelium sustains host-commensal symbiosis in sickness. Nature. 2014 Oct 30;514(7524):638–41.

159. Kruglov AA, Grivennikov SI, Kuprash DV, Winsauer C, Prepens S, Seleznik GM, et al. Nonredundant Function of Soluble LT alpha(3) Produced by Innate Lymphoid Cells in Intestinal Homeostasis. Science. 2013;342(6163):1243–6.

160. Magri G, Miyajima M, Bascones S, Mortha A, Puga I, Cassis L, et al. Innate lymphoid cells integrate stromal and immunological signals to enhance antibody production by splenic marginal zone B cells. Nature Publishing Group. 2014 Feb 23;15(4):354–64.

161. Cerutti A, Chen K, Chorny A. Immunoglobulin responses at the mucosal interface. Annu Rev Immunol. 2011;29:273–93.

162. Zimmermann K, Haas A, Oxenius A. Systemic antibody responses to gut microbes in health and disease. Gut Microbes. 2012 Jan;3(1):42–7.

163. Cerutti A, Cols M, Puga I. Marginal zone B cells: virtues of innate-like antibody-producing lymphocytes. Nat Rev Immunol. 2013 Feb;13(2):118–32.

164. Hepworth MR, Monticelli LA, Fung TC, Ziegler CGK, Grunberg S, Sinha R, et al. Innate lymphoid cells regulate CD4+ T-cell responses to commensal intestinal bacteria. Nature. Nature Publishing Group; 2013 May 29;498(7452):113–7.

165. Hepworth MR, Fung TC, Masur SH, Kelsen JR, McConnell FM, Dubrot J, et al. Group 3 innate lymphoid cells mediate intestinal selection of commensal bacteria-specific CD4+ T cells. Science. 2015 Apr 23.

166. Mortha A, Chudnovskiy A, Hashimoto D, Bogunovic M, Spencer SP, Belkaid Y, et al. Microbiota-Dependent Crosstalk Between Macrophages and ILC3 Promotes Intestinal Homeostasis. Science. 2014 Mar 27;343(6178):1249288–8.

167. Taube C, Tertilt C, Gyülveszi G, Dehzad N, Kreymborg K, Schneeweiss K, et al. IL-22 Is Produced by Innate Lymphoid Cells and Limits Inflammation in Allergic Airway Disease. Häcker G, editor. PLoS ONE. 2011 Jul 18;6(7):e21799.

168. Dudakov JA, Hanash AM, Jenq RR, Young LF, Ghosh A, Singer NV, et al. Interleukin-22 Drives Endogenous Thymic Regeneration in Mice. Science. 2012;336(6077):91–5.

169. Scandella E, Bolinger B, Lattmann E, Miller S, Favre S, Littman DR, et al. Restoration of lymphoid organ integrity through the interaction of lymphoid tissue–inducer cells with stroma of the T cell zone. Nature Immunology. 2008 Apr 20;9(6):667–75.

170. Monticelli LA, Sonnenberg GF, Abt MC, Alenghat T, Ziegler CGK, Doering TA, et al. Innate lymphoid cells promote lung-tissue homeostasis after infection with influenza virus. Nature Immunology. 2011 Sep 25;12(11):1045–54.

171. Molofsky AB, Nussbaum JC, Liang HE, Van Dyken SJ, Cheng LE, Mohapatra A, et al. Innate lymphoid type 2 cells sustain visceral adipose tissue eosinophils and alternatively activated macrophages. Journal of Experimental Medicine. 2013 Mar 11;210(3):535–49.

172. Hams E, Locksley RM, McKenzie ANJ, Fallon PG. Cutting Edge: IL-25 Elicits Innate Lymphoid Type 2 and Type II NKT Cells That Regulate Obesity in Mice. The Journal of Immunology. 2013 Nov 15;191(11):5349–53.

173. Gordon S, Martinez FO. Alternative Activation of Macrophages: Mechanism and Functions. Immunity. Elsevier Inc; 2010 May 28;32(5):593–604.

174. Nguyen KD, Qiu Y, Cui X, Goh YPS, Mwangi J, David T, et al. Alternatively activated macrophages produce catecholamines to sustain adaptive thermogenesis. Nature. 2011;480(7375):104–U272.

175. Nussbaum JC, Van Dyken SJ, Moltke von J, Cheng LE, Mohapatra A, Molofsky AB, et al. Type 2 innate lymphoid cells control eosinophil homeostasis. Nature. Nature Publishing Group; 2013 Nov 28;502(7470):245–8.

176. Odegaard JI, Chawla A. Alternative Macrophage Activation and Metabolism. Annual Review of Pathology: Mechanisms of Disease, Vol 6. 2011;6:275–97.

177. Chawla A, Nguyen KD, Goh YPS. Macrophage-mediated inflammation in metabolic disease. Nat Rev Immunol. Nature Publishing Group; 2011 Oct 10;11(11):738–49.

178. Wu D, Molofsky AB, Liang H-E, Ricardo-Gonzalez RR, Jouihan HA, Bando JK, et al. Eosinophils Sustain Adipose Alternatively Activated Macrophages Associated with Glucose Homeostasis. Science. 2011;332(6026):243–7.

179. Qiu Y, Nguyen KD, Odegaard JI, Cui X, Tian X, Locksley RM, et al. Eosinophils and Type 2 Cytokine Signaling in Macrophages Orchestrate Development of Functional Beige Fat. Cell. 2014;157(6):1292–308.

180. Brestoff JR, Kim BS, Saenz SA, Stine RR, Monticelli LA, Sonnenberg GF, et al. Group 2 innate lymphoid cells promote beiging of white adipose tissue and limit obesity. Nature. Nature Publishing Group; 2015 Mar 4;519(7542):242–6.

181. Lee M-W, Odegaard JI, Mukundan L, Qiu Y, Molofsky AB, Nussbaum JC, et al. Activated Type 2 Innate Lymphoid Cells Regulate Beige Fat Biogenesis. Cell. Elsevier Inc; 2015 Jan 15;160(1-2):74–87.

182. Cupedo T, Crellin NK, Papazian N, Rombouts EJ, Weijer K, Grogan JL, et al. Human foetal lymphoid tissue–inducer cells are interleukin 17–producing precursors to RORC+ CD127+ natural killer–like cells. Nature Immunology. 2008 Nov 23;10(1):66–74.

183. Cella M, Fuchs A, Vermi W, Facchetti F, Otero K, Lennerz JKM, et al. A human natural killer cell subset provides an innate source of IL-22 for mucosal immunity. Nature. Nature Publishing Group; 2008 Oct 16;457(7230):722–5.

184. Hughes T, Becknell B, McClory S, Briercheck E, Freud AG, Zhang X, et al. Stage 3 immature human natural killer cells found in secondary lymphoid tissue constitutively and selectively express the TH17 cytokine interleukin-22. Blood. 2009 Apr 23;113(17):4008–10.

185. Geremia A, Arancibia-Carcamo CV, Fleming MPP, Rust N, Singh B, Mortensen NJ, et al. IL-23-responsive innate lymphoid cells are increased in inflammatory bowel disease. Journal of Experimental Medicine. 2011 Jun 6;208(6):1127–33.

186. Hoorweg K, Peters CP, Cornelissen F, Aparicio-Domingo P, Papazian N, Kazemier G, et al. Functional Differences between Human NKp44(-) and NKp44(+) RORC(+) Innate Lymphoid Cells. Front Immunol. 2012;3:72.

187. Glatzer T, Killig M, Meisig J, Ommert I, Luetke-Eversloh M, Babic M, et al. RORγt^{+} innate lymphoid cells acquire a proinflammatory program upon engagement of the activating receptor NKp44. Immunity. 2013 Jun 27;38(6):1223–35.

188. Crellin NK, Trifari S, Kaplan CD, Cupedo T, Spits H. Human NKp44+IL-22+ cells and LTi-like cells constitute a stable RORC+ lineage distinct from conventional natural killer cells. Journal of Experimental Medicine. 2010 Feb 15;207(2):281–90.

189. Bernink JH, Peters CP, Munneke M, Velde te AA, Meijer SL, Weijer K, et al. Human type 1 innate lymphoid cells accumulate in inflamed mucosal tissues. Nature Publishing Group. Nature Publishing Group; 2013 Jan 20;:1–10.

190. Salimi M, Barlow JL, Saunders SP, Xue L, Gutowska-Owsiak D, Wang X, et al. A role for IL-25 and IL-33-driven type-2 innate lymphoid cells in atopic dermatitis. Journal of Experimental Medicine. 2013 Dec 16;210(13):2939–50.

191. Fuchs A, Vermi W, Lee JS, Lonardi S, Gilfillan S, Newberry RD, et al. Intraepithelial type 1 innate lymphoid cells are a unique subset of IL-12- and IL-15-responsive IFN-γ-producing cells. Immunity. 2013 Apr 18;38(4):769–81.

192. Montaldo E, Teixeira-Alves LG, Glatzer T, Durek P, Stervbo U, Hamann W, et al. Human RORγt(+)CD34(+) cells are lineage-specified progenitors of group 3 RORγt(+) innate lymphoid cells. Immunity. 2014 Dec 18;41(6):988–1000.

193. Tang Q, Ahn Y-O, Southern P, Blazar BR, Miller JS, Verneris MR. Development of IL-22-producing NK lineage cells from umbilical cord blood hematopoietic stem cells in the absence of secondary lymphoid tissue. Blood. 2011 Apr 14;117(15):4052–5.

194. Ahn YO, Blazar BR, Miller JS, Verneris MR. Lineage relationships of human IL-22 producing CD56+ ROR t+ innate lymphoid cells and conventional NK cells. Blood. 2013 Jan 17.

195. Hughes T, Becknell B, Freud AG, McClory S, Briercheck E, Yu J, et al. Interleukin-1beta selectively expands and sustains interleukin-22+ immature human natural killer cells in secondary lymphoid tissue. Immunity. 2010 Jun 25;32(6):803–14.

196. Cella MM, Otero KK, Colonna MM. Expansion of human NK-22 cells with IL-7, IL-2, and IL-1beta reveals intrinsic functional plasticity. PNAS. 2010 Jun 14;107(24):10961–6.

197. Takayama T, Kamada N, Chinen H, Okamoto S, Kitazume MT, Chang J, et al. Imbalance of NKp44+NKp46− and NKp44−NKp46+ Natural Killer Cells in the Intestinal Mucosa of Patients With Crohn's Disease. Gastroenterology. 2010 Sep;139(3):882–3.

198. Powell N, Lo JW, Biancheri P, Vossenkämper A, Pantazi E, Walker AW, et al. Interleukin-6 Increases Production of Cytokines by Colonic Innate Lymphoid Cells in Mice and Patients with Chronic Intestinal Inflammation. Gastroenterology. Elsevier Ltd; 2015 Apr 24;:1–54.

199. Nausch N, Appleby LJ, Sparks AM, Midzi N, Mduluza T, Mutapi F. Group 2 Innate Lymphoid Cell Proportions Are Diminished in Young Helminth Infected Children and Restored by Curative Anti-helminthic Treatment. Brindley PJ, editor. PLoS Negl Trop Dis. 2015 Mar 23;9(3):e0003627.

200. Chang JH, Kim S, Koo J, Lane PJL, Yoon SO, Park AY, et al. The Chronicity of Tonsillitis Is Significantly Correlated with an Increase in an LTi Cell Portion. Inflammation. 2013 Sep 11.

201. Doherty TA, Scott D, Walford HH, Khorram N, Lund S, Baum R, et al. Allergen challenge in allergic rhinitis rapidly induces increased peripheral blood type 2 innate lymphoid cells that express CD84. J Allergy Clin Immunol. 2014 Apr;133(4):1203–5.

202. Walford HH, Lund SJ, Baum RE, White AA, Bergeron CM, Husseman J, et al. Increased ILC2s in the eosinophilic nasal polyp endotype are associated with corticosteroid responsiveness. Clinical Immunology. Elsevier Inc; 2014 Nov 1;155(1):126–35.

203. Doherty TA, Broide DH. Group 2 innate lymphoid cells: new players in human allergic diseases. J Investig Allergol Clin Immunol. 2015;25(1):1–11–quiz2pfollowing11.

204. Teunissen MBM, Munneke JM, Bernink JH, Spuls PI, Res PCM, Velde te A, et al. Composition of innate lymphoid cell subsets in the human skin: enrichment of NCR(+) ILC3 in lesional skin and blood of psoriasis patients. Journal of Investigative Dermatology. 2014 Sep;134(9):2351–60.

205. Dyring-Andersen B, Geisler C, Agerbeck C, Lauritsen JPH, Gúdjonsdottir SD, Skov L, et al. Increased number and frequency of group 3 innate lymphoid cells in nonlesional psoriatic skin. British Journal of Dermatology. 2014 Mar 12;170(3):609–16.

206. Villanova F, Flutter B, Tosi I, Grys K, Sreeneebus H, Perera GK, et al. Characterization of innate lymphoid cells in human skin and blood demonstrates increase of NKp44+ ILC3 in psoriasis. Journal of Investigative Dermatology. 2014 Apr;134(4):984–91.

207. Ward NL, Umetsu DT. A new player on the psoriasis block: IL-17A- and IL-22-producing innate lymphoid cells. Journal of Investigative Dermatology. Nature Publishing Group; 2014 Sep 1;134(9):2305–7.

208. Kim BS, Siracusa MC, Saenz SA, Noti M, Monticelli LA, Sonnenberg GF, et al. TSLP Elicits IL-33-Independent Innate Lymphoid Cell Responses to Promote Skin Inflammation. Science Translational Medicine. 2013 Jan 30;5(170):170ra16–6.

209. Barnig C, Cernadas M, Dutile S, Liu X. Lipoxin A4 regulates natural killer cell and type 2 innate lymphoid cell activation in asthma. Science Translational Medicine. 2013 Feb; 174 (5): 1-11.

210. Bartemes KR, Kephart GM, Fox SJ, Kita H. Enhanced innate type 2 immune response in peripheral blood from patients with asthma. J Allergy Clin Immunol. 2014 Sep;134(3):671–4.

211. Jackson DJ, Makrinioti H, Rana BMJ, Shamji BWH, Trujillo-Torralbo M-B, Footitt J, et al. IL-33-dependent type 2 inflammation during rhinovirus-induced asthma exacerbations in vivo. Am J Respir Crit Care Med. 2014 Dec 15;190(12):1373–82.

212. Male V, Hughes T, McClory S, Colucci F, Caligiuri MA, Moffett A. Immature NK Cells, Capable of Producing IL-22, Are Present in Human Uterine Mucosa. The Journal of Immunology. 2010 Sep 21;185(7):3913–8.

213. Vacca P, Montaldo E, Croxatto D, Loiacono F, Canegallo F, Venturini PL, et al. Identification of diverse innate lymphoid cells in human decidua. Mucosal Immunology. Nature Publishing Group; 2014 Jul 23;8(2):254–64.

214. Perry JSA, Han S, Xu Q, Herman ML, Kennedy LB, Csako G, et al. Inhibition of LTi Cell Development by CD25 Blockade Is Associated with Decreased Intrathecal Inflammation in Multiple Sclerosis. Science Translational Medicine. 2012 Aug 1;4(145):145ra106–6.

215. Sherlock JP, Joyce-Shaikh B, Turner SP, Chao C-C, Sathe M, Grein J, et al. IL-23 induces spondyloarthropathy by acting on ROR-γt+ CD3+CD4-CD8- entheseal resident T cells. Nat Med. 2012 Jul;18(7):1069–76.

216. Ciccia F, Guggino G, Rizzo A, Ferrante A, Raimondo S, Giardina A, et al. Potential involvement of IL-22 and IL-22-producing cells in the inflamed salivary glands of patients with Sjogren's syndrome. Annals of the Rheumatic Diseases. 2011 Dec 28;71(2):295–301.

217. Al-Mossawi MH, Ridley A, Kiedel S, Bowness P. The role of natural killer cells, gamma delta T-cells and other innate immune cells in spondyloarthritis. Current Opinion in Rheumatology. 2013 Jul;25(4):434–9.

218. Bekiaris V, Sedy JR, Rossetti M, Spreafico R, Sharma S, Rhode-Kurnow A, et al. Human CD4+CD3- Innate-Like T Cells Provide a Source of TNF and Lymphotoxin- and Are Elevated in Rheumatoid Arthritis. The Journal of Immunology. 2013 Oct 18;191(9):4611–8.

219. Crellin NK, Trifari S, Kaplan CD, Satoh-Takayama N, Di Santo JP, Spits H. Regulation of Cytokine Secretion in Human CD127+ LTi-like Innate Lymphoid Cells by Toll-like Receptor 2. Immunity. Elsevier Inc; 2010 Nov 24;33(5):752–64.

220. Baychelier F, Sennepin A, Ermonval M, Dorgham K. Identification of a cellular ligand for the natural cytotoxicity receptor NKp44. Blood. 2013.

221. Vieillard V, Strominger JL, Debré P. NK cytotoxicity against CD4+ T cells during HIV-1 infection: a gp41 peptide induces the expression of an NKp44 ligand. Proc Natl Acad Sci USA. 2005 Aug 2;102(31):10981–6.

222. Spencer SP, Wilhelm C, Yang Q, Hall JA, Bouladoux N, Boyd A, et al. Adaptation of innate lymphoid cells to a micronutrient deficiency promotes type 2 barrier immunity. Science. 2014 Jan 24;343(6169):432–7.

223. Xavier RJ, Podolsky DK. Unravelling the pathogenesis of inflammatory bowel disease. Nature. 2007 Jul 26;448(7152):427–34.

224. Stange EF, Travis SPL, Vermeire S, Reinisch W, Geboes K, Barakauskiene A, et al. European evidence-based Consensus on the diagnosis and management of ulcerative colitis: Definitions and diagnosis. Journal of Crohn's and Colitis. 2008 Mar;2(1):1–23.

225. Van Assche G, Dignass A, Panés J, Beaugerie L, Karagiannis J, Allez M, et al. The second European evidence-based Consensus on the diagnosis and management of Crohn's disease: Definitions and diagnosis. 2010. pp. 7–27.

226. Cho JH. The genetics and immunopathogenesis of inflammatory bowel disease. Nature Publishing Group. 2008 Jun;8(6):458–66.

227. Bernstein CN, Blanchard JF, Rawsthorne P, Yu N. The prevalence of extraintestinal diseases in inflammatory bowel disease: a population-based study. The American Journal of Gastroenterology. 2001 Apr;96(4):1116–22.

228. Ott C, Schölmerich J. Extraintestinal manifestations and complications in IBD. Nature Publishing Group. Nature Publishing Group; 2013 Jul 9;10(10):585–95.

229. Bernstein CN, Blanchard JF, Kliewer E, Wajda A. Cancer risk in patients with inflammatory bowel disease: a population-based study. Cancer. 2001 Feb 15;91(4):854–62.

230. Peyrin-Biroulet L, Loftus EV, Colombel J-F, Sandborn WJ. The natural history of adult Crohn's disease in population-based cohorts. The American Journal of Gastroenterology. 2010 Feb;105(2):289–97.

231. Monteleone G, Monteleone I, Fina D, Vavassori P, Del Vecchio Blanco G, Caruso R, et al. Interleukin-21 enhances T-helper cell type I signaling and interferon-γ production in Crohn’s disease. Gastroenterology. 2005 Mar;128(3):687–94.

232. Xie J. Cancer in inflammatory bowel disease. WJG. 2008;14(3):378.

233. Cosnes J, Gower Rousseau C, Seksik P, Cortot A. Epidemiology and Natural History of Inflammatory Bowel Diseases. Gastroenterology. 2011 May;140(6):1785–1794.e4.

234. Khor B, Gardet A, Xavier RJ. Genetics and pathogenesis of inflammatory bowel disease. Nature. 2011 Jun 15;474(7351):307–17.

235. Molodecky NA, Soon IS, Rabi DM, Ghali WA, Ferris M, Chernoff G, et al. Increasing Incidence and Prevalence of the Inflammatory Bowel Diseases With Time, Based on Systematic Review. Gastroenterology. 2012 Jan;142(1):46–54.e42.

236. Goodman WA, Garg RR, Reuter BK, Mattioli B, Rissman EF, Pizarro TT. Loss of estrogen-mediated immunoprotection underlies female gender bias in experimental Crohn’s-like ileitis. Mucosal Immunology. Nature Publishing Group; 2014 Mar 12;7(5):1255–65.

237. Saibeni S, Cortinovis I, Beretta L, Tatarella M, Ferraris L, Rondonotti E, et al. Gender and disease activity influence health-related quality of life in inflammatory bowel diseases. Hepatogastroenterology. 2005;52(62):509–15.

238. Loftus EV. Clinical epidemiology of inflammatory bowel disease: Incidence, prevalence, and environmental influences. Gastroenterology. 2004 May;126(6):1504–17.

239. Carter MJ, Lobo AJ, Travis SPL, IBD Section, British Society of Gastroenterology. Guidelines for the management of inflammatory bowel disease in adults. Gut. 2004. pp. V1–16.

240. Brant SR, Wang M-H, Rawsthorne P, Sargent M, Datta LW, Nouvet F, et al. A population-based case-control study of CARD15 and other risk factors in Crohn's disease and ulcerative colitis. Am J Gastroenterol. 2007 Feb;102(2):313–23.

241. Brant SR. Update on the Heritability of Inflammatory Bowel Disease: The Importance of Twin Studies. Inflamm Bowel Dis. 2011 Jan;17(1):1–5.

242. Orholm M, Munkholm P, Langholz E, Nielsen OH, Sørensen TI, Binder V. Familial occurrence of inflammatory bowel disease. N Engl J Med. 1991 Jan 10;324(2):84–8.

243. Jostins L, Ripke S, Weersma RK, Duerr RH, McGovern DP, Hui KY, et al. Host-microbe interactions have shaped the genetic architecture of inflammatory bowel disease. Nature. 2012 Nov 1;491(7422):119–24.

244. Glocker E-O, Kotlarz D, Boztug K, Gertz EM, Schäffer AA, Noyan F, et al. Inflammatory bowel disease and mutations affecting the interleukin-10 receptor. N Engl J Med. 2009 Nov 19;361(21):2033–45.

245. Cho JH, Brant SR. Recent insights into the genetics of inflammatory bowel disease. Gastroenterology. Elsevier Inc; 2011 May 1;140(6):1704–1712.e2.

246. Hugot JP, Chamaillard M, Zouali H, Lesage S, Cézard JP, Belaiche J, et al. Association of NOD2 leucine-rich repeat variants with susceptibility to Crohn's disease. Nature. 2001 May 31;411(6837):599–603.

247. Noguchi E, Homma Y, Kang X, Netea MG, Ma X. A Crohn's disease-associated NOD2 mutation suppresses transcription of human IL10 by inhibiting activity of the nuclear ribonucleoprotein hnRNP-A1. Nature Immunology. 2009 May;10(5):471–9.

248. Abraham C, Cho JH. Functional consequences of NOD2 (CARD15) mutations. Inflamm Bowel Dis. 2006 Jul;12(7):641–50.

249. Watanabe T, Kitani A, Murray PJ, Strober W. NOD2 is a negative regulator of Toll-like receptor 2-mediated T helper type 1 responses. Nature Immunology. 2004 Aug;5(8):800–8.

250. Brain O, Owens BMJ, Pichulik T, Allan P, Khatamzas E, Leslie A, et al. The Intracellular Sensor NOD2 Induces MicroRNA-29 Expression in Human Dendritic Cells to Limit IL-23 Release. Immunity. 2013;39(3):521–36.

251. Cooney R, Baker J, Brain O, Danis B, Pichulik T, Allan P, et al. NOD2 stimulation induces autophagy in dendritic cells influencing bacterial handling and antigen presentation. Nat Med. Nature Publishing Group; 2009 Dec 6;16(1):90–7.

252. Wehkamp J, Harder J, Weichenthal M, Schwab M, Schäffeler E, Schlee M, et al. NOD2 (CARD15) mutations in Crohn's disease are associated with diminished mucosal alpha-defensin expression. Gut. 2004 Nov;53(11):1658–64.

253. Casanova JL, Abel L. Revisiting Crohn's disease as a primary immunodeficiency of macrophages. Journal of Experimental Medicine. 2009 Aug 31;206(9):1839–43.

254. Korzenik JR. Is Crohn's disease due to defective immunity? Gut. 2007 Jan 1;56(1):2–5.

255. Glocker E, Grimbacher B. Inflammatory bowel disease: is it a primary immunodeficiency? Cell Mol Life Sci. 2011 Oct 14;69(1):41–8.

256. Abraham C, Cho JH. IL-23 and Autoimmunity: New Insights into the Pathogenesis of Inflammatory Bowel Disease. Annu Rev Med. 2009 Feb;60(1):97–110.

257. Tsironi E, Feakins RM, Probert CSJ, Roberts CSJ, Rampton DS, Phil D. Incidence of inflammatory bowel disease is rising and abdominal tuberculosis is falling in Bangladeshis in East London, United Kingdom. Am J Gastroenterol. 2004 Sep;99(9):1749–55.

258. Bernstein CN, Shanahan F. Disorders of a modern lifestyle: reconciling the epidemiology of inflammatory bowel diseases. Gut. 2008 Sep;57(9):1185–91.

259. Ananthakrishnan AN. Epidemiology and risk factors for IBD. Nat Rev Gastroenterol Hepatol. 2015 Apr;12(4):205–17.

260. Sellon RK, Tonkonogy S, Schultz M, Dieleman LA, Grenther W, Balish E, et al. Resident enteric bacteria are necessary for development of spontaneous colitis and immune system activation in interleukin-10-deficient mice. Infect Immun. 1998 Nov;66(11):5224–31.

261. Rath HC, Herfarth HH, Ikeda JS, Grenther WB, Hamm TE Jr, Balish E, et al. Normal luminal bacteria, especially Bacteroides species, mediate chronic colitis, gastritis, and arthritis in HLA-B27/human beta2 microglobulin transgenic rats. J Clin Invest. American Society for Clinical Investigation; 1996 Aug 15;98(4):945–53.

262. Veltkamp C, Tonkonogy SL, De Jong YP, Albright C, Grenther WB, Balish E, et al. Continuous stimulation by normal luminal bacteria is essential for the development and perpetuation of colitis in Tg(epsilon26) mice. Gastroenterology. 2001 Mar;120(4):900–13.

263. Taurog JD, Richardson JA, Croft JT. The germfree state prevents development of gut and joint inflammatory disease in HLA-B27 transgenic rats. The Journal of Experimental Medicine. 1994, 180 (6): 2359-64.

264. RUTGEERTS P, GOBOES K, PEETERS M, HIELE M, PENNINCKX F, AERTS R, et al. Effect of Fecal Stream Diversion on Recurrence of Crohns-Disease in the Neoterminal Ileum. Lancet. 1991;338(8770):771–4.

265. D'Haens GR, Geboes K, Peeters M, Baert F, Penninckx F, Rutgeerts P. Early lesions of recurrent Crohn's disease caused by infusion of intestinal contents in excluded ileum. Gastroenterology. 1998 Feb;114(2):262–7.

266. Khan KJ, Ullman TA, Ford AC, Abreu MT, Abadir A, Marshall JK, et al. Antibiotic Therapy in Inflammatory Bowel Disease: A Systematic Review and Meta-Analysis. Am J Gastroenterol. 2011 Apr;106(4):661–73.

267. Frank DN, Amand ALS, Feldman RA, Boedeker EC, Harpaz N, Pace NR. Molecular-phylogenetic characterization of microbial community imbalances in human inflammatory bowel diseases. Proc Natl Acad Sci USA. 2007;104(34):13780–5.

268. Matsuoka K, Kanai T. The gut microbiota and inflammatory bowel disease. Semin Immunopathol. 2014 Nov 25;37(1):47–55.

269. Chassaing B, Darfeuille Michaud A. The Commensal Microbiota and Enteropathogens in the Pathogenesis of Inflammatory Bowel Diseases. Gastroenterology. 2011 May;140(6):1720–3.

270. Mazmanian SK, Liu CH, Tzianabos AO, Kasper DL. An immunomodulatory molecule of symbiotic bacteria directs maturation of the host immune system. Cell. 2005;122(1):107–18.

271. Sokol H, Pigneur B, Watterlot L, Lakhdari O, Bermudez-Humaran LG, Gratadoux J-J, et al. Faecalibacterium prausnitzii is an anti-inflammatory commensal bacterium identified by gut microbiota analysis of Crohn disease patients. Proc Natl Acad Sci USA. 2008;105(43):16731–6.

272. Wang W, Chen L, Zhou R, Wang X, Song L, Huang S, et al. Increased Proportions of Bifidobacterium and the Lactobacillus Group and Loss of Butyrate-Producing Bacteria in Inflammatory Bowel Disease. J Clin Microbiol. 2014 Feb;52(2):398–406.

273. Gaboriau-Routhiau V, Rakotobe S, Lécuyer E, Mulder I, Lan A, Bridonneau C, et al. The Key Role of Segmented Filamentous Bacteria in the Coordinated Maturation of Gut Helper T Cell Responses. Immunity. 2009;31(4):677–89.

274. Salzman NH, Hung K, Haribhai D, Chu H, Karlsson-Sjoeberg J, Amir E, et al. Enteric defensins are essential regulators of intestinal microbial ecology. Nature Immunology. 2010 Jan;11(1):76–U1.

275. Varela E, Manichanh C, Gallart M, Torrejon A, Borruel N, Casellas F, et al. Colonisation by Faecalibacterium prausnitzii and maintenance of clinical remission in patients with ulcerative colitis. Aliment Pharmacol Ther. 2013 Jul;38(2):151–61.

276. David LA, Maurice CF, Carmody RN, Gootenberg DB, Button JE, Wolfe BE, et al. Diet rapidly and reproducibly alters the human gut microbiome. Nature. 2014;505(7484):559–.

277. Wu GD, Chen J, Hoffmann C, Bittinger K, Chen Y-Y, Keilbaugh SA, et al. Linking Long-Term Dietary Patterns with Gut Microbial Enterotypes. Science. 2011;334(6052):105–8.

278. Barnich N, Darfeuille Michaud A. Adherent-invasive Escherichia coli and Crohn's disease. Curr Opin Gastroenterol. 2007 Jan;23(1):16–20.

279. Martin HM, Campbell BJ, Hart CA, Mpofu C, Nayar M, Singh R, et al. Enhanced Escherichia coli adherence and invasion in Crohn's disease and colon cancer. Gastroenterology. 2004 Jul;127(1):80–93.

280. Glasser AL, Boudeau J, Barnich N, Perruchot MH, Colombel JF, Darfeuille-Michaud A. Adherent Invasive Escherichia coli Strains from Patients with Crohn's Disease Survive and Replicate within Macrophages without Inducing Host Cell Death. Infect Immun. 2001 Sep 1;69(9):5529–37.

281. Feller M, Huwiler K, Stephan R, Altpeter E, Shang A, Furrer H, et al. Mycobacterium avium subspecies paratuberculosis and Crohn's disease: a systematic review and meta-analysis. The Lancet Infectious Diseases. 2007 Sep;7(9):607–13.

282. Selby W, Pavli P, Crotty B, Florin T, Radford-Smith G. Two-Year Combination Antibiotic Therapy With Clarithromycin, Rifabutin, and Clofazimine for Crohn’s Disease. Gastroenterology. 2007.

283. Bernstein CN, Blanchard JF, Rawsthorne P, Collins MT. Population-based case control study of seroprevalence of Mycobacterium paratuberculosis in patients with Crohn's disease and ulcerative colitis. J Clin Microbiol. 2004 Mar;42(3):1129–35.

284. Hugot JP, Alberti C, Berrebi D, Bingen E, Cézard JP. Crohn's disease: the cold chain hypothesis. The Lancet. 2003.

285. Norman JM, Handley SA, Baldridge MT, Droit L, Liu CY, Keller BC, et al. Disease-Specific Alterations in the Enteric Virome in Inflammatory Bowel Disease. Cell. Elsevier Inc; 2015 Jan 29;160(3):447–60.

286. Yen D, Cheung J, Scheerens H, Poulet F, McClanahan T, Mckenzie B, et al. IL-23 is essential for T cell–mediated colitis and promotes inflammation via IL-17 and IL-6. J Clin Invest. 2006 May 1;116(5):1310–6.

287. Izcue A, Hue S, Buonocore S, Arancibia-Cárcamo CV, Ahern PP, Iwakura Y, et al. Interleukin-23 Restrains Regulatory T Cell Activity to Drive T Cell-Dependent Colitis. Immunity. 2008 Apr;28(4):559–70.

288. Hue S, Ahern P, Buonocore S, Kullberg MC, Cua DJ, McKenzie BS, et al. Interleukin-23 drives innate and T cell-mediated intestinal inflammation. Journal of Experimental Medicine. 2006 Oct 16;203(11):2473–83.

289. Elson CO, Cong Y, Weaver CT, Schoeb TR, McClanahan TK, Fick RB, et al. Monoclonal Anti–Interleukin 23 Reverses Active Colitis in a T Cell–Mediated Model in Mice. Gastroenterology. 2007 Jun;132(7):2359–70.

290. Uhlig HH, McKenzie BS, Hue S, Thompson C, Joyce-Shaikh B, Stepankova R, et al. Differential Activity of IL-12 and IL-23 in Mucosal and Systemic Innate Immune Pathology. Immunity. 2006 Aug;25(2):309–18.

291. Ahern PP, Izcue A, Maloy KJ, Powrie F. The interleukin-23 axis in intestinal inflammation. Immunol Rev. 2008 Dec;226:147–59.

292. Fuss IJ, Becker C, Yang Z, Groden C, Hornung RL, Heller F, et al. Both IL-12p70 and IL-23 are synthesized during active Crohn's disease and are down-regulated by treatment with anti-IL-12 p40 monoclonal antibody. Inflamm Bowel Dis. 2006 Jan;12(1):9–15.

293. Leung JM, Davenport M, Wolff MJ, Wiens KE, Abidi WM, Poles MA, et al. IL-22-producing CD4+ cells are depleted in actively inflamed colitis tissue. Mucosal Immunology. 2014 Jan;7(1):124–33.

294. Liu Z, Yadav PK, Xu X, Su J, Chen C, Tang M, et al. The increased expression of IL-23 in inflammatory bowel disease promotes intraepithelial and lamina propria lymphocyte inflammatory responses and cytotoxicity. J Leukoc Biol. 2011 Mar 31;89(4):597–606.

295. Ogino T, Nishimura J, Barman S, Kayama H, Uematsu S, Okuzaki D, et al. Increased Th17-Inducing Activity of CD14+ CD163low Myeloid Cells in Intestinal Lamina Propria of Patients With Crohn’s Disease. Gastroenterology. 2013 Dec;145(6):1380–1.

296. Kamada N, Hisamoto T, Okamoto S, Chinen H, Kobayashi T, Sato T, et al. Unique CD14+ intestinal macrophages contribute to the pathogenesis of Crohn disease via IL-23/IFN-γ axis. The Journal of Clinical Investigation. American Society for Clinical Investigation; 2008 Jun 2;118(6):2269.

297. Kvedaraite E, Lourda M, Ideström M, Chen P, Olsson-Åkefeldt S, Forkel M, et al. Tissue-infiltrating neutrophils represent the main source of IL-23 in the colon of patients with IBD. Gut. 2015 Jul 9;:gutjnl–2014–309014.

298. Kleinschek MA, Boniface K, Sadekova S, Grein J, Murphy EE, Turner SP, et al. Circulating and gut-resident human Th17 cells express CD161 and promote intestinal inflammation. Journal of Experimental Medicine. 2009 Mar 16;206(3):525–34.

299. Murphy CA. Divergent Pro- and Antiinflammatory Roles for IL-23 and IL-12 in Joint Autoimmune Inflammation. Journal of Experimental Medicine. 2003 Dec 15;198(12):1951–7.

300. Kobayashi T, Okamoto S, Hisamatsu T, Kamada N, Chinen H, Saito R, et al. IL23 differentially regulates the Th1/Th17 balance in ulcerative colitis and Crohn's disease. Gut. 2008 Jul 30;57(12):1682–9.

301. Bending D, La Peña De H, Veldhoen M, Phillips JM, Uyttenhove C, Stockinger B, et al. Highly purified Th17 cells from BDC2.5NOD mice convert into Th1-like cells in NOD/SCID recipient mice. J Clin Invest. 2009 Mar 2;119(3):565–72.

302. Lee YK, Turner H, Maynard CL, Oliver JR, Chen D, Elson CO, et al. Late Developmental Plasticity in the T Helper 17 Lineage. Immunity. Elsevier Inc; 2009 Jan 16;30(1):92–107.

303. Heller F, Fuss IJ, Nieuwenhuis EE, Blumberg RS, Strober W. Oxazolone colitis, a Th2 colitis model resembling ulcerative colitis, is mediated by IL-13-producing NK-T cells. Immunity. 2002 Nov;17(5):629–38.

304. Jin W, Dong C. IL-17 cytokines in immunity and inflammation. Emerg. Microbes Infect. 2013;2, e60; doi:10.1038/emi.2013.58

305. Maloy KJ, Kullberg MC. IL-23 and Th17 cytokines in intestinal homeostasis. Mucosal Immunology. 2008 Jul 2;1(5):339–49.

306. Bamba S, Andoh A, Yasui H, Araki Y, Bamba T, Fujiyama Y. Matrix metalloproteinase-3 secretion from human colonic subepithelial myofibroblasts: role of interleukin-17. J Gastroenterol. 2003;38(6):548–54.

307. Ye P, Rodriguez FH, Kanaly S, Stocking KL, Schurr J, Schwarzenberger P, et al. Requirement of interleukin 17 receptor signaling for lung CXC chemokine and granulocyte colony-stimulating factor expression, neutrophil recruitment, and host defense. J Exp Med. 2001 Aug 20;194(4):519–27.

308. Caruso R, Fina D, Peluso I, Stolfi C, Fantini MC, Gioia V, et al. A Functional Role for Interleukin-21 in Promoting the Synthesis of the T-Cell Chemoattractant, MIP-3α, by Gut Epithelial Cells. Gastroenterology. 2007 Jan;132(1):166–75.

309. Neurath MF. Cytokines in inflammatory bowel disease. Nat Rev Immunol. 2014 May;14(5):329–42.

310. O'Connor W, Zenewicz LA, Flavell RA. The dual nature of TH17 cells: shifting the focus to function. Nat Immunol. Nature Publishing Group; 2010 May 18;11(6):471–6.

311. Eken A, Singh AK, Treuting PM, Oukka M. IL-23R+ innate lymphoid cells induce colitis via interleukin-22-dependent mechanism. Mucosal Immunology. 2014 Jan;7(1):143–54.

312. Kaser A, Zeissig S, Blumberg RS. Inflammatory Bowel Disease. Annu Rev Immunol. 2010 Mar;28(1):573–621.

313. Ito R, Shin-Ya M, Kishida T, Urano A, Takada R, Sakagami J, et al. Interferon-gamma is causatively involved in experimental inflammatory bowel disease in mice. Clinical & Experimental Immunology. 2006 Nov;146(2):330–8.

314. Chiba H, Kojima T, Osanai M, Sawada N. The significance of interferon-gamma-triggered internalization of tight-junction proteins in inflammatory bowel disease. Sci STKE. 2006 Jan 3;2006(316):pe1.

315. Madara JL, Stafford J. Interferon-gamma directly affects barrier function of cultured intestinal epithelial monolayers. J Clin Invest. 1989 Feb;83(2):724–7.

316. Cua DJ, Sherlock J, Chen Y, Murphy CA, Joyce B, Seymour B, et al. Interleukin-23 rather than interleukin-12 is the critical cytokine for autoimmune inflammation of the brain. Nature. 2003 Feb 13;421(6924):744–8.

317. Heller F, Florian P, Bojarski C, Richter J, Christ M, Hillenbrand B, et al. Interleukin-13 Is the Key Effector Th2 Cytokine in Ulcerative Colitis That Affects Epithelial Tight Junctions, Apoptosis, and Cell Restitution. Gastroenterology. 2005 Aug;129(2):550–64.

318. Bailey JR, Bland PW, Tarlton JF, Peters I, Moorghen M, Sylvester PA, et al. IL-13 Promotes Collagen Accumulation in Crohn's Disease Fibrosis by Down-Regulation of Fibroblast MMP Synthesis: A Role for Innate Lymphoid Cells? PLoS ONE. 2012 Dec 31;7(12):e52332.

319. Burger D, Travis S. Conventional Medical Management of Inflammatory Bowel Disease. Gastroenterology. 2011 May;140(6):1827–1837.e2.

320. European Medicines Agency - Find medicine - European public assessment reports [Internet]. ema.europa.eu. [cited 2015 Aug 25]. Available from: http://www.ema.europa.eu/ema/index.jsp?curl=pages/includes/medicines/medicines_landing_page.jsp

321. Viget N, Vernier-Massouille G, Salmon-Ceron D, Yazdanpanah Y, Colombel JF. Opportunistic infections in patients with inflammatory bowel disease: prevention and diagnosis. Gut. 2008 Apr;57(4):549–58.

322. Vermeire S, Van Assche G, Rutgeerts P. Vaccination and infection prevention in inflammatory bowel disease. F1000 Med Rep. 2010;2:80.

323. McGovern DPB. Risks and benefits of azathioprine therapy. Gut. 2005 Aug 1;54(8):1055–9.

324. Frei P, Biedermann L, Nielsen OH, Rogler G. Use of thiopurines in inflammatory bowel disease. World J Gastroenterol. 2013 Feb 21;19(7):1040–8.

325. Sternthal MB, Murphy SJ, George J, Kornbluth A, Lichtiger S, Present DH. Adverse events associated with the use of cyclosporine in patients with inflammatory bowel disease. The American Journal of Gastroenterology. 2008 Apr;103(4):937–43.

326. Wahed M, Louis-Auguste JR, Baxter LM, Limdi JK, McCartney SA, Lindsay JO, et al. Efficacy of methotrexate in Crohn's disease and ulcerative colitis patients unresponsive or intolerant to azathioprine /mercaptopurine. Aliment Pharmacol Ther. 2009 Sep 15;30(6):614–20.

327. Hagan M, Cross RK. Safety of vedolizumab in the treatment of Crohn's disease and ulcerative colitis. Expert Opin Drug Saf. 2015 Jul 3;:1–7.

328. Hefti MM, Chessin DB, Harpaz NH, Steinhagen RM, Ullman TA. Severity of Inflammation as a Predictor of Colectomy in Patients With Chronic Ulcerative Colitis. Diseases of the Colon & Rectum. 2009 Feb;52(2):193–7.

329. Goldberg R, Prescott N, Lord GM, MacDonald TT, Powell N. Powell. Nature Publishing Group. Nature Publishing Group; 2015 May 1;12(5):271–83.

330. Neurath MF. New targets for mucosal healing and therapy in inflammatory bowel disease. Mucosal Immunology. Nature Publishing Group; 2013 Oct 2;7(1):6–19.

331. Buonocore S, Ahern PP, Uhlig HH, Ivanov II, Littman DR, Maloy KJ, et al. Innate lymphoid cells drive interleukin-23-dependent innate intestinal pathology. Nature. Nature Publishing Group; 2010 Apr 21;464(7293):1371–5.

332. Coccia M, Harrison OJ, Schiering C, Asquith MJ, Becher B, Powrie F, et al. IL-1 mediates chronic intestinal inflammation by promoting the accumulation of IL-17A secreting innate lymphoid cells and CD4+ Th17 cells. Journal of Experimental Medicine. 2012 Aug 27;209(9):1595–609.

333. Powell N, Walker AW, Stolarczyk E, Canavan JB, Gökmen MR, Marks E, et al. The Transcription Factor T-bet Regulates Intestinal Inflammation Mediated by Interleukin-7 Receptor+ Innate Lymphoid Cells. Immunity. Elsevier Inc; 2012 Oct 10;:1–11.

334. Wynn TA. Type 2 cytokines: mechanisms and therapeutic strategies. Nature Publishing Group. Nature Publishing Group; 2015 Apr 17;15(5):271–82.

335. Hardman CS, Panova V, McKenzie ANJ. IL-33 citrine reporter mice reveal the temporal and spatial expression of IL-33 during allergic lung inflammation. Eur J Immunol. 2012 Dec 26;43(2):488–98.

336. Meylan F, Hawley ET, Barron L, Barlow JL, Penumetcha P, Pelletier M, et al. The TNF-family cytokine TL1A promotes allergic immunopathology through group 2 innate lymphoid cells. Mucosal Immunology. 2014 Jul;7(4):958–68.

337. Yu X, Pappu R, Ramirez-Carrozzi V, Ota N, Caplazi P, Zhang J, et al. TNF superfamily member TL1A elicits type 2 innate lymphoid cells at mucosal barriers. Nature Publishing Group; 2013 Nov 13;7(3):730–40.

338. Camelo A, Barlow JL, Drynan LF, Neill DR, Ballantyne SJ, Wong SH, et al. Blocking IL-25 signalling protects against gut inflammation in a type-2 model of colitis by suppressing nuocyte and NKT derived IL-13. J Gastroenterol. 2012 Apr 27.

339. Schneider CA, Rasband WS, Eliceiri KW. NIH Image to ImageJ: 25 years of image analysis. Nat Methods. 2012 Jul;9(7):671–5.

340. Rovedatti L, Kudo T, Biancheri P, Sarra M, Knowles CH, Rampton DS, et al. Differential regulation of interleukin 17 and interferon gamma production in inflammatory bowel disease. Gut. 2009 Dec;58(12):1629–36.

341. Dambacher J, Beigel F, Zitzmann K, De Toni EN, Goke B, Diepolder HM, et al. The role of the novel Th17 cytokine IL-26 in intestinal inflammation. Gut. 2009 Aug 11;58(9):1207–17.

342. Maloy KJ, Powrie F. Intestinal homeostasis and its breakdown in inflammatory bowel disease. Nature. 2011 Jun 15;474(7351):298–306.

343. Fell JM, Walker-Smith JA, Spencer J, MacDonald TT. The distribution of dividing T cells throughout the intestinal wall in inflammatory bowel disease (IBD). Clinical & Experimental Immunology. 1996 May;104(2):280–5.

344. Brynskov J, Tvede N, Andersen CB, Vilien M. Increased concentrations of interleukin 1 beta, interleukin-2, and soluble interleukin-2 receptors in endoscopical mucosal biopsy specimens with active inflammatory bowel disease. Gut. 1992 Jan;33(1):55–8.

345. Rennert PD, James D, Mackay F, Browning JL, Hochman PS. Lymph node genesis is induced by signaling through the lymphotoxin beta receptor. Immunity. 1998 Jul;9(1):71–9.

346. Cupedo T. An unexpected role for IL-17 in lymphoid organogenesis. Nature Immunology. Nature Publishing Group; 2011 Jul 1;12(7):590–2.

347. Rangel-Moreno J, Carragher DM, la Luz Garcia-Hernandez de M, Hwang JY, Kusser K, Hartson L, et al. The development of inducible bronchus-associated lymphoid tissue depends on IL-17. Nature Immunology. Nature Publishing Group; 2011 Jun 12;12(7):639–46.

348. Owens BMJ, Simmons A. Intestinal stromal cells in mucosal immunity and homeostasis. Nature Publishing Group; 2012 Dec 12;6(2):224–34.

349. Wynn TA. IL-13 effector functions. Annu Rev Immunol. 2003;21:425–56.

350. Wolk K, Haugen HS, Xu W, Witte E, Waggie K, Anderson M, et al. IL-22 and IL-20 are key mediators of the epidermal alterations in psoriasis while IL-17 and IFN-gamma are not. J Mol Med. 2009 May;87(5):523–36.

351. Ma H-L, Liang S, Li J, Napierata L, Brown T, Benoit S, et al. IL-22 is required for Th17 cell-mediated pathology in a mouse model of psoriasis-like skin inflammation. J Clin Invest. 2008 Feb;118(2):597–607.

352. Boniface K, Bernard F-X, Garcia M, Gurney AL, Lecron J-C, Morel F. IL-22 inhibits epidermal differentiation and induces proinflammatory gene expression and migration of human keratinocytes. J Immunol. 2005 Mar 15;174(6):3695–702.

353. Geboes L, Dumoutier L, Kelchtermans H, Schurgers E, Mitera T, Renauld JC, et al. Proinflammatory role of the Th17 cytokine interleukin-22 in collagen-induced arthritis in C57BL/6 mice. Arthritis Rheum. 2009 Feb;60(2):390–5.

354. Bishop JL, Roberts ME, Beer JL, Huang M, Chehal MK, Fan X, et al. Lyn activity protects mice from DSS colitis and regulates the production of IL-22 from innate lymphoid cells. Mucosal Immunology. Nature Publishing Group; 2013 Sep 18;7(2):405–16.

355. Mielke LA, Jones SA, Raverdeau M, Higgs R, Stefanska A, Groom JR, et al. Retinoic acid expression associates with enhanced IL-22 production by γδ T cells and innate lymphoid cells and attenuation of intestinal inflammation. Journal of Experimental Medicine. 2013 Jun 3;210(6):1117–24.

356. Kim S, Han S, Withers DR, Gaspal F, Bae J, Baik S, et al. CD117+CD3−CD56−OX40Lhigh cells express IL-22 and display an LTi phenotype in human secondary lymphoid tissues. Eur J Immunol. 2011 May 25;41(6):1563–72.

357. Withers DR, Jaensson E, Gaspal F, McConnell FM, Eksteen B, Anderson G, et al. The Survival of Memory CD4+ T Cells within the Gut Lamina Propria Requires OX40 and CD30 Signals. The Journal of Immunology. 2009 Oct 2;183(8):5079–84.

358. Gaspal FMC, Kim M-Y, McConnell FM, Raykundalia C, Bekiaris V, Lane PJL. Mice deficient in OX40 and CD30 signals lack memory antibody responses because of deficient CD4 T cell memory. J Immunol. 2005 Apr 1;174(7):3891–6.

359. Malek TR. The biology of interleukin-2. Annu Rev Immunol. 2008;26:453–79.

360. Almeida ARM, Zaragoza B, Freitas AA. Indexation as a novel mechanism of lymphocyte homeostasis: the number of CD4+CD25+ regulatory T cells is indexed to the number of IL-2-producing cells. J Immunol. 2006 Jul 1;177(1):192–200.

361. Setoguchi R, Hori S, Takahashi T, Sakaguchi S. Homeostatic maintenance of natural Foxp3(+) CD25(+) CD4(+) regulatory T cells by interleukin (IL)-2 and induction of autoimmune disease by IL-2 neutralization. J Exp Med. 2005 Mar 7;201(5):723–35.

362. Reboldi A, Coisne C, Baumjohann D, Benvenuto F, Bottinelli D, Lira S, et al. C-C chemokine receptor 6–regulated entry of TH-17 cells into the CNS through the choroid plexus is required for the initiation of EAE. Nature Immunology. 2009 Mar 22;10(5):514–23.

363. Yamazaki T, Yang XO, Chung Y, Fukunaga A, Nurieva R, Pappu B, et al. CCR6 Regulates the Migration of Inflammatory and Regulatory T Cells. The Journal of Immunology. 2008 Dec 2;181(12):8391–401.

364. Hirota K, Yoshitomi H, Hashimoto M, Maeda S, Teradaira S, Sugimoto N, et al. Preferential recruitment of CCR6-expressing Th17 cells to inflamed joints via CCL20 in rheumatoid arthritis and its animal model. Journal of Experimental Medicine. 2007 Oct 29;204(12):2803–12.

365. Varona R, Cadenas V, Flores J, Martínez-A C, Márquez G. CCR6 has a non-redundant role in the development of inflammatory bowel disease. Eur J Immunol. 2003 Oct;33(10):2937–46.

366. Katchar K, Kelly CP, Keates S, O'Brien MJ, Keates AC. MIP-3 neutralizing monoclonal antibody protects against TNBS-induced colonic injury and inflammation in mice. AJP: Gastrointestinal and Liver Physiology. 2006 Dec 7;292(5):G1263–71.

367. Kwon JH, Keates S, Bassani L, Mayer LF, Keates AC. Colonic epithelial cells are a major site of macrophage inflammatory protein 3alpha (MIP-3alpha) production in normal colon and inflammatory bowel disease. Gut. 2002 Dec;51(6):818–26.

368. Kaser A, Ludwiczek O, Holzmann S, Moschen AR, Weiss G, Enrich B, et al. Increased expression of CCL20 in human inflammatory bowel disease. J Clin Immunol. 2004 Jan;24(1):74–85.

369. Uchida K, Koike Y, Hashimoto K, Saigusa S, Inoue M, Otake K, et al. The Increased Expression of CCL20 and CCR6 in Rectal Mucosa Correlated to Severe Inflammation in Pediatric Ulcerative Colitis. Gastroenterology Research and Practice. 2015;2015(4):1–6.

370. Barrett JC, Hansoul S, Nicolae DL, Cho JH, Duerr RH, Rioux JD, et al. Genome-wide association defines more than 30 distinct susceptibility loci for Crohn's disease. Nat Genet. 2008 Jun 29;40(8):955–62.

371. Mackley EC, Houston S, Marriott CL, Halford EE, Lucas B, Cerovic V, et al. CCR7-dependent trafficking of RORγ$^+$ ILCs creates a unique microenvironment within mucosal draining lymph nodes. Nature Communications. 2015;6:5862.

372. Seidelin JB, Bjerrum JT, Coskun M, Widjaya B, Vainer B, Nielsen OH. IL-33 is upregulated in colonocytes of ulcerative colitis. Immunology Letters. 2010 Jan;128(1):80–5.

373. Beltrán CJ, Núñez LE, Díaz-Jiménez D, Farfan N, Candia E, Heine C, et al. Characterization of the novel ST2/IL-33 system in patients with inflammatory bowel disease. Inflamm Bowel Dis. 2010 Jul;16(7):1097–107.

374. Pastorelli L, Garg RR, Hoang SB, Spina L, Mattioli B, Scarpa M, et al. Epithelial-derived IL-33 and its receptor ST2 are dysregulated in ulcerative colitis and in experimental Th1/Th2 driven enteritis. Proc Natl Acad Sci USA. 2010 Apr 27;107(17):8017–22.

375. Mannon P, Reinisch W. Interleukin 13 and its role in gut defence and inflammation. Gut. 2012 Sep 1.

376. Desreumaux P, Ernst O, Geboes K, Gambiez L, Berrebi D, Müller-Alouf H, et al. Inflammatory alterations in mesenteric adipose tissue in Crohn's disease. Gastroenterology. 1999 Jul;117(1):73–81.

377. Zulian A, Cancello R, Ruocco C, Gentilini D, Di Blasio AM, Danelli P, et al. Differences in visceral fat and fat bacterial colonization between ulcerative colitis and Crohn's disease. An in vivo and in vitro study. PLoS ONE. 2013;8(10):e78495.

378. Kredel LI, Batra A, Stroh T, Kuhl AA, Zeitz M, Erben U, et al. Adipokines from local fat cells shape the macrophage compartment of the creeping fat in Crohn's disease. Gut. 2013 Apr 30;62(6):852–62.

379. Facchetti F, Blanzuoli L, Ungari M, Alebardi O, Vermi W. Lymph node pathology in primary combined immunodeficiency diseases. Springer Seminars in Immunopathology. 1998;19(4):459–78.

380. Aloisi F, Pujol-Borrell R. Lymphoid neogenesis in chronic inflammatory diseases. Nat Rev Immunol. 2006 Mar;6(3):205–17.

381. Buckley CD, Barone F, Nayar S, Bénézech C, Caamaño J. Stromal cells in chronic inflammation and tertiary lymphoid organ formation. Annu Rev Immunol. 2015 Mar 21;33:715–45.

382. Kim M-Y, Gaspal FMC, Wiggett HE, McConnell FM, Gulbranson-Judge A, Raykundalia C, et al. CD4(+)CD3(-) accessory cells costimulate primed CD4 T cells through OX40 and CD30 at sites where T cells collaborate with B cells. Immunity. 2003 May;18(5):643–54.

383. Rogers PR, Song J, Gramaglia I, Killeen N, Croft M. OX40 promotes Bcl-xL and Bcl-2 expression and is essential for long-term survival of CD4 T cells. Immunity. 2001 Sep;15(3):445–55.

384. Gaspal F, Bekiaris V, Kim M-Y, Withers DR, Bobat S, MacLennan ICM, et al. Critical synergy of CD30 and OX40 signals in CD4 T cell homeostasis and Th1 immunity to Salmonella. J Immunol. 2008 Mar 1;180(5):2824–9.

385. Lane PJL, Gaspal FM, McConnell FM, Kim M-Y, Anderson G, Withers DR. Lymphoid tissue inducer cells: innate cells critical for CD4+ T cell memory responses? Annals of the New York Academy of Sciences. 2012 Jan 19;1247(1):1–15.

386. Muhlethaler-Mottet A, Otten LA, Steimle V, Mach B. Expression of MHC class II molecules in different cellular and functional compartments is controlled by differential usage of multiple promoters of the transactivator CIITA. EMBO J. 1997 May 15;16(10):2851–60.

387. Reith W, LeibundGut-Landmann S, Waldburger J-M. Regulation of MHC class II gene expression by the class II transactivator. Nat Rev Immunol. 2005 Oct;5(10):793–806.

388. Reinhardt RL, Khoruts A, Merica R, Zell T, Jenkins MK. Visualizing the generation of memory CD4 T cells in the whole body. Nature. 2001;410(6824):101–5.

389. Majowicz SE, Musto J, Scallan E, Angulo FJ, Kirk M, O'Brien SJ, et al. The Global Burden of Nontyphoidal Salmonella Gastroenteritis. CLIN INFECT DIS. 2010 Mar 15;50(6):882–9.

390. Griffin AJ, McSorley SJ. Development of protective immunity to *Salmonella*, a mucosal pathogen with a systemic agenda. Mucosal Immunology. Nature Publishing Group; 2011 Feb 9;:1–12.

391. Burg von N, Chappaz S, Baerenwaldt A, Horvath E, Bose Dasgupta S, Ashok D, et al. Activated group 3 innate lymphoid cells promote T-cell-mediated immune responses. Proc Natl Acad Sci USA. 2014 Sep 2;111(35):12835–40.

392. Kirman I, Nielsen OH. Increased numbers of interleukin-15-expressing cells in active ulcerative colitis. Am J Gastroenterol. 1996 Sep;91(9):1789–94.

393. Bouchery T, Kyle R, Camberis M, Shepherd A, Filbey K, Smith A, et al. ILC2s and T cells cooperate to ensure maintenance of M2 macrophages for lung immunity against hookworms. Nature Communications. 2015;6:6970.

394. Guha M, Mackman N. LPS induction of gene expression in human monocytes. Cell Signal. 2001 Feb;13(2):85–94.

395. Wolk K, Kunz S, Crompton NEA, Volk HD, Sabat R. Multiple Mechanisms of Reduced Major Histocompatibility Complex Class II Expression in Endotoxin Tolerance. Journal of Biological Chemistry. 2003 May 16;278(20):18030–6.

396. Landmann R, Knopf HP, Link S, Sansano S, Schumann R, Zimmerli W. Human monocyte CD14 is upregulated by lipopolysaccharide. Infect Immun. 1996 May;64(5):1762–9.

397. Zanoni I, Ostuni R, Marek LR, Barresi S, Barbalat R, Barton GM, et al. CD14 Controls the LPS-Induced Endocytosis of Toll-like Receptor 4. Cell. Elsevier Inc; 2011 Nov 11;147(4):868–80.

398. Benoit M, Desnues B, Mege JL. Macrophage Polarization in Bacterial Infections. The Journal of Immunology. 2008 Sep 3;181(6):3733–9.

399. Yrlid U, Svensson M, Johansson C, Wick MJ. Salmonella infection of bone marrow-derived macrophages and dendritic cells: influence on antigen presentation and initiating an immune response. FEMS Immunol Med Microbiol. 2000 Apr;27(4):313–20.

400. Chen L, Flies DB. Molecular mechanisms of T cell co-stimulation and co-inhibition. Nat Rev Immunol. 2013 Mar 8;13(4):227–42.

401. Korn LL, Thomas HL, Hubbeling HG, Spencer SP, Sinha R, Simkins HM, et al. Conventional CD4+ T cells regulate IL-22-producing intestinal innate lymphoid cells. Mucosal Immunology. 2014 Sep;7(5):1045–57.

402. Roediger B, Kyle R, Tay SS, Mitchell AJ, Bolton HA, Guy TV, et al. IL-2 is a critical regulator of group 2 innate lymphoid cell function during pulmonary inflammation. J Allergy Clin Immunol. 2015 May 26.

403. Sallusto F, Lanzavecchia A. Efficient presentation of soluble antigen by cultured human dendritic cells is maintained by granulocyte/macrophage colony-stimulating factor plus interleukin 4 and downregulated by tumor necrosis factor alpha. J Exp Med. 1994 Apr 1;179(4):1109–18.

404. Iwamoto S, Iwai S-I, Tsujiyama K, Kurahashi C, Takeshita K, Naoe M, et al. TNF-alpha drives human CD14(+) monocytes to differentiate into CD70(+) dendritic cells evoking Th1 and Th17 responses. J Immunol. 2007;179(3):1449–57.

405. Coquet JM, Rausch L, Borst J. The importance of co-stimulation in the orchestration of T helper cell differentiation. Immunol Cell Biol. 2015 Apr 21.

406. Pen JJ, De Keersmaecker B, Maenhout SK, Van Nuffel AMT, Heirman C, Corthals J, et al. Modulation of Regulatory T Cell Function by Monocyte-Derived Dendritic Cells Matured through Electroporation with mRNA Encoding CD40 Ligand, Constitutively Active TLR4, and CD70. J Immunol. 2013;191(4):1976–83.

407. Xiao Y, Peperzak V, Keller AM, Borst J. CD27 instructs CD4(+) T cells to provide help for the memory CD8(+) T cell response after protein immunization. J Immunol. 2008;181(2):1071–82.

408. Soares H, Waechter H, Glaichenhaus N, Mougneau E, Yagita H, Mizenina O, et al. A subset of dendritic cells induces CD4(+) T cells to produce IFN-gamma by an IL-12 independent but CD70-dependent mechanism in vivo. J Exp Med. 2007;204(5):1095–106.

409. Van Oosterwijk MF, Juwana H, Arens R, Tesselaar K, van Oers MHJ, Eldering E, et al. CD27-CD70 interactions sensitise naive CD4+ T cells for IL-12-induced Th1 cell development. Int Immunol. 2007 May 9;19(6):713–8.

410. Kuchroo VK, Das MP, Brown JA, Ranger AM, Zamvil SS, Sobel RA, et al. B7-1 and B7-2 costimulatory molecules activate differentially the Th1/Th2 developmental pathways: application to autoimmune disease therapy. Cell. 1995 Mar 10;80(5):707–18.

411. Ranger AM, Das MP, Kuchroo VK, Glimcher LH. B7-2 (CD86) is essential for the development of IL-4-producing T cells. Int Immunol. 1996 Oct;8(10):1549–60.

412. Zhang Z, Zhong W, Hinrichs D, Wu X, Weinberg A, Hall M, et al. Activation of OX40 Augments Th17 Cytokine Expression and Antigen-Specific Uveitis. The American Journal of Pathology. 2010 Dec;177(6):2912–20.

413. Nakae S, Saijo S, Horai R, Sudo K, Mori S, Iwakura Y. IL-17 production from activated T cells is required for the spontaneous development of destructive arthritis in mice deficient in IL-1 receptor antagonist. Proc Natl Acad Sci USA. 2003;100(10):5986–90.

414. Ohshima Y, Yang LP, Uchiyama T, Tanaka Y, Baum P, Sergerie M, et al. OX40 costimulation enhances interleukin-4 (IL-4) expression at priming and promotes the differentiation of naive human CD4(+) T cells into high IL-4-producing effectors. Blood. 1998;92(9):3338–45.

415. Flynn S, Toellner KM, Raykundalia C, Goodall M, Lane P. CD4 T cell cytokine differentiation: The B cell activation molecule, OX40 ligand, instructs CD4 T cells to express interleukin 4 and upregulates expression of the chemokine receptor, Blr-1. J Exp Med. 1998;188(2):297–304.

416. Ishii N, Ndhlovu LC, Murata K, Sato T, Kamanaka M, Sugamura K. OX40 (CD134) and OX40 ligand interaction plays an adjuvant role during in vivo Th2 responses. Eur J Immunol. 2003 Sep;33(9):2372–81.

417. Xiao X, Balasubramanian S, Liu W, Chu X, Wang H, Taparowsky EJ, et al. OX40 signaling favors the induction of T(H)9 cells and airway inflammation. Nature Immunology. 2012 Oct;13(10):981–90.

418. Lee MT, Kaushansky K, Ralph P, Ladner MB. Differential expression of M-CSF, G-CSF, and GM-CSF by human monocytes. J Leukoc Biol. 1990 Mar;47(3):275–82.

419. van der Bruggen T, Nijenhuis S, van Raaij E, Verhoef J, van Asbeck BS. Lipopolysaccharide-induced tumor necrosis factor alpha production by human monocytes involves the raf-1/MEK1-MEK2/ERK1-ERK2 pathway. Infect Immun. 1999 Aug;67(8):3824–9.

420. Schroder K. Interferon-γ: an overview of signals, mechanisms and functions. J Leukoc Biol. 2003 Dec 23;75(2):163–89.

421. Zhang X, Mosser DM. Macrophage activation by endogenous danger signals. Altmann DM, Douek DC, editors. J Pathol. 2008 Jan;214(2):161–78.

422. Parameswaran N, Patial S. Tumor necrosis factor-α signaling in macrophages. Crit Rev Eukaryot Gene Expr. 2010;20(2):87–103.

423. Krakauer T, Oppenheim JJ. IL-1 and tumor necrosis factor-alpha each up-regulate both the expression of IFN-gamma receptors and enhance IFN-gamma-induced HLA-DR expression on human monocytes and a human monocytic cell line (THP-1). J Immunol. 1993 Feb 15;150(4):1205–11.

424. Frucht DM, Fukao T, Bogdan C, Schindler H, O'Shea JJ, Koyasu S. IFN-gamma production by antigen-presenting cells: mechanisms emerge. Trends in Immunology. 2001 Oct;22(10):556–60.

425. Mosser DM. The many faces of macrophage activation. J Leukoc Biol. 2003 Feb 1;73(2):209–12.

426. Bogdan C, Schleicher U. Production of interferon-γ by myeloid cells – fact or fancy? Trends in Immunology. 2006 Jun;27(6):282–90.

427. Verneris MR, Ahn Y-O, Weeres MA, Blazar BR, Miller JS. Death Receptor 3 (DR3) Is Expressed By Innate Lymphoid Cells (ILC) and Ligation By Tumor Like Antigen-1 (TL1A) Leads To Costimulation and Significant ILC Expansion. Blood. 2013;122(21).

428. Meylan F, Richard AC, Siegel RM. TL1A and DR3, a TNF family ligand-receptor pair that promotes lymphocyte costimulation, mucosal hyperplasia, and autoimmune inflammation. Immunol Rev. 2011 Nov;244:188–96.

429. Franke A, McGovern DPB, Barrett JC, Wang K, Radford-Smith GL, Ahmad T, et al. Genome-wide meta-analysis increases to 71 the number of confirmed Crohn's disease susceptibility loci. Nature Genetics. Nature Publishing Group; 2010 Nov 21;42(12):1118–25.

430. Morandi B, Bougras G, Muller WA, Ferlazzo G, Münz C. NK cells of human secondary lymphoid tissues enhance T cell polarization via IFN-gamma secretion. Eur J Immunol. 2006 Sep;36(9):2394–400.

431. Crome SQ, Lang PA, Lang KS, Ohashi PS. Natural killer cells regulate diverse T cell responses. Trends in Immunology. Elsevier Ltd; 2013 Jul 1;34(7):342–9.

432. Sutton CE, Lalor SJ, Sweeney CM, Brereton CF, Lavelle EC, Mills KHG. Interleukin-1 and IL-23 induce innate IL-17 production from gammadelta T cells, amplifying Th17 responses and autoimmunity. Immunity. 2009 Aug 21;31(2):331–41.

433. Cui Y, Shao H, Lan C, Nian H, O'Brien RL, Born WK, et al. Major role of gamma delta T cells in the generation of IL-17+ uveitogenic T cells. The Journal of Immunology. 2009 Jul 1;183(1):560–7.

434. Gasteiger G, Rudensky AY. Interactions between innate and adaptive lymphocytes. Nat Rev Immunol. Nature Publishing Group; 2014 Aug 18;14(9):631–9.

435. Hart AL, Al-Hassi HO, Rigby RJ, Bell SJ, Emmanuel AV, Knight SC, et al. Characteristics of intestinal dendritic cells in inflammatory bowel diseases. Gastroenterology. 2005 Jul;129(1):50–65.

436. Bain CC, Scott CL, Mowat AM. Resident and pro-inflammatory macrophages in the colon represent alternative context dependent fates of the same Ly6Chi monocyte precursors. Immunology. 2012 Sep;137:218–8.

437. Rydstrom A, Wick MJ. Monocyte recruitment, activation, and function in the gut-associated lymphoid tissue during oral Salmonella infection. J Immunol. 2007;178(9):5789–801.

438. Bain CC, Mowat AM. The monocyte-macrophage axis in the intestine. Cell Immunol. 2014;291(1-2):41–8.

439. Donohue JH, Rosenberg SA. The fate of interleukin-2 after in vivo administration. J Immunol. 1983 May;130(5):2203–8.

440. Barrila J, Radtke AL, Crabbé A, Sarker SF, Herbst-Kralovetz MM, Ott CM, et al. Organotypic 3D cell culture models: using the rotating wall vessel to study host-pathogen interactions. Nat Rev Microbiol. 2010 Nov;8(11):791–801.

441. Haraguchi Y, Shimizu T, Sasagawa T, Sekine H, Sakaguchi K, Kikuchi T, et al. Fabrication of functional three-dimensional tissues by stacking cell sheets in vitro. Nat Protoc. 2012 May;7(5):850–8.

442. Pereira C, Araújo F, Barrias CC, Granja PL, Sarmento B. Dissecting stromal-epithelial interactions in a 3D in vitro cellularized intestinal model for permeability studies. Biomaterials. 2015 Jul;56:36–45.

443. Rongvaux A, Takizawa H, Strowig T, Willinger T, Eynon EE, Flavell RA, et al. Human hemato-lymphoid system mice: current use and future potential for medicine. Annu Rev Immunol. 2013;31:635–74.

444. Rongvaux A, Willinger T, Martinek J, Strowig T, Gearty SV, Teichmann LL, et al. Development and function of human innate immune cells in a humanized mouse model. Nature Biotechnology. Nature Publishing Group; 2014 Mar 16;32(4):364–72.

445. Köck K, Pan WJ, Gow JM, Horner MJ, Gibbs JP, Colbert A, et al. Preclinical development of AMG 139, a human antibody specifically targeting IL-23. Br J Pharmacol. 2014 Dec 15;172(1):159–72.

446. Gaffen SL, Jain R, Garg AV, Cua DJ. The IL-23-IL-17 immune axis: from mechanisms to therapeutic testing. Nat Rev Immunol. 2014 Sep;14(9):585–600.

447. Sandborn WJ, Gasink C, Gao L-L, Blank MA, Johanns J, Guzzo C, et al. Ustekinumab Induction and Maintenance Therapy in Refractory Crohn's Disease. N Engl J Med. 2012 Oct 18;367(16):1519–28.

448. Niederreiter L, Adolph TE, Kaser A. Anti-IL-12/23 in Crohn's disease: bench and bedside. Current drug targets. 2013 Nov;14(12):1379-84.

449. Ito H, Takazoe M, Fukuda Y, Hibi T, Kusugami K. A pilot randomized trial of a human anti-interleukin-6 receptor monoclonal antibody in active Crohn's disease. Gastroenterology. 2004 April;12(4):989-96.

450. Jones SA, Scheller J, Rose-John S. Therapeutic strategies for the clinical blockade of IL-6/gp130 signaling. J Clin Invest. 2011 Sep;121(9):3375–83.

451. Nam JL, Ramiro S, Gaujoux-Viala C. Efficacy of biological disease-modifying antirheumatic drugs: a systematic literature review informing the 2013 update of the EULAR recommendations for the management of rheumatoid arthritis. Ann Rheum Dis. 2014 Jan; 73:516-28.

452. Ruperto N, Brunner HI, Quartier P, Constantin T, Wulffraat N, Horneff G, et al. Two Randomized Trials of Canakinumab in Systemic Juvenile Idiopathic Arthritis. N Engl J Med. 2012;367(25):2396–406.

453. Ilowite NT, Prather K, Lokhnygina Y, Schanberg LE, Elder M, Milojevic D, et al. Randomized, Double-Blind, Placebo-Controlled Trial of the Efficacy and Safety of Rilonacept in the Treatment of Systemic Juvenile Idiopathic Arthritis. Arthritis & Rheumatology. 2014 Sep;66(9):2570–9.

454. Colombel J-F, Sendid B, Jouault T, Poulain D. Secukinumab failure in Crohn's disease: the yeast connection? Gut. 2013 May;62(5):800–1.

455. Hueber W, Sands BE, Lewitzky S. Secukinumab, a human anti-IL-17A monoclonal antibody, for moderate to severe Crohn's disease: unexpected results of a randomised, double-blind placebo-controlled trial. Gut. 2012 May;61(12):1693-1700.

456. Reinisch W, de Villiers W, Bene L. Fontolizumab in moderate to severe Crohn's disease: A phase 2, randomized, double-blind, placebo-controlled, multiple-dose study. Inflamm Bowel Dis. 2010 July;16(2):233-42.

457. Sandborn WJ, Ghosh S, Panés J, Vranic I, Wang W, Niezychowski W, et al. A Phase 2 Study of Tofacitinib, an Oral Janus Kinase Inhibitor, in Patients With Crohn's Disease. Clinical Gastroenterology and Hepatology. Elsevier, Inc; 2014 Sep 1;12(9):1485–1493.e2.

458. Sandborn WJ, Ghosh S, Panés J, Vranic I, Su C, Rousell S, et al. Tofacitinib, an Oral Janus Kinase Inhibitor, in Active Ulcerative Colitis. N Engl J Med. 2012 Aug 16;367(7):616–24.

459. Zenewicz LA, Yancopoulos GD, Valenzuela DM, Murphy AJ, Stevens S, Flavell RA. Innate and Adaptive Interleukin-22 Protects Mice from Inflammatory Bowel Disease. Immunity. Elsevier Inc; 2008 Dec 19;29(6):947–57.

460. Sugimoto K, Ogawa A, Mizoguchi E, Shimomura Y, Andoh A, Bhan AK, et al. IL-22 ameliorates intestinal inflammation in a mouse model of ulcerative colitis. J Clin Invest. 2008 Feb;118(2):534–44.

461. Kirchberger S, Royston DJ, Boulard O, Thornton E, Franchini F, Szabady RL, et al. Innate lymphoid cells sustain colon cancer through production of interleukin-22 in a mouse model. Journal of Experimental Medicine. 2013 May 6;210(5):917–31.

462. Okada S, Markle JG, Deenick EK, Mele F, Averbuch D, Lagos M, et al. Immunodeficiencies. Impairment of immunity to Candida and Mycobacterium in humans with bi-allelic RORC mutations. Science. 2015 Aug 7;349(6248):606–13.